Geochemical Perspectives

Volume 2, number 1 | April 2013

Fred T. Mackenzie
Andreas J. Andersson

The Marine Carbon System and Ocean Acidification during Phanerozoic Time

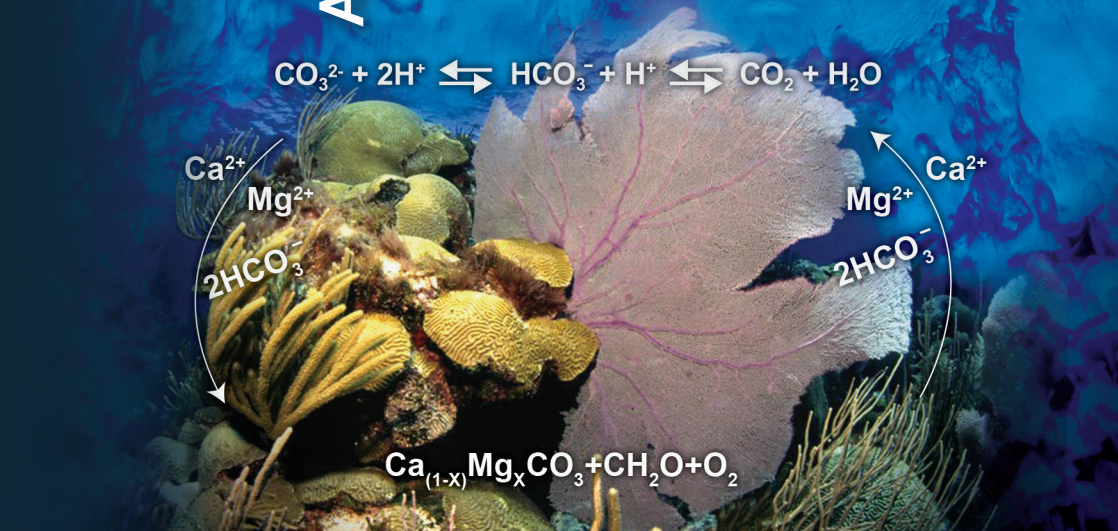

Geochemical Perspectives

Each issue of ***Geochemical Perspectives*** presents a single article with an in-depth view on the past, present and future of a field of geochemistry, seen through the eyes of highly respected members of our community. The articles combine research and history of the field's development and the scientist's opinions about future directions. We welcome personal glimpses into the author's scientific life, how ideas were generated and pitfalls along the way. *Perspectives* articles are intended to appeal to the entire geochemical community, not only to experts. They are not reviews or monographs; they go beyond the current state of the art, providing opinions about future directions and impact in the field.

ISSN 2223-7755 (print)
ISSN 2224-2759 (online)
DOI 10.7185/geochempersp.2.1

Principal Editor for this issue
Eric H. Oelkers
Reviewer
Sigurður R. Gíslason, University of Iceland

Cover Layout **Pouliot Guay Graphistes**
Typesetter **Info 1000 Mots**
Printer **J.B. Deschamps**

ABOUT THE COVER

The cover illustrates the general schematic of the cycling of carbon on coral reefs owing to primary production, calcification, respiration and $CaCO_3$ dissolution under aerobic conditions. The picture is from a Bermuda coral reef showing coral colonies of *Diploria strigosa* and *D. labyrinthiformis*, and the purple sea fan *Gorgonia ventalina*

Photo credit: Alex Venn, CSM

CONTENTS

DEDICATION

We dedicate this volume to the loving memory of four individuals who had enormous impact on the fields of sedimentary and marine geochemistry and to our knowledge of carbonate biogeochemistry: *Robert M. Garrels, Keith E. Chave, Roland Wollast, and John W. Morse*.

The "giants" who had enormous impact on the field of the geochemistry of sedimentary carbonates: Robert M. Garrels, Keith E. Chave, Roland Wollast, and John W. Morse.

PREFACE

When I (*Fred*) was first contacted to write a monograph for the European Association of Geochemistry series *Geochemical Perspectives* by the Editorial Board of *Liane Benning, Tim Elliott, Eric Oelkers*, and *Susan Stipp*, and strongly encouraged by *Eric* to do so, I was somewhat uncertain as to the expectations of such an article. My original assumption was that it would deal with a scientific issue(s) but would have a personal perspective and insights into what my life as a scientist was like. Because of some surgeries that were not life threatening but disrupting, my writing of the monograph was considerably delayed and by now, several excellent *Perspectives* by outstanding scientists have already been published. So *Andreas Andersson (Andreas)*, my former Ph.D. student now at Scripps Institution of Oceanography and co-author of this volume, and I had the opportunity to see the approaches taken by these authors.

Early in my ruminations, I had decided that because many of my contributions to science were based on friendships and interactions I had with more than 200 co-authors and mentoring of 35 Ph.D.s and 15 M.S. students at Northwestern University and the University of Hawaii that in recognition and affirmation of this "standing on the shoulders of giants", I would ask my last Ph.D. student, *Andreas*, to co-author the article with me, which he happily consented to do. Thus, the story we present here is a little different than that of the previous articles in this series, but perhaps the approach is most similar to Rob Raiswell and Don Canfield's (2012) excellent synthesis of the past and present of the iron biogeochemical cycle in that we often use the first person to enable the story to develop both scientifically and personally. At times we diverge from one another and tell

our personal adventures in the world of science and at other times, especially in the discussion of the behaviour of the carbon cycle and ocean acidification, we converge and emphasise our scientific and personal interactions, which started in the early part of the twenty-first century in the Hawaiian Islands.

The narrative starts with the beginning of *Fred's* career and progresses through some of the major scientific topics that he dealt with during his career and the trials, tribulations, and rewards of engaging in the enterprises of research and education. This is followed by *Andreas'* personal, but obviously much shorter, life perspective to date. We then come together in the major theme of this monograph, that of the co-evolution of the Phanerozoic ocean-atmosphere-carbonate sediment system, with emphasis on the behaviour of the biogeochemical cycle of carbon, the acidification of ocean surface waters, and the future of the carbon cycle. It is a long journey and we hope the reader will enjoy it and stay with us until the end. For those readers who wish to get directly at the scientific "meat" of this *Perspectives* volume, they can proceed directly to Section 3.

Fred T. Mackenzie
Department of Oceanography
School of Ocean and Earth Science and Technology
University of Hawaii at Manoa
Honolulu, Hawaii 96822
USA
http://www.soest.hawaii.edu/oceanography/faculty/mackenzie.html

Andreas J. Andersson
Scripps Institution of Oceanography
University of California at San Diego
La Jolla, California 92093-0202
USA
http://scrippsscholars.ucsd.edu/aandersson/

ACKNOWLEDGEMENTS

We first acknowledge with much gratitude our colleagues *Abraham Lerman, Rolf S. Arvidson*, and *Michael W. Guidry* with whom we have had many discussions concerning some of the topics in this *Perspectives* volume and with whom we have written a number of papers over the years. I (*Fred*) professionally would like to acknowledge *Don Ryan* and *Keith Chave*, my Ph.D. advisors at Lehigh University, for setting me off on the academic track, a path that I have never regretted. *Keith* also encouraged me to depart from working for Shell Oil Company and start my research career at the Bermuda Biological Station for Research. I also would like to acknowledge my colleagues and students at Northwestern University, where as a professor for 16 years, I had an incredible academic experience in daily interchanges about all facets of geochemistry, sedimentology, stratigraphy, geochemical modelling, and the like with *Bob Garrels, Hal Helgeson, Bill Krumbein, Larry Sloss, Larry Nobles, Ed Dapples, Bob Speed, Art Howland, Finley Bishop, Abe Lerman*, and my very talented graduate students, including *Ken Roy, Don Thorstenson, Neil Plummer, Byron Ristvet, Mike Lafon, Sam Upchurch, Len Vacher, Art White, Bill Stuart, Dick Beane, Richard Lantzy, Foster Brown, Jane Schoonmaker, Patricia Egli, Marc Stoffyn, Bill Bischoff, John Pigott, Khosrow Badiozamani, Jim Hill, Rick Arnseth, Cliff Dodge, Steve Smith*, and *Huang Chang*.

It was at Northwestern that I first met *Steve Smith* who, along with *Keith Chave*, was one of the persons who convinced me to move to the University of Hawaii in 1981 and to adopt a pleasant life style living and doing science in 'paradise'. *Steve* and I became close friends and that led to a fruitful research interaction dealing with such topics as the trophic state of the world's oceans, among

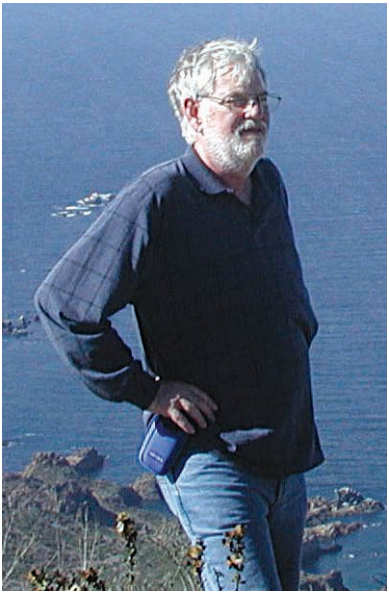

Photo courtesy of Stephen V. Smith.

Figure 1 Stephen V. Smith overlooking the kelp beds near Ensenada, Baja California, Mexico in 2002. Steve has been a pioneering contributor to our knowledge of coral reefs, the ocean carbon cycle, and the biogeochemical behaviour of carbon, nitrogen, and phosphorus in coastal ocean environments. His most recent synthesis contribution is an Association for the Sciences of Limnology and Oceanography (ASLO) e-Book entitled: *Parsing the Oceanic Calcium Carbonate Cycle: A Net Atmospheric Carbon Dioxide Source, or a Sink* (Smith, 2013).

many others, which at times we dealt with in exciting and challenging (to me at least) debates (Fig. 1).

At Hawaii I was blessed by daily interactions with an outstanding faculty and a very productive graduate student body, including, to name just a few faculty, *Steve Smith, Eric De Carlo, Mike Mottl, Tony Clarke, Barry Hubert, Chris Measures, Frank Sansone, Telu Li, Jane Schoonmaker, Richard Zeebe, Jim Cowen, Chris Winn, Klaus Wyrtki, Lorenz Magaard, Ed Laws, Ricky Grigg, Dave Karl, Brian Glazer,* and *Kathleen Ruttenberg. Eric De Carlo* in particular in recent years became a close colleague of mine in studies of air-sea CO_2 exchange and the problem of ocean acidification (Fig. 2).

My graduate students at the University of Hawaii included *Steve Dollar, Miriam Bertram, Chris Sabine, Michael Guidry, Somasundar Krothapalli, Catherine Agegian, Josef Urmos, Lynn Miller, Dan Sadler, Rolf Arvidson, May Ver, Katsumasa Tanaka, Stephanie Ringuet, Kathryn Fagan, Dan Hoover,* and *Andreas Andersson,* all of whom contributed to a superb and intellectually very dynamic academic atmosphere and have gone on to important careers of their own. It is amazing to me how all the people mentioned here and others have come to shape me as a scientist and a person. It is their shoulders I stand on! I would also like to acknowledge my extended family, who always offered me encouragement over the years and put up with my endless hours in the office, at the computer, and in the laboratory. I especially would like to thank my wife *Judy* for her love and support, and my son *Scott*, daughter *Michele,* and stepdaughter *Deborah* for standing by me throughout the years.

Photo courtesy of Eric De Carlo.

Figure 2 Eric De Carlo (in blue shirt) hooking one of the buoys equipped with instrumentation to measure atmospheric and surface ocean water CO_2 and a variety of biogeochemical parameters in Kanoehe Bay, Hawaii, USA. Several of these buoy platforms are operative in coastal waters around Oahu, Hawaii. The work is done in cooperation with the Pacific Marine Environmental Laboratory of the National Oceanic and Atmospheric Administration in the USA.

I (*Andreas*) would like to thank *Fred* for inviting me to co-author this *Perspectives* article, which I consider a great honour. I especially would like to acknowledge *Fred* for the eminent guidance, support, and friendship he has provided me since the day I started graduate school at the University of Hawaii (UH) and until my current capacity as Assistant Professor at the Scripps Institution of Oceanography. Not only have I learned a tremendous deal about science from *Fred*, but he has also served as a major role model in his ways of teaching, mentoring, life philosophy, and the way he interacts and treats other people. On top of everything, it has been (and still is) a great deal of fun to work with *Fred* (Fig. 3)! I also would like to acknowledge *Chris Winn* and *Varis Grundmanis* at the Hawaii Pacific University for opening my eyes to the field of oceanography; *Yuan-Hui Li* (*Telu*), *Jane Schoonmaker, Craig Glenn, Richard Zeebe*, and *Ed Laws* for guidance during my time at UH; Nicholas Bates for giving me the opportunity to explore the North Atlantic and the coral reefs of Bermuda; *Ilsa Kuffner, Paul Jokiel, Ku'ulei Rodgers, Dwight Gledhill, Sam DePutron, Andrew Collins, Kyra Freeman, Alex Venn, Eric Tambutte, Aline Tribollet, David Kadko, Chris Langdon, Alyson Venti, Chris Sabine, Jean-Pierre Gattuso, Joanie Kleypas, Anne Cohen, Frank Sansone, Eric De Carlo, May Ver, Abe Lerman, Rolf Arvidson, Mike Guidry, Scott Doney, Ken Anthony, Todd Martz, Andrew Dickson*, and *Mario Lebrato* for past and ongoing research collaborations and interactions. I also would like to acknowledge many of my

ocean acidification colleagues around the world whom I have interacted with one way or the other and especially the members of *No-aa*. Finally, I would like to thank all my past and current students, interns, and volunteers for their curiosity, enthusiasm, and hunger to learn, which I find tremendously rewarding.

Figure 3 The Mackenzie lab anno 2001 following Michael Guidry's successful Ph.D. dissertation defense. From left to right: Dan Hoover, May Ver, Jane Schoonmaker, Michael Guidry, Fred Mackenzie, Stephanie Ringuet, and Andreas Andersson.

Finally, we are extremely grateful to our principal editor *Eric Oelkers* who was very patient in terms of receiving this article and helped to improve the first version with insightful comments. Mahalo nui loa to *Siggi Gislason* (University of Iceland) for his review and extensive and helpful comments on the manuscript and *Rob Raiswell* (University of Leeds) for the thorough copy-editing. Our editorial manager *Marie-Aude Hulshoff* was exceptional in keeping us on track toward our finished manuscript and providing support in our efforts. *Juan Diego Rodriguez Blanco* (University of Copenhagen) is thanked for the excellent coloration of the figures and for redrawing many of the figures. Although there was no direct financial support of this work from U.S. agencies, the project required resources and we thank the U.S. National Science Foundation, the American Chemical Society Petroleum Research Foundation, and the National Oceanic and Atmospheric Administration for the funding of our research efforts over these many years.

THE MARINE CARBON SYSTEM AND OCEAN ACIDIFICATION DURING PHANEROZOIC TIME

ABSTRACT

The global CO_2-carbonic acid-carbonate system of seawater, although certainly a well-researched topic of interest in the past, has risen to the fore in recent years because of the environmental issue of ocean acidification (often simply termed OA). Despite much previous research, there remain pressing questions about how this most important chemical system of seawater operated at the various time scales of the deep time of the Phanerozoic Eon (the past 545 Ma of Earth's history), interglacial-glacial time, and the Anthropocene (the time of strong human influence on the behaviour of the system) into the future of the planet. One difficulty in any analysis is that the behaviour of the marine carbon system is not only controlled by internal processes in the ocean, but it is intimately linked to the domains of the atmosphere, continental landscape, and marine carbonate sediments.

For the deep-time behaviour of the system, there exists a strong coupling between the states of various material reservoirs resulting in an homeostatic and self-regulating system. As a working hypothesis, the coupling produces two dominant chemostatic modes: (Mode I), a state of elevated atmospheric CO_2, warm

climate, and depressed seawater Mg/Ca and SO_4/Ca mol ratios, pH (extended geologic periods of ocean acidification), and carbonate saturation states (**Ω**), and elevated Sr concentrations, with calcite and dolomite as dominant minerals found in marine carbonate sediments (Hothouses, the calcite-dolomite seas), and (Mode II), a state of depressed atmospheric CO_2, cool climate, and elevated seawater Mg/Ca and SO_4/Ca ratios, pH, and carbonate saturation states, and low Sr concentrations, with aragonite and high magnesian calcites as dominant minerals found in marine carbonate sediments (Icehouses, the aragonite seas).

Investigation of the impacts of deglaciation and anthropogenic inputs on the CO_2–H_2O–$CaCO_3$ system in global coastal ocean waters from the Last Glacial Maximum (LGM: the last great continental glaciation of the Pleistocene Epoch, 18,000 year BP) to the year 2100 shows that with rising sea level, atmospheric CO_2, and temperature, the carbonate system of coastal ocean water changed and will continue to change significantly. We find that 6,000 Gt of C were emitted as CO_2 to the atmosphere from the growing coastal ocean from the Last Glacial Maximum to late preindustrial time because of net heterotrophy (state of gross respiration exceeding gross photosynthesis) and net calcification processes. Shallow-water carbonate accumulation alone from the Last Glacial Maximum to late preindustrial time could account for ~24 ppmv of the ~100 ppmv rise in atmospheric CO_2, lending some support to the ''coral reef hypothesis''. In addition, the global coastal ocean is now, or soon will be, a sink of atmospheric CO_2, rather than a source. The pH_T (pH values on the total proton scale) of global coastal seawater has decreased from ~8.35 to ~8.18 and the CO_3^{2-} ion concentration declined by ~19% from the Last Glacial Maximum to late preindustrial time. In comparison, the decrease in coastal water pH_T from the year 1900 to 2000 was ~8.18 to ~8.08 and is projected to decrease further from about ~8.08 to ~7.85 between 2000 and 2100. During these 200 years, the CO_3^{2-} ion concentration will fall by ~ 45%. This decadal rate of decline of the CO_3^{2-} ion concentration in the Anthropocene is 214 times the average rate of decline for the entire Holocene!

In terms of the modern problem of ocean acidification and its effects, the "other CO_2 problem", we emphasise that most experimental work on a variety of calcifying organisms has shown that under increased atmospheric CO_2 levels (which attempt to mimic those of the future), and hence decreased seawater CO_3^{2-} ion concentration and carbonate saturation state, most calcifying organisms will not calcify as rapidly as they do under present-day CO_2 levels. In addition, we conclude that dissolution of the highly reactive carbonate phases, particularly the biogenic and cementing magnesian calcite phases, on reefs will not be sufficient to alter significantly future changes in seawater pH and lead to a buffering of the CO_2-carbonic acid system in waters bathing reefs and other carbonate ecosystems on timescales of decades to centuries. Because of decreased calcification rates and increased dissolution rates in a future higher CO_2, warmer world with seas of lower pH and carbonate saturation state, the rate of accretion of carbonate structures is likely to slow and dissolution may even exceed calcification. The potential of increasing nutrient and organic carbon inputs from land, occurrences of mass bleaching events, and increasing intensity (and perhaps frequency of hurricanes and cyclones as a result of sea surface warming) will only complicate

matters more. This composite of stresses will have severe consequences for the ecosystem services that reefs perform, including acting as a fishery, a barrier to storm surges, a source of carbonate sediment to maintain beaches, and an environment of aesthetic appeal to tourist and local populations. It seems obvious that increasing rates of dissolution and bioerosion owing to ocean acidification will result in a progressively increasing calcium carbonate ($CaCO_3$) deficit in the $CaCO_3$ budget for many coral reef environments. The major questions that require answers are: will this deficit occur and when and to what extent will the destructive processes exceed the constructive processes?

1. INTRODUCTION

The global CO_2-carbonic acid-carbonate system of seawater, although certainly a well-researched topic of interest in the past (see *e.g.*, Zeebe, 2012b and references therein), has risen to the fore in recent years because of the environmental issue of ocean acidification (OA, defined as an increase in the hydrogen ion concentration, or decrease in pH, of seawater). Despite much previous research, there remain pressing questions about how this most important chemical system of seawater operated at the various time scales of the deep time of the Phanerozoic Eon, interglacial-glacial time, and the Anthropocene into the future of the planet. One difficulty that arises is that internal processes in the ocean do not alone control the behaviour of the marine carbon system, but its behaviour is intimately linked to the domains of the atmosphere, continental landscape, and marine carbonate sediments. Thus, we contend that to understand the system requires an holistic approach based not only on observational and experimental information but also modelling activities that can integrate across the various domains. This is the overall approach that we attempted to use in this *Geochemical Perspectives* monograph.

After a short foray through the journeys that have led us (Fig. 2.1) to the present stage of our scientific careers, we discuss the Phanerozoic (the past 545 Ma of Earth history) compositional history of the coupled system of atmosphere, ocean, and carbonate sediments with emphasis on the global biogeochemical cycle of carbon. We then continue our tour through the geologic time of the carbon system by investigating the impacts of deglaciation and anthropogenic inputs on the CO_2–H_2O–$CaCO_3$ system in global coastal ocean waters from the Last Glacial Maximum (LGM: 18,000 years BP) to the year 2100. This time scale includes the Anthropocene, the period of major human intervention in the Earth's surficial system, and the modern environmental problem of ocean acidification, the so-called "other CO_2 problem". At all these various time scales, the global CO_2-carbonic acid-carbonate system of the ocean is shown to respond to and feedback into the behaviour of the other major Earth surface domains, and that the compositional changes in the system affect and respond to changes in the nature of the biogenic and abiotic carbonate mineral precipitates from seawater.

2. OUR SCIENTIFIC JOURNEYS

Photo courtesy of Fred Mackenzie and Andreas Andersson.

Figure 2.1 Fred Mackenzie and Andreas Andersson on the summit of Mauna Kea (4,205 m, 13,796 ft), Big Island of Hawaii, Hawaii, USA, the tallest mountain in the world from seafloor to summit.

2.1 Fred's Journey

I was ambivalent about my early career decision: mountaineering or geophysics? After climbing all the major peaks in the eastern USA, I had already hitch-hiked by the time I finished high school in 1952 across the country three times to get to mountains in the Rockies, Sierras, and Cascades and to a failed attempt on the West Buttress route of Denali (Mount McKinley) in Alaska. It was my mother, *Bessie Mackenzie,* who convinced me that mountaineering could be an avocation and that returning to school after my service in the U.S. Army to complete my bachelor's degree in physics and geology was the path to follow. That in turn was my passport to adventure enabling me to start work in the oil patch from backing pipe to exploration geologist with the Shell Oil Company during my

summers away from the halls of academe. It also was my introduction to the wonderful world of carbonate sediments in that to earn enough money to get through my early years of college, I sat a diamond drill rig for a cement company in the highlands of New Jersey, USA. This involved sitting the rig, recording the stratigraphic section, boxing the cores, and rushing them back to campus at Lehigh University in Bethlehem, Pennsylvania, USA for analysis and evaluation as limestone rock suitable for making cement. I finally received my doctoral degree at Lehigh University in geology and geochemistry in 1962 after a brief stint at Johns Hopkins University, which had been interrupted by another tour of duty in the U.S. Army. It was at Lehigh University where I first met my Ph.D. thesis advisors, *Donald Ryan* and *Keith Chave*, the latter had only recently joined the faculty at Lehigh after working for Chevron Oil Company in the State of California, USA. It was *Keith* who would lead me by his powers of persuasion away from the field of sedimentology – a palaeocurrent study of the Cretaceous rocks of the western interior of the U.S. was the subject of my Ph.D. dissertation – and into geochemistry. I was privileged during my last year in graduate school to write my first paper in geochemistry with *Keith* as co-author (Chave and Mackenzie, 1961). The paper was written at a time when the distribution of major and trace chemical elements in the mineral phases of pelagic muds was largely unknown or at least problematic. *Keith* and I employed a statistical technique originally proposed for biometric work, that of correlation and partial correlation analysis, to eke out elemental groups formed by the correlation analysis. Later research efforts using this technique and more data than available to us at the time were able to arrive at general conclusions related to the distribution, mechanisms of deposition, and sources of the elemental constituents of pelagic muds. Thus began my professional career in science in 1962.

Following completion of my Ph.D., I went to work for Shell Oil Company as an Exploration and Research Geologist. Interestingly, two of my assignments at the time involved studies of the stratigraphy and structure (Shell had shot innumerable seismic lines across the Appalachian Basin from the continental interior through the folded Appalachians to the coastal plain from New York State south to Georgia, USA) of Ordovician carbonates as targets for oil exploration and of the Devonian Marcellus Shale, which in recent years has become a horizon for gas production by fracking and a subject of strong environmental concern. Then in 1963, I accepted a position as Staff Geochemist and Assistant Director at the Bermuda Biological Station for Research (BBSR, now the Bermuda Institute of Ocean Sciences), and my research career in geochemistry, with a foot both in geology and oceanography, finally took off. At that time there were three scientists, including me, and a handful of staff at the station who would keep each other company during the cool, often grey, windy, humid winters. The Institute now has a staff of more than 75 people.

One of my tasks at BBSR was to manage Hydrostation S, the longest continuously occupied hydrostation in the world. The summers were very pleasant going to sea but in the winter in the North Atlantic, it was a different matter and I was seasick every two weeks! At Bermuda my initial research involved the

Pleistocene history of sea level and palaeowind directions of limestones exposed on the Bermuda islands and the diagenesis of the limestones as deduced from their stratigraphic, sedimentologic, and geochemical features. I had the distinct privilege of working on these issues doing field studies with *Lynton S. Land* and *Stephen Jay Gould*, who were graduate students at the time. From investigation of the characteristics of the Pleistocene marine and aeolian carbonates of the Bermuda Islands, we were able to untangle a Late Pleistocene sea level curve and develop a diagenetic pathway of major importance for the stabilisation of carbonate sediments, consisting initially of a melange of metastable carbonate mineral phases, to limestone in meteoric waters (Fig. 2.2).

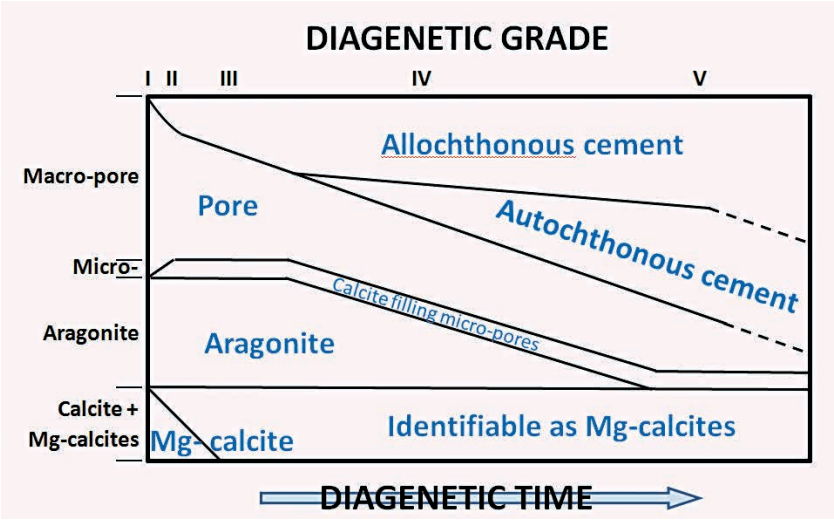

Figure 2.2 Schematic diagram of vadose (above permanent water table) and phreatic (below permanent water table and bathed in fresh or seawater) meteoric diagenesis in terms of percent composition of minerals, porosity, and cement versus time increasing to the right (modified from Land *et al.*, 1967). This interpretation of the pattern of meteoric diagenesis versus age of an initial carbonate sediment containing a mélange of carbonate mineral compositions stabilised to a calcite limestone still holds today.

In Bermuda I also began work on the problem of the physical and biogeochemical controls on the concentration and distribution of dissolved strontium in seawater. This work showed that strontium is not a completely conservative element in seawater but at mid-depth in the North Atlantic exhibits a maximum in concentration caused by the dissolution of the very soluble $SrSO_4$ (the mineral celestite) skeletons of sinking Acantharia protozoa (Fig. 2.3). However, this work, which involved time-consuming atomic absorption spectrometry, also convinced me that I was not born to be an analytical geochemist and I peaked at being so

very young! Nevertheless, it also initiated and stimulated my interests in the field of oceanography and ever since I have had my feet in two major fields of research and teaching: geology/geochemistry and oceanography.

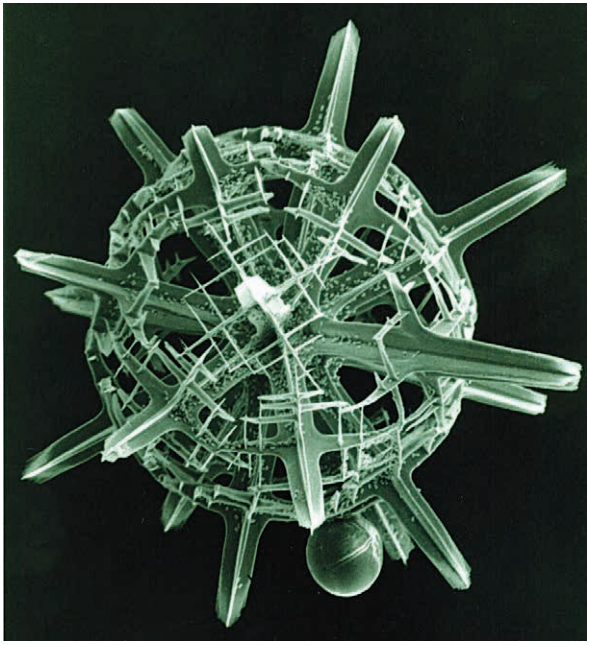

Figure 2.3 Photomicrograph of a skeletal $SrSO_4$ (the mineral celestite) Acantharia protozoan presented to Fred Mackenzie by Renate Bernstein at one of his Distinguished Lectureships at the College of Marine Science, University of South Florida, St Petersburg, Florida, USA.

It was at BBSR that I would meet many of the individuals who would have a major impact on my career in science and who would become close friends and research collaborators. The Director at the time, *Bill Sutcliffe*, was a strong supporter of mine and gave me ample time to do research supported by the U.S. Office of Naval Research and the National Science Foundation. I first met *Bob Garrels* at the Station in 1962. Our collaboration was spontaneous from the moment we met, and from then until *Bob's* untimely death in 1988, we carried on research blending geochemistry, sedimentology, and elemental mass balances in attempts to interpret the sedimentary record in terms of changes in the Earth's near-surface environment (its exogenic system or ecosphere). It should be mentioned that not only did *Bob* and I do research together but we were also fairly competitive athletes. In high school and college, we both played sports and this "love of the game" carried on into later life. I had always had mountaineering and running as avocations and *Bob* continued his gymnastics and playing

tennis, which I participated in with him. In Bermuda we would swim for long distances across the lagoon into the open ocean and *Bob* would time me as I ran 440s around the Biostation parking lot. We also set up an athletic committee (Bermuda Biological Station Athletic Committee, BBSAC) that included at one time or another such notables as *Bob Berner, John Morse, Owen Bricker,* and *John Frantz*, which governed competitive competitions at the Biostation. For every swimming lap of about 100 metres completed, the "athlete" would receive one gin and tonic! Thus, *Bob's* and my relationship was not all work but a great deal of play. Indeed, when we first considered the global phosphorus cycle in our research, *Bob* wrote the little ditty:

"I put some P into the sea the biomass did swell
But settling down soon overcame and P went down toward Hell
From purgatory soon released it moved up to the land
To make a perfect rose for thee to carry in thy hand
But roses wilt and die you know then P falls on the ground
Gobbled up as ferric P a nasty brown compound
The world is moral still you know and Nature's wheels do grind
Put ferric P into the sea and a rose someday you'll find."

Bob's and my initial cooperative research in Bermuda involved the experimental dissolution of aluminosilicate minerals in seawater in which we demonstrated that these minerals are rapidly reactive in seawater mainly through dissolution. These experiments laid the basis for our hypothesis of "reverse weathering", in which some portion of the very degraded weathering products on land, when transported to the marine environment, react to form newly formed marine minerals removing cations and dissolved silica from seawater. Although we published papers on this issue in the mid- and late-1960s (*e.g.*, Mackenzie and Garrels, 1966a,b), because of the strong appeal at the time of basalt-seawater chemical reactions as sinks for the elements in the ocean, it was not until field work by my students *Byron Ristvet, Don Thorstenson*, and *Richard Leeper*, and I in Kaneohe Bay, Hawaii, USA in the 1970s and later by Michalopoulos and Aller (1995) on the Amazon shelf of Brazil demonstrated unequivocal field evidence of reverse weathering reactions involving neoformed sedimentary minerals (minerals newly formed near the sediment-water interface and during shallow burial) as sinks for potassium, magnesium, iron, and silica that the hypothesis gained credence. The generalised theoretical reverse weathering reaction we first considered was:

$$\text{Amorphous aluminosilicate} + \text{cations Mg, K, Na} + SiO_{2aq} + HCO_3^- = \text{cation-rich aluminosilicate} + CO_2 + H_2O, \quad (2.1)$$

but Ristvet (1971), Mackenzie *et al*. (1981), and Michalopoulos and Aller (1995) in field studies showed that the reactions, although occurring and accounting for cation removal, were more varied and complex in nature.

At about the same time that *Bob Garrels* and I were working on the hypothesis of reverse weathering, we also developed a model for the origin of the chemical composition of freshwater springs and lakes using the waters associated with the Sierra Nevada granites of the USA as an illustration of the processes involved (Garrels and Mackenzie, 1967). The studies of reverse weathering and the origin of the composition of freshwaters encouraged my belief, probably an outcome of my original training in physics, that observations must go hand in hand with theory and modelling for a fundamental understanding of Earth's systems.

At Bermuda, I also met *Roland Wollast* and *Hal Helgeson*, both of whom were to influence me in different ways. *Roland* shared his experimental and kinetic expertise with me, enabling my graduate students and I to do thoughtful and careful experiments on the thermodynamics and kinetics of important sedimentary mineral groups, including calcite, aragonite, magnesian calcites, dolomite, and carbonate fluorapatite (Fig. 2.4). For example, in the years to follow, my Ph.D. student *Art White* (1977, 1978) would study Na and K coprecipitation in aragonite and Na coprecipitation in calcite and dolomite. Ph.D. students *Neil Plummer, Don Thorstenson, Bill Bischoff*, and *Miriam Bertram* would work out the stabilities of the abiotic synthetic and the biogenic magnesian calcite phases [$CaCO_3$ rich in Mg; Plummer and Mackenzie, 1974; Thorstenson and Plummer, 1977; Bischoff *et al*., 1987; Bertram *et al*., 1991]. Eventually we would demonstrate that not only did the magnesium content of these phases determine their solubility but also carbonate ion disorder and trace constituent composition. For the same magnesium content, abiotic magnesian calcite phases have lower solubilities than their biogenic counterparts because of the structural and chemical differences between their

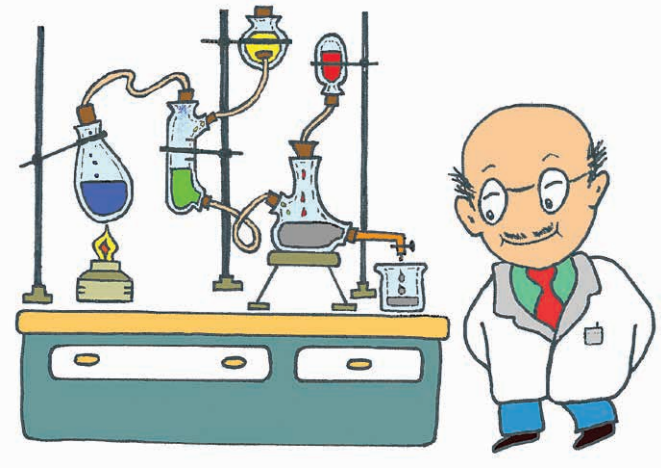

Figure courtesy of Judy Mackenzie.

Figure 2.4 Cartoon of one of Mackenzie's students in the laboratory already showing signs of baldness due to the exciting, but at times exasperating, work of studying mineral-solution reactions in the laboratory.

mineral compositions (see Supplementary Information SI-1). Based on the original experimental composition versus stability curve of Plummer and Mackenzie (1974), *Don Thorstenson* and *Neil Plummer* went on to develop the theory of stoichiometric saturation as applied to the calcite minerals (Thorstenson and Plummer, 1977). This theory is still controversial today (see Garrels and Wollast, 1978; Morse *et al.*, 2006) but in practice remains the *modus operandi* for evaluation of the saturation state of natural waters with respect to the magnesian calcites.

With respect to dolomite, *Rolf Arvidson* was able to synthesise this mineral experimentally at low temperatures down to 60 °C and demonstrate that saturation state and temperature play a major role in the rate of formation of the mineral (Fig. 2.5; Arvidson and Mackenzie, 1997, 1999). This was a yeoman experimental effort and tour de force of *Rolf's* because of the difficulty of maintaining exacting experimental conditions and the relative slowness of the dolomite precipitation process. The work enabled us to conclude that given the right environmental conditions, and lessened competition from other carbonate phases for aqueous components, that the mineral was not as recalcitrant to precipitate at lower temperatures as originally thought. We felt that organogenic and sabkha dolomites, and given the right environmental setting, shelf dolomites in general were not that unusual from a kinetic standpoint. This work forms part of the evidence for the cyclic nature of dolomite in the Phanerozoic sedimentary record discussed later.

Michael Guidry's study of the kinetics of igneous and sedimentary carbonate fluorapatite (CFA, a calcium phosphate mineral containing fluorine and carbonate) precipitation was even more of a nightmare than the work on dolomite. After several botched approaches, *Michael* gave up on attempts to synthesise this sedimentary phase over the range in composition of natural samples because of the difficulty in maintaining constant solution chemistry in the fluidised bed reactor used for precipitation purposes. Thus, we decided to evaluate the rate of dissolution, and the mechanism(s) controlling the rate, of a range of apatite compositions, including sedimentary carbonate fluorapatite. This proved amenable experimentally and *Michael* was able to show that the dissolution rate depends strongly on pH and temperature and that dissolution was a

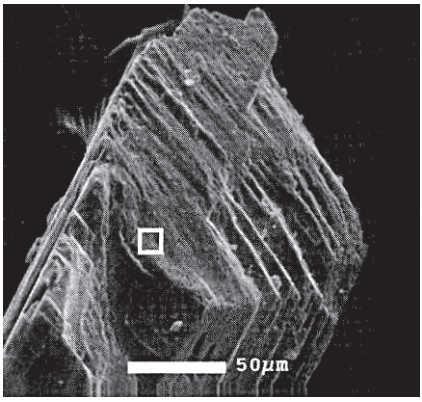

Figure 2.5 Photomicrograph of epitaxial dolomite growing on a dolomite seed at a temperature of 60 °C (after Arvidson and Mackenzie, 1999).

surface controlled reaction. From the experimental results, we were able to develop a simple weathering model and a global biogeochemical cycle of phosphorus (Fig. 2.6) showing that both the surface area of igneous rock available

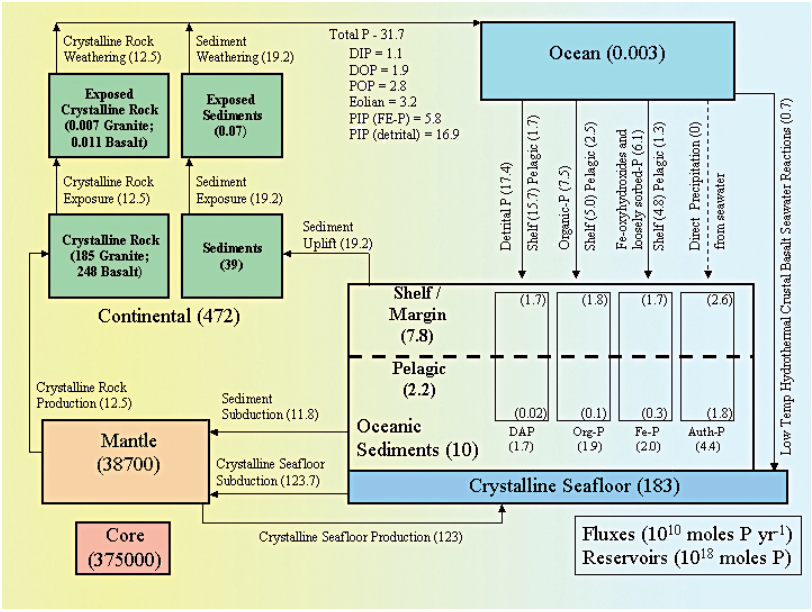

Figure 2.6 Global biogeochemical cycle of phosphorus including both the exogenic (continental crust, ocean, and sediments) and endogenic fluxes (mantle and seafloor basalt).

and the average global temperature were important controlling factors in determining the flux of dissolved phosphorus to the ocean during the Phanerozoic Eon (Guidry and Mackenzie, 2003) and hence bioproductivity in the ocean. This work also has implications for the environmental problems of acid rain and global climatic change. In regions of acid rainfall, particularly on crystalline terrain, the increased acidity of the rain increases the weathering rate of phosphorus-bearing minerals in the soils and bedrock. As atmospheric CO_2 and other greenhouse gases continue to rise and the temperature increases, the rate of weathering of phosphate minerals will increase, even on the centennial time scale.

Returning to Bermuda and early associations with colleagues, *Hal Helgeson* convinced me of the importance of theoretical geochemistry in the solution of problems involving sediments and sedimentary rocks. Indeed, it was on a roll out of computer paper at BBSR that the papers to appear in *Geochimica et Cosmochimica Acta* (Helgeson, 1968; Helgeson *et al.*, 1969) dealing with the evaluation of irreversible thermodynamics in geochemical processes were first worked out

– *Hal* doing theory and *Bob Garrels* and I applications. *Hal* and I even tried to apply equilibrium thermodynamics to silicate-seawater equilibria in the ocean. We evaluated the stability fields of aluminosilicate minerals (including a mixed-layer illite-montmorillonite solid solution formed by interlayers of potassium-rich aluminosilicate and sodium-, calcium-, and magnesium-rich aluminosilicate) in a nine-component model of the ocean system and showed that they can be depicted on isothermal-isobaric activity diagrams in terms of pH and the logarithm of the activity of dissolved silica (Fig. 2.7; Helgeson and Mackenzie, 1970). Following *Lars Gunnar Sillén's* lead (Sillén, 1967), we felt that quantitative consideration of equilibria in the present ocean would provide a frame of reference for investigation of the chemical evolution of seawater and the mass transfer of chemical constituents involved in silicate-sea water reactions through geologic time. This in part proved true but our solid solution model for illlite-montmorillonite was later shown to be too simple. In addition after this work, equilibrium models of the ocean were disbanded and kinetic and material balance models of input and output fluxes involving the ocean reservoir were found to be more rewarding approaches to an understanding of the evolution of seawater (*e.g.*, Broecker, 1971; Mackenzie, 1975).

While working at BBSR and for many summers thereafter, besides my research enterprise, I taught classes in organism-sediment interactions, the carbon cycle and carbonate biogeochemistry, and global change. Probably over the years, at least a few hundred undergraduate and graduate students from a number of countries of the world took part in these courses. It was always a great deal of intellectual stimulation and fun working with these students, especially seeing how quickly they adjusted to a steep learning curve of lectures, field and laboratory studies, scrounging up equipment and supplies, and long days and nights. The latter was true for me also! It was a delightful experience and I am pleased to say that many of these students went on to successful scientific careers of their own. It was in one of these courses that I met *Chris Sabine*, who would become one of my Ph.D. students and study a subject relevant to the topic of this monograph, that of the dissolution of carbonate sediments transported offshore of shallow-water banks in the Hawaiian Archipelago (Sabine and Mackenzie, 1995). He also made some of the initial carbon chemistry measurements for the Hawaii Ocean Time-series program (HOT) at the deep-water station ALOHA (A Long-term Oligotrophic Habitat Assessment) 100 km north of Oahu, Hawaii (see Fig. 9.7). *Chris* is now Director of the Pacific Marine Environmental Laboratory of the National Oceanographic and Atmospheric Administration (NOAA) in the USA.

It seems appropriate to end my story of Bermuda with an experience that has direct application to part of the theme of this monograph, that of the environmental issue of modern ocean acidfication and its effects on reef cacifying organisms. Along with *Bob Ginsburg* of the Rosentiel School of Marine and Atmospheric Science, University of Miami, USA, and *Gene Shinn* of the St. Petersburg Coastal and Marine Science Center of the United States Geological Survey, I was part of a group that in the late 1960s (and with Bermuda government permission)

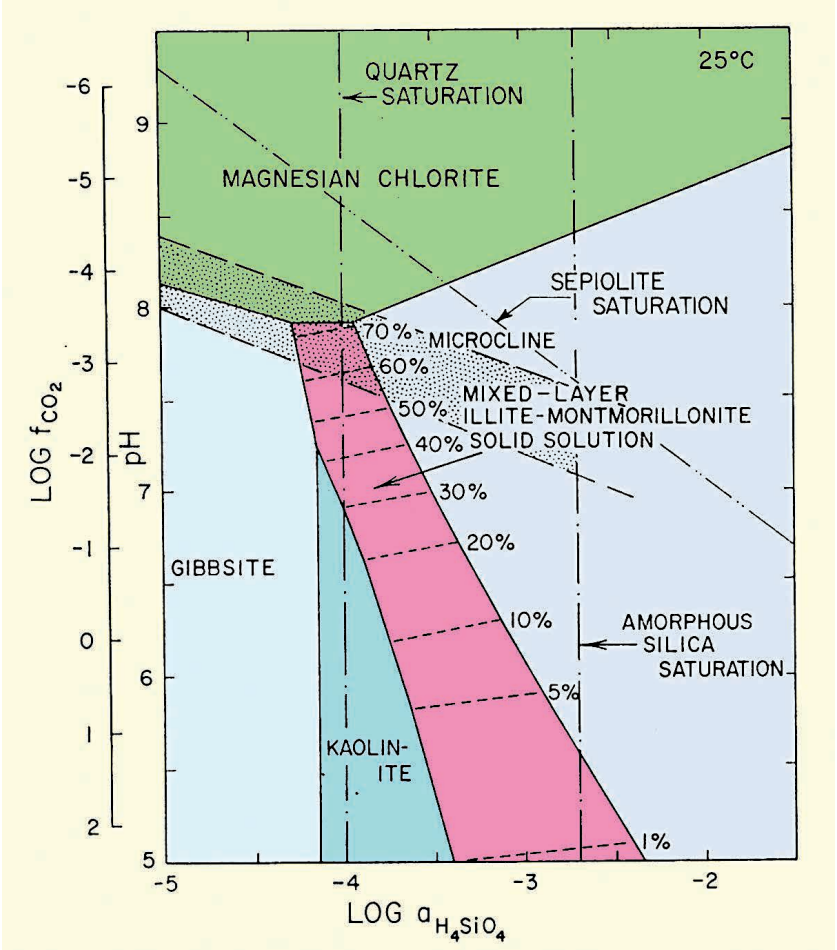

Figure 2.7 pH-dissolved silica diagram in the four component chemical system K_2O-Al_2O_3-SiO_2-H_2O at 25 °C and 1 atm showing the stability fields of important marine mineral compositions and the realm of seawater composition (stippled area) (modified from Helgeson and Mackenzie, 1970). The fact that the range of seawater composition covers the stability fields of important marine minerals led some investigators to conclude that the composition of seawater is not far from that predicted based on an equilibrium model of the seawater-atmosphere-marine mineral system.

dynamited and cracked open a small cup reef on the northern lagoonal fringe of the Bermuda platform to study its vertical succession of biological communties, internal texture and structure, and cementation. Instantly sharks were attracted

and started to swarm about the reef. Needless to say we stopped our diving activities! What was very surprising to discover at that time was that very close to the top of the growing part of the reef, the reef was cemented tight by aragonite ($CaCO_3$) and high Mg-calcite (calcite high in magnesium) cements and "hard as a rock". As our oceans continue to acidify, we will demonstate later in this article that it is this solid edifice composed of growing corals, coralline algae and other organisms, infilling carbonate skeletal debris, and inorganic and biologically produced carbonate cements that is threatened by ocean acidification to the extent that in the future, these coral reef structures may no longer be viable biological communities.

In 1967 I joined the faculty at Northwestern University where *Bob Garrels* and I continued our cooperation and research collaborations with *Hal Helgeson* and *Abe Lerman*. I recall that early in my tenure there, *Bob, Hal*, and I went with a group of graduate students to the Upper Peninsula of Michigan to study the 1.9 Ga year old Biwabik Iron Formation. It did not take long to recognise from the sedimentological characteristics, such as rip up clasts and ooids, of these iron-rich deposits that they were deposited in the shallow waters of a Precambrian aquatic environment. This led us to develop on the outcrop a geochemical model of their formation and to sketch in the field logarithmic activity-activity stability diagrams involving solid phases of iron as related to aqueous components. The students were mightily impressed at the activities of their professors! This activity actually eventually led to publication of a paper on the iron formations by *Bob, Ed Perry*, and me on their origin, depositional history, and diagenesis (Garrels *et al*., 1973).

Early in the 1970s, *Bob* and I published two books, which were to set the stage for much of the rest of my career. One was entitled *Evolution of Sedimentary Rocks* (1971) (Fig. 2.8a) and the second *Chemical Cycles and the Global Environment: Assessing Human Influences* (1975; *Cynthia Hunt* was also a co-author of this book) (Fig. 2.8b). The former book has had a major influence on those scientists interested in the chemical recycling of sediments through the processes of weathering and dissolution, erosion, transportation, sedimentation, burial, and diagenesis, followed by uplift to begin the cycle anew. This circulation of materials is known as the exogenic cycle. The book revived the original concepts of *James Hutton*, which, except for the works of *Willem Van Nieuwenkamp* and *Tom Barth* in the 1950s and 1960s, had lain dormant for more than 150 years. The latter book contained the first attempt at a quantitative representation of the sedimentary rock cycle (Fig. 2.9), which would form, in part, the basis for the Berner, Lasaga, and Garrels (1983) BLAG model of atmospheric CO_2. The book also described in detail how human activities are affecting the global biogeochemical cycles of carbon, nitrogen, sulphur, phosphorus, and selected trace metals like mercury. The fundamental approaches found in these books, abetted by numerical modelling of the Earth's surface environmental system through geological time, are still a major part of my research and teaching programmes today.

Figure 2.8 Book jackets of **(a)** *Evolution of Sedimentary Rocks* by Garrels and Mackenzie (1971); **(b)** *Chemical Cycles and the Global Environment: Assessing Human Influences* by Garrels, Mackenzie, and Hunt (1975); **(c)** *Our Changing Planet: An Introduction to Earth System Science and Global Environmental Change* by Mackenzie (editions of 1998, 2003, 2011); **(d)** *Geochemistry of Sedimentary Carbonates* by Morse and Mackenzie (1990); and **(e)** *Carbon in the Geobiosphere: Earth's Outer Shell* by Mackenzie and Lerman (2006).

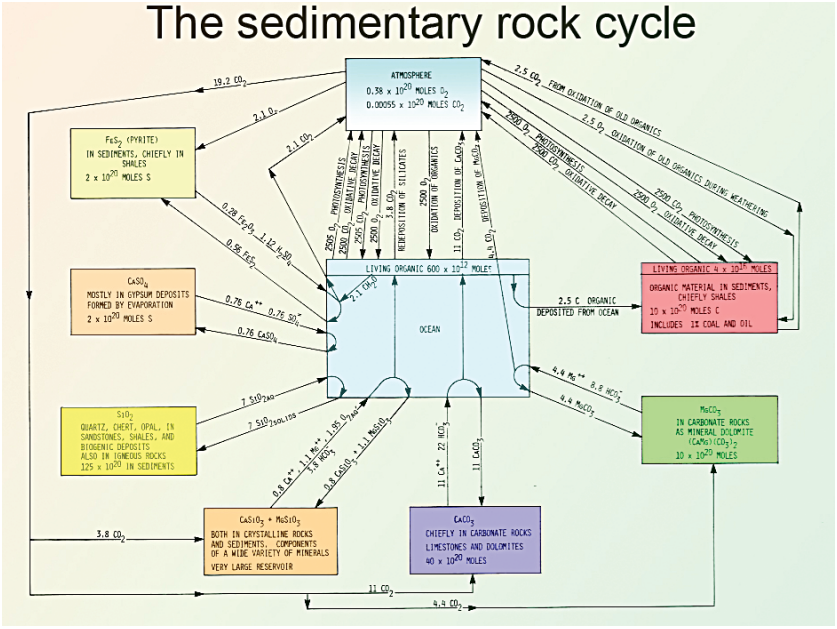

Figure 2.9 The sedimentary rock cycle of reservoirs and fluxes as it appeared in the book *Chemical Cycles and the Global Environment: Assessing Human Influences* by Garrels, Mackenzie, and Hunt (modified from Garrels *et al.*, 1975).

I should mention at this stage that the teaching enterprise, both at the graduate and undergraduate levels, has been an important focus of my career. I have always enjoyed both teaching and research. The books mentioned above were written around courses that *Bob Garrels* and I taught initially at the undergraduate level but because of their unique approaches were later used in graduate level courses and even as general reading material by professional scientists. My last book to date *Our Changing Planet: An Introduction to Earth System Science and Global Environmental Change* (Fig. 2.8c) is also an undergraduate text dealing with the history of our planetary ecosphere, its biogeochemical cycles, and human interference in those cycles resulting in human-induced environmental change, including climatic change, within the newly named Anthropocene Epoch.

It was at Bermuda that I first met *John Morse* of Texas A&M University, then a student of *Bob Berner,* and *Bob Berner* himself, then at Yale University. *John* and I continued an active research collaboration until his untimely death in 2009, culminating in the publication of our book *Geochemistry of Sedimentary Carbonates* in 1990 (Figure 2.8d). This book followed that of *Robin Bathhurst's* classic volume of 1974, *Carbonate Sediments and their Diagenesis*, and was a synthesis work devoted to the solid phase and aqueous biogeochemistry of the sedimentary carbonates, including their role in the climatic change issues of the geologic past and present. *Bob Berner* and I have spent many years discussing scientific problems and recently co-authored a paper for a Special Issue of *Aquatic Geochemistry* honouring *John Morse's* life and career. We are currently working on another honouring the life and career of *Owen Bricker.* As an aside, *Bob Berner* and his wife *Betty* spent many spring times here in the Hawaiian Islands enjoying the beauty and weather of the islands and visiting me.

Sadly, my first five professional colleagues and close friends who had major influences on my career have all passed on: *Keith, Bob, Roland, Hal*, and *John*. However, their remarkable contributions to the field of geochemistry are not forgotten.

Abe Lerman at Northwestern University and I began our fruitful research interaction and friendship in the early 1970s that continue to this day. One of our more recent efforts was publication of the book *Carbon in the Geobiosphere – Earth's Outer Shell* in 2006 (Fig. 2.8e). This book is an overview of the origins and behaviour of the carbon and nutrient biogeochemical cycles and atmospheric carbon dioxide and their fate under human influence. As such it represents a systems approach to the biosphere as defined by *Vladimir Vernadsky* (Fig. 2.10), which was a fundamental look at the Earth surface system and the pivotal role of the carbon cycle in the system, including the environmental impacts of humankind. This *Geochemical Perspectives* memoir is in part a synthesis and continuation of my ongoing attempts at making sense of the complexities of the ocean-atmosphere-carbonate system through Phanerozoic time.

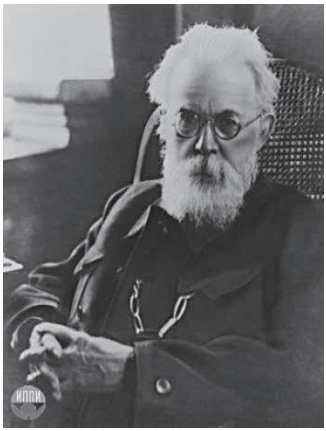

Source: russia-ic.com.

Figure 2.10 Vladimir Vernadsky (left) and his spheres of the planet Earth (right).

2.2 Andreas' Journey

I began my science journey on the island of Va'vau, in the kingdom of Tonga located in the South Pacific and not far from the international dateline. I had recently completed my service in the Royal Swedish Navy and I was contemplating what to do with my life. My first step was to buy a round-the-world airline ticket to get the chance to experience other cultures and to see something else than pine trees, lakes, and the rolling hills that my native Sweden had to offer. I was also keen to experience a more pleasant climate. For some reason I was obsessed about the South Pacific and after several hours in the local library in my hometown reading all the available Lonely Planet guides for the area, I set my mind on Tonga. To say the least, it was a life changing decision. Many of my friends had chosen careers in civil engineering, and although this did not excite me, I was also heading in that direction. This changed when for the first time in my life I slipped into the warm waters of Tonga with a mask and snorkel on my face. I simply could not believe what I saw under the sea surface. Experiencing a healthy coral reef with myriads of corals and fish of all colours of the rainbow in real life was something out of the ordinary. None of the nature documentaries I had watched on TV had prepared me for the thrill I felt. I instantaneously realised that I wanted to study and work in the ocean.

Following six months on the road exploring Tonga, Fiji, Australia, and Bali, I returned to Sweden with about two dollars of combined assets in my wallet and bank account, but with a mindset to study marine science in a place where the average temperature significantly exceeded the annual average of 5-6 °C experienced in my hometown in Sweden. With some hard work, a little bit of

luck, and a very generous student loan provided by the Swedish government, I eventually ended up at the Hawaii Pacific University on Oahu, Hawaii, USA to study marine biology. Nevertheless, due to a couple of inspiring teachers and mentors in oceanography, Drs. *Varis Grundmanis* and *Chris Winn,* my area of interest rapidly transitioned to the field of oceanography.

My first encounter with *Fred Mackenzie* took place in his corner office overlooking Honolulu and the Pacific Ocean at the UH Manoa campus in the spring of 2001. I had applied to graduate school at UH but my area of interest was highly uncertain, as I was pretty much interested in everything related to oceanography; my application letter covered everything from plate tectonics and seafloor mapping to chemical oceanography and climate change. Although this letter was against everybody's advice for getting accepted to graduate school (it was rather a great recipe for rejection), this was a true reflection of my intellectual interests at the time.

My introduction to *Fred* was highly orchestrated by *Chris Winn*, my main mentor at Hawaii Pacific University (I did not understand this until several years later after I had started working with *Fred*), and my first research experience was in *Dr. Winn's* lab where I worked as a student research assistant for $8/hour for a year. I am not exactly sure what went down before *Fred* admitted me (I had only applied to the UH and my backup plan was to return to the South Pacific on a surf safari), but I am convinced *Chris Winn* had a great deal to do with it. (As a side note, *Chris* also had a lot to do with *Fred* meeting his lovely wife *Judy* as the two of them met at *Chris'* wedding). Despite my broad and scattered scientific interests, my grade point average and graduate record exam scores were quite OK apart from a B+ in microbiology and an embarrassingly low score on the verbal section of the GRE. However, I am still convinced that I earned an A in the microbiology class, but that this became a B+ after I and a group of fellow students managed to sink the microbiology professor's dinghy in his pool during one of our graduation parties. This was to the delight of his teenage sons watching as I went down with the dinghy dressed in a brown polyester suit and beer in hand (the beer was the last thing to go under). During my first meeting with *Fred*, we discussed my undergraduate honours thesis, and during my second visit to his office, he broke the news that he was willing to offer me a position as a graduate student. However, at the time I was not certain whether I had understood him correctly or not, and I spent several weeks becoming increasingly convinced that I must have misunderstood him until I received the admission letter in the mail. It was quite a relief!

My first year with *Fred* as a graduate student was interesting to say the least and I got to take on roles that I had never imagined I would do as a graduate student in oceanography! It started out quite normal as I would imagine most students experience their first year in graduate school with mostly classes and exams, and a little bit of research. Nevertheless, at the end of the year, *Fred* was hosting and organising the Sixth International Symposium on the Geochemistry of the Earth's Surface (GES-6) meeting at the University of Hawaii, which gathers the world's top geochemists every four years. As the budget was limited, it fell on the post-docs and students of *Fred's* lab to take on the various roles associated

with every possible aspect of organising a conference. I started out editing and helping *Dr. May Ver* put together the abstracts book; then I was the bartender at the welcoming party at the Waikiki aquarium; then *Dr. Michael Guidry* and I were in charge of the audio-visual at the actual conference (most people were using powerpoint presentations at this time, but the best talk was delivered by *Vaclav Smil*; he had one overhead slide that he told me he may or may not show. He ended up not showing it and gave a 40 minute fascinating science talk about nitrogen that had the audience totally enraptured); then we were responsible for the clean-up after the banquet at the Bishop museum, followed by taking on roles as tour guides and shuttle van drivers for a field trip on the "Big Island" of Hawaii! The latter was an adventure in itself. One of the activities included hiking to the active lava flows of the Kilauea volcano on the "Big Island" over rugged lava terrain for several miles (Fig. 2.11). Sixty extremely excited scientists scattered in every possible direction as we started the hike and it would have been easier to control a herd of sheep. At the end of the day, we had also managed to loose a few scientists and had to execute a search and rescue mission, which luckily had a happy ending. For a first year graduate student, it was quite a treat to be engaged in every possible aspect of the conference. I not only got the opportunity

Photo courtesy of Judy Mackenzie.

Figure 2.11 The visit to the active lava flow on the "Big Island" of Hawaii, Hawaii, USA of participants at the *Sixth International Symposium on the Geochemistry of the Earth's Surface (GES-6)*, May, 2002.

to meet all the big names in geochemistry and biogeochemistry, including *Bob Berner, Dick Holland, Lee Kump, John Morse, Dick Feely, Abe Lerman, David Archer,* and *Vaclav Smil* to name a few, but I also got a chance to interact with them in both formal and informal settings.

The first research project I started working on with *Fred* involved refining the coastal compartment of *TOTEM* (Fig. 2.12). At the time, little attention had been given to the role of the carbon cycle in the coastal ocean in the context of global environmental change despite the fact that this region is highly important at the global scale, as discussed in Section 9.

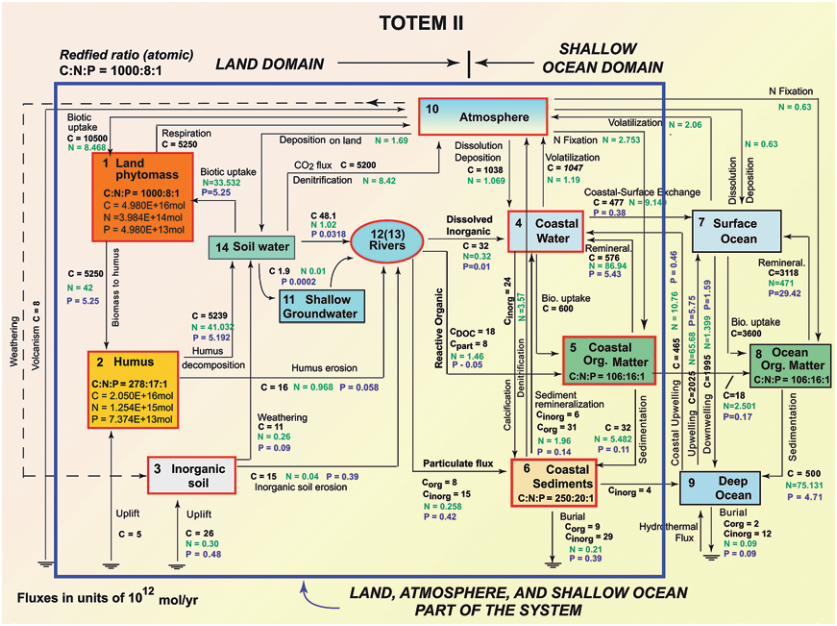

Figure 2.12 The model *TOTEM* (*T*errestrial *O*cean a*T*mosphere *E*cosystem *M*odel) for the global carbon, nitrogen, and phosphorus coupled biogeochemical cycles in the land-ocean-atmosphere-sediment system showing reservoirs, processes of transfer, and fluxes in 10^{12} mol per year of the elements (after Ver *et al.*, 1999 as modified in Mackenzie *et al.*, 2011).

Furthermore, the coastal ocean is heavily impacted by human activities, as nearly 40% of the global population lives within 100 km of the coastline (Cohen *et al.*, 1997). Our goal was to model how anthropogenic changes including rising atmospheric CO_2, temperature, and increasing material input via rivers and run-off had altered global coastal ocean biogeochemical processes, including inorganic and organic carbon production. At the time some researchers had pointed out that rising atmospheric CO_2 would lead to decreasing seawater pH and saturation

state with respect to calcium carbonate minerals (*i.e.*, ocean acidification, OA) that could have negative effects on marine organisms depositing shells and skeletons of calcium carbonate including corals (*e.g.*, Gattuso *et al.*, 1998; 1999; Kleypas *et al.*, 1999). Nonetheless, at the coral reef symposium in Bali in the year 2000, a couple of abstracts appeared claiming that OA would not have a negative effect on coral reef organisms because the seawater pH would be rapidly buffered by dissolution of metastable carbonate minerals such as biogenic high Mg-calcite phases. The hypothesis was referred to as the Magnesian Salvation Theory (MST). Hence, *Fred* and I decided to use our model and evaluate quantitatively whether this was true or not. The MST was proven incorrect (Section 10.1), but this exercise marked the starting point for my research focus on ocean acidification, which is still my main research and teaching emphasis today.

During my PhD, *Fred* brought me along to the BBSR as a teaching assistant for a summer class on coral reefs and climate change. There I met *Nick Bates* (Fig. 2.13) for the first time and we immediately started a fruitful collaboration investigating carbon chemistry and biogeochemical processes in a mangrove environment and in an environment called Devil's Hole located within Harrington Sound, Bermuda. Once I had completed my PhD, it was a natural move for me to continue my collaboration with *Nick* in Bermuda as a post-doctoral researcher continuing the work on ocean acidification, but also exploring the problem of the uptake and fate of CO_2 in North Atlantic subtropical mode waters. As a side note, it was *Fred* who introduced *Nick* to ocean carbon chemistry and the marine carbon cycle when *Nick* participated in one of *Fred's* summer courses in Bermuda. *Nick* subsequently switched focus from being a geologist to the study of ocean carbon chemistry. He has remained in this field of research ever since, including maintaining the inorganic carbon program of the Bermuda Atlantic Time-series Station (BATS; *e.g.*, Bates *et al.*, 2012).

Photo courtesy of Judy Mackenzie.

Figure 2.13 Fred, Nick, and Andreas gathered at a dock in Harrington Sound, Bermuda in 2010.

My science career almost ended in Bermuda since after a couple of years, I began to run out of funding, and being a 100% soft-money institution, no funding meant no job. Rather than heading back to the South Pacific on a surf safari, my backup plan this time involved moving to Margarita Island in Venezuela to pursue two passions of mine, kite surfing and salsa dancing, while learning to play the guitar and to speak Spanish. Two months before the implementation of my backup plan, I received my first NSF grant, and my career in science was saved. For the past several years, my research has focused on the effects of ocean acidification on coral reefs using Bermuda as a natural laboratory, which I hope to pursue for several more years. However, I am now an Assistant Professor at the Scripps Institution of Oceanography, University of California San Diego, California, USA, and I am developing a growing scientific interest for what is going on in my own backyard of the Pacific Ocean.

Working with *Fred* throughout my scientific career has been a tremendous privilege and honour, not only is he an outstanding scientist, he is also the kindest and most generous person I ever met, and he has served as the ultimate role model in all aspects of my life (Fig. 2.14).

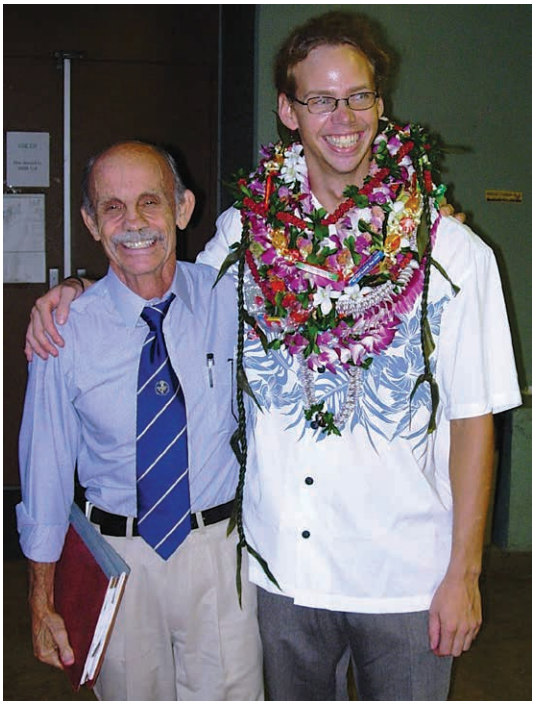

Figure 2.14 Fred and Andreas outside the Marine Science Building at the University of Hawaii after Andreas' successful Ph.D dissertation defense in October 2006.

When *Fred* asked if I wanted to co-author this *Perspectives* article with him, I accepted without hesitation. Nevertheless, as the University of California at San Diego for some reason unknown to me strongly discourages its Assistant Professors to work with their previous Ph.D. or post-doctoral advisors if we want to get tenure, I may yet again have to resort to one of my backup plans in a few years. The road of life never stops being exciting and apparently it is never straight (Fig. 2.15)!

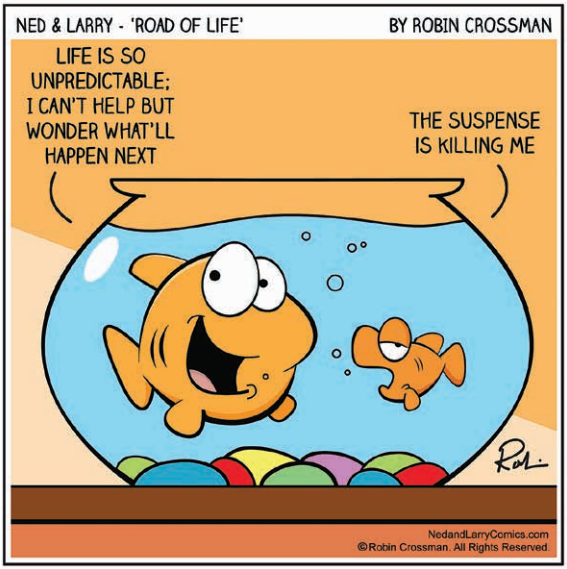

Figure 2.15 Cartoon of the tortuous and unpredictable road of life.

3. INTRODUCTION TO THE GEOCHEMICAL EVOLUTION OF THE EARTH'S ECOSPHERE

The chemical evolution of the Earth's near-surface environmental system, its ecosphere or exogenic system, and in particular the composition of the atmosphere and ocean, has long been of central interest to scientists from several disciplines. The more modern issue of chemical changes in the atmosphere and oceans deriving from human activities has engaged not only scientists but also policy makers and the public at large. Coupled to the interest in the history of the atmosphere and ocean have been questions about the relationship between their composition and the evolution of life, and the two have often been closely intertwined, As an example of this relationship, despite the appearance of oxygenic photosynthesis early in the Precambrian by the ancestral cynaobacteria ("blue-green algae"), the rise in atmospheric oxygen was delayed due to the scavenging of the initial O_2 fluxes produced by the reduced inorganic materials found in the Earth's oceans, atmosphere, and crust (Catling and Claire, 2005). In the modern world, the effects of changing atmospheric and oceanic composition have become a problem of concern for human society and natural ecosystems. During the past several centuries, the "Anthropocene Epoch", human activities have become a "geologic force" in the ecosphere, modifying its chemistry and biology due to fluxes of anthropogenically generated materials into the environment. These fluxes are the cause of a plethora of modern environmental problems.

Attempts to unravel the history of seawater and atmospheric composition, particularly CO_2, through geologic time are not new, going back as far back as Halley (1715) and Joly (1899), and more recently, Rubey (1951) and Holland (1972) among others for seawater and Ebelmen (1845) and later Berner *et al.* (1983; see summary in Berner, 2004) for the carbon cycle and atmospheric CO_2. *Fred's* interest in these problems initially began back in the early- and mid-1960's with a series of papers co-authored with *Bob Garrels*, including as mentioned above, those on the experiments dealing with the reactions of aluminosilicate minerals with seawater and the formulation of the "reverse weathering hypothesis". *Fred's* work on modelling the Earth's ocean-atmosphere-sediment system started with *Bob Garrels* on the evolution of sedimentary rocks (Garrels and Mackenzie, 1971) and the development of a quantitative model of the sedimentary rock cycle (Garrels and Mackenzie, 1972). As my scientific career developed, studies of biogeochemical processes in the context of gaining an understanding of the behaviour of the Earth's exogenic system or ecosphere at various time scales strengthened by Earth system modelling became central foci of my career. This work engaged quite a few students and other colleagues mentioned below, several of whom continue to do work with both *Fred* and *Andreas*.

During much of the latter half of the twentieth century, the prevailing view of the major ion composition of seawater was that it did not vary significantly during the Phanerozoic Eon. Although arguable, this view also extended to the CO_2-carbonic acid-carbonate system of seawater consisting of dissolved

CO_2 (CO_{2aq}), HCO_3^- and CO_3^{2-} ions, carbonate minerals, and atmospheric CO_2. Examples from books by leading geochemists of the period that strongly influenced this view of seawater chemistry include the *Evolution of Sedimentary Rocks* by Garrels and Mackenzie (1971):

> *"Many, if not most, geologists today would contend that the chemical composition of ocean water has not varied markedly for an interval of time greater than a few million years, at least as far back as the Cambrian time." (p. 285). "If so, sea water with ion ratios close to those of today may be the "mean sea water" of about half the geologic past."* (p. 297).

and

The Chemical Evolution of the Atmosphere and Oceans by Holland (1984):

> *"The apparent invariance of mineral sequences in marine evaporites, the relatively small variation in the Br and Cl ratio of basal halites in marine evaporites, and the composition of fluid inclusions in halites all suggest that the concentration of major ions in seawater have not varied a great deal during the Phanerozoic Eon."* (p. 536).

However, subsequently both *Garrels* and *Mackenzie* (*e.g.*, Morse and Mackenzie, 1992) and *Holland* (*e.g.*, Holland *et al.*, 1996) did allow the possiblity that seawater composition may have undergone significant variations during the Phanerozoic Eon. This was largely attributable to processes involving changes in the extent of dolomite formation, the shift from shoal (shallow)-water to deep-water deposition of carbonates in the Jurassic Period, excursions in the carbon and sulphur stable isotopic records, changes in the rate of circulation of seawater through mid-ocean ridge hydrothermal systems, and changes in the fluxes of dissolved constituents from the land to the ocean. Also in 1971 *Broecker* put forward his kinetic model of modern seawater composition challenging Sillén (1967) thermodynamic approach to the problem. In addition, starting in the 1980s, based on models of Phanerozoic atmospheric CO_2 compositional changes, it was demonstrated that atmospheric CO_2 concentrations had varied greatly during the Phanerozoic (Berner *et al.*, 1983; Berner and Kothavala, 2001; Berner, 2004, 2006) and as we will show in this article, in concert with seawater compositional changes. In addition, modelled atmospheric CO_2 concentration changes were confirmed to some degree by proxy data involving mainly fossil stomatal numbers and density, carbon isotopes in palaeosol (ancient soils) organic matter and carbonate, and the carbon isotopic composition of the organic remains of phytoplankton (*e.g.*, Royer *et al.*, 2001). On the shorter time scales of the Pleistocene glaciation-interglaciation stages and in the Anthropocene, evidence for varying atmospheric CO_2 concentrations is also abundant (Petit *et al.*, 1999; Siegenthaler *et al.*, 2005). Accompanying these compositional changes were changes in both biotic and abiotic carbonate mineral precipitates.

Research supporting the near constancy of seawater major ion composition included the calculations of Harvie *et al.* (1982) and Hardie (1991), which indicated that based on their studies of primary evaporite deposits (salt deposits of halite), Permian seawater was similar to modern seawater in composition. Studies of fluid inclusions in Permian marine evaporites also led to the same conclusion that

ancient seawater was similar in composition to that of modern seawater (Horita *et al.*, 1991; Stein and Krumhansl, 1988). However, subsequent studies of fluid inclusions in evaporite deposits of differing geologic ages demonstrated that the Permian results were unique in predicting an agreement with modern seawater composition and that seawater composition did vary during Phanerozoic time (see Horita *et al.*, 2002 and Holland, 2004 for extensive reviews and discussion of this literature). Also, various property-age trends of carbonate rocks, such as oolite mineralogy, dolomite distribution, and biotic and abiotic precipitates (see following and *e.g.*, Mackenzie and Pigott, 1981; Sandberg, 1983; Wilkinson and Algeo, 1989; Wilkinson and Given, 1986; Stanley and Hardie, 1998; Morse and Mackenzie, 1990; Kump *et al.*, 2009; and Veizer and Mackenzie, 2004 for summary), as well as Earth system models of seawater composition (Hardie, 1996; Zeebe, 2001; Tyrrell and Zeebe, 2004; Ridgwell and Zeebe, 2005; Arvidson, *et al.*, 2006; 2011; Guidry *et al.*, 2007; Mackenzie *et al.*, 2008), including its carbon chemistry, corroborated to some extent the fluid inclusion data reflecting variations in seawater chemistry and potential ties to atmospheric CO_2 concentrations.

The modern issue of changes in the marine CO_2-carbonic acid–carbonate system and ocean acidification as a result of human activities became a major focus of scientific investigation in the early twenty-first century. However, recognition that fossil fuel and land-use fluxes of CO_2 to the atmosphere and absorption of part of the gas emissions by surface seawater would lead to ocean acidification dates back at least four decades (Broecker and Takahashi, 1966; Broecker *et al.*, 1971; Bacastow and Keeling, 1973). In addition, increased land-to-sea nutrient and organic carbon fluxes and their effects on coastal ecosystems were viewed as a major problem by the latter part of the twentieth century. It is well known that excess nutrient loading of coastal ecosystems has led to hypoxia and anoxia in these environments, resulting in their deterioration and loss of aquatic life and changes in biological community structures. These changes in the oxygen content and the abundance and distribution of biological populations (trophic state) of coastal waters have modified the behaviour of the marine CO_2-carbonic acid system and the magnitude (and possibly the direction of air-sea exchange of CO_2) in some coastal environments.

The future effects of a decrease in the pH of surface seawater are still inadequately known and model predictions of increased acidity of seawater on individual calcifying and non-calcifying marine organisms, communities, and ecosystems carry large uncertainties. Despite these limitations, it is likely that the increasing acidity of the modern oceans will have significant effects, both direct and indirect, on individual marine organisms, communities, and ecosystems. These changes may translate into shifts in community and trophic structures, and perhaps even biodiversity. It is more or less certain that anthropogenically induced ocean acidification will lead to *decreasing* calcification rates for numerous marine calcifiers, and thus, lessened production of carbonate substrates, and *increasing* dissolution rates of abiotic and biotic carbonates. This assertion is derived from numerous field, laboratory, and model studies of corals, calcifying

algae, and other taxa, as well as calcium carbonate dominated ecosystems in general (Caldeira and Wickett, 2003; Andersson *et al.*, 2005, 2006; Silverman *et al.*, 2009).

Because of the renewed interest in modern ocean acidification, there has been increased research interest in the history of the seawater CO_2-carbonic acid-carbonate system and OA over deep geologic time (Arvidson *et al.*, 2006; 2011; Guidry *et al.*, 2007; Mackenzie *et al.*, 2008; Kump *et al.*, 2009; Zeebe and Ridgwell, 2011; Hönisch *et al.*, 2012), in part motivated by the need to constrain and quantify the response of the carbon cycle to the modern perturbation of anthropogenic CO_2 emissions, but also to identify how past marine ecosystems responded to CO_2 perturbation events. In the remainder of this article, we consider the behaviour of the seawater CO_2-carbonic acid-carbonate system through the Phanerozoic Eon, emphasising the coupling between the history of atmospheric CO_2 levels, carbonate sediment composition, the living biota, and the chemistry of the ocean, including the acidification of its surface waters in response to changing atmospheric CO_2, temperature, and land-to-sea inputs on various time scales: geologic deep time, the current glacial-interglacial, and the Anthropocene Epoch.

4. DEEP TIME: OBSERVATIONAL EVIDENCE FROM THE SEDIMENTARY ROCK RECORD

4.1 Introduction

In the following section on deep time, we have borrowed liberally from a book manuscript that was in preparation by *Fred, Andreas,* and *John Morse*, who regrettably passed away before the effort could be brought to fruition. At this point, *Fred* and *Andreas* wish to acknowledge once more *John's* friendship and valuable scientific interactions with us. Some of the material discussed in this section and Sections 5 and 6 will be revisited in Section 7, which is our attempt to articulate a synthesis of current knowledge concerning the evolution of the global CO_2-carbonic acid-carbonate system of seawater during Phanerozoic time.

There have been different approaches utilised to try to establish the variations in atmospheric and seawater chemistry over Phanerozoic time (the past 545 Ma of Earth's history). However, any discussion of ocean-atmosphere chemical changes during the Phanerozoic should start with considerations of the chemical, mineralogical, and isotopic attributes of sedimentary rocks. These are relevant to and constrain interpretations of the behaviour of the ocean-atmosphere system during the geologic past. *Fred* encouraged his former Ph.D. student *John Pigott* to begin collecting data of this nature in the late-1970s beginning with a synthesis of several hundred petrographic analyses of thin sections of carbonate rocks with the goal of establishing the inferred mineralogical composition (composition at the time of formation) of ooids (small sand-size internally concentrically banded carbonate grains found originally on the sea floor) during Phanerozoic time (see below). These studies placed a bound on the ancient history of ocean and atmospheric composition (Mackenzie and Pigott, 1981).

Only 12% of geologic time is represented by the Phanerozoic Eon, the rest by Precambrian time. However in terms of preserved sedimentary rock mass, the Phanerozoic contains about 60-70% of the total rock mass and much of this mass, although altered by diagenesis and metamorphism in some areas or buried at currently inaccessible depths, contains retrievable information on the mineralogy, chemistry, and isotopic composition of the deposited sediments. For the Phanerozoic carbonates, Figure 4.1 shows the carbonate preserved (the survival rate) versus the burial flux of carbonates on the sea floor as calculated from the model *GEOCARB III* (Berner and Mackenzie, 2011). Notice that much of the carbonate buried has been lost from the rock column, mainly, but not exclusively, by subduction.

We should also keep in mind for the carbonate rock column, that it is biased in terms of preservation of various types of carbonate rocks. Pelagic, deep-sea carbonate deposits [the calcareous pteropod (aragonitic pelagic sea snails), foraminifera (calcitic pelagic amoeboid protists), and coccolithophore

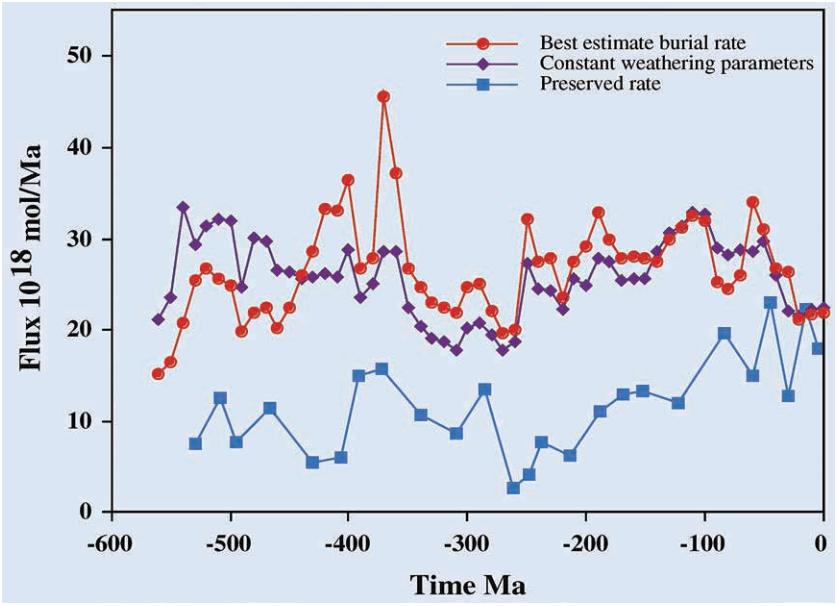

Figure 4.1 Plots of preserved rate and burial rate of carbonate sediments during Phanerozoic time. Two curves are shown for the burial rate of carbonates to illustrate the sensitivity of the model *GEOCARBSULFvolc* calculations to changes in weathering parameters: best estimate and time-invariant (constant) values for parameters affecting carbonate weathering (see Berner, 2004 for complete information concerning the parameters involved and their changes during Phanerozoic time). The preserved rate curve is derived from a number of compilations of carbonate rock mass-age data, which show a similar mass distribution with time (Ronov, 1980; Hay, 1985; Wilkinson and Walker, 1989; Mackenzie and Morse, 1992). Note that both the preserved rate and the burial rate curves converge to the same value at t = 0. This provides a check on the accuracy of calculations of the two entirely independent methods (after Berner and Mackenzie, 2011).

(calcitic pelagic algae) oozes] are representative of post-Permian time and not found in the Palaeozoic and Precambrian. Shallow-water, continental organo-detrital carbonates (deposits of fragmental shells and tests of mainly shoal-water benthic calcifying organisms) characterise the Palaeozoic but are also found later in Earth's history. These shallow-water carbonates were commonly deposited in vast seaways on the palaeo-continents, so-called epeiric or epicontinental, platform seas, for example, of the Ordovician and Cretaceous Periods of geologic time. These carbonate deposits can differ significantly in their mineralogical, chemical, and isotopic compositions from the coeval carbonates deposited in the much greater volume of the open ocean. For example, present-day, shallow-water carbonates are characterised by organo-detrital, aragonite, and magnesian calcite mineralogies with little pure calcite, while the deep-sea pelagic oozes are

nearly pure aragonite and calcite. This has been the case for at least much of the Cenozoic. In addition and of interest to the later discussion on the carbon isotopic composition of carbonates through geologic time is the observation that the carbon isotopic composition of the dissolved inorganic carbon (DIC) of shallow buried pore waters of shelf carbonate sediments generally differs from that of the open surface ocean.

For example, the DIC of Florida Bay pore waters is significantly depleted in ^{13}C owing to respiration of organic matter in the sediments as compared to the DIC of adjacent open ocean surface seawater (Walter *et al.*, 2007). The data accumulated by Walter *et al.* (2007) indicated that biogenic carbonates undergo extensive syndepositional (at the time of deposition and early in the burial history of the sediment) recrystallisation (solid-state transformation of the biogenic carbonate) in the sediments of Florida Bay at rates that are comparable to net dissolution rates of carbonate mineral phases in the sediments. This permits significant exchange between isotopically depleted organic carbon (depleted in the stable isotope ^{13}C relative to ^{12}C) and isotopically enriched inorganic carbon (enriched in the stable isotope ^{13}C relative to ^{12}C) pools in the sediment-pore water system. The authors concluded that the observed magnitude of isotopic exchange between organic and inorganic carbon pools during the earliest stages of sediment accumulation has important ramifications for the interpretation of the $\delta^{13}C$ isotopic record of marine carbonate rocks (see Section 4.4.1) and contributes significant uncertainty to reconstructions of palaeoocean and palaeoatmospheric chemistry. Thus, the $\delta^{13}C$ values of pre-Mesozoic carbonates that are largely shallow-water deposits may not reflect that of the ocean as whole. The above considerations should be kept in mind as we discuss the attributes of carbonate rocks in the following sections and their relevance to Phanerozoic ocean-atmosphere evolution.

4.2 Sea Level and Accretion Rate

We will start our observations relevant to ocean-atmosphere evolution during the Phanerozoic Eon by looking at the relationship between the generalised first-order sea level curve and the mid-ocean ridge accretion rate curve for the Phanerozoic (Fig. 4.2). The figure also shows atmospheric CO_2 concentrations during the Phanerozoic, which we will discuss later. Notice the reasonable correlation between the ridge accretion rate and the sea level curve. Mid-ocean ridge morphology and crustal accretion are known to depend on the spreading rate at the ridge. Although still somewhat contentious, the volume of the globally encircling mid-ocean ridge system appears to depend on the seafloor generation rate; the faster the rate, the greater the volume and hence the greater the displacement of ocean water onto the continents and the higher the sea level. The opposite is the case for slow generation rates. Changes in sea floor accretion rates modify high and low temperature basalt-seawater reaction elemental exchange fluxes, hence ocean chemistry, and also the rate at which volcanic CO_2 is emitted to the atmosphere, and thus atmospheric CO_2 concentration levels. A rise in sea level

floods continents providing shelf area for the deposition of dolomite, an important sedimentary mineral that controls in part the long-term CO_2-carbonic acid system chemistry of seawater (see discussion in further sections).

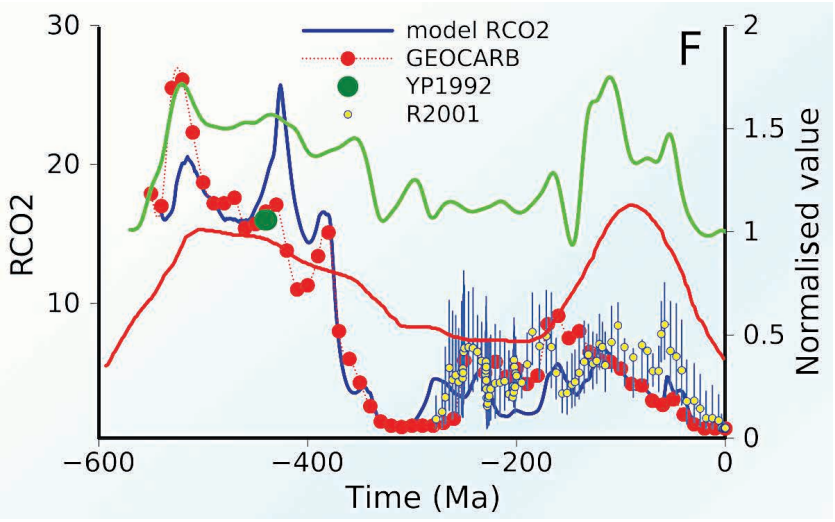

Figure 4.2 First order sea level changes, accretion rate, and palaeoatmospheric CO_2 through the Phanerozoic Eon. The green curve is a normalised forcing function used in the *GEOCARB* and *MAGic* (*M*ackenzie, *A*rvidson, *G*uidry *i*nteractive cycles) models to simulate sea floor accretion rate (*e.g.*, Berner and Kothavala, 2001); the red curve is an estimate of relative eustatic sea level variation, based on data from Vail *et al.* (1977) as modified by Arvidson and Mackenzie (1997). Atmospheric CO_2 (red dots GEOCARB and blue line MAGic) is shown as plotted relative to its present day concentration (RCO_2). The proxy (red dots GEOCARB and blue line MAGic) CO_2 data from Yapp and Poths obtained from palaeosols (YP1992) and from fossil plant stomata from Retallack (R2001) with ranges in blue are also shown (after Mackenzie *et al.*, 2011).

4.3 Distribution of Dolomite

The changes in sea level have important consequences for carbonate sedimentation during the Phanerozoic resulting in changes in the locus of the sedimentation, as mentioned above, and the distribution of dolomite through time. Massive dolomite accumulations do not form in the open ocean and based on their sedimentologic features appear to have been deposited in mainly continental shallow-water environments. Thus, dolomites in the sedimentary record are found predominantly at times of high sea level when the continental free board is flooded (Fig. 4.3). As we will see later, dolomite appears to exert a major control on the oceanic sink for magnesium and on the seawater CO_2-carbonic

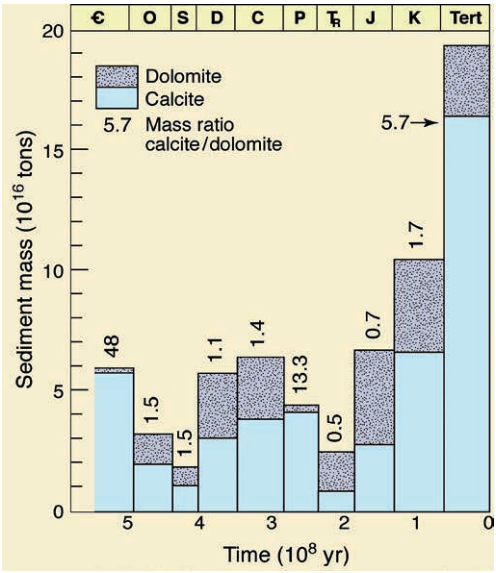

Figure 4.3 **(top)** Period-averaged preserved distribution of dolomite and calcite and mass ratio of calcite/dolomite through Phanerozoic time. Although controversial, it appears that dolomite accumulations vary cyclical over this time interval with scant dolomite observed in the more recent rock record when sea level was relatively low, considerable mass in the Mesozoic as sea level rose and reached the maximum transgression of the Cretaceous, little mass during the low stand of the Permo-Carboniferous with increasing mass during the high stand of the Palaeozoic decreasing into the Cambrian at a lower sea level stand (after Mackenzie and Morse, 1992). **(bottom)** View of dolomite cliffs in the Dolomite Mountains of Italy.

acid system chemistry. Thus, a rigorous evaluation of the mass-age distribution of dolomite through the Phanerozoic Eon is required to help constrain the evolution of seawater chemistry during this time interval. Regrettably despite all the work that has been done on this problem, including that of *Fred* and *John Morse* in a synthesis compilation of the data (Mackenzie and Morse, 1992), the dolomite mass-age distribution and its meaning still remain controversial and this fact should be kept in mind in the discussions below.

4.4 Carbon, Oxygen, and Sulphur Isotopic Compositions of Sedimentary Materials

The isotopic composition of sedimentary materials provides strong constraints on the evolution of the composition of the atmosphere, ocean, and carbonate sediments throughout the Phanerozoic Eon. Major factors of importance are that biological processes involving carbon and sulphur generally fractionate the light isotope of the element from its heavier counterpart, whereas physical processes are important in the fractionation of the oxygen isotopes. This enables one, for example, to determine the relative fluxes of carbon to the organic carbon and carbonate carbon reservoirs through geologic time, to assess the relative fluxes of sulphur to the oxidised versus reduced sulphur reservoirs, and to determine the history of Earth's surface temperature. Determination of the carbon and sulphur fluxes is one constraint on ocean-atmosphere compositional evolution during the Phanerozoic. In this section, we discuss the carbon, oxygen, and sulphur isotopic composition of sedimentary materials, such as organic carbon, carbonate, and sulphur-bearing compounds, in light of the evolution of the ocean-atmosphere-carbonate sediment system.

4.4.1 Carbon

There are two stable isotopes of carbon, ^{13}C and ^{12}C, used in environmental interpretations. The heavier ^{13}C isotope is less abundant than the lighter ^{12}C isotope. The isotopic ratio of these two isotopes of carbon is usually expressed in the form of a del (δ) value where

$$\delta^{13}C = [(^{13}C/^{12}C_{sample})/(^{13}C/^{12}C_{standard}) - 1] \times 1000‰. \quad (4.1)$$

The common reference standard for $\delta^{13}C$ was originally the Chicago Pee Dee Belemnite Marine Carbonate Standard obtained from a fossilised $CaCO_3$ cephalopod (the belemnite *Belemnitella americanus*) found in the Cretaceous Pee Dee Formation in South Carolina, USA. All original supplies of this material have been used up and replaced by secondary standards obtained from the U. S. National Bureau of Standards.

Carbon isotope systematics and the isotopic fractionation of $^{13}C/^{12}C$ during the biological production of organic matter by photosynthesis and in the carbon transfers between the atmosphere, continental and ocean waters, and carbonate

sediments are reasonably well known (see Mackenzie and Lerman, 2006, for review). Here we briefly review these in terms of the changes in the isotopic composition of the Phanerozoic carbon isotope rock-age record and the bearing of these changes on the evolution of the ocean-atmosphere-carbonate sediment system. The two dominant exogenic (surface plus near-surface) reservoirs of carbon are carbonate rocks and organic matter in sediments. They are linked in the carbon cycle (Fig. 4.4) via atmospheric CO_2 and the carbon species dissolved in the hydrosphere.

^{12}C in carbon dioxide is preferentially utilised by photosynthesising organisms for production of organic carbon as a result of kinetic differentiation of ^{12}C and ^{13}C (because ^{13}C is heavier than ^{12}C) and a higher affinity for ^{12}C by the enzyme Rubisco, which acts as the catalyst of the reaction. As marine phytoplankton and benthic organisms preferentially incorporate ^{12}C, this causes enrichment in ^{13}C in seawater that accounts for near-surface ocean waters being usually enriched in ^{13}C relative to deep waters, where much of the sinking organic matter is respired, adding ^{12}C to intermediate and deep waters of the ocean (Kroopnick, 1980; Tan, 1988). The majority of carbon in organic compounds in the biosphere is ultimately derived from photosynthetically produced material, thus all organic carbon compounds in the biosphere are isotopically very light, largely as a result of the kinetic effects occurring during photosynthesis. The isotope values for aquatic plants are somewhat different than those of land plants because the former utilise dissolved and not gaseous CO_2 and thus tend to be more enriched in ^{13}C.

While the isotopic composition of CO_2 in the atmosphere is about $\delta^{13}C$ = -6‰ to -7‰, marine phytoplankton exhibit a range of $\delta^{13}C$ values between -10‰ and -31‰, with most values between -17‰ and -22‰. In contrast, in most land plants utilising the C_3 or Calvin-Benson pathway of metabolism, the $\delta^{13}C$ of the organic tissue carbon is about -23‰ to -33‰, with an average of about -26‰. Plants using the C_4 pathway (most tropical and marsh grasses; spreading across the landscape in the Cenozoic) average about -13‰, with values ranging from -9‰ to -16‰. It is important to stress in the context of this section the fact that organic carbon is strongly depleted in ^{13}C relative to its carbon source. This organic matter, which is very labile, is easily oxidised to CO_2 and its ambient environment inherits a ^{13}C-depleted signal (Fig. 4.5).

The $\delta^{13}C$ of mantle inorganic carbon is approximately –5‰ to –7‰ and in the absence of life and its photosynthetic capabilities, this would also be the isotopic composition of seawater. Yet, as far back as 3.5 to 4 billion years ago, carbonate rocks and, hence seawater, had a $\delta^{13}C$ of about 0‰ (Shields and Veizer, 2002; Veizer and Mackenzie, 2004; Lerman and Clauer, 2004, 2013). This suggests that a reservoir of reduced organic carbon that accounted for approximately 20% of the entire exogenic carbon existed some 4 Ga ago, and raised the residual 4/5 of carbon, present in the oxidised form in the ocean-atmosphere system, from –5 to 0‰. This oxidised/reduced partitioning of carbon is very similar to that found today.

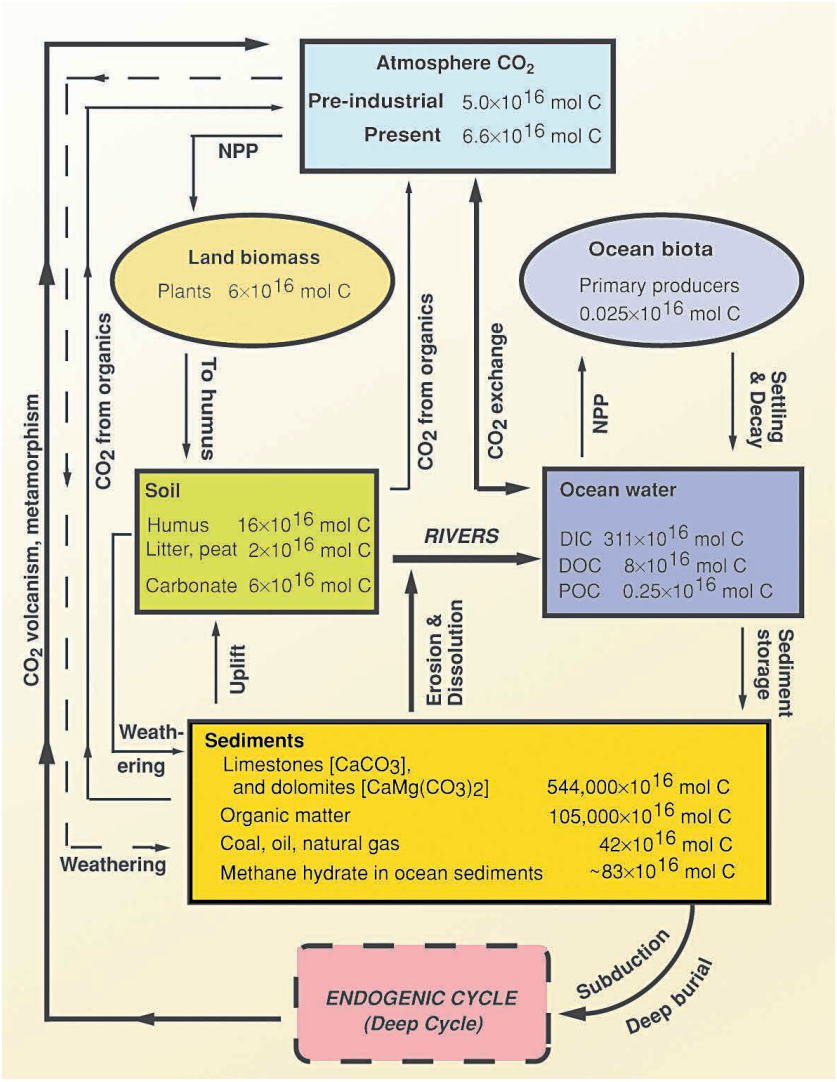

Figure 4.4 Global biogeochemical cycle of carbon. Reservoirs on the Earth's surface represent the exogenic cycle, which is coupled to the endogenic cycle via subduction of sea floor sediments, deep burial, volcanism and metamorphism. Masses of the major reservoirs are shown along with processes transferring carbon between the reservoirs. NPP is net primary production, Mass units: 1 mol C = 12.011 g C and 1×10^{16} mol C = 120 Gt C (after Mackenzie and Lerman, 2006).

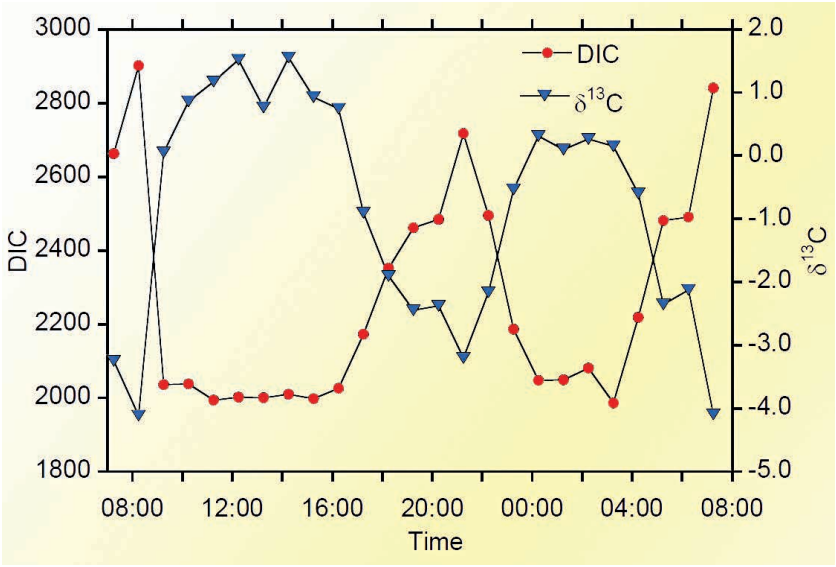

Figure 4.5 Diel cycle of seawater DIC and DIC-$\delta^{13}C$ in a mangrove embayment in Bermuda. During low tide (~16:00 to 04:00 hours), the influence of groundwater enriched in CO_2 from respiration and decomposition of organic material is observed by high seawater DIC and low $\delta^{13}C$.

The sampling density and temporal resolution of $\delta^{13}C$ in the Phanerozoic Eon enable the delineation of a well-constrained $\delta^{13}C$ versus age secular curve that exhibits a maximum in the Permo-Carboniferous (Fig. 4.6). However even in this case, we are dealing with a band of data, reflecting the fact that the $\delta^{13}C$ of the DIC of seawater is not uniform in time and space, that organisms can incorporate metabolic carbon into their shells and also exert a vital effect on shell isotopic composition, and that some samples may have an isotopic composition modified by diagenesis. The main factors that control the long-term variations in the $\delta^{13}C$ record in carbonates are biological production of organic matter and subsequent storage in sediments of some portion of the ^{13}C-depleted organic carbon produced. In addition, tectonic processes can play a role through sea floor spreading by additions of isotopically lighter CO_2 to the Earth's ocean-atmosphere system. Another potential control is the weathering and erosion of sedimentary organic matter in continental rocks that can add isotopically lighter CO_2 to the atmosphere and to the ocean via river runoff of ^{13}C-depleted organic carbon. In addition, storage of ^{13}C-depleted organic carbon in the ocean may depend to some extent on changes in sea level as more or less of the continental surface is flooded providing additional or less area, respectively, for the accumulation of organic carbon.

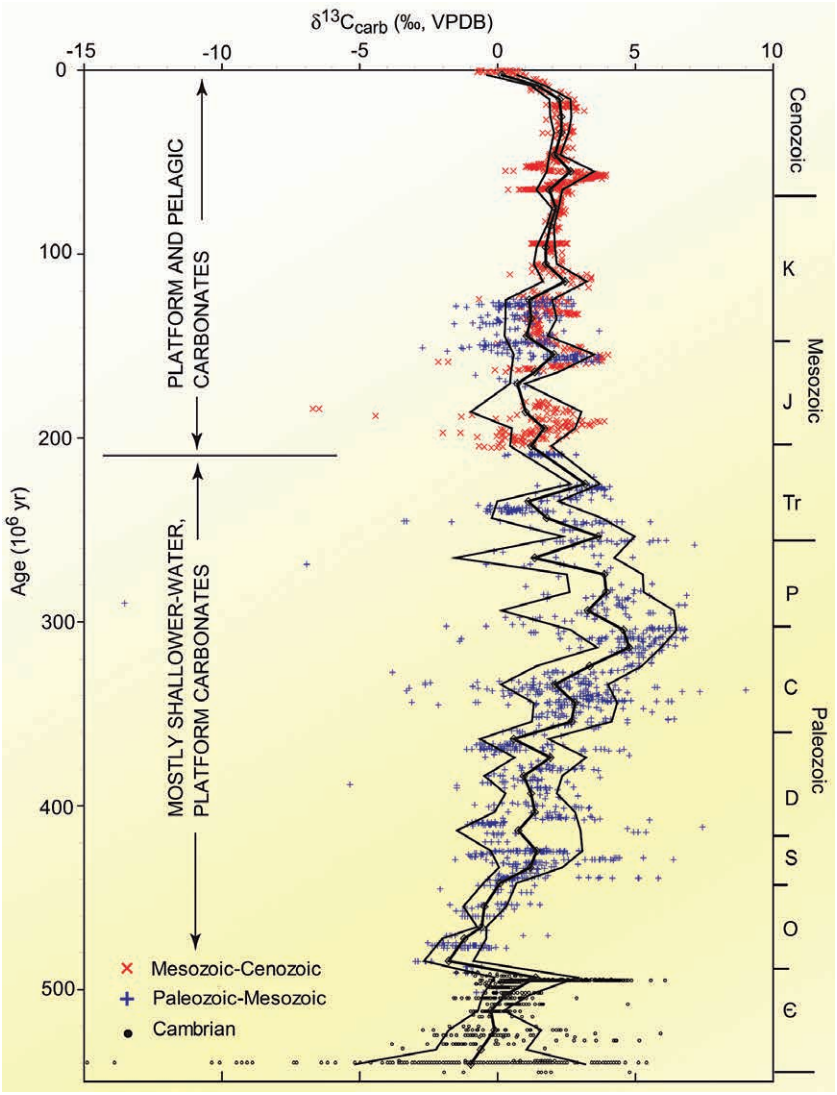

Figure 4.6 $\delta^{13}C$ values of Phanerozoic carbonates. Cambrian to Jurassic (black • and blue +) data from Veizer *et al.* (1999); Jurassic to Recent (red ×) from Katz *et al.* (2005). The reference scale is the Vienna Pee Dee Belemnite (VPDB) scale. Stratigraphic time scale is from Gradstein *et al.* (2004). Thick line is the consecutive 10-Ma-interval means (5-Ma for the most recent 10-Ma interval); thin lines are the ±1 standard deviation (after Lerman and Clauer, 2013).

Frakes *et al*. (1992) proposed that the $\delta^{13}C$ of carbonates (hence seawater) becomes particularly heavy at times of glaciations because of ^{12}C being sequestered in continental ice caps, and that low CO_2 levels also characterise such times. The coincidences of the $\delta^{13}C$ peaks with the Late Ordovician and Permo-Carboniferous glacial episodes appear to support this proposition, but the Mesozoic-Cenozoic record is divergent (Fig. 4.6). This is not surprising, since as mentioned above, the rate of accumulation of organic carbon on the seafloor plays a very strong role in the $\delta^{13}C$ of carbonates. The Permo-Carboniferous, a time of continental glaciation and ^{13}C-enriched carbonates, is the time of the emergence and spread of lowland plants living in coastal marine settings and a time of relatively high organic carbon to inorganic carbon burial rates. The important burial at this time of ^{12}C-enriched organic matter in organic-rich sediments would drive the ocean toward higher $\delta^{13}C$ values as the ^{12}C was preferentially removed from the ocean water DIC pool and incorporated in organic matter. These events probably account for much of the enrichment of ^{13}C-enriched inorganic carbon in carbonates. Furthermore, the great swamps of the Permo-Carboniferous would eventually become the vast reserves of coal that we mine today through processes involving the maturation of the organic matter buried in them. In addition, the emergence and spread of land plants in the late Palaeozoic also played an important role in the drawdown of atmospheric CO_2 at this time and the large amounts of buried coastal organic matter led to increased levels of oxygen in the atmosphere (since this carbon was not oxidised), and also increased levels of methane derived from microbial reactions in the muds of the swampy lowlands of the time (Berner and Canfield, 1989; Beerling *et al*., 2009; see Section 7). The drawdown of CO_2 from the atmosphere led to changes in the CO_2-carbonic acid system chemistry of seawater (see below).

4.4.2 Oxygen

The stable isotopes of oxygen, ^{18}O and ^{16}O, found in the calcium carbonate ($CaCO_3$) skeletons of corals, brachiopods, belemnites, and foraminifera can provide a record of the temperature of the environment in which the $CaCO_3$ precipitated. This is fundamentally due to the fact that one of the oxygen atoms in the $CaCO_3$ is derived from the water of the environment of formation. The other two oxygen atoms are from the carbon dioxide dissolved in the water. $\delta^{18}O$ is a measure of the ratio of the stable isotopes of ^{18}O to ^{16}O in the oxygen of the $CaCO_3$ and is defined as:

$$\delta^{18}O = [(^{18}O/^{16}O_{sample})/(^{18}O/^{16}_{standard})) \text{ -1}] \text{ x } 1000‰. \quad (4.2)$$

The standards used are Vienna Standard Mean Ocean Water (VSMOW) or the $CaCO_3$ of a belemnite originally found in the Cretaceous Pee Dee Formation in South Carolina, USA (see above). $\delta^{18}O$ can be used as a proxy to interpret the temperature of seawater at the time the $CaCO_3$ precipitated since this ratio depends on the temperature of the water. Other factors, such as the salinity of

the water and the volume of water locked up in ice sheets, need to be corrected for to obtain a temperature only signal. For example, a $\delta^{18}O$ increase of +0.22‰ is equivalent to about a 1 °C cooling, if there is no salinity or ice volume effect.

The Phanerozoic oxygen isotope record based on 4,500 samples of calcite and aragonite shells (Veizer *et al.*, 1999; Shields and Veizer, 2002; Veizer and Mackenzie, 2004) shows a clear trend of ^{18}O depletion with the age of the rocks (Fig. 4.7). This isotopic ^{18}O record in ancient marine carbonate deposits is one of the more controversial topics of sedimentary isotope geochemistry. The controversy centres on the issue of the primary versus post-depositional origin of the secular trend (Land, 1995, as opposed to Veizer, 1995). An extensive review of $\delta^{18}O$ and $\delta^{13}C$ data for numerous taxonomic groups secreting $CaCO_3$ shells and skeletons (see Land, 1989) led to the conclusion that the spread of values is much greater than can be accounted for by temperature–dependent fractionation or variation of the oxygen isotopic ratios in ocean water, and that diagenetic alteration of biogenic carbonates involves dissolution and *in situ* reprecipitation of calcite rather than a reaction in the solid state.

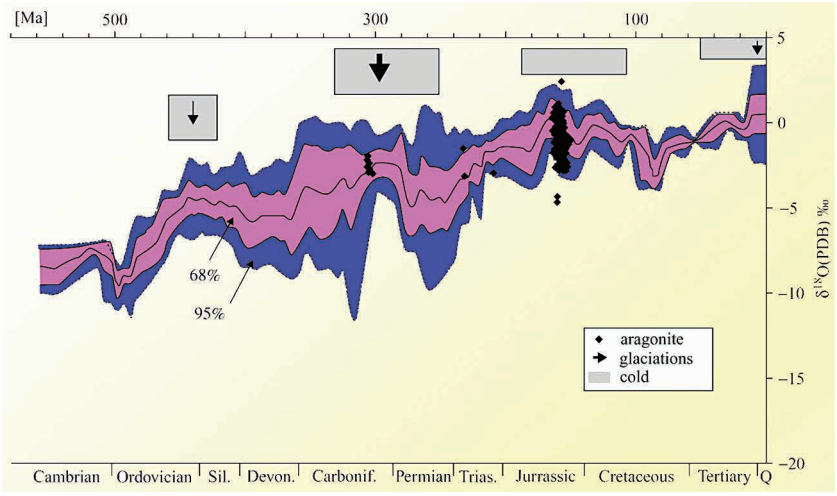

Figure 4.7 Phanerozoic variation in the oxygen isotope composition of marine carbonates based on 4,500 samples of calcite and aragonite shells. Periods of inferred cold climate and glaciations are also shown (after Veizer *et al.*, 1999).

Undoubtedly, diagenesis may reset the $\delta^{18}O$ signature, usually to more negative values, during stabilisation of original metastable carbonate phases (aragonite and high Mg calcite) into the stable phase, low-Mg calcite (Bathurst, 1974; Morse and Mackenzie, 1990). Virtually every carbonate rock during its history is subjected to this stabilisation process, or to replacement by dolomite,

and much of the original chemistry and mineralogy can be altered. An exception to this can be the original low magnesium calcitic shells of some organisms, such as brachiopods, belemnites, and foraminifera.

The Phanerozoic trend shown in Figure 4.7 is based on samples of low-Mg calcitic fossils from about 100 localities worldwide and is thought to be primary in nature. The reasons for believing that this is essentially a primary trend are discussed in detail by Veizer *et al.* (1999). If we accept that the $\delta^{18}O$ of past seawater was evolving towards ^{18}O-enriched values (Wallmann, 2001) and if we account for this evolutionary trend in the data of Figure 4.7 accordingly, the superimposed second-order structure of the curve appears to correlate reasonably well with the Phanerozoic palaeoclimatic record (Veizer and Mackenzie, 2004). Therefore, the observed structure in the $\delta^{18}O$ secular trend to some degree likely reflects palaeotemperatures. However, the structure does not correlate that well with the palaeoatmospheric CO_2 curve; the $\delta^{18}O$ curve suggests four periods of cooling (^{18}O-enriched) in the Phanerozoic, whereas if CO_2 alone is the major driving force of climatic change, one would conclude there are only two major coolings during which there were continental glaciations. However, it should be pointed out that the pH of seawater also affects the $\delta^{18}O$ record of contemporary carbonates (Zeebe, 1999; Royer *et al.*, 2004) and may account to some extent for variations in the record. Indeed, Royer *et al.* (2004) have found that if you correct the Phanerozoic $\delta^{18}O$ record for seawater pH variations, the corrected record matches the glacial record of cooling much better with important episodes of cooling and large-scale continental glaciations in the Permo-Carboniferous and late Cenozoic correlating with low atmospheric CO_2 levels. Some care must be taken in terms of this conclusion because the seawater pH trend for much of the Palaeozoic is based mainly on various modelling approaches with different assumptions.

4.4.3 Sulphur

Sulphur is found in carbonate minerals as a minor constituent. Its importance to the history of the carbon cycle stems mainly from the fact that the isotopes of sulphur in sedimentary precipitates provide boundary conditions on the evolution of some organism groups over geologic time and the relative accumulation rates of sulphate-sulphur to sulphide-sulphur on the sea floor. The latter is tied to the carbon cycle through the fact that organic matter contains important amounts of sulphur primarily strengthening protein bonds and sulphur as dissolved sulphate in sediment pore waters is an important oxidising agent of organic matter.

As with the carbon and oxygen stable isotopes, the isotopic compositions of different materials in terms of the two isotopes ^{34}S and ^{32}S of sulphur can be expressed as a δ value, where for sulphur the $\delta^{34}S$ is:

$$\delta^{34}S = [(^{34}S_{sample}/^{32}S_{sample})/(^{34}S_{standard}/^{32}S_{standard}) - 1] \times 1000‰. \quad (4.3)$$

The original standard for this sulphur isotopic ratio was based on the sulphur found in the mineral troilite (FeS) of the Cañon Diablo iron meteorite (CDT). Sulphur isotope values are still reported relative to the Cañon Diablo troilite, but the scarcity of this material and its lack of homogeneity led the International Atomic Energy Agency (IAEA) to develop a new standard. The IAEA standard for $\delta\,^{34}S$ of -0.30‰ is presently used in sample analysis.

As with carbon, the isotopes of sulphur are strongly fractionated by biological processes, particularly during dissimilatory (as the opposite of an assimilatory biological process, sulphur is released) bacterial reduction of sulphate to sulphide. The laboratory results for this step are anywhere from $\delta^{34}S$ = +4 to -46‰ relative to the standard Cañon Diablo Troilite meteorite, but even larger fractionations have been observed in natural systems. The Phanerozoic record of evaporitic sequences, including sulphate evaporites, is certainly not very complete (see Fig. 4.13). Therefore sulphur found in calcitic shells has also been used to obtain a record.

The variations in the $\delta^{34}S$ of sulphate in Phanerozoic evaporites and sulphur structurally bound in calcitic shells (and hence a record of the ^{34}S of the oceans) form an overall trough-like trend similar to that for Sr isotopes (Fig. 4.8; Sr not

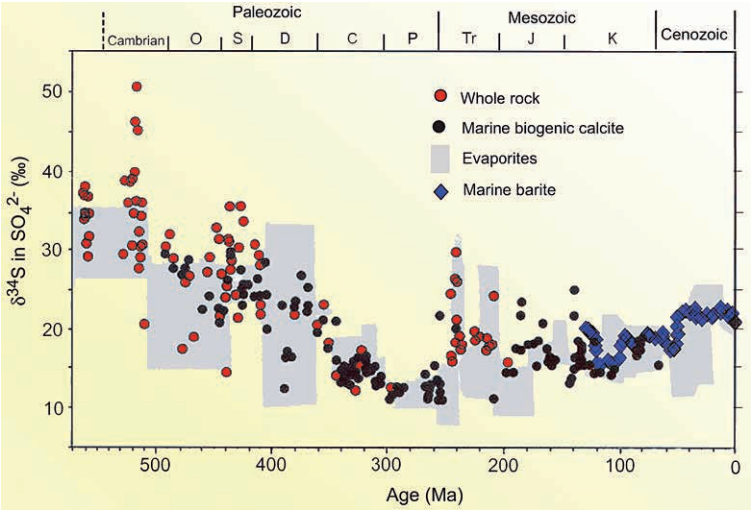

Figure 4.8 Sulphur isotopic composition of sulphate (‰,Cañon Diablo Troilite or CDT meteorite standard) in evaporites and in sulphur structurally bound in calcite shells during the Phanerozoic. The red circles represent data from whole rock analyses of $\delta^{34}S$ whereas the black circles are data from biologically produced marine calcite. The shaded gray areas represent data from evaporite deposits. This trend reflects the sulphur isotopic composition of Phanerozoic seawater (after Kampschulte, 2001, modified from Veizer and Mackenzie, 2004). Blue diamonds are Cretaceous and Cenozoic marine barites from Paytan *et al.* (1998, 2004) (after Lerman and Clauer, 2013).

shown in the figure). However, there are large age uncertainties and temporal gaps between the evaporitic sequences investigated. This is due to their episodic occurrence and uncertain chronology and is part of the reason for the large spread in the coeval $\delta^{34}S$ values despite the fact that the $\delta^{34}S$ sulphate in seawater is spatially essentially homogeneous. Another reason for this large spread in the $\delta^{34}S$ values is the evolution of sulphur isotopes in the course of the evaporation process involving seawater, from Ca-sulphate to Na-chloride deposits to later rocks bearing complex sulphate and chloride salts. A recent development of the technique that enabled measurement of $\delta^{34}S$ in structurally bound sulphate in carbonates (Kampschulte and Strauss, 1998; Kampschulte, 2001) has yielded the Phanerozoic secular curve of Figure 4.8, which has a much greater temporal resolution.

The $\delta^{34}S$ of sulphate and $\delta^{13}C$ of carbonate secular curves correlate negatively, suggesting that it is the redox balance (exchange of oxygen between the carbon and sulphur cycles) that controls the $\delta^{34}S$ variations in Phanerozoic rocks and hence oceans. If the redox balance is indeed a major controlling mechanism, it suggests that the withdrawal of ^{32}S into pyrite (FeS_2) burial in sediments was twice as large as today in the early Palaeozoic versus about one half of that in the late Palaeozoic (Kump, 1989).

4.5 Distribution of Abiotic Sedimentary Carbonates

Much of the early impetus for the concept that seawater chemistry was not constant, but varied substantially during the Phanerozoic Eon, came from studies of ancient sedimentary carbonates. The primary concept that formed the basis of interpretation was that the original mineralogy of abiotic carbonate cements and ooids (sand-sized approximately spherical abiotic carbonate particles with internal concentric banding) could be deduced from their morphologies, even though their original mineralogical compositions had been altered due to diagenesis (Sorby, 1879; Bathurst, 1975; Wilson and Dickson, 1996). The basic idea was that these abiotic carbonates formed directly from seawater and that changes in their mineralogy reflected changes in seawater composition. To some extent based on experimental studies (discussed below), attention focused on potential changes in the ratio of dissolved Mg to Ca in seawater that conceivably could cause a change from calcite (low ratio) to aragonite (high ratio) seas. It was also argued that the relative abundance of dolomite could potentially be influenced by changes in seawater sulphate concentration because it has been shown that sulphate may inhibit dolomite formation (Warthmann *et al.*, 2000).

Figure 4.9 presents the most recent summary (Mackenzie and Lerman, 2006) of work on the relative abundance of calcitic versus aragonitic ooids based on the work of several investigators, including Mackenzie and Pigott (1981), Sandberg (1983, 1985a,b), and Wilkinson *et al.* (1985). The data were obtained from petrographic analysis of hundreds of thin sections of carbonate rocks from around the world. In addition to the ooid trend, Sandberg (1983) also

demonstrated a trend for carbonate cements that closely matches the mineralogical trend found for ooids. He contended that these trends were driven by plate tectonics and reflected changes in pCO_2 rather than the Mg/Ca mol ratio of seawater. The book *Geochemistry of Sedimentary Carbonates* (1990) by Morse and Mackenzie and a paper by Hardie (1996) were particularly influential in tying together the concepts of sea floor spreading rates, seawater chemistry, sea level changes, and carbonate mineralogy. Many subsequent papers (*e.g.,* Holland, 2005; Arvidson *et al.*, 2006) have expanded on and refined these basic concepts.

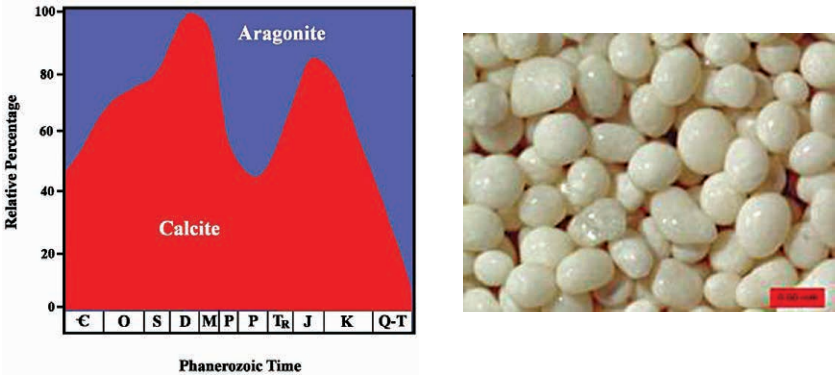

Figure 4.9 **(left)** Trend in original ooid mineralogies at deposition during the Phanerozoic Eon [after Mackenzie and Lerman (2006) and based on petrographic data from several hundreds of thin sections of carbonate rocks from Mackenzie and Pigott, 1981; Sandberg, 1983; and Wilkinson and Given, 1986]. **(right)** Sand-sized aragonitic ooid grains with internally concentric banding found on the modern sea floor of the Joulters Cay, Bahamas (red scale bar = 0.5 mm).

There is no doubt that the Mg/Ca ratio in an aqueous solution can affect the composition of both biogenic and abiogenic carbonate minerals (Mackenzie *et al.*, 1983; Ries, 2009). However, although the concept that "calcite versus aragonite seas" (Sandberg, 1983; now called calcite-dolomite versus aragonite seas; Mackenzie *et al.*, 2008) may to some extent reflect the Mg/Ca ratio of seawater is currently accepted by a number of scientists, *Bruce Wilkinson* at the University of Michigan and his associates have urged that caution be taken in acceptance of this hypothesis. Their concerns are several and include: (1) palaeolatitude distributions of carbonate accumulations at the time of deposition (Opdyke and Wilkinson, 1990), (2) the fact that at any given time the preponderance of one carbonate mineralogy over the other changes but it is never an "either or" situation (Wilkinson *et al.*, 1984), (3) that carbonate mineral growth rates may be more important in controlling crystal morphology than the Mg/Ca ratio of seawater (Wilkinson *et al.*, 1985; Arvidson and Morse, 2013), (4) the lack of any constraints afforded by deep-sea carbonate deposition prior to the Jurassic Period (Wilkinson and Walker, 1989), and (5) that the composition of modern carbonate cements

appears to be largely controlled by latitude and alteration through diagenetic processes. Furthermore, Balthasar *et al.* (2011) found relic aragonite in Ordovician and Silurian trimerellid brachiopods showing that aragonite can be a favoured precipitate in some warm tropical seas even during episodes of calcite-dolomite seas.

In addition, Bates and Brand (1990) have seriously questioned whether there has indeed been a statistically demonstrable change at all during the Phanerozoic Eon away from the current dominance of aragonitic ooids and micritic (fine-grained) cements. Furthermore, recently Bots *et al.* (2011) on the basis of controlled laboratory experiments showed that increases in experimental solutions of dissolved SO_4 decrease the Mg/Ca ratio at which calcite is no longer stable and aragonite becomes the dominant $CaCO_3$ dimorph precipitate. Their data suggest that the Mg/Ca and SO_4 thresholds for the formation of calcite seas may be significantly lower than previous estimates and are not mutually independent. These considerations point to the need for a new and detailed look at the carbonate mineralogical database on which the aragonite seas versus calcite-dolomite seas concept to some extent rests and at the relationship between changes in seawater chemistry and the models that tie that chemistry to the mineralogy of the primary $CaCO_3$ precipitate. However as shown in the next sections, there is evidence from fluid inclusion studies of evaporite deposits that the dissolved Mg/Ca and SO_4/Ca of seawater tracks that of the inferred original composition of abiotic carbonate materials. The question obviously is: Is there a causal link?

4.6 Dissolved Mg/Ca Ratio and Aragonite versus Calcite-Dolomite Seas

As mentioned above, a possible tie has been suggested between the dissolved Mg/Ca ratio of seawater and the composition of abiotic marine carbonate sediment constituents such as ooids and cements during the Phanerozoic Eon**.** The inference is largely based on a few experimental studies that will be discussed later. The point of central importance is that at ~25 °C the polymorph of $CaCO_3$ that nucleates from seawater changes from aragonite to calcite at about a Mg/Ca ratio of 1 (Morse *et al.*, 1997). As shown in Figure 4.10, there is a reasonable match of time intervals at which the Mg/Ca ratio of seawater (as based on studies of the chemical composition of fluid inclusions in evaporite deposits) approached this value and when there was a change from a dominance of abiotic aragonite production to calcite production. Thus, it appears that to some extent the composition of the original mineralogy of carbonate ooids and cements is controlled by the changing Mg/Ca seawater ratio and that these carbonate precipitates do reflect changing seawater composition. Because the dissolved SO_4/Ca mol ratio reasonably well tracks the Mg/Ca ratio of seawater composition as determined from fluid inclusions in evaporites, it is not unreasonable to assume that both

chemical ratio parameters play a role in the nature of the $CaCO_3$ precipitate. However, we will see in further sections of this article that these conclusions are not that straightforward.

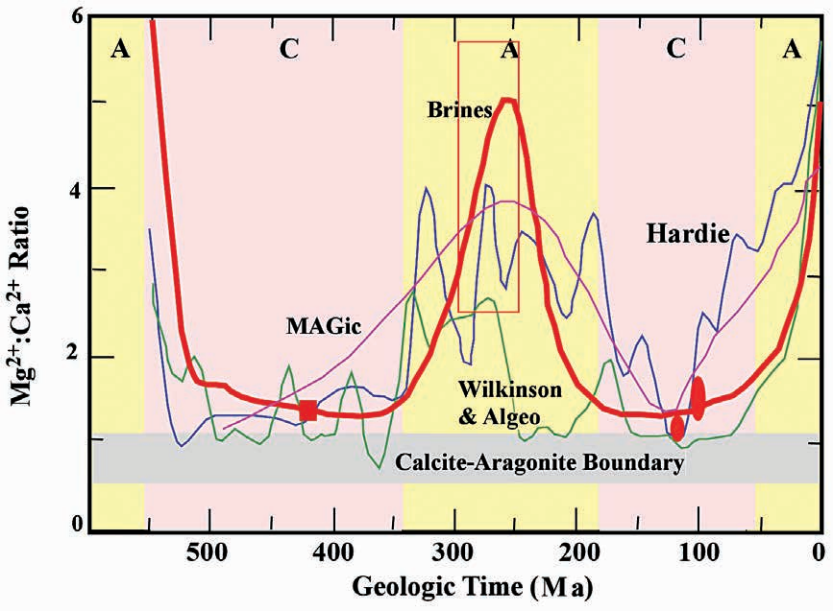

Figure 4.10 Estimated variations in the dissolved Mg/Ca ratio of seawater during the Phanerozoic Eon. The heavy red line and red symbols are based on marine evaporite fluid inclusions. Examples of model results for the Mg/Ca ratio of seawater from Wilkinson and Algeo (1989), Hardie (1996), and *MAGic* (Arvidson *et al.*, 2006) are also shown. A stands for "aragonite seas" and C for "calcite-dolomite seas" (*e.g.*, Hardie, 1996). The calcite-aragonite grey horizontal boundary is based on the experimental studies of the onset of carbonate mineral nucleation from seawater between 20 °C and 30 °C of Morse *et al.* (1997).

4.7 Carbonate-Secreting Organisms Mineralogy, Chemistry, and the Proliferation of Reefs

An important issue that has generated a substantial number of papers in the past two decades is how the changing chemistry of seawater may be linked to the evolution of carbonate secreting organisms and the mineralogy of the biotic calcium carbonate that is produced (*e.g.*, Wilkinson, 1979; Railsback and Anderson, 1987; Stanley and Hardie, 1998, 1999; Kerr, 2002; Montañez, 2002; Brennan *et al.*,

2004; Riding and Liang, 2005a,b; Stanley *et al*., 2005). Attempts have also been made to determine the original composition of the biotic carbonate phases and then use this information to predict the chemistry of the original seawater at the time of formation of the biogenic phases (*e.g.*, Macqueen and Ghent, 1970, Macqueen *et al*., 1974; Railsback, 1993; Dickson, 1995, 2002, 2004; Ries, 2004). For example, Ries *et al*. (2006) in laboratory experiments showed that three species of modern aragonite-producing scleractinian corals began producing calcite in artificial seawater with an ambient Mg/Ca ratio below that of modern seawater of 5:1. The corals produced progressively higher percentages of calcite and calcified at lower rates with progressively further reductions in the ambient Mg/Ca ratio. In experimental artificial seawater of Late Cretaceous composition (Mg/Ca = 1.0), as deduced from the evaporite fluid inclusion record of seawater composition, the scleractinian corals produced skeletons containing more than 30% calcite. These results indicate that the skeletal mineral used by scleractinian corals may be partially determined by seawater chemistry. Ries *et al*. further concluded that slow calcification rates, resulting from the production of largely aragonitic skeletons in chemically unfavourable seawater (Mg/Ca < 2), probably contributed to the scleractinians' diminished reef-building capacity in the calcite seas of Late Cretaceous and early Cenozoic time. It should be kept in mind that application of experimental investigations to past seawater chemistry are necessary but can be fraught with potential difficulties that include necessary assumptions about biomineralisation processes and diagenesis. Many of these issues have been explored with regard to carbon and oxygen stable isotopes and in studies of how well modern carbonate secreting organisms record the environmental conditions of their formation.

As an example of variable biogenic carbonate mineralogy during the Phanerozoic, reef-building organisms and their evolution have received major attention (*e.g.*, Kiessling *et al*., 2003). A recent compilation of the data for the inferred mineralogies of the skeletal components of reef-building organisms in terms of calcite versus aragonite plus Mg-calcite mineralogies is shown in Figure 4.11. The relative percentage of calcite in the reef-building organisms is generally lower than that for abiotic ooid calcites and highly variable. However, although the correlation is not strong, there appears to be a long-term cyclic pattern in both skeletal and abiotic ooid mineralogy. In addition, the Sr content of the reef-building organisms also follows a pattern mimicking the mineralogy of the organisms: calcitic-rich intervals coincide with times when Sr concentrations in biologically produced calcite were high and vice versa. This observation probably reflects changes in the Sr content of seawater with higher seawater Sr content coinciding with biogenic calcitic mineralogies due to the reduced incorporation of Sr in the calcitic phase as opposed to the aragonitic phase.

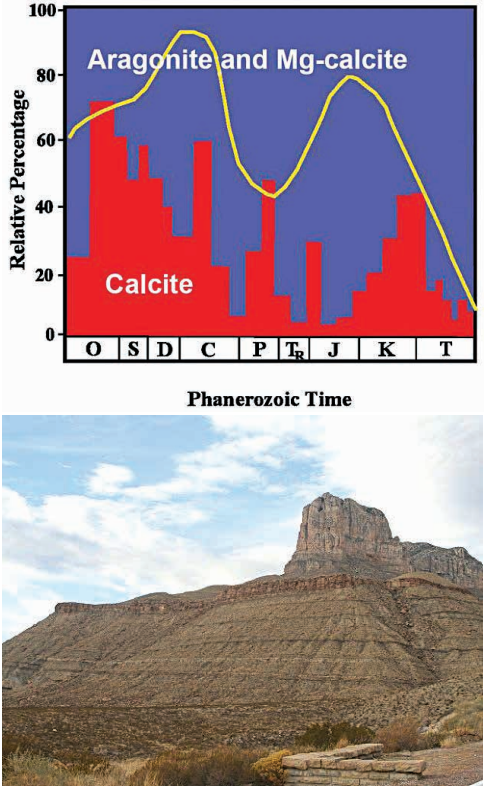

Photo courtesy of Ron Schott (geology.about.com).

Figure 4.11 **(top)** The inferred mineralogy of skeletal components of main reef-building organisms during much of the Phanerozoic. Modified after Mackenzie and Lerman (2006) and Veizer and Mackenzie (2004, based on the data of Kiessling, 2002). The yellow line is the ooid calcite versus aragonite curve from Figure 4.9. **(bottom)** The Permian (~ 265 Ma years ago) reef complex of the Guadalupe Mountains, Texas.

Concurrent with changes in the skeletal mineralogy of shallow water calcifiers throughout the Phanerozoic, the number of reef sites and the dominant calcifiers found in these reefs have also undergone major changes during this time interval (Fig. 4.12). The geologic record suggests that the proliferation of reef types has undergone several boom and bust events throughout the Phanerozoic with boom events being dominated by hypercalcifiers (organisms with high skeleton to biomass ratio) such as corals, sponges, and algae (Kiessling, 2009). On average these events did not last longer than 20 million years. One hypothesis put forward is that the variation in the abundance of reefs could be linked to the same forcings responsible for the observed variations in skeletal mineralogy such as seawater

Mg/Ca ratios and/or CO_2-carbonic acid chemistry, and thus, linked to the variation in dominant calcifiers observed between aragonite and calcite-dolomite seas (Stanley and Hardie, 1998; Kiessling, 2009). However, there is no unequivocal evidence that this is the case as expansions of coral reefs have occurred both at times of rising Mg/Ca in the Cenozoic and falling Mg/Ca in the late Jurassic (Kiessling, 2009). However, there are many other factors that control the success and distribution of reefs such as temperature, nutrients, and sea level and there may be multiple and different parameters at play for any given boom and bust event. Kiessling (2009) concluded based on the currently available data that the biotic composition of major reef builders appears to be correlated with long-term climatic changes while their abundance and geographic distribution are not.

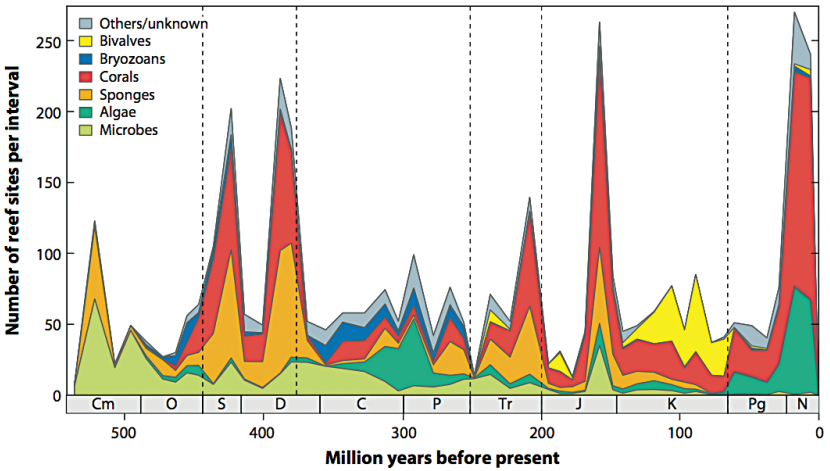

Figure 4.12 Number of reef sites per 10 million years interval throughout the Phanerozoic. A reef site is defined by several reef structures of the same age and environment within 20 km. The dashed lines indicate the documented major mass extinction events (after Kiessling, 2009).

4.8 Evaporite Deposits and Fluid Inclusions

Marine evaporites provide important clues to the history of seawater composition, including the CO_2-carbonic acid system, because they can be used to place compositional bounds on the two major seawater components that are part of carbonate minerals, calcium and magnesium. Evaporites owe their existence to an unique combination of tectonic, palaeogeographic, and sea level conditions. Seawater bodies must be restricted to some degree, but also must exchange with the open ocean to permit large volumes of seawater to enter these restricted basins and evaporate, leaving precipitated salts behind. Environmental settings

of evaporite deposition may occur on cratons or in rifted basins. Figure 4.13 illustrates that because evaporite deposition requires an unusual combination of circumstances (a "geological accident"; Holser, 1984), the intensity of deposition has varied significantly during geologic time. This conclusion implies that the volume preserved of NaCl and $CaSO_4$ per unit of time in the Phanerozoic reasonably reflects nearly the volume deposited and because of the lack of any secular trend in evaporite mass per unit time, there has been only minor differential recycling (Garrels and Mackenzie, 1971) of these rocks relative to other lithologies. As the oceans are the main reservoirs for these components, such large variations in the rate of NaCl and $CaSO_4$ output from the ocean to evaporite deposits imply changes in the salinity and chemistry of seawater. Indeed, seawater salinity may have decreased from roughly 40‰ at Cambrian time to the 35.5‰ of today (Babel and Schreiber, 2013) in part due to removal of salts from the ocean and lack of their recycling.

As mentioned previously, the near constancy of seawater composition during the Phanerozoic was advocated by a number of investigators who at the same time recognised that there could be deviations in its composition (Holser, 1963; Mackenzie and Garrels, 1966a,b; Garrels and Mackenzie, 1971; Holland, 1978). Calculations based on mineral sequences found in evaporite rocks and the development of a new method for extracting brines from fluid inclusions and determining their composition using ion chromatography provided some confirmation for Holser's (1963) earlier discovery that the Mg/Cl and Br/Cl mol ratios in brines extracted from fluid inclusions in Permian halite deposits were similar to those of modern brines (Holland, 1978; Harvie and Weare, 1980; Lazar and Holland, 1988; Hardie, 1991; Horita *et al.*, 1991). As mentioned previously, these works implied that Permian seawater composition was similar to that of today and lent some support to the assertion that seawater composition has been conservative during the Phanerozoic. Were we in for a shock! The choice of a comparison between Permian and modern seawater was unfortunate because both atmospheric CO_2 concentration and seawater chemistry were indeed similar to the modern ocean with relatively low atmospheric CO_2 and a similar seawater chemical composition**.** The similarity between Permian and modern seawater (and, indeed, atmospheric CO_2) turned out to be the exception rather than the rule.

Despite potential problems arising from the alteration of the composition of fluid inclusion brines owing to diagenesis and the fact that marine halite deposits are sporadic and unevenly distributed throughout the Phanerozoic**,** it appears at this stage that fluid inclusion data from carefully selected marine halite sequences provide a reasonably good guide to the composition of the Phanerozoic parent seawater from which the halite formed. However, one must take care in interpretation of trends with time because brine chemistry is far removed from the parent seawater and reconstruction of the chemical evolution of these brines is a considerable challenge (Holland, 2004; Babel and Schreiber, 2013).

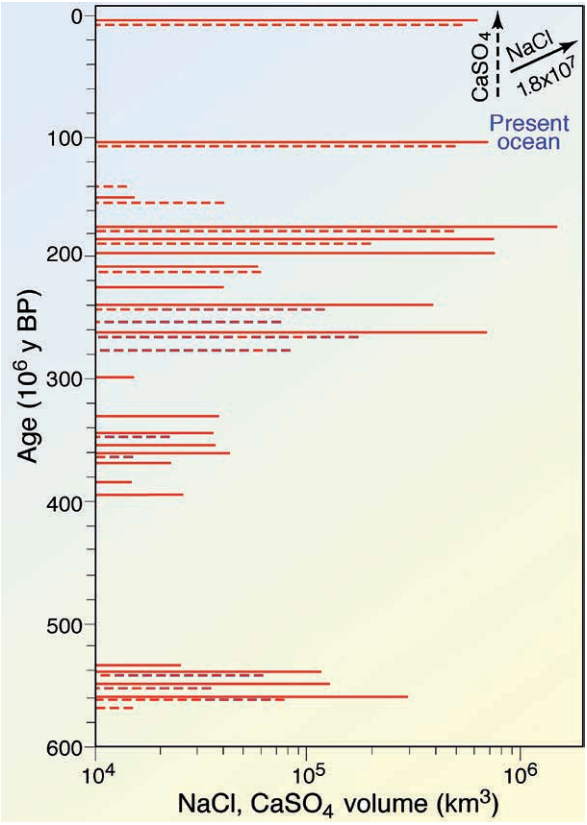

Figure 4.13 Sporadic distribution of NaCl (halite, solid lines) and $CaSO_4$ (gypsum and anhydrite, dashed lines) in marine evaporites during the Phanerozoic. There are approximately 1.8×10^7 km^3 of NaCl and 9×10^5 km^3 of $CaSO_4$ in the modern oceans (after Holser, 1984).

With these caveats in mind, Figure 4.14 shows the concentrations of dissolved Mg, Ca, and SO_4 in seawater during the Phanerozoic Eon based on marine evaporite, (halite) fluid inclusions as reviewed by Horita *et al.* (2002). (Note K appears not to have changed significantly during the Phanerozoic). One can see from the trends with age that seawater concentrations of Mg, Ca, and SO_4 have varied considerably during Phanerozoic time. Other more recent estimates by Brennan and Lowenstein (2002) for Silurian seawater, Lowenstein *et al.* (2005) for Permian seawater, and Timofeeff *et al.* (2006) for Cretaceous seawater are shown in this figure as well. Mg varies by about a factor of two, whereas Ca and SO_4 vary by about a factor of three. The relative changes of Mg and SO_4 closely track each other, but the changes in Ca over Phanerozoic time are largely the opposite of

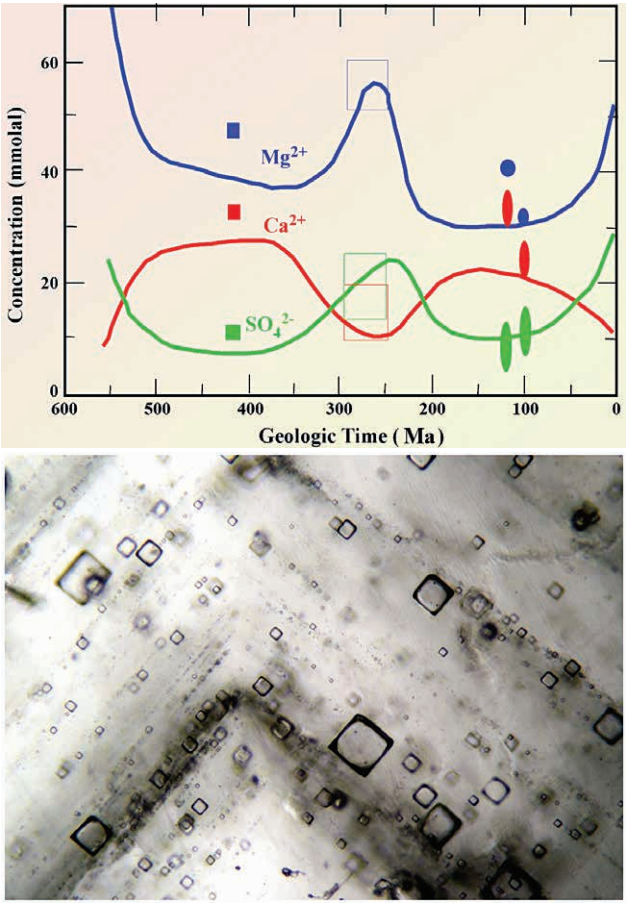

Figure 4.14 **(top)** Variation of major seawater ion concentrations during the Phanerozoic Eon as obtained from the composition of fluid inclusions in evaporites. Solid lines are based on the summary of Horita *et al.* (2002) of data from fluid inclusions in marine evaporites. Circular and ellipsoidal symbols are for Cretaceous (Timofeeff *et al.*, 2006), open squares are for Permian (Lowenstein *et al.*, 2005), and solid squares for Silurian (Brennan and Lowenstein, 2002) fluid inclusions. **(bottom)** Fluid inclusions in halite (NaCl) from the Bochnia Salt Mine, upper Zuber deposits, the Badenian of the Carpathian Foredeep in Poland. Length of the crystal equals 65 mm.

Mg and SO_4. The inverse behaviour of Mg and Ca has resulted in major changes in the dissolved Mg/Ca and SO_4/Ca ratios of seawater during the Phanerozoic Eon. The variation of Ca and Mg in seawater also implies that the dissolved inorganic carbon chemistry and speciation of seawater has changed over time,

including its saturation state with respect to carbonate minerals. In addition, the variation in SO_4 concentrations most likely affected the formation of dolomite because the precipitation of this mineral appears to be promoted by lower sulphate concentrations in seawater-like fluids**.** While these values should be taken with caution, as demonstrated by the at times significant differences of the newer data from the Horita *et al.* (2002) compilation, they are probably a reasonable representation of the current thinking that indicates very substantial variations in seawater major ion chemistry during the Phanerozoic Eon.

It is also noteworthy that other relatively direct evidence for changes in seawater chemistry has been sought using basinal brines that might be considered "mega-fluid inclusions". Although these subsurface waters suffer from a host of potential diagenetic reactions and mixing processes that could alter their composition, some of the observations are intriguing. The paper by Lowenstein *et al.* (2003) is particular interesting in this regard. It discusses how earlier work, based on the presumption of the constancy of seawater, sought to explain the composition of Silurian-Devonian Illinois basin brines through complex diagenetic processes. However, the brine's composition is similar to that estimated from fluid inclusions in marine halites of that time indicating little diagenetic alteration.

These observations have led to a variety of models and considerable discussion in the literature regarding the geologic processes and their relative importance that might have led to the variations in the major ion composition of seawater (*e.g.*, Spencer and Hardie, 1990; Hardie, 1996; Stanley and Hardie, 1998, 1999; Cicero and Lowman, 2001; Steuber and Veizer, 2002; Mackenzie *et al.*, 2008; Arvidson *et al.*, 2003, 2006, 2011; Hansen and Wallmann, 2003; Berner, 2004; Demicco, 2004; Demicco *et al.*, 2005; Locklair and Lerman, 2005; Holland, 2005, 2013). Chief controls on Phanerozoic major ion seawater variations are related to processes involving changes in weathering fluxes to the ocean, mid-ocean ridge spreading and accretion rates, with associated fluxes of seawater ridge brines, and impacts on sea level. Other factors, such as the rate of dolomite formation (Holland, 2005; Arvidson *et al.*, 2006), and the rise of the pelagic calcifiers have also been considered to be of importance at various times.

5. DEEP TIME: SOME PERTINENT EXPERIMENTAL STUDIES

Some of the basic underlying concepts about calcite-dolomite versus aragonite seas and seawater composition stem from a long series of experimental studies of calcite and aragonite nucleation and growth kinetics (for the most recent review of studies relevant to the marine environment see Morse *et al.*, 2007, which contains ~340 references). Here we discuss some of the history of those experimental results. These results are discussed in more detail and expanded on in Section 7. A central point is the strong inhibitory influence of dissolved Mg on calcite nucleation and growth which has been recognised for nearly 100 years (Leitmeier, 1909) and was extensively investigated from the mid-1950s to the early-1970s (*e.g.*, Monoghan and Lytle, 1956; Lippmann, 1960; Cloud, 1962; Curl, 1962; Simkiss, 1964; Taft and Harbaugh, 1964; Fyfe and Bischoff, 1965; Pytkowicz, 1965, 1973; Chave and Suess, 1967; Bischoff, 1968; Bischoff and Fyfe, 1968; Berner, 1971; Wollast, 1971). A similar influence of Mg on aragonite nucleation and precipitation was not observed by Berner (1975). This led to several papers in the 1980s and 1990s arguing that the Mg to Ca ratio during times of calcite seas must be considerably lower (close to 1) than the present ratio of about 5 (see previous discussion).

Experimental studies of calcite precipitation kinetics during the 1980s demonstrated not only the influence of the Mg/Ca ratio but also that of SO_4 on calcite precipitation kinetics (Reddy *et al.*, 1981; Mucci and Morse, 1983; Walter, 1986; Fig. 5.1). The difference in reaction rates caused by a change from no SO_4 to a concentration close to that of seawater was similar to the influence of changing the Mg to Ca ratio from 1 to 5. Walter (1986) also found that such a change in sulphate concentration at a Mg/Ca ratio of 1 had a much greater inhibitory influence on the aragonite precipitation rate than on the calcite rate causing a reversal in the reaction rate at a given calcium and carbonate ion activity

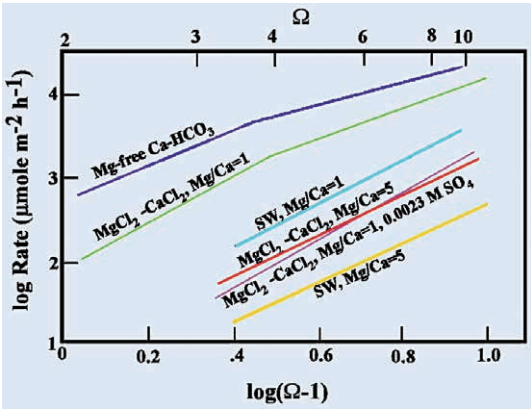

Figure 5.1 Influence of the dissolved Mg/Ca ratio and dissolved sulphate on the precipitation kinetics of calcite at ~25 °C and 1 atm. Ω is the saturation state with respect to calcite. Based on the data of Reddy *et al.*, 1981; Mucci and Morse, 1983; and Walter, 1986 (after Morse and Mackenzie, 1990).

product. It is interesting to note that this major influence by sulphate has attracted little attention in the literature on calcite-dolomite versus aragonite seas until recently (Bots *et al.*, 2011).

It has been widely observed that aragonite and calcite with significant Mg contents are dominant forms of calcium carbonate in warm tropical to subtropical waters, but in cooler high latitude waters and at depth in the ocean, the Mg content becomes gradually lower and calcite of lower Mg content becomes increasingly dominant (*e.g.,* Chave, 1954; Lees and Butler, 1972; Schlager and James, 1978; Nelson, 1988; Opdyke and Wilkinson, 1990; Rao and Jayawardane, 1994; Videtich, 1985). These trends are due to both increasing pressure with increasing depth, and most importantly decreasing temperature with depth and higher latitude, exerting some control on the formation and the preservation of calcium carbonate. Consequently, the combination of major ion seawater composition, aqueous carbonate chemistry, temperature, and pressure appear to influence carbonate mineralogy. Morse *et al.* (1997) experimentally investigated the combined influences of seawater Mg/Ca ratio and temperature on abiotic calcium carbonate precipitation. They found (Fig. 5.2) that as temperature decreased, the Mg/Ca ratio at which calcite could precipitate instead of aragonite increased such that at the current seawater Mg/Ca ratio and below about 8 ^{o}C, only calcite would precipitate. A major influence of temperature and solution chemistry on the morphology of the aragonite precipitated was also observed.

Although the Mg content in both abiotic and biotic carbonate precipitates appears to decrease with increasing geographic latitude and ocean depth, the exact mechanism(s) controlling the Mg content is poorly understood. Marine calcifiers depositing aragonite contain almost no or very little magnesium (<1 mol%) and the same is true for open ocean calcite producers, which are mostly represented by pelagic calcifiers including coccolithophorids and foraminifera. Among organisms depositing Mg calcite of various compositions, ranging from a few mol% Mg to as much as 30 mol%, there are distinct differences between different species. Clearly, there is a strong taxonomic control on the magnesium content of calcitic skeletons (Chave, 1954), but the observed latitudinal trends suggest a direct or indirect control by environmental parameters such as aqueous carbonate chemistry, temperature, and light. One hypothesis suggests that variations in organism growth rates, which depend on environmental conditions and also are a function of the availability of food and nutrients, may explain the observed latitudinal trend in skeletal Mg content (Moberly 1968; Mackenzie *et al.*, 1983). *Fred* encouraged his and *Keith Chave*'s Ph.D. student *Kitty Agegian* to investigate this problem by some carefully performed mesocosm experiments in which the coralline algal *Porolithon gardineri* was grown in a flowing seawater mesocosm chamber subjected to differing temperatures and carbonate mineral saturation state conditions. These experimental manipulations confirmed that growth rate may be important in determining the Mg content of the *Porolithon gardieneri* but temperature and saturation state also have an effect. (*e.g.,* Agegian, 1985; Mackenzie and Agegian, 1989). More recently Ries (2011) reached an opposite conclusion with respect to growth rate and its effect on the Mg content of coralline

algae. These variables are not necessarily mutually independent in nature, and it is not always easy to separate the influence of one variable from another on the Mg content of a biotic Mg-calcite phase. There is obviously still a strong need for some cleverly designed experiments that would elucidate the mechanistic controls on the Mg content in calcareous shells and skeletons.

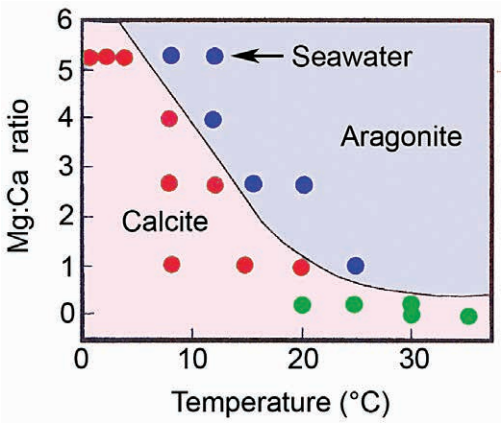

Image courtesy of Chip Clark, Smithsonian Institution (catalog number 104908-00; photo number: 97-35096).

Image credit: Volker Betz.

Figure 5.2 **(top)** Influences of seawater dissolved Mg/Ca ratio and temperature on the mineralogy of the calcium carbonate nucleated (after Morse *et al*., 2007; based on Morse *et al*., 1997). Blue dots are aragonite; yellow dots calcite; green dots indicate first calcite precipitated followed by some later aragonite due to increasing Mg to Ca ratio with extent of precipitation. **(bottom)** Photographs of a calcite twined crystal from Deming, New Mexico, USA (left) and an aragonite specimen from Auvergne, France (right).

In Section 7 we use the experiments described here and others to complement the observational evidence discussed above and modelling efforts below (Section 6) to arrive at a tentative picture of the evolution of the ocean-atmosphere-carbonate sediment system during Phanerozoic time.

6. DEEP TIME: MODELLING OF ATMOSPHERIC CO_2 AND THE MARINE CO_2-CARBONIC ACID-CARBONATE SYSTEM

6.1 Initial Considerations

In this section we investigate the changes in the CO_2-carbonic acid system of seawater as coupled to atmospheric CO_2 variations and weathering inputs from land during the Phanerozoic Eon based mainly on modelling efforts. We recognise the fact that modelling has its drawbacks as expressed in the phrase "garbage in, garbage out", but modelling constrained by both observational data and experimental information is in our opinion the most robust approach to understanding the behaviour of complex systems like the Earth's exogenic system or ecosphere, including its ocean and atmosphere. For *Fred* these efforts in modelling the Earth's exosphere were initially a delightful collaboration, among others, on two papers between him and his colleagues *Bob Garrels* and *Abraham Lerman*. The first paper (Lerman *et al*., 1975), using the phosphorus cycle as an example, set up the mathematical methodology for the modelling of geochemical cycles. The second paper was published in the *American Scientist* (Garrels *et al*., 1976) and considered the controls of atmospheric CO_2 and O_2 on the multi-million year geologic time scale. Interestingly because of the generalised nature of the journal in which the paper was published, it was not a widely disseminated paper and a number of the ideas were not picked up on until later.

At the completion of the Garrels *et al.* (1976) paper involving the global cycle of CO_2 and O_2, *Fred* diverted his attention somewhat to global models of the behaviour of a variety of trace elements in the atmosphere and of the minor elements aluminum and lithium in the ocean (*e.g.*, Mackenzie *et al*., 1979; Lantzy and Mackenzie, 1979; Stoffyn and Mackenzie, 1982; Egli-Stoffyn and Mackenzie, 1984). However at the same time, he encouraged his Ph.D. student, *John Pigott*, to investigate the original mineralogy of ooids through the Phaerozoic Eon in the anticipation that their mineralogy might be a clue to the evolution of the Earth's ocean and atmosphere. This hypothesis was based on *Philip Sandberg's* initial comparison of the differences in the original mineralogy and fabric of Pleistocene and Recent Great Salt Lake ooids with those of Mississippian age (1975). *John* painstakingly looked at several hundred petrographic thin sections of various Phanerozic carbonate rock units from a number of sedimentary basins. His work led to the dataset for the original depositional mineralogy of ooids depicted in Figure 4.9. The results of this work were published in the *Journal of the Geological Society of London* (Mackenzie and Pigott, 1981) and included a model interpretation of the data that involved two alternating cycles of originally calcite and aragonite/magnesian calcite mineralogies. *John* and *Fred* concluded that these cycles were ultimately driven by global tectonic changes and labeled the cycles accordingly submergent and emergent tectonic cycles. The former were

hypothesised to be times of high plate accretion rates, high sea levels, and high atmospheric CO_2 levels; the latter the opposite. The former become the calcite seas and the latter the aragonite seas of *Sandberg* (Sandberg, 1983). This work initiated *Fred's* next stage in modelling the Earth's exosphere discussed in further sections of this article.

In part constrained by the observational and experimental data discussed previously and other considerations, numerous models have been constructed to estimate changes in atmospheric carbon dioxide partial pressure (pCO_2) during the Phanerozoic Eon (*e.g.*, Berner *et al*., 1983; Mora *et al*., 1996; Pearson and Palmer, 2000; Wallmann, 2001; Nordt *et al*., 2002; Demicco *et al*., 2003; Edmond and Huh, 2003; Hansen and Wallmann, 2003; Royer *et al*., 2004; Haworth *et al*., 2005; Guidry *et al*. 2007; Mackenzie *et al*., 2008; Arvidson *et al*., 2006, 2011; Berner, 2004, 2006; Royer, 2006; Li and Elderfield, 2013). Estimates of maximum atmospheric pCO_2 values exceed 6,000 μatm or more than 20 times the preindustrial modern value at times (Fig. 6.1). For modern seawater with a salinity of 35‰ and a total alkalinity (TA) of 2.3 mmol kg^{-1} at 0 °C and one atmosphere pressure, seawater in equilibrium with this atmospheric CO_2 concentration would be undersaturated with respect to both calcite ($\Omega c = 0.54$) and aragonite ($\Omega a = 0.36$) at these conditions. It would have a pH of about 7 on the seawater pH scale and a dissolved inorganic carbon content of 2.44 mmol kg^{-1}. Equilibrium with aragonite would be obtained only at an alkalinity of about 4.0 mmol kg^{-1}. For comparison, it should be noted that modern seawater composition of S = 35‰ at 25 °C and when at equilibrium with the atmosphere (pCO_2 = 390 μatm) is about 4 times supersaturated with respect to aragonite and 6 times supersaturated with respect to calcite.

There also have been many model-based papers attempting to estimate the impact of variable pCO_2 values on seawater saturation state with respect to carbonate minerals and the CO_2-carbonic acid system parameters, such as pH, during all or parts of the Phanerozoic Eon (*e.g.*, Arvidson *et al*., 2000, 2006, 2011; Zeebe, 2001; Tyrrell and Zeebe, 2004; Hönish and Hemming, 2005; Riding and Liang, 2005a,b; Locklair and Lerman, 2005; Guidry *et al*., 2007; Mackenzie *et al*., 2008, 2011). Seawater DIC, based on the *MAGic* (*M*ackenzie, *A*rvidson, *G*uidry *i*nteractive *c*ycles, see below for more detailed discussion of the model) model estimates of Arvidson *et al*. (2006), may have undergone large relative changes of up to about five times the current value of roughly 2.2 mmol kg^{-1} (Fig. 6.1). A significant amount, but not all of this variation, is believed to be the result of large changes in the partial pressure of atmospheric carbon dioxide. It should be kept in mind that *MAGic* seawater chemistry is calculated using a one-box global ocean reservoir with no proviso for geographical or depth variations in ocean chemistry. Also as we will see later, the depositional flux of dolomite to the sea floor significantly affects the DIC content of seawater through Phanerozoic time and this flux is problematic.

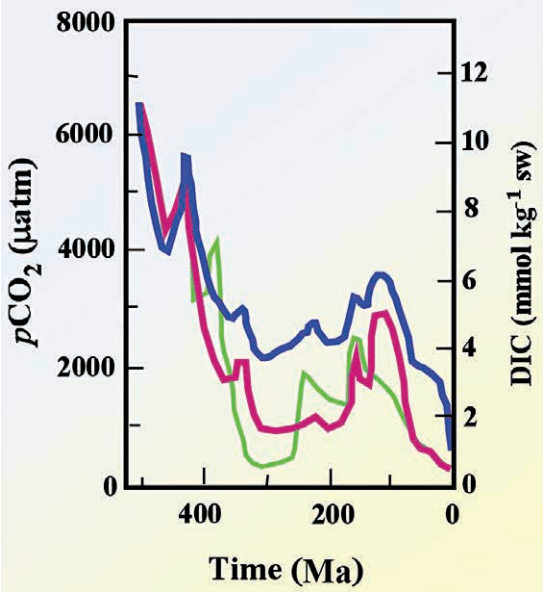

Figure 6.1 Changes in dissolved inorganic carbon (DIC, heavy purple line; Arvidson *et al.*, 2006) and pCO_2 during the Phanerozoic Eon (heavy dark blue line from *MAGic*, Arvidson *et al.*, 2006; thinner light green line from *GEOCARB III*, Berner and Kothavala, 2001).

In the initial modelling runs using the *MAGic* model, Arvidson *et al.* (2006) also attempted to estimate the saturation state of the global ocean with respect to calcite, aragonite, and dolomite. The results are shown in Figure 6.2 as the modelled seawater ion activity product (IAP) to solubility product (K_{sp}) ratio for aragonite and dolomite (note this ratio for calcite is 1.51 times that of aragonite at 25 °C). Although absolute values should be taken with caution, two important conclusions can be made from this preliminary work: (1) during much of the Phanerozoic Eon, the saturation state of seawater with respect to carbonate minerals varied significantly, and (2) although the changes in calcite and aragonite saturation state must inherently track each other, dolomite does not always track aragonite saturation state because of other confounding factors that influence its saturation state such as the Mg concentration of seawater. In a later synthesis section of this article, *MAGic* model results for the atmosphere, ocean, and sediment compositional changes during the Phanerozoic will be discussed in more detail.

Based on the observation that the calcite compensation depth (CCD), *i.e.* the depth at which calcite is no longer found in the sediments, in the ocean has varied relatively little during the past 100 million years, an alternative modelling approach for a portion of the Phanerozoic Eon was used by Tyrrell and Zeebe (2004) to conclude that for this interval of time, the saturation state of seawater with respect to $CaCO_3$ has been close to constant. Based on this conclusion, the carbonate ion concentration was estimated to have more than quadrupled since the Cretaceous Period. Surface ocean pH was calculated to have increased in a close to linear fashion from about 7.5 in the Mesozoic to the modern value of 8.2. Model reconstructions of long-term changes in Phanerozoic mean ocean surface

pH have also been calculated at 20 million year intervals by Ridgwell (2005; Kump *et al.*, 2009; Zeebe and Ridgwell, 2011).

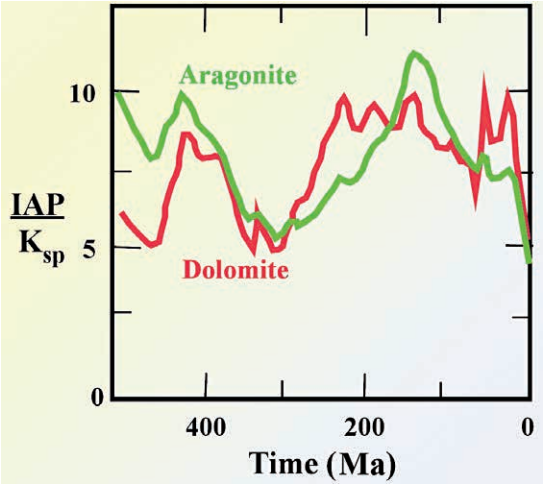

Figure 6.2 The variation in the saturation state of seawater (IAP/K_{sp}) in equilibrium with the atmosphere with respect to aragonite and dolomite. The saturation state with respect to calcite is 1.51 times that of aragonite (modified from Arvidson *et al.*, 2006).

Based on the considerations described in this section, Table 6.1 has been constructed for the estimated composition of seawater at times of what appear to be the most extreme differences from modern seawater. The times chosen were the Albian Stage of the Cretaceous Period and the Ordovician Period (calcite-dolomite seas). The data for the Albian for K, Mg, Ca, and SO_4 concentrations were primarily obtained from Timofeeff *et al.* (2006). The composition of the seawater was initially set at the Cl concentration of modern seawater and the charge was balanced using Na^+. The pCO_2 estimate of Arvidson *et al.* (2006) was used to calculate the DIC concentration for their estimate of a supersaturation with respect to aragonite (Ω_{arag}) of 10, resulting in a value of ~9 mmol kg^{-1} of DIC which is close to their estimate of 10 mmol kg^{-1}. The calculations were based on a Pitzer equation-based program (*e.g.*, Pitzer, 1973, 1975). The calculations were also carried out for DIC for a Ω_{arag} = 1. pH values were also calculated and are in reasonable agreement with the estimates of Zeebe (2001) for seawater pH during the Cretaceous.

The same general approach was taken with Ordovician seawater composition except Mg, Ca, and SO_4 concentrations were estimated from the data of Horita *et al.* (2002). K and Cl concentrations of modern seawater were used and the charge balance was obtained using Na^+. The pCO_2 estimate of Arvidson *et al.* (2006) was used to calculate the DIC concentration for their estimate of a supersaturation with respect to aragonite (Ω_{arag}) of 10, resulting in a value of ~7 mmol kg^{-1} DIC which is lower than their estimate of ~10 mmol kg^{-1}. Discussions of the details of the estimated composition of seawater for calcite-dolomite seas as given in the table are left for a further section.

Table 6.1 Estimated composition and related parameters of "calcite-dolomite seas" seawater for the Albian Stage of the Cretaceous Period and the Ordovician Period. Ion concentrations and DIC are mmol kg^{-1}. pCO_2 values are in μatm. See text for sources and discussion. Note that DIC and pH were calculated at both a Ω_{arag} of 10 and 1 (in parentheses).

	Albian (~106 Ma)		Ordovician (~425 Ma)	
Parameter	**Value**	**% Mod SW**	**Value**	**% Mod SW**
Na^+	425	86	443	90
K^+	11	100	11	100
Mg^{2+}	42	58	38	73
Ca^{2+}	36	214	28	272
Cl^-	565	100	565	100
SO_4^{2-}	9	39	7	25
DIC	9 (1)	409 (46)	7 (2)	318 (91)
pCO_2	2800	1000	5300	1893
pH	8.0 (7.2)	Δ= 0.2 (1.0)	7.8 (7.1)	Δ= 0.4 (1.1)
Ω arag	10 (1)	2.5x (0.25x)	10 (1)	2.5x (0.25x)
Mg/Ca	1.2		1.4	

6.2 Some New Modelling Results and Synthesis

In this section we present, in the context of the information previously discussed, an updated synthesis picture of the long-term evolution of the Phanerozoic land-ocean-atmosphere-carbonate sediment system with emphasis on the biogeochemical cycle of carbon. We use primarily the numerical output from the Earth system model *MAGic* (Arvidson *et al.*, 2006, 2011) to explore the evolution of the Earth's surface system. The data we present are for the standard runs of *MAGic* based on the original *MAGic* model (Arvidson *et al.*, 2006) as revised in Arvidson *et al.* (2011).

There are a number of Earth system models in the literature (*e.g.*, Berner and Canfield 1989; Hansen and Wallmann, 2003; Berner 2004; Bergman *et al.*, 2004; Ridgwell, 2005; Arvidson *et al.*, 2006; Arndt *et al.*, 2010; Zeebe, 2012a; Li and Elderfield, 2013) that discuss one aspect or another of the carbon cycle for a specific reservoir or a specific period of time. However, there is only one model that we are aware of dealing with the long-term evolution of the carbon cycle as coupled to 10 other relevant element cycles in the exogenic system of

land-ocean-atmosphere-sediment and includes interactions with the deeper endogenic system; this is the model *MAGic*. The foundation for *MAGic* was originally laid out in the paper by Garrels and Mackenzie, *A Quantitative Model for the Sedimentary Rock Cycle* (1972), which described the steady-state cycling of 11 elements important in the formation and destruction of sedimentary rocks: Al, C, Ca, Cl, Fe, K, Mg, Na, S, Si, and Ti. This model, which incorporated much of the thinking of Garrels and Mackenzie previously set forth in their book *Evolution of Sedimentary Rocks* (1971), was based on a steady state mass balance of the elements in the atmosphere, ocean, and sedimentary lithosphere that was consistent with the observed composition of the atmosphere, ocean, stream and groundwater reservoirs, as well as the mass–age distribution of the chemical and mineralogical composition of sedimentary rocks. Conditions were incorporated in the model that allowed for rapidly recycling and more slowly recycling sedimentary reservoirs with material transfers between each due mainly to post-depositional diagenetic processes. The model was secular and cannabilistic and did not allow for inputs involving endogenic processes that act to reconstitute primary igneous crystalline phases and volatile acids, like CO_2, from sediments, organic matter, and dissolved constituents. This implied that there was little exchange of materials between the sedimentary lithosphere and the endogenic cycle involving the mantle. Garrels and Mackenzie recognised this but were impressed how well the 11-element sedimentary system balanced without including these exchanges.

In a later reconstruction of the model (Garrels *et al*., 1975), the original model was constructed as a biogeochemical box model (Fig. 2.9). This model formed, with the addition of endogenic fluxes, the basis of the first model dealing quantitatively with the carbonate-silicate geochemical cycle and variations in atmospheric CO_2 concentrations for part of Phanerozoic time (Berner *et al*., 1983). It is also the foundation of *MAGic* with the provisos that: (1) *MAGic* is set up in an initial steady state condition that can be perturbed and accounts for the temporal changes in atmosphere, ocean, and sediment composition followed through Phanerozoic time; (2) the model includes provision for the interactions between seawater and oceanic crust, the cycling and complex feedbacks between O_2, iron, phosphorus, and organic matter, the complex feedback relationships between atmospheric CO_2, global temperature, the terrestrial biosphere, and the rate of chemical weathering; and (3) not only can the compositional changes in atmospheric CO_2 and O_2 be explored in *MAGic* but also that of seawater and carbonate sediment composition through the Phanerozoic Eon.

It should be pointed out that the primary drivers for the mid to late Palaeozoic and the late Cenozoic decreases in atmospheric CO_2 levels in both *MAGic* and the various renditions of the models *BLAG* (*B*erner, *L*asaga, *a*nd *G*arrels, 1983) and *GEOCARB* (Berner *et al*., 1983; Berner and Kothavala, 2001; Berner, 2004, 2006) are, among other factors, mainly through the negative weathering feedbacks involving reduction of atmospheric CO_2 levels, and hence temperature, because of lessened degassing of volcanic CO_2, and importantly, the evolution of land plants and their succession. For the past 100 Ma, an "uplift driven climate

change" hypothesis (Raymo *et al.*, 1988; Raymo and Ruddiman, 1992; Li and Elderfield, 2013), has been proposed involving the late Cenozoic tectonic uplift of mainly the Tibetan Plateau, which may have enhanced physical erosion and monsoonal rainfall, thus enabling the increased drawdown of atmospheric CO_2 levels by silicate weathering.

The model *MAGic* was initially fully put together by *Rolf Arvidson*, a former Ph.D. student of *Fred's*, who studied in *Fred's* laboratory and graduated in 1998 with a dissertation entitled *Kinetics of Dolomite Precipitation with Application to Changes in Seawater Saturation State over the Past 100 Ma*, and gone on to be a Researcher at Rice University in Houston, Texas, USA and subsequently a Professor at the Universitat Bremen in Germany. After his Ph.D., *Rolf* spent some time with *Fred* in Hawaii in the early twenty-first century developing the conceptual and initial numerical model of *MAGic*. *Fred* then encouraged another of his former Ph.D. students, *Michael Guidry*, after graduation in 2002 to engage in the modelling efforts. *Michael* studied apatite dissolution kinetics with application to the problem of the role of tectonics and phosphorus weathering fluxes in the Phanerozoic phosphorus cycle. Since this time *MAGic* has been updated and revised a number of times. The numerical output described in further sections of this monograph is mainly from the latest version of the model (Arvidson *et al.*, 2011; see also Arvidson *et al.*, 2006; Guidry *et al.*, 2007; Mackenzie *et al.*, 2008), with some exceptions as noted.

Image from Michael Guidry collection.

Figure 6.3 Michael Guidry, Fred Mackenzie, and Rolf Arvidson at the 15th Goldschmidt Conference, Moscow, Idaho, USA in 2005. This was just prior to the first publication of the *MAGic* model (Arvidson *et al.*, 2006).

Figure 6.4 is a schematic diagram of the *MAGic* global biogeochemical model illustrating its general features. The Earth's surface and near-surface global environment is divided into a series of entities termed reservoirs (boxes) and material transports among the boxes are described by physical, chemical, and biological processes that move materials from one box to the other. Associated with each process is a flux, that is, a rate of transfer usually given in terms of mass per unit time. Such an Earth system model is a global biogeochemical model (see Supplementary Information SI-4), and in *MAGic,* 11 element cycles are explicitly coupled to corresponding cycles of other elements via a reaction network. This network incorporates the basic reactions controlling atmospheric carbon dioxide and oxygen concentrations, continental and seafloor weathering of silicate and carbonate rocks, net ecosystem productivity, basalt-seawater exchange reactions, precipitation and diagenesis of chemical sediments and authigenic silicates, oxidation–reduction reactions involving C, S, and Fe, and subduction-decarbonation reactions. Coupled reservoirs include shallow and deep cratonic silicate and carbonate rocks and sediments, seawater, atmosphere, oceanic sediments and basalts, and the shallow mantle (see Arvidson *et al.*, 2006 for details).

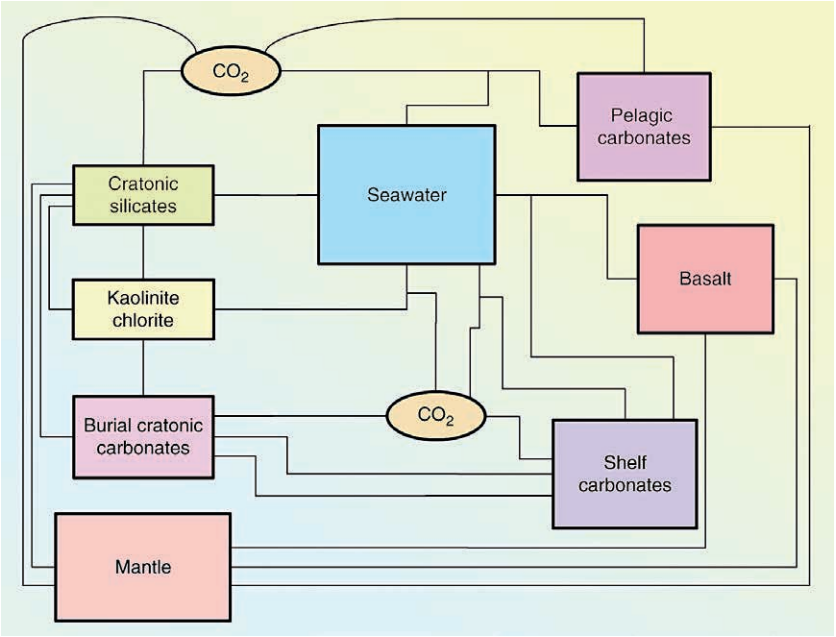

Figure 6.4 Schematic diagram of the Earth system model *MAGic* showing the major reservoirs and the coupling network among the reservoirs (after Arvidson *et al.*, 2006, 2011). Figure 6.5 illustrates in detail one subcycle of the model, that of the calcium, magnesium, silicate, carbonate, carbon dioxide subcycle.

The model *MAGic* has been mainly employed to investigate the long-term, millions to tens of million-year compositional history of the Phanerozoic ocean-atmosphere-carbonate sediment system. Relatively short-term events like the changes accompanying mass extinctions (Table 6.2) have not been dealt with to date in any detail in the model. This should be kept in mind in the following discussion since these events, whatever their ultimate cause, be they meteorite impacts, volcanic eruptions, or rapid sea level changes, can reset the "compositional clock" and disturb the otherwise smoother changes in geochemical and environmental parameters calculated for the long time scale.

Table 6.2 Brief summary of geochemical and environmental phenomena associated with mass extinctions (modified from Kump, 2004).

Extinction	$\delta^{13}C$ excursion	$\delta^{34}S$ excursion	$^{87}Sr/^{86}Sr$ excursion	Extra-terrestrial iridium?	Anoxia?	Global temperature change	Sea level change
Cretaceous-Palaeogene ~65Ma	(-)	(0)	(+) (short term)	Yes	No		After Maastrichtian. lowstand
Triassic-Jurassic ~208 Ma	(-)	(0)	(0)	Yes	No		After late Triassic
End of Permian ~245 Ma	(-)	(+)	(+) (from Palaeozoic minimum)	No, but Fe-Si-Ni grains and fullerenes present	Yes		From late Permian low stand
Late Devonian ~360 Ma	Generally (+) but (-) right at boundary	(+)	(+) (from Devonian minimum)	No (but yes above and below boundary)	Yes (but may have ended just before boundary)		
Late Ordovician ~438 Ma	(+) (1^{st} wave) (-) (2^{nd} wave)	(0)	(+) (from Ordovician minimum)	No	Yes, before and after glaciation	then	then

Also, before going further, it is important to remind ourselves that changes in seawater composition, which are partly tied to changes in atmospheric composition and vice versa, play a strong role in biological evolution that, in turn, leads to feedbacks on the compositional changes in these reservoir systems (Katz *et al*., 2007; Guidry *et al*., 2007; Kump *et al*., 2009). As an example of the coupling between changes in atmosphere–seawater chemistry and biological evolution, one may look at the emergence of the coral organisms that formed massive reefs. Some palaeontologists have noted that massive coral reefs are less common in the Palaeogene than in the Neogene (Budd, 2000; Perrin, 2002). This change in abundance has been attributed to the decline in atmospheric CO_2 during the Cenozoic, thus leading to a less acidic ocean water and/or to the rising Mg/Ca ratio of seawater from the Palaeogene to the Neogene that led to a transition from ocean waters whose chemical composition favoured calcite precipitation (calcite seas, Sandberg, 1983; calcite-dolomite seas, Mackenzie *et al*., 2011) to waters that favoured aragonite precipitation (aragonite seas, Sandberg, 1983). This change, in turn, gave rise to the expansion of coral reefs dominated by corals that secrete carbonate skeletons of aragonite (Stanley, 2006). Now let us explore some of the details of the *MAGic* model and its output in terms of the Phanerozoic evolution of the Earth's exogenic system, basically its ecosphere.

6.2.1 *Calcium-Magnesium-Silicate-Carbonate-CO_2 subcycle cycle of MAGic*

The global biogeochemical cycle of Ca and Mg is the most important in terms of its interactions with carbon and the consequent long-term controls on seawater alkaline earth and carbon chemistry, as well as atmospheric CO_2. In turn, changes in seawater chemistry and atmospheric CO_2 have influenced pelagic and benthic carbonate mineral biomineralisation and production over geologic time. The calcium-magnesium-silicate-carbonate-CO_2 subcycle of the model *MAGic,* which is most applicable to the discussion here, is shown in Figure 6.5. It should be recognised that although this subcycle appears complex, it is coupled in the reaction network to several other relevant biogechemical element cycles in *MAGic* and thus the picture of the true natural behaviour of the system is even more complex, but "this is the nature of the beast".

With reference to Figure 6.5, Ca and Mg are initially weathered from continental silicates and carbonates by carbonic and sulphuric acids. The Ca in river water is mainly derived from the weathering of calcite and dolomite and the dissolution of silicate minerals, particularly felsic plagioclase (Ca, Na aluminosilicate). Magnesium is derived from $CaMg(CO_3)_2$ weathering and the weathering of mafic silicate minerals such as amphibole, pyroxene, and biotite (Fe- and Mg-rich silicate minerals). The dissolved inorganic carbon (mainly bicarbonate) is derived from the weathering of carbonate and silicate rocks in the presence of CO_2-charged soil and ground waters; the CO_2 being mainly derived from terrestrial plant photosynthesis and subsequent degradation of organic carbon and root respiration in soils. Ca and Mg are also produced during weathering

from dissolution of evaporite minerals. The resultant dissolved constituents are transported to the oceans by rivers, and less importantly, by ground waters. Once present in seawater, these components are re-deposited in shelf environments as primary or secondary calcite and aragonite, dolomite and $CaSO_4$ and $MgSO_4$ salts in evaporite deposits (Babel and Schreiber, 2013). Subsequent to deposition, these minerals either re-enter the weathering cycle through uplift and exposure or can be removed to deeper burial regimes.

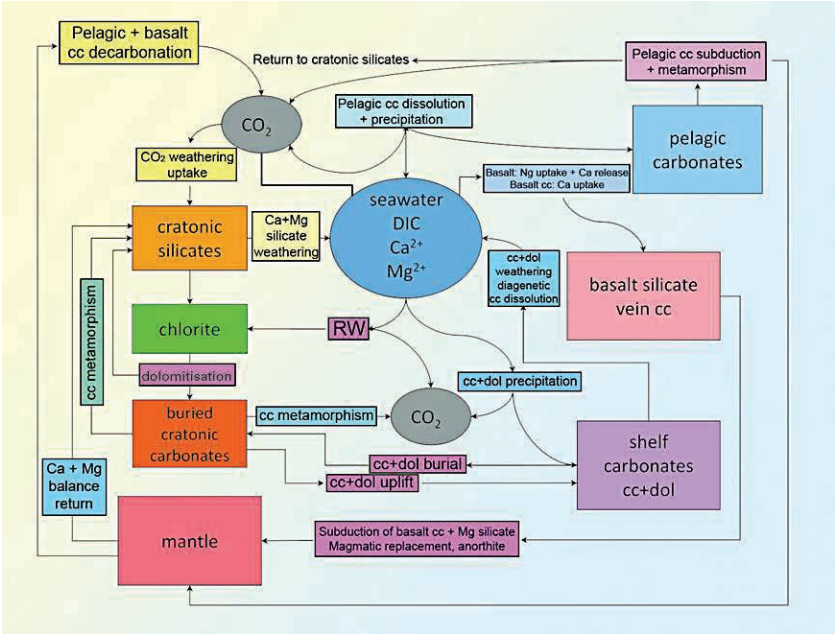

Figure 6.5 The calcium-magnesium-silicate-carbonate-CO_2 subcycle of the model *MAGic* showing reservoirs and processes moving constituents from reservoir to reservoir. This subcycle is coupled to several others in the reaction network of *MAGic* and is important in terms of the controls on atmospheric CO_2 and ocean carbon chemistry on the geologic deep time scale. The oval boxes denote the reservoirs of seawater and the atmosphere and the large rectangular boxes other material reservoirs as designated. The arrows represent the direction of transfer of materials from one reservoir to another, and the small rectangular boxes denote the processes involved in the model *MAGic*. CC is calcite and aragonite ($CaCO_3$) and dol is dolomite [$CaMg(CO_3)_2$]; RW is reverse weathering; and DIC is dissolved inorganic carbon (modified from Arvidson *et al.*, 2006).

In pelagic environments encompassing the continental slope and rise and deep ocean, only calcium carbonate is deposited, and as far as we are aware in the present and past oceans, no dolomite; thus, the total carbonate flux is partitioned between shelf and pelagic regimes. Although other factors may play

a role (Arvidson *et al.*, 2011), the precipitation rate of shelf dolomite in *MAGic* is controlled by seawater saturation state and temperature (Arvidson and Mackenzie, 1999). In addition, the accumulation of dolomite is a function of the shelf area available for deposition of carbonate sediment. This function is estimated from Quaternary dolomite depositional fluxes in shallow water environments and the submerged shelf area as a function of time and is normalised to its Quaternary value. Dolomite is also formed in the shelf environment where the oxidation of organic matter (so-called organogenic dolomitisation) is tied to the rate of microbial sulphate reduction and production of dissolved inorganic carbon. After deposition, pelagic calcite is either subducted to the mantle or removed to a metamorphic regime, such as deep burial in sedimentary basins like the Gulf Coast, USA. Both of these pathways lead to decarbonation reactions that serve to return material to the weathering cycle. This is the classic Urey-Ebelmen reaction simply written:

$$CaCO_3 + SiO_2 = CaSiO_3 + CO_2, \tag{6.1}$$

leading to the release of CO_2 to the atmosphere via volcanism and metamorphism in the subsurface of deep sedimentary basins. The latter process can be more precisely represented by the burial metamorphic reaction involving the reactants dolomite, kaolinite, quartz, and water and the products of chlorite, calcite, and CO_2 (Hutcheon *et al.*, 1980; Holser *et al.*, 1988)

$$5CaMg(CO_3)_2 + Al_2Si_2O_5(OH)_4 + SiO_2 + 2H_2O = Mg_5Al_2Si_3O_{10}(OH)_8 + 5CaCO_3 + 5CO_2, \tag{6.2}$$

where $CaMg(CO_3)_2$, $Al_2Si_2O_5(OH)_4$, SiO_2, H_2O, $Mg_5Al_2Si_3O_{10}(OH)_8$, $CaCO_3$, and CO_2 are, respectively, dolomite, kaolinite, quartz, water, chlorite, calcite, and carbon dioxide.

The mantle itself does not constitute a reservoir *per se* in the *MAGic* model but simply represents a collection point for return fluxes to either the silicate (basaltic or continental crust) or atmospheric reservoirs. Basalt-seawater reactions result in the uptake of Mg and DIC from seawater and the release of Ca to seawater. Mg uptake is assumed to be first order with respect to the Mg concentration in seawater and its uptake is modified by a time-dependent parameter reflecting the rate at which the seafloor spreads. The complementary release of Ca from basalt during seawater–basalt reactions, although identical to the Mg uptake flux in the steady state (Quaternary) condition, is allowed to vary during time to balance with the uptake fluxes. This variation is related to the maintenance of the proton (*i.e.* CO_2) balance between seawater and hydrothermal fluids within the basalt (see detailed explanation in Arvidson *et al.*, 2006). In addition, some of the Ca derived from reactions with mafic silicate minerals in seafloor basalts during basalt-seawater reactions in the shallow seafloor is precipitated within the basalt and can be subducted to depth where its decarbonisation leads to release of CO_2 to the atmosphere via volcanism.

Diagenetic alteration of shelf and pelagic sediments also results in release of Ca to seawater that is considered for modelling purposes to be a first order flux with respect to sediment mass. Magnesium uptake by the sediment to form chlorite, a composition representative of a neoformed magnesium silicate clay mineral, is allowed to vary according to the mass of Mg in the ocean. The Mg from the chlorite is transferred from the chlorite reservoir to react with buried calcite to form burial dolomite, an important process of secondary dolomite formation (Holland and Zimmerman, 2000; Arvidson *et al.*, 2006; 2011). The rate of burial dolomite formation is consequently limited by the size of the chlorite reservoir. This dolomite is eventually returned by uplift to the continental weathering regime, and burial calcite not consumed by dolomitisation or uplift eventually returns CO_2 to the atmosphere and Ca to the silicate reservoir by metamorphic decarbonation.

The above cycle of Ca, Mg, carbonate, and CO_2 is tied to that of the biogeochemical cycle of silica. Silica is released to river and ground waters during the chemical weathering of silicate minerals in rocks and in more recent geologic time, but less importantly, because of the dissolution of silica phytoliths in plants (see *e.g.*, Katz *et al.*, 2007). Since the appearance of organisms such as diatoms, radiolarians, dinoflagellates, and sponges that secrete siliceous opal-A skeletons, the dissolved silica entering the ocean from the weathering source, and from both low- and high-temperature basalt–seawater reactions, has been removed from the ocean primarily by the precipitation of the biogenic silica phase opal-A ($SiO_2 \cdot 2H_2O$). During early diagenesis on the seafloor, some of this silica, upon dissolution in the pore waters of sediments, may precipitate in reverse weathering reactions, leading to the neoformation of silicate phases in the sediments (Mackenzie and Garrels, 1966a,b; Mackenzie *et al.*, 1981; Michalopoulas and Aller, 1995). The net amount of opal-A buried in the sediments goes through a series of diagenetic reactions that convert it to quartz (SiO_2) on the longer time scale. Some of the buried quartz subsequently reacts with calcite at the higher temperatures of the subducted slab of the seafloor to form calcium silicate minerals represented by wollastonite ($CaSiO_3$) in the Urey-Ebelmen reaction (equation 6.1) and release CO_2 to the atmosphere via volcanism. The quartz can also undergo reactions as represented schematically in Equation (6.2) leading to seepage of CO_2 from deep sedimentary basins (Mackenzie and Pigott, 1981; Berner *et al.*, 1983; Berner and Kothavala, 2001; Berner, 2004; Milliken, 2004). However, most of the quartz silica is uplifted to the surface environment where it can be dissolved during weathering or recycled in the solid phase (Wollast and Mackenzie, 1983).

Now with some appreciation of the scheme for the Ca-Mg-carbonate-CO_2-Si subcycle of the *MAGic* model, we can consider some of the numerical results of the model and their accordance with proxy or other data for the evolution of the ocean-atmosphere-carbonate sediment system during the Phanerozoic. Let us start with the weathering and basalt-seawater reaction fluxes.

6.2.2 *Ca, Mg, and DIC weathering and basalt-seawater reaction fluxes through Phanerozoic time*

Figures 6.6 to 6.8 show the calculated Ca, Mg, and DIC weathering and basalt-seawater reaction fluxes during the Phaneozoic.

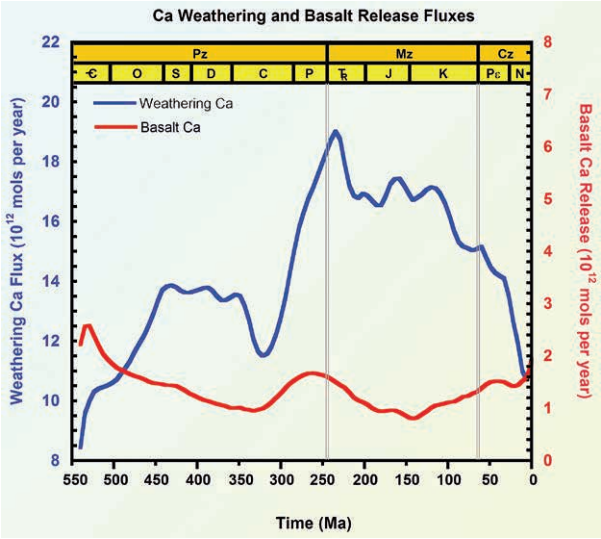

Figure 6.6 The results of numerical calculations from *MAGic* showing the calcium flux to the ocean via rivers and groundwaters from weathering reactions on land and the calcium released to the ocean due to basalt-seawater reactions in the seafloor in 10^{12} mol yr^{-1}. Notice in particular the rough cyclic pattern of higher weathering fluxes of the mid-Palaeozoic and much of the Mesozoic and the lower fluxes of the early Phanerozoic, late Palaeozoic, and Cenozoic. The basalt calcium release fluxes vary by about a factor of two and appear slightly higher at times of low plate accretion rates and lower at times of higher plate accretion rates [data from numerical model output of *MAGic* (Arvidson *et al.*, 2006) as modified in Arvidson *et al.* (2011)].

Notice first the roughly long-term, multi-million year cyclic pattern in these fluxes. The Phanerozoic starts out with low values of the weathering fluxes, gradually increasing into the middle of the Palaeozoic and then falling to the Carboniferous, at which time the fluxes began to increase into the Mesozoic and then fall dramatically into the Cenozoic. Despite some time lags, this general pattern is remarkably similar to the calculated long-term palaeoatmospheric CO_2 curves of the models *MAGic* and *GEOCARB* (*e.g.*, Berner, 2004) and to proxy data for this atmospheric variable (Fig. 6.9). As atmospheric CO_2 concentrations rose, the radiative forcing due to this greenhouse gas increased and planetary temperatures rose leading to enhanced loading of the atmosphere with water vapour and hence increased precipitation (Kasting *et al.*, 1988). The increase in

temperature and precipitation rate led in turn to increasing chemical weathering rates on land. The opposite combination of decreasing atmospheric CO_2, radiative forcing, and precipitation appears to be responsible for falling weathering rates. The overall pattern of weathering fluxes is modified by sea level changes, a reflection at least in part of plate accretion rate, and the carbonate land area and carbonate rock type available for weathering, plus the location of the continents during Phanerozoic time. Notice that the cyclic weathering flux changes are somewhat muted for magnesium. This probably reflects the more rapid dissolution rate of calcite than that of dolomite and the mass distribution of dolomite versus limestone, and hence surface exposure to weathering (Garrels *et al.*, 1976), as a function of geologic age in the sedimentary rock column.

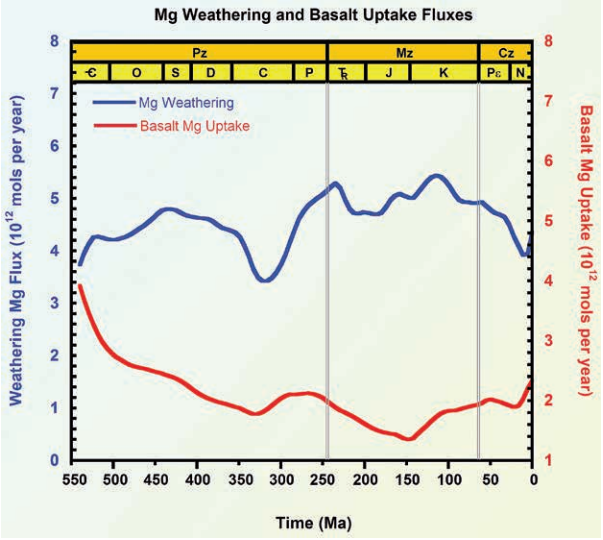

Figure 6.7 The results of numerical calculations from *MAGic* showing the magnesium flux to the ocean via rivers and groundwaters from weathering reactions on land and the magnesium taken up from seawater due to basalt-seawater reactions in the seafloor in 10^{12} mol yr^{-1}. Similar to the calcium fluxes in Figure 6.6 but not as pronounced, notice in particular the rough cyclic pattern of higher weathering fluxes of the mid-Palaeozoic and much of the Mesozoic and the lower fluxes of the early Phanerozoic, late Palaeozoic, and Cenozoic. The basalt magnesium uptake fluxes vary by about a factor of 2.5 and appear slightly higher at times of low plate accretion rates and lower at times of higher plate accretion rates [data from numerical model output of *MAGic* (Arvidson *et al.*, 2006) as modified in Arvidson *et al.* (2011)].

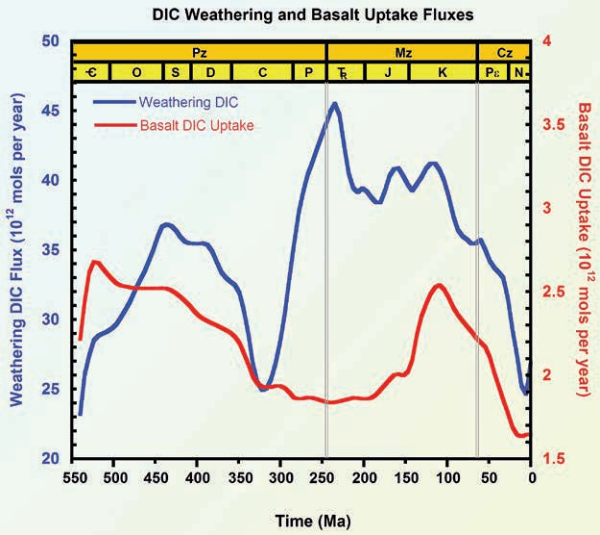

Figure 6.8 The results of numerical calculations from *MAGic* showing the DIC, (mainly bicarbonate) flux to the ocean via rivers and groundwaters from weathering reactions on land and the DIC taken up from seawater due to basalt-seawater reactions in the seafloor in 10^{12} mol yr^{-1}. Similar to the calcium fluxes in Figure 6.6, notice in particular the pronounced cyclic pattern of higher weathering fluxes of the mid-Palaeozoic and much of the Mesozoic and the lower fluxes of the early Phanerozoic, late Palaeozoic, and Cenozoic. The basalt DIC uptake fluxes also exhibit a cyclic pattern and vary by about a factor of 1.5, appearing higher at times of high plate accretion rates and lower at times of lower plate accretion rates [data from numerical model output of *MAGic* (Arvidson *et al*., 2006) as modified in Arvidson *et al*. (2011)].

Figures 6.6 to 6.8 also show the Ca, Mg, and DIC combined low and high temperature exchange fluxes due to basalt-seawater reactions in the seafloor during the Phanerozoic. These fluxes only vary by about a factor of 1.5 to 2.5 in magnitude. The uptake-age trend of the DIC basalt uptake flux exhibits a distinct cyclic pattern with uptake fluxes low in the early Palaeozoic climbing slightly into the Ordovician and then falling into the late-Palaeozoic/early-Mesozoic minimum, followed by a rise into the Cretaceous and then falling again into the Cenozoic. To some extent this pattern roughly mimics that of the seafloor accretion rate (Fig. 4.2), with lower fluxes at times of low accretion rate and higher fluxes at times of high accretion rates. This might be anticipated as more DIC (mainly HCO_3^-) is flushed through the global ridge system and precipitates as $CaCO_3$ (the Ca being derived mainly from minerals like the Ca-rich anorthite component of plagioclase feldspar within the basalt) releasing CO_2 as accretion rates increase; the converse is true for lower accretion rates. Calcite found in seafloor basalts as veins and other void fillings is recognised as an important

sink of carbon (Alt and Teagle, 1999). This seafloor calcite on subduction acts as a CO_2 source to the atmosphere owing to the Urey-Ebelmen reaction (equation 6.1). Much lesser amounts of CO_2 are added to the exogenic system by primordial CO_2, that is CO_2 derived directly from the mantle that has never been at Earth's surface before (see *e.g.,* Garrels and Mackenzie, 1971; Gregor *et al.,* 1988).

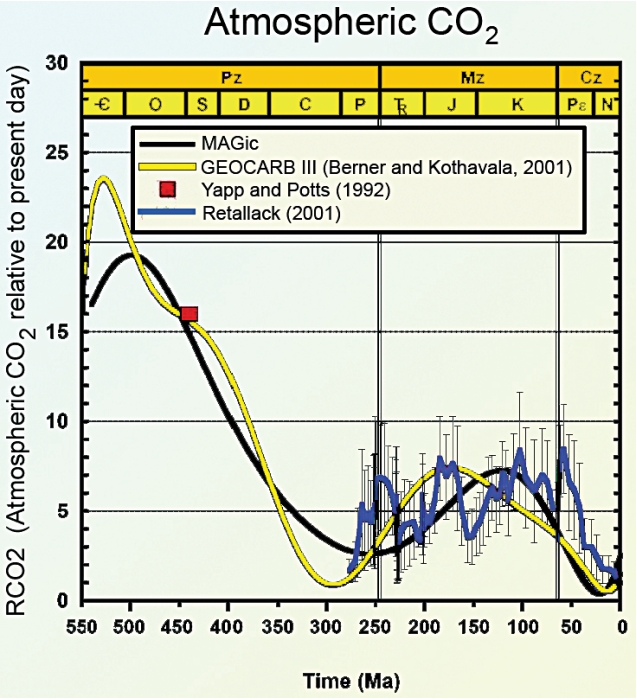

Figure 6.9 Phanerozoic long-term generalised palaeoatmospheric CO_2 concentrations relative to the pre-Anthropocene value of ~300 ppmv. Model calculations from *MAGic* (Arvidson *et al.*, 2006, 2011) and *GEOCARB III* (Berner and Kothavala (2001) are shown for comparison. The blue line is a trend line through the ranges (bars) in proxy fossil plant stomatal data for atmospheric CO_2 of Retallack (2001). The red square is Yapp and Poths (1992) data point of palaeoatmospheric CO_2 derived from palaeosols. Notice the overall cyclic pattern in Phanerozoic atmospheric CO_2 levels with concentration values increasing from the beginning of the Cambrian into the mid-Palaeozoic and then falling toward the end of the Palaeozoic and rising once more into the mid-Mesozoic and then falling into the Cenozoic.

The Ca basalt release and Mg uptake fluxes due to basalt-seawater exchange reactions in the seafloor show only moderate variations over Phanerozoic time. This is to be expected because of the strong buffering of these exchange fluxes controlled by the stoichiometry of basalt-seawater reactions (Arvidson *et al.,*

2006). However, the temporal patterns of uptake of Mg and release of Ca due to basalt-seawater reactions are similar and their exchange is not simply one to one due to the complex nature of the processes giving rise to the basalt exchange fluxes (Arvidson *et al.*, 2006).

6.2.3 Sinks of Ca, Mg, and DIC through Phanerozoic time

The dissolved constituents delivered to the ocean by rivers and ground water discharges and those from other sources during Phanerozoic time must be removed from the oceans by various mechanisms and processes, otherwise the ocean would become very salty. Variations in the input and output fluxes of dissolved constituents involving the ocean determine seawater composition during geologic time. The *MAGic* model permits one to make calculations of the magnitude of these fluxes, and in addition, the changes in seawater and atmospheric CO_2 and O_2 composition deriving from changes in these fluxes. These variations in composition exert an influence on the evolution of life in the Phanerozoic that in turn through feedback mechanisms influence the composition of the ocean and atmosphere. In this section, we present a description and quantification of the sinks of Ca, Mg, and DIC, three major components related to carbonate biomineralisation and production and to organic productivity through Phanerozoic time. The oceanic uptakes or sinks of Ca, Mg, and DIC into solid marine deposits are shown in Figures 6.10 to 6.12. The strength of each sink is shown as a percentage of the total constituent flux into the solid phase. Let us first consider the nature of the sinks for Ca, Mg, and DIC.

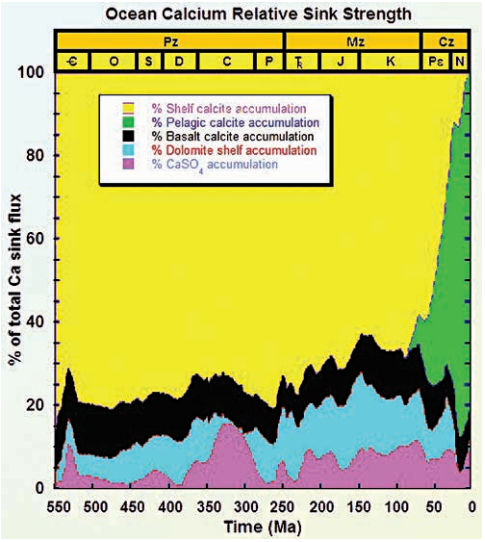

Figure 6.10 The relative sink strengths of various solid phase marine reservoirs of calcium in percent of total calcium flux to the reservoirs through Phanerozoic time [data from numerical model output of *MAGic* (Arvidson *et al.*, 2006) as modified in Arvidson *et al.* (2011)].

The flux of dissolved Ca to the oceans from weathering on land of carbonate and silicate rocks plus that released through reactions at the seafloor involving basalt and seawater at low and high temperatures (Thompson 1983; Wollast and

Mackenzie, 1983; Mottl and Wheat, 1994; de Villiers and Nelson, 1999; Arvidson *et al.*, 2006) is removed from the ocean in five sinks (Fig. 6.10): accumulation of $CaCO_3$ (calcite and aragonite) on the shelf and in deep sea sediments; accumulation of $CaMg(CO_3)_2$ on the shelf; accumulation of $CaCO_3$ in the pores, cracks, and fractures in submarine basalts; and accumulation as evaporite $CaSO_4$. Until the dawn and rapid expansion of the planktonic coccolithophoridae and foraminiferal calcifiers in the mid Mesozoic, unless there were inorganic deposition of calcium carbonate in the deep sea (see previous discussion and Berner and Mackenzie, 2011), there was no accumulation of laterally extensive, thick beds of carbonate sediments in the pre-Mesozoic deep sea.

Magnesium mainly derived from weathering reactions on land of carbonate and silicate rocks is primarily removed from the ocean during dolomite formation on the shelves, and to a much lesser extent in calcite rich in magnesium (the magnesian calcites) (Morse and Mackenzie, 1990; Mackenzie and Morse, 1992); in low-temperature, diagenetic reverse weathering reactions in seafloor sediments (*e.g.*, Mackenzie and Garrels, 1966a; Mackenzie *et al.*, 1981; Michalopoulos and Aller, 1995; Holland, 2004); during reactions involving basalts and seawater (Thompson, 1983; Mottl and Wheat, 1994); and during formation of evaporite $MgSO_4$ (Babel and Schreiber, 2013) (Fig. 6.11).

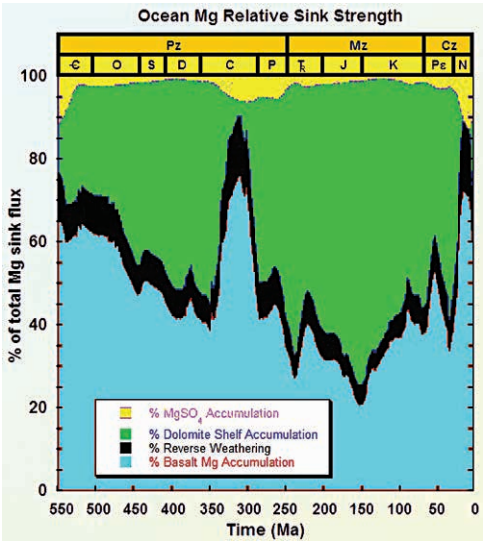

Figure 6.11 The relative sink strengths of various solid phase marine reservoirs of magnesium in percent of total magnesium flux to the reservoirs through Phanerozoic time [data from numerical model output of *MAGic* (Arvidson *et al.*, 2006) as modified in Arvidson *et al.* (2011)].

The sinks for dissolved inorganic C released via weathering of carbonate and silicate rocks (in the latter the CO_2 comes ultimately only from the atmosphere) and seafloor basalt-seawater reactions are the accumulation of inorganic carbon in shelf $CaCO_3$ (aragonite and calcite) and dolomite, the accumulation of $CaCO_3$ in seafloor basalts, and the accumulation of calcite and aragonite in the deep sea (Morse and Mackenzie, 1990) (Fig. 6.12). Organic carbon sinks include shelf and pelagic storage of organic matter and the burial of organic matter in coal basins. Variations in the flux to the latter sink are especially important to the history of atmospheric oxygen (Berner and Canfield, 1989; Berner, 2004; Arvidson *et al.*, 2006). Pelagic organic

carbon accumulation is a very small flux in terms of total organic carbon burial through the Phanerozoic. Indeed, in today's ocean only ~0.1% of the total organic carbon photosynthesised annually in surface waters accumulates in marine sediments; the rest is respired and decomposed.

Now let us consider how these sinks of Ca, Mg, and DIC vary throughout the Phanerozic. First, we will consider the pattern of Ca and Mg flux variations as shown in Figures 6.10 and 6.11. It can be seen from the figures that an important sink of Mg, and less so for Ca, through the Phanerozoic Eon is in the accumulation of dolomite on the shelf. Storage of these elements in dolomite is relatively high for much of the Mesozoic and mid-Palaeozoic and low in the Cenozoic and Permo-Carboniferous. The downward trend from the high dolomite accumulation rate of the Cretaceous toward the present is well established by observational records of the distribution of dolomite through Phanerozoic time (Wilkinson and Walker, 1989; Wilkinson and Algeo, 1989; Morse and Mackenzie, 1990; Holland and Zimmerman, 2000). The high of the mid-Palaeozoic and the subsequent low of the Permo-Carboniferous have been debated in the literature based on interpretations of observations of the dolomite mass-age distribution (Wilkinson and Algeo, 1989; Mackenzie and Morse, 1992; Holland and Zimmerman, 2000; Veizer and Mackenzie, 2004, 2013), but nevertheless, the results of the numerical simulations from *MAGic* suggest the possibility of a cyclic pattern in the dolomite accumulation flux-age distribution. This is in accord with the dolomite mass-age curve of Figure 4.3. This cyclic pattern mimics to some extent the first-order sea level curves of Vail *et al.* (1977) and Hallam (1984), with high sea level stands being times of high dolomite accumulation rates. This would be anticipated since dolomite is a shallow-water deposit and is not deposited as vast extensive beds of dolomite in the deep sea. One can see from Figure 6.11 that as the sink for

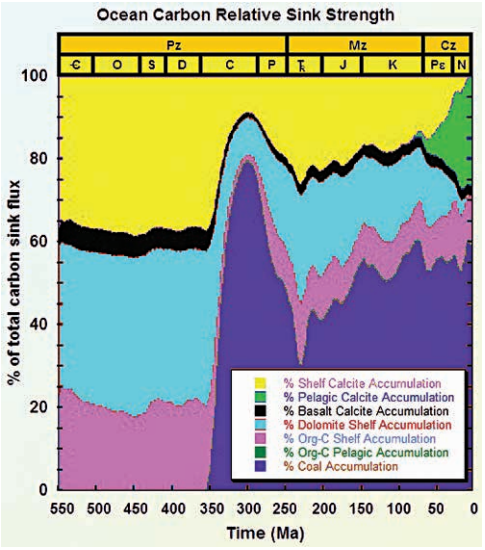

Figure 6.12 The relative sink strengths of various solid phase marine reservoirs of carbon in percent of total carbon flux to the reservoirs through Phanerozoic time. Pelagic accumulation of organic carbon is not shown in the figure in detail because it is so small [data from numerical model output of *MAGic* (Arvidson *et al.*, 2006) as modified in Arvidson *et al.* (2011)].

Mg in dolomite accumulation becomes more significant, the sink in submarine basalt uptake, the second most important sink of Mg, weakens as more of the Mg entering seawater is removed in the accumulation of dolomite.

For Ca, the most important sink through Phanerozoic time is in the accumulation of $CaCO_3$ in shelf carbonate deposits (Fig. 6.10). Until the advent of open ocean pelagic calcifying organisms, there probably was scant accumulation of biogenic $CaCO_3$ in the deep sea (Boss and Wilkinson, 1991), and as mentioned previously, there may or may not have been inorganic deposition of $CaCO_3$ in the deep sea. The accumulation of deep-sea biogenic carbonates only became significant in the early Mesozoic, resulting in the transfer of $CaCO_3$ from the shallow water continental regime to the deep sea. Most, if not all, extant Palaeozoic carbonates were deposited in cratonic, continental environments as mainly organo-detrital limestones and not in the deep sea, as evidenced by the sedimentologic characteristics of the carbonate rock record and the near-absence of deep-sea carbonate deposits associated with Palaeozoic ophiolites (ancient sea floor metamorphosed basalt complexes; Boss and Wilkinson, 1991). The latter authors contend that some of the occurrences of dark limestone and rhythmically layered marble associated with the scant record of Palaeozoic ophiolites may represent inorganic $CaCO_3$ deposition on the deep seafloor. This observation would lend credence to the hypothesis of Berner and Mackenzie (2011) mentioned previously that there was inorganic accumulation of carbonate in the Palaeozoic deep sea. The accumulation of calcite in submarine basalts is of further importance to the record of Ca accumulation in the deep sea. In this case the Ca is derived from the reaction of primary basaltic minerals with seawater mainly at hydrothermal temperatures and accumulates during the precipitation of $CaCO_3$ in the pores, cracks, and fractures of submarine basalt. Arvidson *et al*. (2006) hypothesise that this sink can be an important source of CO_2 to the atmosphere. Subduction of this $CaCO_3$, along with pelagic calcareous oozes, results in decarbonation at higher temperatures and pressures and ultimate release of CO_2 by volcanism to the Earth's atmosphere. Evaporite minerals form an additional, albeit minor, sink for both Ca and Mg.

As mentioned previously, the age distribution of extant evaporites in the sedimentary rock record is irregular, reflecting the infrequent coincidence of requisite tectonic, palaeogeographic, and palaeoclimatic conditions necessary for evaporite deposition. For example, vast quantities of evaporite salts accumulated in the Upper Permian that may actually have resulted in a lowering of the mean salinity of seawater at this time by 1% to 4% (Holser, 1984). The current version of the *MAGic* model does not incorporate these episodic evaporite depositional events and thus the modelled pattern of Ca and Mg accumulation reflects more the integrated strength of these evaporite sinks over time and not specific variations in their depositional history.

The Phanerozoic oceanic sinks of inorganic and organic C derived from land and organic C produced *in situ* by productivity in the ocean are shown in Figure 6.12. Shelf and bank (Fig. 6.13) accumulation of both C in organic matter and inorganic C in calcite, aragonite, and dolomite are very important sinks of C

Figure 6.13 Aerial view of the Bahama Banks east of southern Florida, USA. The peacock blue ocean water coincides with shallow depths and extensive areas of organo-detrital and oolitic carbonate deposits characteristic of much of the Phanerozoic.

during the Phanerozoic. The trend in the rate of accumulation of inorganic C in dolomite, as might be expected, mimics the trend in accumulation of Mg in this phase. Pelagic calcite accumulation of inorganic C begins to become important in the Mesozoic and inorganic accumulation of $CaCO_3$ in submarine basalts occurs with only minor variation in magnitude through the past 500 million years. Accumulation of terrestrially derived organic C is particularly important in the Permo-Carboniferous, a time of vast coal deposits, whereas pelagic accumulation of organic C varies only slightly throughout Phanerozoic time (not shown).

Because to a significant extent, the ratio of the reduced carbon (as organic C) flux to the oxidised carbon (as inorganic carbonate) flux determines the $\delta^{13}C$ ratio of seawater and hence that of sedimentary carbonates, it is possible to

calculate using *MAGic* this ratio during Phanerozoic time and compare its trend with the carbon isotopic curve of Figure 4.6. The trend in calculated ratio agrees well with the isotopic curve with intervals of high organic C accumulation being periods of ^{13}C-enriched carbonate deposits, and hence presumably seawater, at the time (Guidry *et al.*, 2007). This finding lends some credence to the temporal distribution of carbon sinks shown in Figure 6.12.

6.2.4 *Changes in Ca, Mg, DIC, pH, and carbonate saturation state of seawater through Phanerozoic time*

The balance between the fluxes of dissolved constituents to seawater and their accumulation fluxes is the basic control on variations in seawater chemistry through geologic time. Several authors have tried to document variations in the CO_2-carbonic acid system and carbonate saturation state of seawater for portions of the Phanerozoic (*e.g.*, Lasaga *et al.*, 1985; Tyrrell and Zeebe, 2004; Locklair and Lerman, 2005; Guidry *et al.*, 2007; Arvidson *et al.*, 2006, 2011). The changes in Ca, Mg, and DIC concentrations, pH, and seawater saturation state with respect to calcite in the ocean during Phanerozoic time calculated from the *MAGic* model are shown in Figure 6.14. In addition, the sulphate concentration trend with age is also shown in Figure 6.14 since the concentration-age trend of this dissolved species is one that is recorded in the fluid inclusions of evaporites (Babel and Schreiber, 2013) and can be compared with model output. It should be pointed out that the model trends shown for Ca, Mg, and sulphate are supported by the evaporite fluid inclusion data for these constituents and that the pH trend from the late Mesozoic through the Cenozoic is confirmed to some extent by the boron isotope proxy data for pH (Pearson and Palmer, 2000), and pH computed from palaeoceanographic reconstructions (Tyrrell and Zeebe, 2004) and $\delta^{18}O$ data (Zeebe, 2001). The earlier pH trend for the Phanerozic is also similar to other reconstructions (*e.g.*, Kump *et al.*, 2009; Zeebe, 2012b).

In general there is a cyclic pattern of variation in the Ca, Mg, and DIC concentrations of seawater and hence the Mg/Ca and SO_4/Ca ratios through Phanerozoic time. Times of slow plate accretion rates and low sea level are times of high Mg/Ca and SO_4/Ca ratios; the converse is true for high plate accretion rates and high sea levels. The composition of fluid inclusions in evaporites in terms of Ca, Mg, and sulphate tracks the modelled compositional trends (Fig. 4.14). As would be expected, the pH and carbonate mineral saturation state of seawater track each other closely, with a decrease in pH and saturation state with respect to calcite, and therefore aragonite and dolomite, at times of dolomite accumulation during first order high sea level stands and flooded continental freeboards. The cyclicity in seawater pH and calcite saturation state to some degree also tracks the palaeoatmospheric CO_2 curve with high CO_2 levels correlating with lower seawater pH and calcite saturation state; the converse is true for lower pCO_2 levels. The extended times of low seawater pH and likely carbonate saturation state are natural periods of ocean acidification.

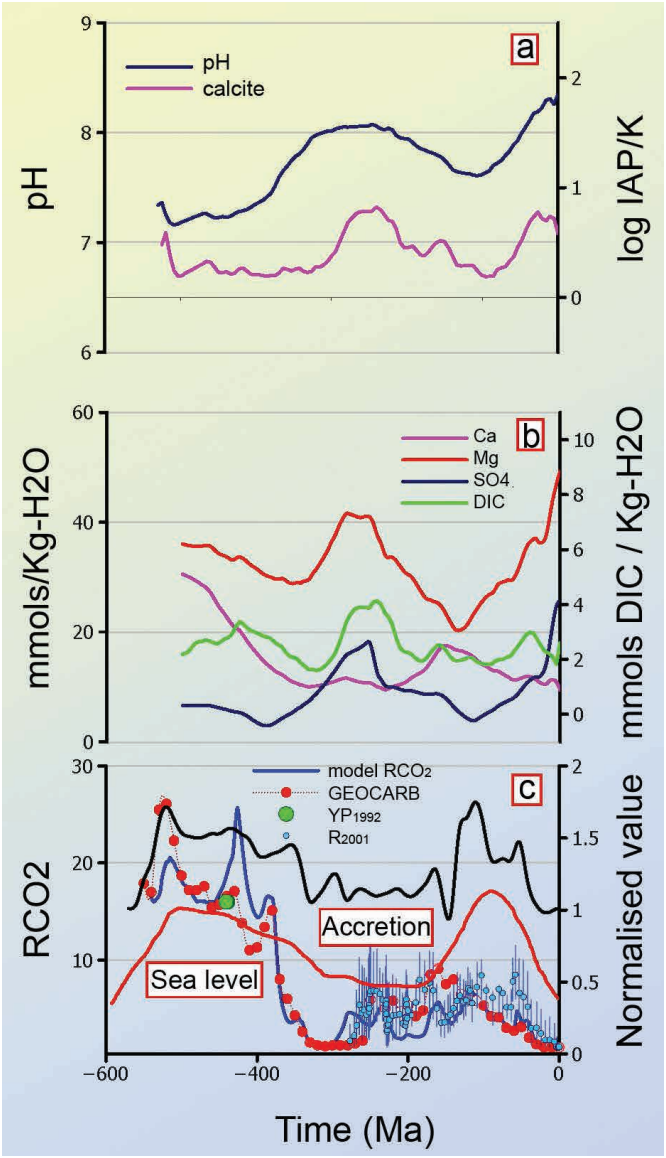

Figure 6.14 Seawater concentration-age trends through the Phanerozoic Eon calculated using the model *MAGic*. **(a)** pH and saturation state of seawater with respect to calcite; **(b)** seawater dissolved Ca, Mg, DIC, and sulphate concentrations. Concentrations are in units of mmol kg^{-1} of solution and were calculated using

Pitzer type equations. In general, there is a cyclic pattern of variation in the Mg/Ca and SO_4/Ca ratios through Phanerozoic time. **(c)** Times of slow plate accretion rates, low sea levels, and relatively low CO_2 levels are times of high Mg/Ca and SO_4/Ca ratios; the converse is true for the values of the ratios for periods of high plate accretion rates, sea levels, and CO_2 levels. YP1992 is the estimate (open green circle) from Upper Ordovician natural ironstone goethites (Yapp and Poths, 1992) and R2001 is the stomatal data (small bluish-green dots) with error bars from Retallack (Rettalack, 2001) for palaeoatmospheric CO_2. The composition of fluid inclusions in evaporites in terms of Ca, Mg, and sulphate tracks the modelled chemical compostional trends (Fig. 4.14). Also, notice the cyclicity in pH and calcite saturation state that to some degree tracks the palaeoatmospheric CO_2 curve with high CO_2 levels correlating with lower seawater pH and calcite saturation state; the converse is true for lower pCO_2 levels. These extended times of low seawater pH are natural extended periods of ocean acidification [data from numerical model output of *MAGic*, Arvidson *et al*. (2006) as modified in Arvidson *et al*. (2011)].

With respect to DIC concentrations, the total inventory of DIC in the ocean reflects the sum of fluxes derived from continental weathering, basalt-seawater exchange, reverse weathering, and global deposition of carbonate. In the *MAGic* model, the pattern of DIC concentrations through the Phanerozoic is very sensitive to the dolomite accumulation rate, which acts to buffer the DIC concentration. Indeed varying the dolomite flux alone in the *MAGic* model can produce quite a different pattern of the DIC versus age trend as shown in Figure 6.14 (cf., Fig. 6.1 of this text; Arvidson *et al*., 2006, 2011). Thus, this trend still remains an important question for future investigation, although it is likely that DIC seawater concentrations were elevated during Hothouse intervals (Phanerozoic periods of extended warmth, see following).

7. SYNTHESIS OF OCEAN-ATMOSPHERE-CARBONATE SEDIMENT EVOLUTION DURING THE PHANEROZOIC

Based on the pervious sections dealing with observational, experimental, and modelling efforts applicable to understanding the ocean-atmosphere-carbonate sediment evolution during the Phanerozoic Eon, in this section we integrate the information into a consistent picture of that evolution. As mentioned previously, geological and biological processes have acted in concert to alter atmospheric and seawater chemistry during the Phanerozoic Eon. Stanley and Hardie (1998, 1999, Stanley *et al*., 2002; see also Morse and Mackenzie, 1990) concluded that the Phanerozoic long-term oscillations in the carbonate mineralogy of calcifying organisms that produced massive skeletons, large reefs, or voluminous bodies of carbonate sediment (termed hypercalcifying organisms such as tabulate, rugose, and scleractinian corals, coralline algae, and calcareous nannoplankton) are related to the Mg/Ca ratio of seawater. For example, during the time of the generally low Mg/Ca ratio and high Ca concentration of seawater approximately coinciding with the last Hothouse (extended period of warm temperatures, also termed Greenhouse) and climaxing in the Cretaceous, chalks dominated by the coccolith plates of planktonic Coccolithophoridae, formed massive carbonate deposits in the warm shallow seas of the Late Cretaceous. Stanley and Hardie (1998) further concluded that it was variable seafloor spreading rates that led to the changing Mg/Ca ratios of seawater and hence to effects on biocalcification and the long-term cyclical distribution patterns of the chemistry and mineralogy of calcareous taxa, marine carbonate sedimentation, and reef growth during the Phanerozoic Eon. However, the tie between the carbonate mineralogy of calcifying organisms and seawater chemistry is still somewhat tenuous and problematic.

The basis for the conclusion that the Mg/Ca ratio is the governing factor in the biomineralisation of the hypercalcifying organisms is the fact that the Mg/Ca ratio of a solution can control the Mg/Ca ratio and the skeletal mineralogy of both inorganic and biogenic carbonate precipitates (*e.g.*, Mackenzie *et al*., 1983; Lowenstam and Weiner, 1989; Morse and Mackenzie, 1990; Stanley *et al*., 2002). This is certainly true to some extent, but other factors can influence significantly both the mineralogy and chemistry of marine carbonate precipitates. In the case of both inorganic and biogenic precipitates, temperature is an important factor: at lower temperatures the same group of magnesian calcite calcifying organisms will contain less Mg in their skeletons than at high temperatures (Chave, 1954), and magnesian calcite precipitated inorganically at low temperature will contain less Mg than that at high temperature (Morse and Mackenzie, 1990). In addition, the saturation state of the seawater, particularly as reflected in its carbonate ion activity, will play a role in the nature of the carbonate precipitate: Obviously it is difficult for an organism to precipitate a certain carbonate composition if the ambient bulk solution is undersaturated with respect to that phase, and this will not happen if the precipitate is inorganic. Furthermore and importantly, the rate of precipitation of an inorganic carbonate phase and the rate of calcification

of many modern calcifying organisms are related to several factors, including temperature, carbonate saturation state, and the DIC content of the water. The rate can influence the composition of the precipitate.

As an example of this perplexing situation, Stanley *et al*. (2002) grew the coralline algal *Amphiroa* sp. in artificial seawater of differing Mg/Ca mol ratios and observed that the lower the ratio in the seawater, the less Mg incorporated in the coralline algal skeleton. They used the results of these experiments to conclude that the Mg/Ca ratio of seawater controls the composition of the biogenic magnesian calcite precipitate and postulated that many taxa producing calcite high in Mg content in the modern oceans may have produced calcite low in Mg content in the Late Cretaceous Hothouse seas. However, Mackenzie and Agegian (1989; Agegian, 1985) grew another coralline algal, *Porolithon gardineri,* under varying conditions, but constant seawater Mg/Ca ratio, and showed that the Mg content of the organism varied with all three parameters of carbonate saturation state, temperature, and growth rate: the higher the value of any of these three variables, the higher the Mg content of the *Porolithon* skeleton (Andersson *et al*., 2005). Thus, the controls on the mineralogy and chemistry of both inorganic and biogenic precipitates are complex and most likely are not simply related to a single environmental variable but more likely to the confluence of variables.

For all inorganic carbonate precipitates, their overall rates of precipitation have been shown to be a function of at minimum the two variables of seawater carbonate saturation state and temperature (Morse and Mackenzie, 1990; Arvidson and Mackenzie, 1999; Arvidson and Morse, 2013) and generally follow the parabolic rate law

$$R = k(\Omega - 1)^n, \tag{7.1}$$

where Ω is the carbonate saturation index, n is the order of reaction, and k is the rate constant (see Supplementary Information SI-3). Thus, during Hothouse intervals (calcite-dolomite seas) of time with higher temperatures and lower seawater pH, carbonate saturation state, and Mg/Ca and SO_4/Ca ratios, one would anticipate that warm temperatures would favour increased rates of precipitation of at least the inorganic carbonate phases of ooids and carbonate cements, and perhaps the biogenic phases. Indeed, Burton and Walter (1987) showed experimentally that the precipitation rates of inorganic calcites of less than 5 mol% to 14 mol% and aragonite vary with temperature and saturation state. However, the precipitation rates of aragonite relative to those of calcite were demonstrated to increase strongly with temperature and were not affected greatly by changes in seawater saturation state. This simple finding would imply that as temperature increased during Hothouse conditions, aragonite could outcompete calcite as the major carbonate mineral precipitate, contrary to the observation that calcitic abiotic and biota precipitates are apparently more common during Hothouse (calcite-dolomite seas) conditions than during Icehouse (extended periods of relatively cool temperatures, aragonite seas) conditions. However, the situation is confounded by the role of decreased pH (and seawater carbonate saturation state) and decreased Mg/Ca and SO_4/Ca seawater ratios of Hothouse ocean waters in the precipitation rates of carbonate minerals.

As mentioned previously, it has been known for some time from experimental evidence (Weyl, 1965; Berner, 1975; see review in Morse and Mackenzie, 1990) that Mg^{2+} inhibits calcite precipitation from seawater. In particular, Berner showed that in solutions of different Mg^{2+} concentrations, Mg^{2+} does not influence aragonite precipitation kinetics, but he observed major retardation of calcite precipitation rates in seawater solutions containing Mg^{2+}, except at very low Mg^{2+} concentration levels at which no inhibition of calcite growth rate was observed. To further complicate the issue, Morse *et al.* (2007) (Fig. 5.1) demonstrated that both the Mg/Ca ratio and temperature of seawater influence the calcite versus aragonite mineralogy of the carbonate mineral precipitate, with present seawater composition of Mg/Ca = 5.4 favouring an aragonite precipitate down to a temperature of about 8 °C, below which calcite becomes the stable precipitate at lower temperatures. As the Mg/Ca ratio decreases and the temperature increases, calcite is progressively favoured to nucleate from seawater over aragonite as the precipitated dimorph, and at a Mg/Ca ratio of about one, calcite is the stable phase up to temperatures approaching 40 °C. Now even another complication: Bots *et al.* (2011) showed that an increase in the sulphate ion concentration of seawater decreases the Mg/Ca ratio at which calcite is destabilised and aragonite is favoured as the dominant $CaCO_3$ precipitate. The authors further suggested that the Mg/Ca and sulphate thresholds for the formation of calcite over aragonite at times of calcite-dolomite seas are significantly lower than those of the Morse *et al.* (2007) results and furthermore that these variables are not mutually independent.

One more experimental result that is applicable to the discussion here: Lee and Morse (2010) in experiments conducted on $CaCO_3$ mineral nucleation from a Hothouse (calcite-dolomite sea) seawater of estimated Cretaceous composition (Table 6.1) demonstrated that the initial alkalinity of the experimental seawater solution significantly affected the pCO_2 at which a carbonate mineral nucleated and whether calcite or aragonite was precipitated. In seawater with Mg/Ca = 1.2 and ~10 mM TA and a pCO_2 below ~2,500 ppm, calcite was the initial phase nucleated, while aragonite nucleated when the pCO_2 rose above ~2,500 ppm. In seawater with a Mg/Ca = 1.7, only aragonite was produced at lower alkalinities (<~11 mM), but calcite was nucleated when the alkalinity was above ~18 mM. The Lee and Morse results provide evidence that the Mg/Ca ratio, temperature, alkalinity, and pCO_2 level are all important in determining whether seawater can be classified as that of a calcite-dolomite sea or aragonite sea.

The results of the above experiments point to the possibility that for calcite to nucleate directly from a Hothouse Cretaceous seawater composition probably necessitated at least elevated calcium and alkalinity concentrations at the higher pCO_2 levels of the Cretaceous atmosphere. In addition, the precipitation rates of calcite with low Mg content could outcompete those of calcites with high Mg content and aragonite under conditions in which there was less Mg in the seawater to act as an inhibitor of calcite precipitation (Berner, 1975; Morse, 1983). Furthermore, it is likely that the rates of calcite precipitation could be enhanced by higher sea surface temperature and TA. The higher rates of calcite

precipitation with low Mg content during Hothouse intervals could have led to mineralogical shifts favouring the formation and deposition of original ooid, cement, and skeletal carbonates composed of calcite deficient in Mg. The reduction in the accumulation of aragonite in sediments would raise the concentration of strontium in seawater during Hothouse conditions and lead to skeletal calcites with increased strontium concentrations. Indeed, Guidry *et al*. (2007) concluded that the changing cyclic character of inorganic and biogenic aragonite and calcite precipitates through the Phanerozoic Eon strongly reflects the fundamental precipitation kinetics of the carbonate phases calcite and aragonite as mediated by sea surface temperature and seawater chemistry.

Now let us turn to dolomite formation and relationship to seawater chemistry, which is an even more difficult kinetic problem than that of calcite and aragonite; the difficulties are very well summarised by Arvidson and Morse (2013). Dolomite is a recalcitrant precipitate to form experimentally or in nature at low temperatures even at high supersaturations and is not found in abundance in modern marine environments. The mineral is found most commonly in unique environmental settings and typically forming from compositionally modified seawater solutions often with higher seawater solution ionic strengths, Mg/Ca ratio, and/or dolomite saturation states at warm temperatures, like the deposits of the Persian Gulf sabkhas, Caribbean Sea Bonaire Island Pleistocene carbonates, supratidal carbonate sediments of Andros Island, Bahamas, and in Deep Springs Lake in California, USA. These observations have led to the paradigm of the "dolomite problem" of why occurrences of dolomite are so scarce in the modern marine environment, and yet large horizontally and vertically extensive bedded dolomite deposits are characteristic of much of the pre-Tertiary rock record.

As Land (1985) so succinctly pointed out, "there are dolomites and dolomites"; that is, there are a number of environmental settings and solution compositions under which dolomite may form. In addition, bacteria are known to be involved in reactions involving dolomite formation (*e.g.*, Vasconcelos and McKenzie, 1997; Roberts *et al*., 2004) thus compounding the problem. Another type of dolomite, "organogenic" dolomites, can also form early within the realm of shallow burial in organic-rich sediments due to high concentrations of alkalinity derived from microbially mediated oxidation of organic carbon via the pathway of sulphate reduction and high supersaturation of pore water with respect to dolomite. It is important to note that the *MAGic* model results are consistent with the importance of these reactions in dolomite formation. It should also be kept in mind that dolomite often forms through replacement reactions involving precursor calcite and aragonite in the subsurface of sedimentary basins at elevated temperatures and in waters of modified seawater composition. This later stage dolomite formation and its role in the mass-age distribution of dolomite through the Phanerozoic Eon are also evaluated in *MAGic.*

One plausible explanation for the slow precipitation kinetics of dolomite is the requirement that cation ordering of the well-ordered dolomite mineral structure puts a major limit on the rate at which it can form (*e.g.*, the "simplexity"

principle, Goldsmith, 1953). It is also difficult to dehydrate the Mg^{2+} ion so it is likely that the dehydration kinetics of Mg^{2+} also play a role in its rate of precipitation (*e.g.*, Lippmann, 1973). In addition, modern dolomites are calcium-rich "protodolomites" and far from ordered structures; the degree of ordering apparently increases with the age of the dolomite (Land, 1985). Based mainly on observational evidence from the field (Folk and Land, 1975; Morrow, 1982), there have been attempts made to construct kinetic phase boundaries between calcite and dolomite. One such diagram shows that dolomite may be favoured to precipitate over calcite in high ionic strength, Mg/Ca, and CO_3/Ca solution conditions. Seawater has these characteristics to some degree but obviously dolomite does not precipitate from normal modern seawater compositions without their modification.

The relationship between dolomite kinetics and sulphate is even more problematic. Early work by Baker and Kastner (1981) demonstrated that sulphate inhibits dolomite growth at high temperature (200 °C). This result was seen as an initial challenge to the importance of the Mg/Ca ratio in promoting dolomite formation and led to a longstanding notion that current levels of seawater sulphate were at least part of the explanation for the paucity of dolomite in modern sediments. However, the idea that dolomite growth is promoted in low-sulphate or sulphate-free systems may be strictly true only at high temperature, given the observation that dolomite is found in sulphate-rich hypersaline environments. In addition, such environments provide ambient water with a high Mg/Ca ratio and may also promote dolomite formation through a decrease in the activity of water, thus promoting dehydration of Mg^{2+} ion (Folk and Land, 1975; Lippman, 1973). This is a key reaction step that must limit the crystal growth of ordered dolomite. More recent sorption experiments also suggest that aqueous magnesium sulphate (or surface) complexes may facilitate a reaction path involving carbonation–dehydration and lattice attachment of magnesium ion. In this case, sulphate may actually catalyse dolomite nucleation on carbonate surfaces (Brady *et al*., 1996). Thus, the role of sulphate in the precipitation kinetics of dolomite is still controversial and it is difficult to assert without question that seawater sulphate concentrations play a strong role in the formation of dolomite (*e.g.*, Arvidson and Morse, 2013).

In summary, the dependencies of inorganic dolomite precipitation rate on saturation state and temperature are complex and at this date have not been resolved in detail. In addition, the mechanistic role of the Mg/Ca ratio in dolomite formation is also not well understood, and recent work on the interaction of Mg with carbonate mineral surfaces has confirmed complex relationships (Davis *et al*., 2000; Arvidson and Mackenzie, 1997, 1999; Arvidson, personal communication). Despite uncertainties, Arvidson and Mackenzie (1997, 1999) did demonstrate unequivocally that temperature and saturation state control to some extent dolomite precipitation kinetics, with higher temperature and higher saturation state favouring an increased precipitation rate. Figure 7.1 shows mineral-aqueous solution model *calculations* of dolomite versus calcite precipitation rates as a function of temperature (Arvidson and Mackenzie, 1997). Recalling the

caveat about how difficult it is to precipitate dolomite at low temepratures, what is most impressive in this figure is the very strong calculated increase in the rate of dolomite precipitation rate with increasing temperature. The dolomite rate of precipitation changes by four orders of magnitude from 25 °C to 90 °C, whereas the calcite precipitation rate varies by less than an order of magnitude. This finding alone might argue that at higher temperatures, dolomite could outcompete calcite and possibly aragonite for dissolved constituents and be a dominant sedimentary phase under the higher temperature conditions of the Hothouse intervals when dolomite abundance in the rock record appears high.

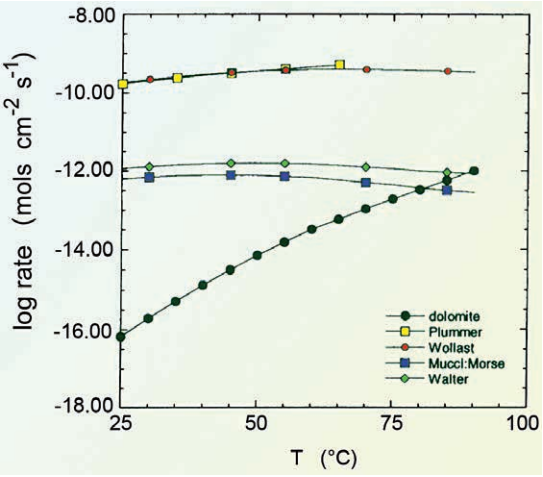

Figure 7.1 Comparison of calculated dolomite and calcite precipitation rates. Dolomite mineral precipitation rates were calculated from the saturation states of a simple closed seawater system heated from 25 °C to 90 °C. Calculated dolomite rates (black circles) are generally lower than those of calcite calculated for dilute Ca-HCO_3 solutions (yellow squares and red circles) and from seawater models (blue squares and green diamonds). Notice the strong convergence of the rates for dolomite versus calcite as temperature increases and the significant depression of the rates for calcite in seawater relative to those in dilute Ca-HCO_3 solutions (after Arvidson and Mackenzie, 1997).

Obviously an elevated Mg/Ca ratio should also favour formation of dolomite but periods of high dolomite accumulation appear to be times of depressed Mg/Ca seawater ratio. *MAGic* model results in terms of the relationship between input fluxes and mineral sinks are consistent with major dolomite deposits being favoured during periods of higher atmospheric CO_2 levels *and hence temperatures*, depressed seawater Mg/Ca and SO_4/Ca ratios, overall lower pH and carbonate mineral saturation states, and perhaps elevated alkalinity, but likely most importantly, in expanded shallow-water depositional environments of warm interior seas with abundant lagoons, shallow banks, and sabhkas, conditions characteristic of Hothouse regimes.

These observations can be used to link the identity of mineral precipitation in the oceans over Phanerozoic time in response to changing chemical and climate conditions with the aid of Figure 7.2. This figure shows the tens of millions of year cyclic changes in the broad-scale evolution of the ocean-atmosphere-carbonate sediment system through the Phanerozoic Eon in concert with climatic changes as presented by Crowley and Berner (2001). At this time scale, variations in atmospheric CO_2 concentrations, seawater chemical parameters, sediment composition, and climate appear to go hand in hand. Basically as discussed by Mackenzie and Pigott (1981; see also *e.g.*, Berner *et al.*, 1983; Morse and Mackenzie, 1990), changes in plate accretion rates drive to some extent changes in atmospheric CO_2 levels and hence climate. Changes in these variables in turn influence first order sea level stands, seawater composition, and chemical, mineralogical, and biological features of the extant sedimentary carbonate rock record. Extended times of high accretion rate correspond reasonably well with global high sea levels, increased atmospheric pCO_2 concentrations, higher temperatures (Hothouse or Greenhouse conditions), lower seawater Mg/Ca and SO_4/Ca ratios, higher seawater strontium concentrations, and lower carbonate saturation state and pH of seawater. The extended periods of time of lower pH conditions of seawater are the natural ocean acidification episodes. DIC concentrations and TA *appear* to be higher during these Hothouse conditions. In addition, it appears that the environmental conditions necessary for enhanced accumulation of dolomite and early dolomitisation, formation of calcitic ooids and cements, and preponderance of calcitic reef-building organisms were best met during extended times of global high sea levels, periods of ubiquitous shallow-water epicontinental seas and increased areas of sabkha-like environments. These are the times of the calcite seas of Sandberg (1983) that probably should be termed the calcite-dolomite seas (Mackenzie *et al.*, 2008). The converse of the calcite-dolomite seas is the low sea level stands and the Icehouse conditions of the Permo-Carboniferous and the late Cenozoic. These are times of aragonite seas with reduced dolomite accumulation rates, abundant aragonitic oolites, and a greater propensity for skeletal carbonate mineralogies and marine carbonate cements of aragonite and calcite containing significant magnesium concentrations.

During Icehouse conditions, major continental-scale glaciations occurred when atmospheric CO_2,, radiative forcing from CO_2, global temperatures, and worldwide sea levels were relatively low. The Earth was cold enough for large ice sheets to form and spread over large geographical areas. Following the major Icehouse of the Late Precambrian, the Permo-Carboniferous and the 30-35 million years ago to present Icehouses occurred with extensive continental glaciations. Also, despite early and middle Palaeozoic atmospheric CO_2 being relatively high, there is evidence of another Icehouse in the Middle and Late Ordovician 440 million years ago, a time of slightly depressed CO_2 concentation levels. The cause(s) of this Icehouse are currently debated (see *e.g.*, Buggisch *et al.*, 2010; Herrmann *et al.*, 2010).

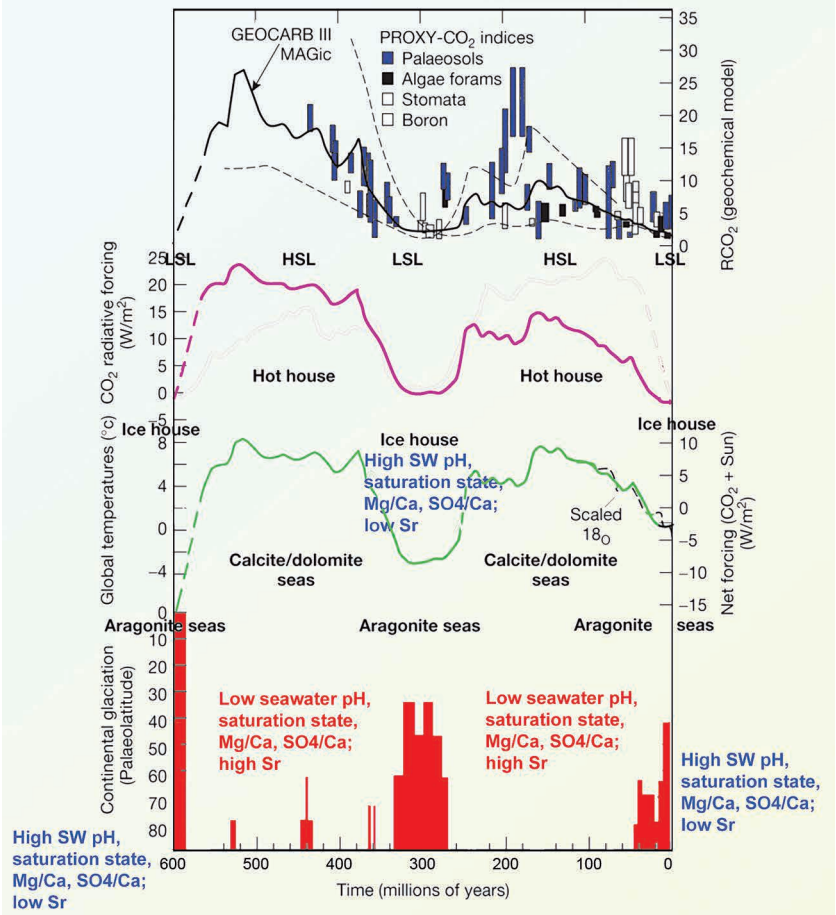

Figure 7.2 Palaeoatmospheric CO_2, seawater chemistry, climate, and glaciations. Notice the broad oscillatory pattern in all parameters and that the three major glaciations occurred at times of relatively low atmospheric CO_2, hence, low radiative forcing and temperature. Various types of proxy data for atmospheric concentrations are compared with the composite *GEOCARB III* and *MAGic* modelled concentrations of CO_2 in the atmosphere relative to average Holocene levels. The dashed lines in the upper panel are upper and lower bounds of CO_2 estimates from *GEOCARB III*. HSL is high sea level; LSL is low sea level. Aragonite seas are Icehouse times when the carbonate minerals aragonite and high Mg-calcite were especially abundant as chemical and biological precipitates from ocean water, and the pH, carbonate saturation state, Mg/Ca and SO_4/Ca ratios were high, and Sr concentration was low. Calcite/dolomite seas are Hothouse (Greenhouse) times when these minerals were abundant as precipitates from ocean water and seawater chemistry and climate differed from Icehouse conditions (modified from Crowley and Berner, 2001, with additional information from Mackenzie *et al.*, 2008 and Arvidson *et al.*, 2006, 2011).

The relatively quick drawdowns of atmospheric CO_2 from the mid-Palaeozoic to the Permo-Carboniferous and from the peak of the late Mesozoic into the Icehouse of the latter part of the Cenozoic deserve some further explanation. As Berner so succinctly pointed out (see summary in Berner, 2004), both of these features in the palaeoatmospheric CO_2-age curve of the Phanerozoic reflect to a significant extent biological evolution. In the former case, the rise of terrestrial plants evolving from primitive green algae and their invasion of the land began about 450 Ma ago. Their expansion across the landscape in the latter part of the Palaeozoic led to the first large accumulations of atmospheric CO_2 in organic matter in terrestrial living plants, possibly initially in lowland coastal swamps and later in highland environments, and as organic carbon in soils and continental aquatic systems. The storage of organic carbon on land and the enhanced weathering rates engendered by root respiration and decomposition of organic carbon in soils led to decreasing atmospheric CO_2 concentrations. This biological storage of carbon was abetted by declining seafloor accretion rates and lessened CO_2 emissions from metamorphism/volcanism, leading to lower atmospheric CO_2 concentrations.

The evolutionarily advanced and most successful plants are the flowering vascular plants that began their spread across the landscape about 130 Ma ago in the early part of the Cretaceous Period. Their root systems and root hairs respire large quantities of CO_2 that led to increasingly enhanced weathering rates on into the Cenozoic drawing down atmospheric CO_2 concentrations as plate accretion rates also slowed and less CO_2 was vented to the atmosphere by metamorphism/volcanism, and hence, atmospheric CO_2 concentrations fell.

It is worth pointing out that plant evolution on land not only had an effect on atmospheric CO_2 but also on O_2 and CH_4 concentrations. Figures 7.3 and 7.4 illustrate model calculations for atmospheric O_2 and CH_4 concentrations, respectively, through the Phanerozoic Eon. There are no sedimentary proxies for these two atmospheric gases applicable on the time scale of the whole Phanerozoic so model estimates must be relied on. The various model calculations for O_2 shown in Figure 7.3, although variable, appear robust in terms of the most important features: (1) atmospheric O_2 concentrations started out at the beginning of the Phanerozoic similar to those of the more recent past; (2) from Cambrian to Devonian time (~545 to 408 Ma), O_2 concentrations were slightly higher or slightly lower than modern day; (3) in the Carboniferous and on into the Permian (~360 to 245 Ma), O_2 concentrations apparently rose dramatically to values reaching 1.5 to 2 times present day values; (4) following the relatively high O_2 concentrations of the Permo-Carboniferous (~360 to 245 Ma), O_2 concentrations fell to values perhaps lower than today during the Triassic/early Jurassic (~245 to 144 Ma) and then rose once more into the late Mesozoic, falling then into the Cenozoic toward present day levels.

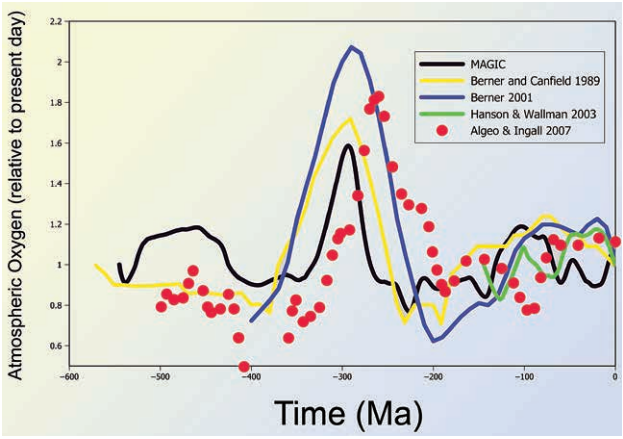

Figure 7.3 Some model calculations for atmospheric oxygen through the Phanerozoic Eon. The models exhibit significant differences but the overall trends and especially the higher O_2 levels of the Permo-Carboniferous (about 300 Ma) and Cretaceous-early Cenozoic (70 to 20 Ma) appear to be a robust feature of the models (Mackenzie, Arvidson and Guidry, MAGic, unpublished; Berner and Canfield, 1989; Berner, 2001; Hansen and Wallmann, 2003; Algeo and Ingall, 2007; see also Bergman *et al*., 2004).

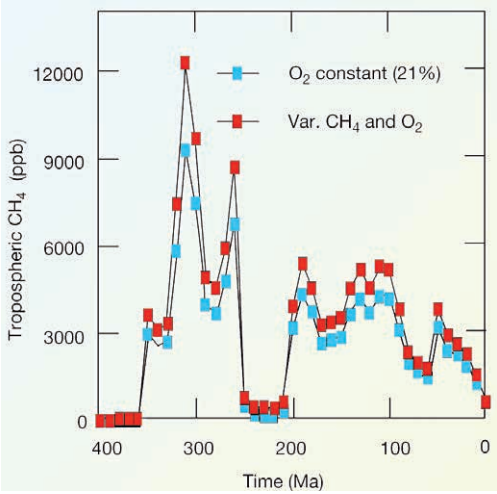

Figure 7.4 Model calculations of the variations in tropospheric methane during much of the Phanerozoic Eon. The model calculations were made using two scenarios for palaeoatmospheric O_2 concentrations: one scenario holds atmospheric O_2 concentration constant at 21%, and a second varies O_2 concentration closely following the Berner and Canfield (1989) model O_2 results of Figure 7.3 (after Beerling *et al*., 2009).

What caused this pattern in palaeoatmospheric O_2 concentrations during the Phanerozoic? The simplest explanation is mainly tied to the development of the vast Permo-Carboniferous and Cretaceous/early Tertiary coal basins that stored large quantities of organic carbon recalcitrant to oxidation (Berner and Canfield, 1989). Oxygen on the geologic time scale is mainly controlled by two major processes: (1) the accumulation of organic carbon and pyrite (FeS_2) in sediments leading to accumulation of O_2 in the atmosphere, and (2) the weathering of uplifted sediments containing fossil organic matter (kerogen) and FeS_2 by atmospheric O_2 that removes O_2 from the atmosphere (Fig. 7.5; *e.g.*, Garrels *et al.*, 1976). During the Permo-Carboniferous and the Cretaceous/early Tertiary, with the large fluxes of organic carbon stored in coal basins, O_2 weathering fluxes could not keep up and atmospheric O_2 concentrations increased. Decreased coal basin development and carbon storage then led to O_2 weathering fluxes being sufficient to drawdown atmospheric O_2 levels.

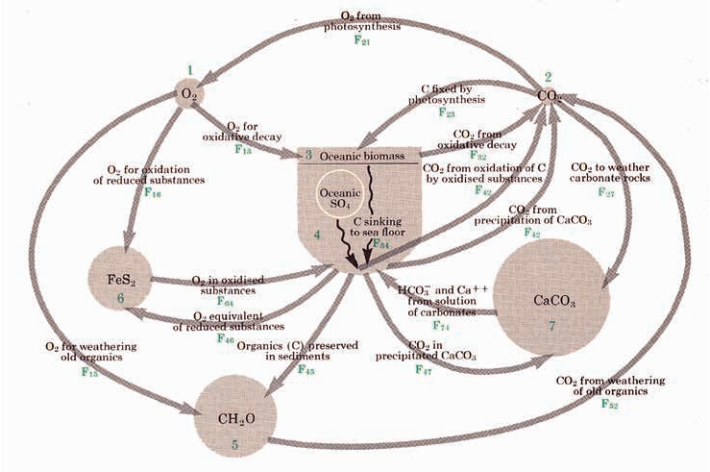

Figure 7.5 Schematic diagram representing the relationships among the processes, reservoirs, and fluxes of the major components of the exogenic cycles of carbon and sulphur involving oceanic biomass and seawater, sediment reservoirs of $CaCO_3$, organic matter (CH_2O), and FeS_2, and atmospheric CO_2 and O_2. F denotes flux (rate of transfer) as F_{ij} from reservoir i to j, where i and j are denoted as 1, 2, 3, 4, 5, 6, and 7 (after Garrels *et al.*, 1976).

The temporal evolution of the development of coal basins in the Phanerozoic also led to changes in atmospheric CH_4 concentrations. In 2008-2009 *Fred* had the opportunity to work with *Dave Beerling, Bob Berner, Michael Harfoot,* and *John Pyle* to consider the behaviour of atmospheric methane over Phanerozoic time. This was a much needed effort at the time since little had been done on the geologic history of atmospheric methane (Beerling *et al.*, 2009; Fig. 7.4). Figure 7.6 shows the natural biogeochemical cycle of CH_4 without human interference

(Beerling *et al.*, 2009). Notice in particular that natural wetlands are a very important source of methane to the atmosphere, with the oceans and termite metabolic processes being less important sources. The sinks of natural emissions are mainly oxidation in the atmosphere by the hydroxyl radical and uptake in soils. As mentioned, the organic matter deposited in natural wetlands and its alteration is the source material for coal deposits. The size and geographical distribution of natural, swampy wetlands and hence coal deposits have varied through geologic time, with the Permo-Carboniferous and the late Jurassic, Cretaceous, and parts of the Tertiary being times of extensive tropical swamplands that resulted in major coal accumulations. These extensive swamplands led to increased emissions of CH_4 to the atmosphere and increased atmospheric CH_4 concentrations. So as we see with Phanerozoic atmospheric CO_2 concentrations, there is also a somewhat cyclic pattern of atmospheric CH_4 concentrations, although fundamentally for a different reason. Because methane is a greenhouse gas, its atmospheric compositional variations also contribute to the natural global warming or cooling of the planet. Furthermore, because methane and carbon dioxide show cyclic patterns in atmospheric concentrations through the Phanerozoic that in part overlap, it is likely that atmospheric nitrous oxide also exhibited such cyclic behaviour (Beerling *et al.*, 2009). All three greenhouse gases played a role in climatic fluctuations through the Phanerozoic but CO_2 was by far the most important.

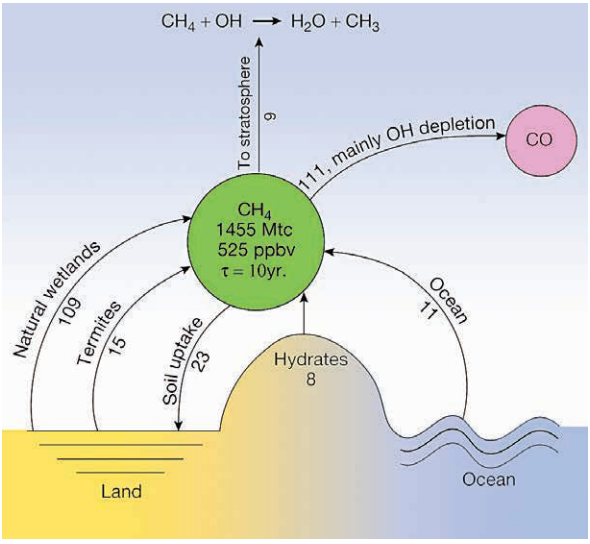

Figure 7.6 The natural biogeochemical cycle of methane. Fluxes are in units of 10^6 metric tons C yr^{-1}. The residence time of CH_4 in the atmosphere is 10 years. Notice the important flux of CH_4 to the atmosphere due to microbial degradation of organic matter in natural wetland sediments, like the ones of ancient coal basins (after Beerling *et al.*, 2009).

In conclusion, we see that fluctuations in climate are tied to atmospheric greenhouse gas concentrations at the millions of years geologic time scale of the Phanerozoic and in turn seawater chemistry and abiotic and biotic carbonate sediment production and composition are linked and feed back into the climatic changes brought about by variations in greenhouse gas concentrations. A variety of biological and inorganic processes played a role in maintaining and regulating the Earth's exogenic system in an homeostatic state (tendency to maintain equilibrium through a network of coupled processes and feedbacks) through the Phanerozoic Eon. What is also important to understand is that similar connections exist at the time scales of Pleistocene glaciations and interglaciations and the recent period of Earth history under human influence, the Anthropocene Epoch. As one example of glacial-interglacial change and controlling processes and forcings of change, we discuss ocean, atmosphere, and carbonate sediment evolution for the transition from the LGM, 18,000 years BP, to late preindustrial time, the beginning of the Anthropocene Epoch, in the following section.

8. COASTAL OCEAN CARBON CYCLE FROM THE LAST GLACIAL MAXIMUM INTO LATE PREINDUSTRIAL TIME

8.1 Introduction

Photo courtesy of May Ver, University of British Columbia.

Figure 8.1 Leah May Ver of the Department of Earth, Ocean and Atmospheric Sciences, University of British Columbia, Vancouver, Canada. May is a former Ph.D. student of Fred's and collaborator of Andreas. May's Ph.D. dissertation at the University of Hawaii dealt with the development and application of the model TOTEM to problems involving the coupled behaviour of C, N, and P in the global coastal ocean interacting with the land, atmosphere, open ocean, and marine sediments (see *e.g.*, Ver *et al.*, 1999).

It is probably fair to say that we know more about the environmental changes occurring during the last glacial to interglacial transition of the Pleistocene Epoch and Holocene Epoch than we do for the longer term geologic record of the Phanerozoic environmental changes in the exogenic system or the ecosphere, although we are still seeking answers to what were the main drivers and the explanatory mechanisms of many of the observed changes in the Pleistocene and Holocene. For example, despite considerable efforts, the mechanism(s) responsible for the rapid rise in atmospheric CO_2 during deglaciations is still unknown although several hypotheses have been put forward. In this Section 8, we discuss some of those changes that have occurred during glacial-interglacial transitions mainly focusing on the LGM, 18,000 years BP, to late preindustrial time. In Section 9, we continue the story into the Anthropocene Epoch and its future. Much of our discussion is based on models developed by our group, and the invaluable contributions to our efforts over the years of *Leah May Ver* at the University of British Columbia, a former Ph.D. student of *Fred's*, *Abraham Lerman* at Northwestern University, a long-time colleague of *Fred's* and also *Andreas*, *Rolf Arvidson* at Universtat Bremen, and *Michael Guidry* at the University of Hawaii are especially noted here (*e.g.*, Ver *et al.*, 1999; Mackenzie *et al.*, 2002; Guidry *et al.*, 2007; Lerman *et al.*, 2011). *May Ver* was responsible for the development of the *T*errestrial *O*cean a*T*mosphere *E*cosystem *M*odel (*TOTEM*), which led to her Ph.D. dissertation

consisting of two volumes and several hundreds of pages and innumerable papers before she went on to the position of Lecturer at the University of British Columbia.

Furthermore, our emphasis for the remaining sections of this monograph is mainly on the global coastal ocean, which was motivated when we started this work by the fact that little attention had been given to the role of the carbon cycle and associated elements of the coastal ocean in the context of global environmental change, despite the fact that this region is highly important at the global scale (Gattuso *et al*., 1998; Ver *et al*., 1999; Chen *et al*., 2003, 2008; Mackenzie *et al*., 2005). At present time, the global coastal ocean (*i.e.* bays, estuaries, lagoons, banks, and continental shelves) constitutes only 7% to 8% of global ocean surface area, but is the location where approximately 10–30% of the world's marine primary production occurs (Jahnke, 2010). Its further importance lies in the fact that 80% of fluvial suspended sediment inputs, containing reactive nutrients, from the land to the sea are deposited in coastal environments. In addition, 85% of organic C and 45% of inorganic C are buried in the sediments within this region (Gattuso *et al*., 1998; Wollast, 1998; Chen *et al*., 2003; Mackenzie *et al*., 2005). Furthermore, the coastal ocean provides a myriad of critical services to a large proportion of the human population in terms of food, nutrition, and income from the fisheries and tourism economies. In addition, the global coastal ocean supports nearly 50% of all species on the planet and helps sustain that life through providing 20% of animal protein and five percent of the total protein in the human diet. Of that resource, coastal ocean waters out to 200 nautical miles supply 99% of the worldwide annual commercial fish catch.

The coastal ocean is and has been heavily impacted by human activities, as nearly 40% of the global population lives within 100 km of the coastline (Cohen *et al*., 1997). To understand the current human perturbation and consequences for the coastal ocean and its marine ecosystems discussed later in this monograph, it is necessary to evaluate the evolution and cycling of carbon in this region since the LGM to late preindustrial time. During the LGM, sea level was approximately 120 m lower compared to today and the submerged coastal area was significantly smaller. Since that time sea level has progressively risen, providing additional varied coastal environments and increasing shallow water surface area, atmospheric greenhouse concentrations have risen and hence global temperatures warmed, and land to sea carbon and nutrient fluxes changed significantly.

The overall land-atmosphere-ocean-sediment carbon cycle dramatically varied in a cyclic pattern during the Pleistocene Period. Figure 8.2 shows the trends with time of several environmental variables as recorded in the composite of the Vostok, Dome C, and Taylor Dome ice core records from Antarctica. The ice core records have been a remarkable contribution to our knowledge of glacial-interglacial environmental changes that form the background against which human intervention in the ecosphere can be evaluated. The 800,000-year record of Figure 8.3 includes the present interglaciation (interglacial stage) plus four previous ones and four continental glaciations (glacial stages). The temperature

record from the ice core that reflects the past temperatures of the environment at Vostok exhibits a strong 100,000-year cyclicity, as predicted by the Milankovitch theory of three main orbital periodicities (Milankovitch, 1941; Imbrie *et al.*, 1984): changes in the ellipticity of the Earth's orbit, with a period of about 100,000 years; the obliquity or tilt of the Earth's axis to the plane of its solar orbit, with a period of about 41,000 years; and the wobble or precession of the axis, with a period of about 23,000 years.

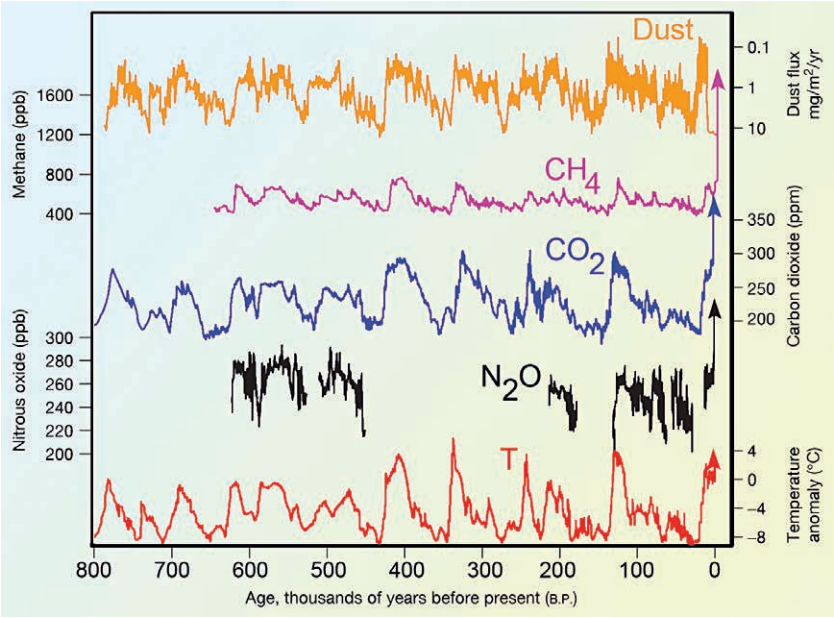

Figure 8.2 The trends in atmospheric CO_2, CH_4, N_2O, temperature, and dust as recorded in the composite of the Vostok, Dome C, and Taylor Dome ice cores records from Antarctica (after Petit *et al.*, 1999; Siegenthaler *et al.*, 2005; Lüthi *et al.*, 2008).

The ice core records of temperature, atmospheric carbon dioxide, and methane roughly track each other in the data from the composite ice cores for the past 800,000 years. The latter two variables reflect global atmospheric concentrations of CO_2 and CH_4. The oxygen isotopic record ($\delta^{18}O$) is that of the oxygen in precipitation trapped in H_2O ice that reflects changes in the oxygen isotope ratio of water vapour that was deposited as snow and consolidated into ice on the Antarctica ice cap. The $\delta^{18}O$ of H_2O in atmospheric precipitation of the cold high latitudes is relatively low due to Rayleigh fractionation, -30‰ to -50‰ on the SMOW scale, whereas tropical surface ocean water has a $\delta^{18}O \approx 0$‰ (Moser and Stichler, 1980; Broecker, 1995). Because the relationship between the isotopic composition of oxygen (and hydrogen) in precipitation and temperature has been

studied intensively and observed empirically many times and a good correlation has been shown to exist, the $\delta^{18}O$ trend in polar ice can be interpreted as a record of polar ice temperature, and with some degree of certainty, the air temperature over the ice at the time of formation. The dust record shows that the precipitation over Vostok contained more dust particles at the climax of each glacial stage, probably reflecting more exposed continental shelf areas, and a more dusty, drier, and windy atmosphere during continental glaciations. Carbon dioxide during this whole time interval oscillated in approximately 100,000-year cycles by about 100 ppmv from 180 to 280 ppmv, and CH_4 by about 0.4 ppmv, and despite time lags of one variable or the other, both track the ice core pattern of the temperature record obtained from the Greenland Ice Core Project (GRIP) since the last interglaciation, the period of time for which the ice cores overlap in age.

The 100,000-year $\delta^{18}O$ cycle observed in the ice cores is also seen in the oxygen isotopic composition of foraminifera collected from deep-sea calcareous oozes that serves as a proxy for ice sheet volume and for ocean water surface temperatures. This record goes back nearly 800,000 years. In addition, the sedimentary record of major, continental glacial advances and retreats found in Pleistocene glacial deposits of North America, Europe, and Asia also exhibits a 100,000-year cyclicity. Thus, the 100,000-year pattern is seen not only in ice core environmental parameters but also in other records from both the terrestrial and marine realms.

As the parameters discussed above varied on a roughly 100,000-year time scale, so did sea level with warmer intervals of time representing higher sea levels and colder intervals, lower sea levels. Figure 8.3 shows the rise in global sea level from its low stand (Fig. 8.4) of the Last Glacial Maximum 18,000 years ago to late preindustrial time. As sea level rose about 120 m with the melting of the last great continental ice sheets, continental freeboard and island shelves were flooded providing the environmental conditions necessary for accumulation of reefs and other shoal-water carbonate deposits. Major accumulations of carbonate sediments shifted from the deep sea to the shelves. Commensurate with this shift

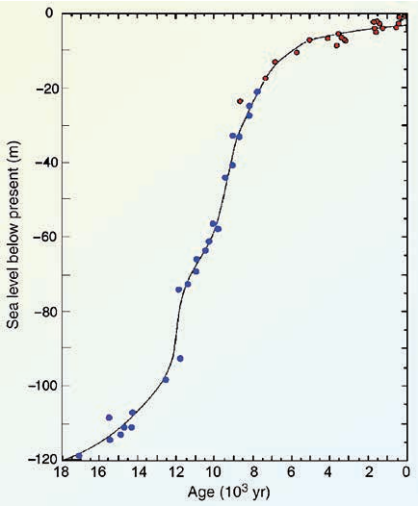

Figure 8.3 Diagram showing the rise in sea level after the last continental glaciation 18,000 years ago. The rise is due to the return of meltwater from the continental ice sheets to the ocean. The curve is based on radiocarbon age dating of fossilised corals found on the island of Barbados (after Fairbanks, 1989; Bard *et al.*, 1990a,b).

were changes in the CO_2-carbonic acid chemistry of seawater and in the nature of carbonate deposits, which probably contributed to some extent to the buildup of CO_2 in the atmosphere from the LGM to late preindustrial time but not to the entire increase of roughly 100 ppmv (Sigman and Boyle, 2000; Ridgwell, 2003; Vecsei and Berger, 2004).

The shift in carbonate deposition from the deep sea to the shelves and its possible relationship to the rise of atmospheric CO_2 led to the development of the "coral reef hypothesis" (Berger, 1982). The coral reef hypothesis is based on the translocation of carbonate deposition from the deep sea to the shelves and the associated redistribution of seawater TA, and thus, the ability of the ocean to take up CO_2. The preservation of $CaCO_3$ in the deep sea is strongly controlled by the depth of the seawater saturation horizon with respect to a specific carbonate mineral phase, *e.g.*, calcite or aragonite, which is partly inferred and recorded in the sediments by the depth of the chemical lysocline horizon (the kinetic boundary which indicates the depth zone where the $CaCO_3$ content rapidly decreases in the sediments). Thus, changes in the average depth of the lysocline over time provide constraints on changes in the DIC to TA ratio balance of the oceans and the expected equilibrium between CO_2 concentrations in the atmosphere and the ocean.

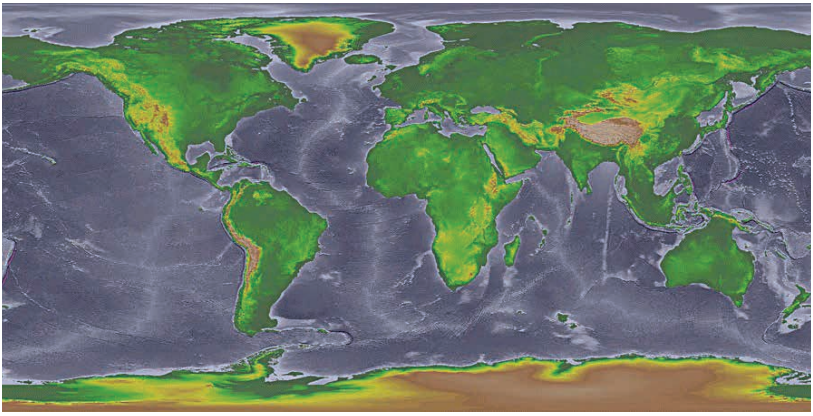

Credit: National Geophysical Data Center (NGDC) at NOAA.

Figure 8.4 Land area (green and brown pattern) during the Last Glacial Maximum 18,000 years ago. During the last ice age, sea level was ~120 m lower than it is today exposing much more area on the continents. As sea level rose, the land bridge from Siberia to Alaska disappeared, Britain and the islands of Southeast Asia appeared, and the region which is now Hudson Bay flooded.

Theoretical considerations suggest that the lysocline should have been approximately 2 km deeper during the LGM than today, if changes in ocean alkalinity owing to increased input from land or less $CaCO_3$ deposition on the shelves were responsible for the lower atmospheric CO_2 concentration at this time (Archer and Maier-Reimer, 1994; Sigman and Boyle, 2000). However, observational data

based on the distribution of seafloor carbonates with age suggest that the average depth of the lysocline during the LGM was less than 1 km deeper than that of the Holocene suggesting that changes in ocean alkalinity probably did not have a major role in the control of atmospheric CO_2 over glacial-interglacial cycles. Nevertheless, model simulations by Ridgwell *et al.* (2003) suggest that CO_2 emissions, owing to shallow water carbonate deposition during the last 8,000 years, could have contributed to a rise in atmospheric CO_2 by 40 ppmv prior to industrialisation. Similarly, evaluations by Vecsei and Berger (2004) of the pattern and timing of significant reef growth suggest that this process mainly contributed to the rise in atmospheric CO_2 during the most recent late deglaciation (6,000 to 8,000 years ago) and post-glacial time (0 to 6,000 years). These authors concluded that approximately 4,200 Gt of $CaCO_3$ accumulated on the flooded shelves since 14,000 years ago, potentially releasing 225 Gt of C as CO_2 to the atmosphere. However, we are just coming to grips with what is known about how much of this carbon remained in the atmosphere and was taken up in other carbon reservoirs (Elsig *et al.*, 2009). Figure 8.5 is one interpretation of how the masses of carbon in the atmosphere, land and oceanic reservoirs, and carbon fluxes between the reservoirs differed between the LGM and late preindustrial time.

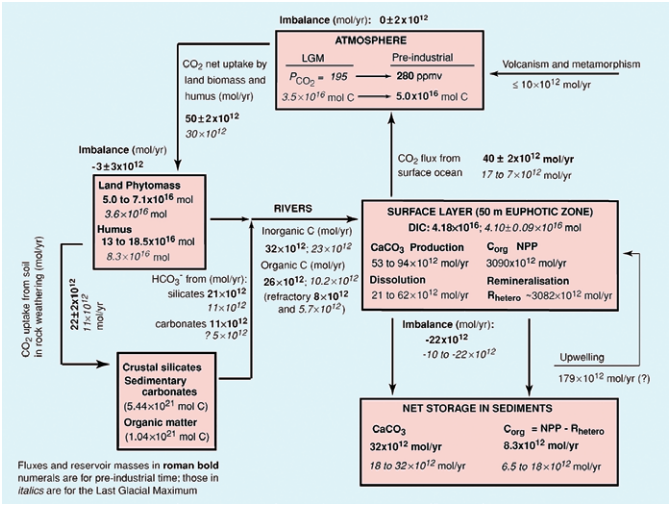

Figure 8.5 Difference between LGM and late preindustrial time atmosphere, land, and oceanic reservoirs and fluxes of carbon. For the crustal silicates reservoir, only one estimate is given for the C stored in sedimentary carbonates and that stored in organic matter and because the reservoirs are so large, significantly valid LGM vs late preindustrial differences cannot be estimated. In the SURFACE LAYER box, ranges are shown for $CaCO_3$ production and dissolution from the LGM to late preindustrial time. C_{org} NPP and Remineralization of organic C are assumed to be the same for LGM and late preindustrial time. Reservoir sizes are in units of 10^{12} mol C and fluxes in units of 10^{12} mol C/yr (modified from Lerman and Mackenzie, 2005).

8.2 Trends in Carbon, Nitrogen, and Phosphorus River Fluxes

Abraham Lerman at Northwestern University in Evanston, Illinois, USA, well recognised for his contributions to our understanding of continental weathering, in collaboration with *Fred*, developed a weathering model for continental weathering fluxes of C, N, and P to the coastal ocean from the LGM to the time just preceding the Industrial Revolution (late preindustrial time). This research was published in the journal *Aquatic Geochemistry* (Lerman *et al.*, 2011) and in the book *Treatise on Coastal and Estuarine Science* (Mackenzie *et al.*, 2011) (Fig. 8.6).

The work showed that profound changes occurred from the LGM to late preindustrial time that significantly affected the transport of carbon, nutrients, and suspended sediments to the ocean. Despite the decreasing land area, since the LGM to the beginning of the Anthropocene, the combined effect of the rising temperature, increasing chemical weathering rates of inorganic and organic materials on land, increasing terrestrial biomass, and most likely increased water discharge was, in general, to increase the inputs of carbon and other nutrient species to the coastal ocean (Fig. 8.7). This occurred along with an increase in the storage of organic carbon on land as deglaciation proceeded, the land being a large reservoir for C, N, and P. One major climatic perturbation that is evident in the overall pattern of increasing riverine fluxes to the coastal ocean is the return to near glacial conditions during the Younger Dryas climatic event (12,800 to 11,500 years BP).

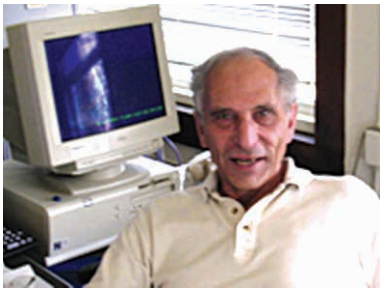

Photo courtesy of Abe Lerman, Northwestern University.

Figure 8.6 Abe Lerman of the Department of Earth and Planetary Sciences, Northwestern University, Evanston, Illinois USA. Abe is Fred's long-time colleague and friend and a recent collaborator with Andreas. Abe is a pioneer in the mathematical modelling of geochemical processes involved in weathering and other Earth surface processes and in our understanding and quantitative modelling of the global biogeochemical cycles of the elements.

It should be pointed out that as important as the riverine input is to the coastal ocean, particularly the proximal, nearshore region, the volume inflow of water is much smaller than the volume of global coastal upwelling of water that also transports the dissolved nutrient elements of C, N, and P to the coastal ocean from intermediate ocean depths. Present-day global coastal upwelling has been estimated as 43.7×10^{13} m^3 yr^{-1} (Chavez and Toggweiler, 1995) to 78.8×10^{13} m^3 yr^{-1} (Walsh, 1991). Both values are considerably larger (~10 to 20 times bigger, respectively) than the river inflow of about 4×10^{13} m^3 yr^{-1}. In addition, a large number of dams on rivers, constructed in the twentieth century and projected to increase in number in the future, disrupt natural river flow by creating water reservoirs from which additional evaporation of water can occur. Furthermore, dams

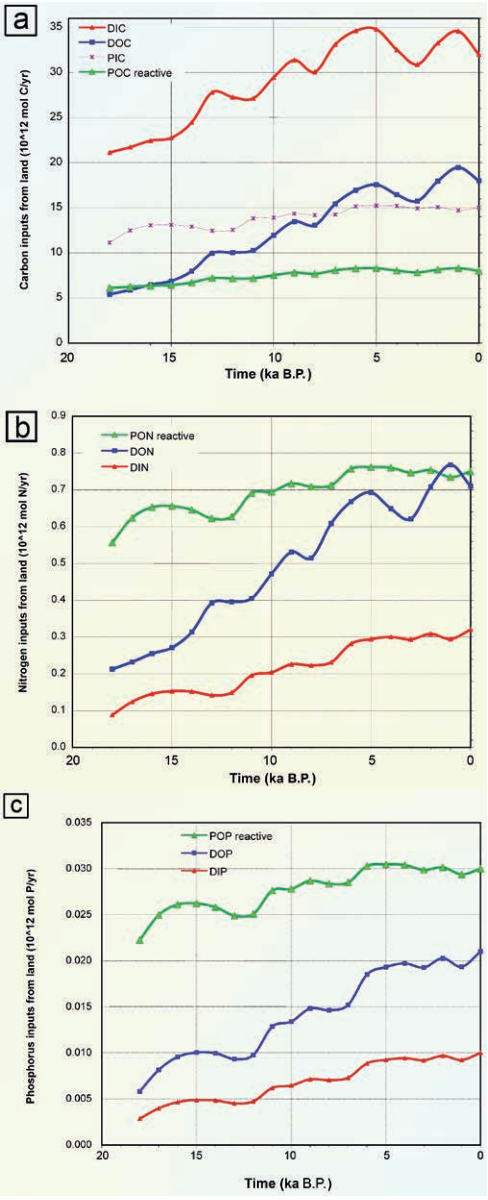

Figure 8.7 Calculated trends in riverine C **(a)**, N **(b)**, and P **(c)** inputs to the coastal ocean from the LGM to late preindustrial time. Notice the general trends of increasing delivery of these materials to the coastal ocean mainly due to

increasing temperature and chemical weathering rates of inorganic and organic materials on land, increasing terrestrial biomass, and most likely increased water dischange. DIC, DOC, PIC, and POC reactive are, respectively, dissolved inorganic carbon, dissolved organic carbon, particulate inorganic carbon, and particulate organic carbon that is reactive owing to remineralisation in the ocean. DIN, DON, and PON reactive are, respectively, dissolved inorganic nitrogen, dissolved organic nitrogen, and particulate organic nitrogen that is reactive owing to remineralisation in the ocean. DIP, DOP, and POP reactive are, respectively, dissolved inorganic phosphorus, dissolved organic phosphorus, and particuate organic phosphorus that is reactive owing to remineralisation and dissolution in the ocean (after Lerman *et al.*, 2011).

trap a large part of the suspended matter carried by rivers and thereby reduce inputs of some of the nutrients to the coastal ocean. Use of river waters for irrigation also reduces river discharge. As opposed to the trapping of solids by dams, increasing land erosion rates due to agricultural and changing land-use activities in general deliver more suspended solids to rivers (Meybeck, 1979; Meybeck and Ragu, 1995; Milliman, 1997, 2001). Moreover, recent acceleration of the global hydrological cycle is occurring because of global warming and probably will continue in the near future. One piece of evidence for this assertion is the salinity change in the global oceans during the period from 1950 to 2008 (Durack and Wijffels, 2010; see also IPCC 2007) that shows salinity increases in evaporation-dominated regions and decreases in precipitation-dominated regions.

8.3 Trends in the Coastal Ocean CO_2-Carbonic-Acid-Carbonate System

The global coastal ocean CO_2-carbonic acid-carbonate system during the rise in sea level since the LGM has been rarely investigated using an Earth system transient modelling approach that couples land-atmosphere-coastal ocean-open ocean-sediment reservoirs. Exceptions to this statement are the papers of Munhoven (2007 and references therein to his earlier work) and Köhler *et al.* (2005), although the approaches of these authors are considerably different from that used in our models. In this section, we describe the long-term trends from the LGM to late preindustrial time, and as discussed in a later section, on into the Anthopocene in coastal ocean carbon chemistry and ancillary parameters. Calculations were generated from the *SOCM* (Shallow-water Ocean Carbonate Model, Fig. 8.8) and the *SOCM-GLACIAL* models. *SOCM-GLACIAL* is used for the LGM to late preindustrial time calculations and *SOCM* for the years 1700 to year 2100. The initial conditions for the calculations for both of these periods of time are the inorganic and organic carbon cycle reservoirs and fluxes in the global coastal ocean as estimated for late preindustrial time as shown in Figure 8.8 (see details in Andersson *et al.*, 2005 and Lerman *et al.*, 2011). The models were forced from the initial quasi-steady state condition by calculated and documented trends in important variables. For the LGM to late preindustrial time, the major external forcings on the coastal ocean CO_2-carbonic acid-carbonate system are (1) the river fluxes of C, N, and P shown in Figure 8.7, (2) the ice core record of atmospheric CO_2 rise, the rise in temperature since the LGM of ~ 6 °C, and

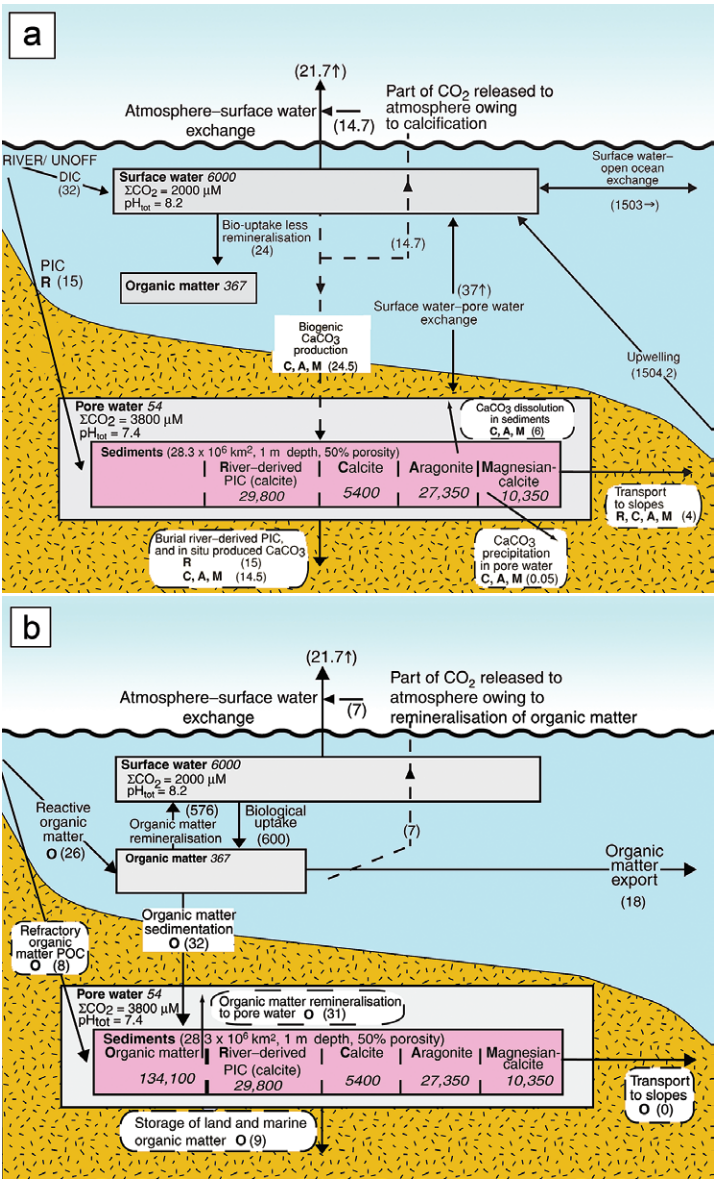

Figure 8.8 Inorganic (carbonate) **(a)** and organic (C_{org}) **(b)** parts of the carbon cycle in the coastal ocean in preindustrial time. Reservoir masses in *italics* are in units of 10^{12} mol C. Arrows denote carbon fluxes between reservoirs in units of

10^{12} mol C yr^{-1} (shown inside parentheses). In **(a)** two major domains are the water column (surface water and dissolved inorganic carbon) and the pore water–sediment system [pore water, dissolved inorganic carbon, river-derived particulate inorganic carbon (PIC), calcite, aragonite, and 15 mol% magnesian calcite]. For two-way arrows the direction of the net flux is shown next to the flux estimate. The dashed lines indicate the carbon flux owing to $CaCO_3$ production. In **(b)** two major domains are the water column (surface water, dissolved inorganic carbon, and organic matter) and the pore water–sediment system (pore water and organic matter in sediments). The dashed lines indicate the carbon flux owing to the net imbalance between Gross Primary Productivity and total remineralisation of organic matter or net ecosystem production, NEP (after Andersson *et al.*, 2005).

the global rise of sea level of 120 m from which the increasing area and water volume of the coastal ocean can be estimated. For late preindustrial time into the future of the Anthropocene, the river fluxes were calculated using *TOTEM* (Fig. 2.12; *e.g.*, Ver *et al.*, 1999) to the year 2040 and then extrapolating beyond that in a business-as-usual scenario of continuous linear changes in these river C, N, P forcings associated with river discharge (Fig. 8.9). In addition, for this period of time, atmospheric CO_2 concentrations were calculated directly from the *TOTEM* and the temperature record was based on the global observational combined land-ocean record and the projection for the future from the IPCC IS92a fossil fuel CO_2 emissions scenario. The emissions scenario itself was also used as an external forcing in *TOTEM*. Land use CO_2 emissions were based on the estimates of Houghton (1995) and the IPCC (2007), with a business as usual projection into the future. Figures 8.10 to 8.14 illustrate the calculated trends in the CO_2-carbonic acid system parameters for both the period of the LGM to late preindustrial time and in expanded detail for that part of the Anthropocene Epoch from 1700 to 2100.

What is most apparent in the temporal trends shown in Figures 8.9 to 8.14 are the significant changes in the slopes, *i.e.* the rate of change, of the external forcings on the system--rise in atmospheric CO_2 concentrations and temperature, and river and groundwater inputs of dissolved inorganic carbon (DIC) and nutrients to the coastal zone--and in the CO_2-carbonic acid system chemical species, seawater carbonate saturation state, net ecosystem calcification (NEC, carbonate calcification minus dissolution), net ecosystem production (NEP, organic production minus gross respiration), and net air-sea exchange of CO_2 of coastal ocean waters. The changes in slope begin most dramatically in the Anthropocene at about the middle of the twentieth century and continue on into the future.

For most of the time since the LGM, the coastal ocean expanded in area and volume, with the strong exception of the Younger Dryas interval. Despite the increasing flux of river DIC to the ocean owing to rising temperature and enhanced continental weathering, coastal seawater DIC concentrations were nearly constant through time due to the riverine DIC flux being rapidly mixed and exchanged with the open ocean waters, but increased slightly. Obviously because of the increase in the volume of the coastal ocean during this period of time, total DIC mass in the coastal ocean increased. The DIC concentration trend was accompanied by a modest decline in TA and carbonate ion concentration and

increase in bicarbonate ion concentration, the former due to melting of ice causing a decrease in salinity and also increasing shallow water $CaCO_3$ deposition. The latter two trends resulted mainly from rising atmospheric CO_2 concentrations during post-glacial time and consequently slightly decreasing pH due to the equilibrium partitioning of this gas between the atmosphere and coastal ocean surface waters (Figs. 8.10 and 8.11).

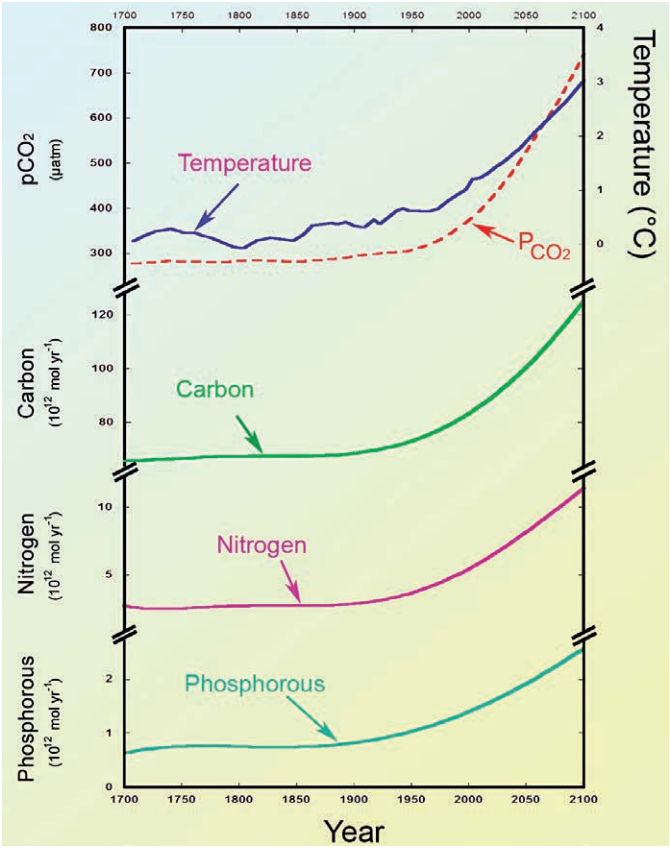

Figure 8.9 Calculated trends in riverine chemical species of carbon, nitrogen, and phosphorus from late preindustrial time around the year 1700 to the year 2100. Notice the rapidly increasing riverine delivery of these materials to the coastal ocean during the Anthropocene, mainly due to land-use activities, particularly deforestation, sewage discharge, and application of N and P fertilisers to the terrestrial landscape. Also shown are the trends in global temperature and atmospheric CO_2 as obtained from historical records and projected to the year 2100 using the Business as Usual scenario IS92a of the IPCC (2001, 2007) and used as forcings in *SOCM* (adapted from Ver *et al.*, 1999).

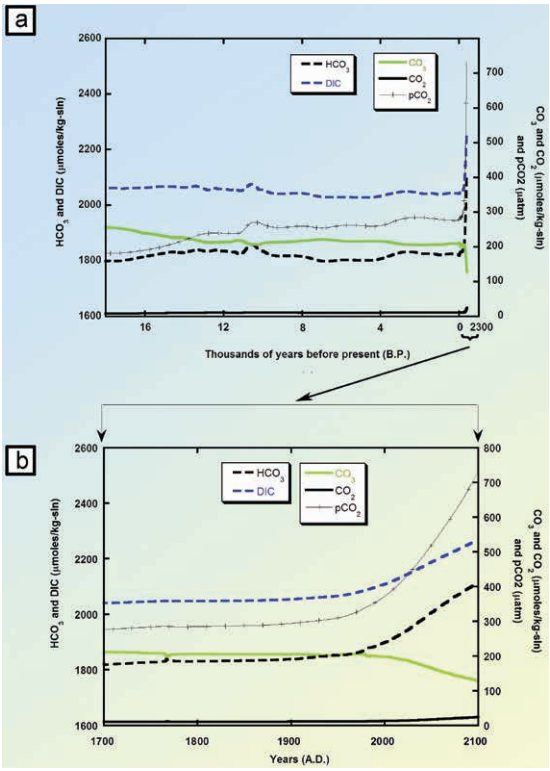

Figure 8.10 Model output from the LGM to the year 2100 **(a)** and enlargement of the trends from 1700 A.D. to 2100 A.D. **(b)** for coastal seawater HCO_3^-, DIC, CO_3^{2-}, and CO_2 (µmol kg^{-1}) and pCO_2 (µatm) (after Lerman *et al.*, 2011).

TA concentrations fell slightly as reef-related and other carbonate deposits increased in area and the coastal ocean volume, and particularly net ecosystem calcification, increased as sea level rose since the LGM, providing shallow-water accommodation space and prerequisite environmental conditions of light, temperature, nutrient availability, etc. for the growth of carbonate-secreting organisms (Kleypas, 1997). However, the main factor contributing to the increase in shallow water carbonate accumulation was most likely the increasing availability of shallow water space with high light levels. For example, for hermatypic corals (corals dependent on photoautotrophic symbionts), the rate of linear extension of the skeleton increases almost exponentially as a function of decreasing depth and increasing light levels (Kleypas, 1997). Kleypas (1997) estimated that the space available for reef growth today was 50 to 75% greater than that available during the LGM. Thus, just decreasing depth with attendant increasing light levels and more space would presumably lead to greater shoal-water carbonate

accumulation. Nevertheless, during the initial flooding of shelves, the success of some calcifiers may have been impaired while others flourished. It is postulated that the initial flooding during sea level rise in some coastal regions was associated with high turbidity and nutrient concentrations, and reduced water clarity. For example in the Caribbean, these conditions constrained the ability of reefs to keep up with the sea level rise to the extent that some reefs actually drowned (Buddemeier and Hopley, 1988; Kleypas, 1997). Similarly, the growth of the Great Barrier Reef in Australia appears to have been suppressed for several hundred years after the initial flooding of the shelf owing to high turbidity and nutrient inputs, but at the same time, *Halimeda* (green algae carbonate secreting organisms) bioherms, particularly on the Sunda Shelf of the Indonesian Archiplego, expanded significantly suggesting that these algae were able to capitalise on the additional nutrients (Kleypas, 1997).

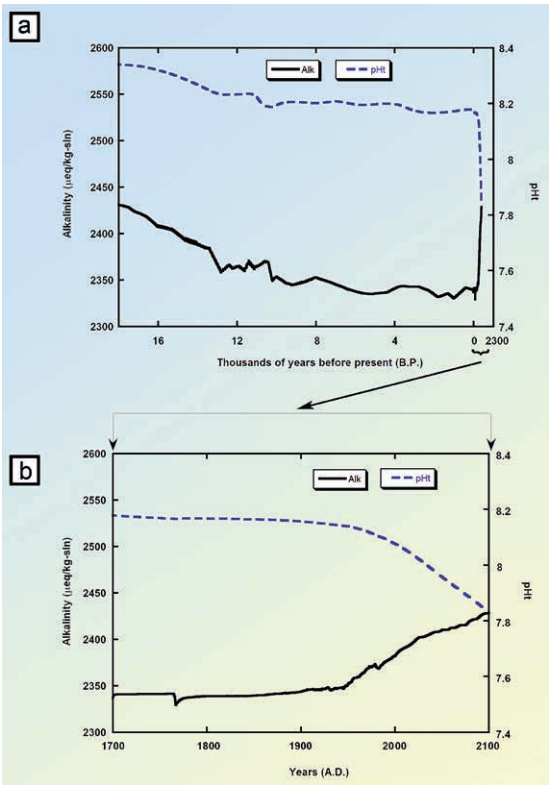

Figure 8.11 Model output from the LGM to the year 2100 **(a)** and enlargement of the trends from 1700 A.D. to 2100 A.D. **(b)** for coastal seawater pH (seawater scale) and total alkalinity (meq kg^{-1}) (after Lerman *et al.*, 2011).

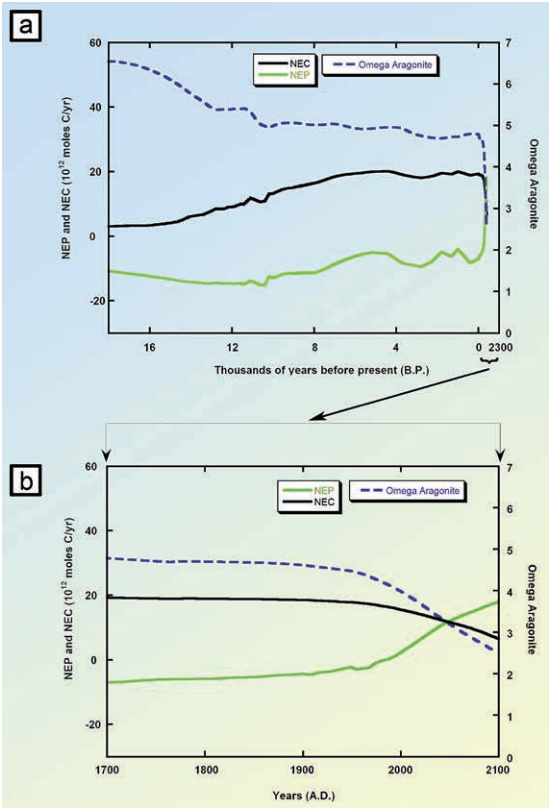

Figure 8.12 Model output from the LGM to the year 2100 **(a)** and enlargement of the trends from 1700 A.D. to 2100 A.D. **(b)** for coastal ocean Net Ecosystem Calcification (NEC) and Net Ecosystem Productivity (NEP) (10^{12} mol C yr^{-1}) and seawater aragonite saturation state omega (Ω) (after Lerman *et al.*, 2011).

Based on our model simulations, NEC rose from 3 x 10^{12} mol C yr^{-1} to 18.8 x 10^{12} mol C yr^{-1}, or more than 600%, during post-glacial time to the year 1850, reflecting the positive imbalance between calcification and $CaCO_3$ dissolution (Figs. 8.12 and 8.13). Estimates by Kleypas (1997) using the model *ReefHab,* which employs environmental parameters to predict the global distribution of reef habitats, suggest total reef calcification during the LGM was at a minimum of 2.6 x 10^{12} mol C yr^{-1} and at a maximum of 10.7 x 10^{12} mol C yr^{-1} about 2,000 years ago. However, this model only considers coral reef calcification and not $CaCO_3$ production for the entire global coastal ocean. At present time, coral reefs constitute about 50% of the total $CaCO_3$ production in the global coastal ocean (Smith and Kinsey, 1976; Milliman, 1993; Milliman and Droxler, 1996; Andersson, 2013). Other estimates by Opdyke and Walker (1992) range from -7 x 10^{12} mol C yr^{-1} to

23 x 10^{12} mol C yr^{-1} and estimates by Vecsei and Berger (2004) in the time range 0-8,000 years ago, the time of maximum $CaCO_3$ accumulation, range from 5 x 10^{12} mol C yr^{-1} to 7.2 x 10^{12} mol C yr^{-1}.

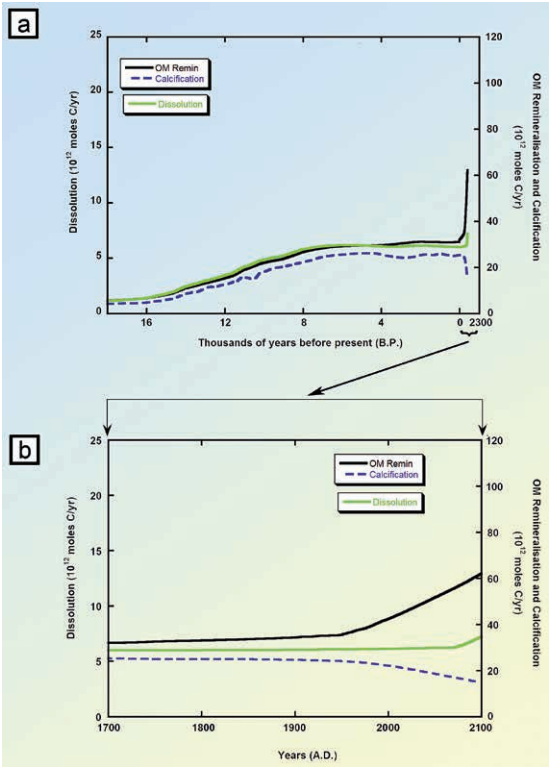

Figure 8.13 Model output from the LGM to the year 2100 **(a)** and enlargement of the trends from 1700 A.D. to 2100 A.D. **(b)** for coastal ocean organic matter (OM) remineralisation, calcification, and dissolution in units of 10^{12} mol C yr^{-1} (after Lerman *et al.*, 2011).

Post-Last Glacial Maximum NEC and reef growth were certainly not continuous and monotonic in time but were punctuated by intervals of more or less growth. For example in the Younger Dryas, the system nearly returned to glacial conditions with decreased reef growth (Montaggioni, 2000; Vecsei and Berger, 2004).

Despite the extensive development of reefs and accumulation of $CaCO_3$ on the shelves, the carbonate saturation state of coastal waters with respect to aragonite fell from about Ω_a = 6.6 to 4.7, or about 30%, from the LGM to the year 1850 (Fig. 8.12) due to the increase in atmospheric CO_2 and decrease in TA

resulting in a reduction in the pH and carbonate ion concentration of coastal waters. Based on experimental results, rates of calcification for most marine calcifiers decrease with decreasing seawater aragonite saturation state, all other factors being constant (*e.g.*, Gattuso *et al.*, 1999; Doney *et al.*, 2009; Andersson *et al.*, 2011), but increasing space, light availability, and temperature that occurred during this extended time period of the last glacial-interglacial transition probably outweighed the potential negative effect from the decrease in seawater carbonate saturation state. Obviously coastal seawaters also became less saturated during this time interval with respect to calcite, which is less soluble than aragonite and a spectrum of Mg-calcite compositions, many compositions of which are more soluble than aragonite.

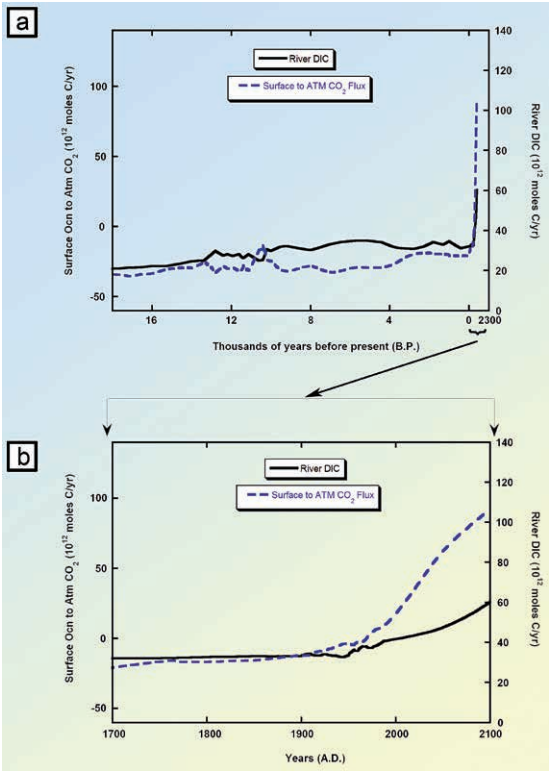

Figure 8.14 Model output from the LGM to the year 2100 **(a)** and enlargement of the trends from 1700 A.D. to 2100 A.D. **(b)** for the river flux of DIC to the coastal ocean and coastal ocean surface seawater air-sea exchange of CO_2 in units of 10^{12} mol C yr^{-1}. Negative values imply a net release of CO_2 to the atmosphere and positive values the opposite. Because the river flux of DIC, mainly total alkalinity, can buffer the magnitude of this exchange, this flux is also illustrated (after Lerman *et al.*, 2011).

The NEP of coastal waters from the LGM to 1850 increased from being net heterotrophic of -11 x 10^{12} mol C yr^{-1} to net heterotrophy of about -5 x 10^{12} mol C yr^{-1}, or 55% (Fig. 8.12). This change in NEP mainly reflected increasing total organic productivity by benthic and pelagic organisms in coastal ocean waters due to the increasing area of this region, but also due to rising temperature and increasing riverine nutrient fluxes to the coastal ocean.

Coastal surface water air-sea exchange flux of CO_2 was reduced from about -34 x 10^{12} mol C yr^{-1} (*i.e.* from water to air) at the LGM to about -16 x 10^{12} mol C yr^{-1} in the year 1850, or 53%, (Fig. 8.14) due to the relative decrease in the ratio of the volume of upwelling seawater with a high CO_2 content to the total coastal ocean volume (the model assumes that the rate of upwelling is constant, an unknown and problematic assertion), but also due to relatively greater increases in organic productivity relative to remineralisation of organic matter in shallowly buried sediments, and an increase in organic carbon deposition and sequestration in sediments in parts of the coastal ocean waters with suboxic to anoxic conditions (*e.g.*, Andersson *et al*., 2007). Contrary to this reduction in the air-sea CO_2 exchange flux due to enhanced organic production and subsequent organic carbon burial in sediments, resulting in sequestration of atmospheric CO_2, the increase in NEC alone actually led to an increasing release of CO_2 to the atmosphere from ~2 mol C yr^{-1} at the LGM to ~11 mol C yr^{-1} in late preindustrial time.

In addition, increasing remineralisation of organic material in coastal marine sediments probably led to increasing dissolution of biotically and abiotically produced carbonate minerals (Fig. 8.13) due in part to the reaction

$$CaCO_3 + CH_2O + O_2 = Ca^{2+} + 2HCO_3^-, \quad (8.1)$$

where $CaCO_3$ is calcite (or other carbonate minerals) and CH_2O a simplified representation of organic matter. Equation (8.1) is the summation reaction for organic remineralisation under oxygenated conditions coupled to carbonate mineral dissolution (Smith and Veeh, 1989). Under anoxic conditions the following reaction plays a role

$$2CH_2O + Ca^{2+} + SO_4^{2-} = CaCO_3 + H_2S + H^+ + HCO_3^-, \quad (8.2)$$

in which during the early stages of sulphate reduction, sediment pore waters can become undersaturated with respect to carbonate minerals owing to the generation of H^+, as well as in Fe-poor sediments where reoxidation of sulphide-generated acid can also drive undersaturation and dissolution. However, further sulphate reduction below about 30% of the modern seawater concentration of 28 mmol kg^{-1} and accompanying deposition of FeS_2 can lead to an increase of pore water saturation states with respect to carbonate minerals as TA increases in solution (Ku *et al*., 1999; Walter and Burton, 1990; Walter *et al*., 1993; Morse and Mackenzie, 1990), resulting in the potential for precipitation of carbonate cements.

Although we are still looking for the unequivocal explanation for the mechanisms and associated changes that took the Earth out of the LGM, this transition was no doubt part of Earth's natural cycle. The resolution of the mechanisms

controlling the rise of atmospheric CO_2 and changes in seawater carbon chemistry during the last Pleistocene deglaciation are not fully resolved but from the consistent cyclic patterns of variables that can be seen in Figure 8.2 for the past 800,000 years, the changes are consistent with a tightly coupled system, one that is self regulating and homeostatic. It seems to us that the only driver proposed to date that can qualify for this distinction is that of Milankovitch forcing. Once the system is nudged by this forcing a whole cascade of events follow that amplify the changes in the system.

Wally Broecker (Broecker, 2002, 2012) at the Lamont-Doherty Earth Observatory of Columbia University, USA, has concluded that there are potentially three types of forcing that can be responsible for the general pattern of climatic change observed during much of Pleistocene-Holocene time. These include: (1) changes in seasonality associated with the Earth's orbital cycles, the Milankovich forcing; (2) reorganisation of the ocean's thermohaline conveyor belt circulation pattern that is associated with catastrophic inputs of fresh water to the northern Atlantic; and (3) fluctuations in the sun's energy output associated with the appearance and disappearance of sunspots, that is sunspot activity. However, these three forcings are all too weak to account for the intensity of climatic change during glacial-interglacial transitions. There must be powerful amplifiers of the initial forcing also operating. Once the climate is nudged by one of the three forcings, the amplifiers play a major role in the pattern of climatic change that follows. The potential amplifiers include (1) feedbacks in the biogeochemical cycles of the natural greenhouse gases of CO_2, CH_4, N_2O, and tropospheric O_3 and resulting changes in atmospheric composition; (2) continental dust and sea salt aerosol loading of the atmosphere; (3) sea ice coverage in the northern Atlantic; (4) water vapour content of the atmosphere; (5) cloud cover; (6) ice sheets and their geographical extent, and (7) changes in net ecosystem calcification and net ecosystem productivity in the coastal ocean. One intriguing feature of these amplifiers is that most were certainly stronger during times of glaciation than during times of interglaciation. The resolution of the story of glacial-interglacial climatic and environmental change still has long way to go.

During the last glacial-interglacial transition, the human population was small; people lived nomadic life styles and had little impact on the ecosphere. With the event of the Neolithic Revolution about 10,000 years BP and the initial transition from hunting and gathering to settled agriculture and animal domestication, the human population started to increase more rapidly. As time progressed the combination of an increasing population and land use changes, such as deforestation, farmed and grazed lands, and construction of settlements, meant that humans started to have a direct and greater impact on their surrounding environment. Based on the previous glacial-interglacial cycles observed during the previous ~800,000 years, one might expect that the planet is due to start its entrance slowly into a glaciation stage in another several thousand years. It is possible but contentious that human agricultural and industrial activities may slow the Earth from venturing down this route. Ruddiman (2003) has promoted the concept that the Anthropocene Epoch started with the clearing of forests in

Eurasia 8,000 years ago contributing to an anomalous increase in atmospheric CO_2 (Fig. 8.15), and an increase in CH_4 about 5,000 years ago owing to rice irrigation. Furthermore he suggested without the beginnings of human intevention in the carbon cycle at this time, the world would have plunged into another glacial stage. However, the observed increase in CO_2 would require an area of the size of the Amazon forest to be deforested without compensatory regrowth of forested areas, an unlikely situation. In addition, the anticipated decrease due to the extensive deforestation necessary to satisfy Ruddiman's hypothesis in the $\delta^{13}C$ record of atmospheric CO_2 trapped in polar ice and that of foraminteral shells over this period of time is not observed (see *e.g.*, Broecker and Stocker, 2006; Broecker, 2012; Elsig *et al*., 2009). Nevertheless, the early human activities marked the beginning of human intervention in the ecosphere, which blossomed with the Industrial Revolution in the mid-nineteenth century. As shown by our model results, the coastal ocean went through major changes between the LGM and late pre-industrial time, albeit at a relatively slow rate compared to those changes that have occurred since the Industrial Revolution of 1850, and those changes anticipated for the next future several decades to century of the Anthropocene.

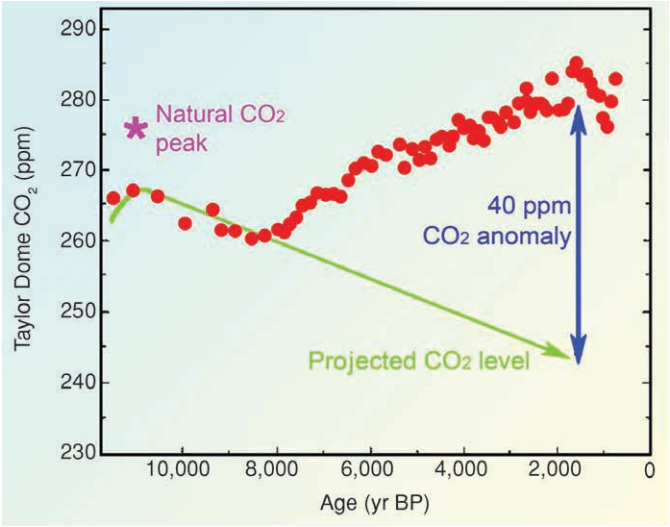

Figure 8.15 Atmospheric CO_2 record inferred from Taylor Dome ice cores on Antarctica. According to Ruddiman, without human activities modifying atmospheric CO_2 levels beginning at about 8,000 years ago, there would be 40 ppmv less of the gas in the atmosphere. The purple star represents the atmospheric concentration of CO_2 one would expect under natural conditions (Indermühle *et al*., 1999; modified from Ruddiman, 2003).

9. COASTAL OCEAN IN THE ANTHROPOCENE

9.1 Some General Statements

Since preindustrial time until present, the influence of external inputs and the forcings (an environmental influence that causes change in a system) on the global coastal ocean has increased enormously, and consequently, the role of the coastal ocean in the cycling of carbon and other elements has changed significantly. Increased industrialisation, transportation, and agricultural activities globally, particularly since the end of World War II, and the dramatic rise in the growth of the world's economies are responsible for the enhanced fluxes that add materials from human activities to the Earth's landscape, its atmosphere, and ocean (Fig. 9.1).

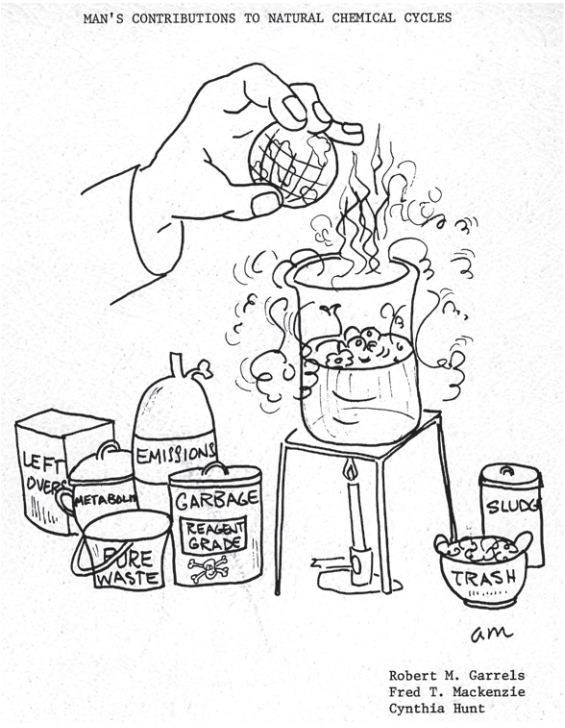

Courtesy of A. Conrad Neumann.

Figure 9.1 Cartoon of human interference in the natural biogeochemical cycles of the ecosphere from the cover of the book *Man's Contributions to Natural Chemical Cycles* by Garrels *et al.* (1976).

Human interference in the natural biogeochemical cycles, including the activities of land-use changes such as deforestation, agriculture, mining, and construction of factories, homes, roads, etc., have increased rates of erosion and the load of nutrients and organic material transported via rivers and groundwater runoff toward the coastal ocean (Fig. 8.9). Erosion may have increased by a factor of three to four at the global scale compared to natural levels and probably has increased by an order of magnitude locally (Vörösmarty *et al.*, 2004). However, the construction of dams and irrigation practices have increased the residence time of continental runoff on land, led to the retention of increasing amounts of sediments behind dams, and generally altered the hydrological cycle. Although human-controlled regulation of the flow of rivers has stabilised the flow for use by humans, it has changed habitats and migration paths for aquatic organisms (Vörösmarty *et al.*, 2004). The total river load of dissolved N and P has doubled at the global scale, but in some regions such as Europe and North America, it has increased by as much as a factor of 10 to 50 (Meybeck, 1982). In addition, more than 80% of the world's rivers exhibit a human imprint. In concert with changes in the material inputs to the coastal ocean, atmospheric CO_2, other greenhouse gas concentrations, global temperature (Fig. 8.9), and the average heat content and sea surface temperature of the ocean (Fig. 9.2) have also increased during the Anthropocene.

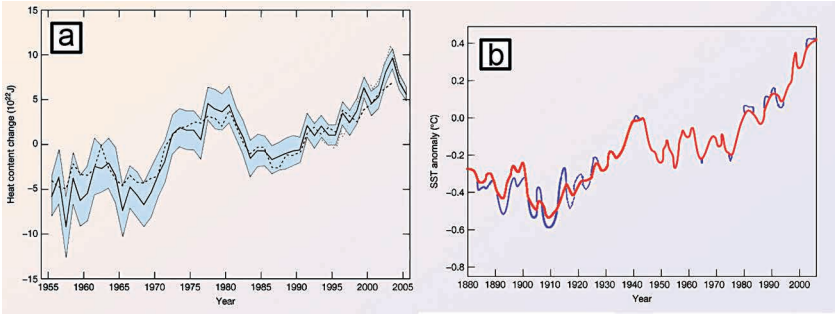

Figure 9.2 Trends in ocean heat content **(a)** and sea surface temperature (SST) **(b)**. The time series for global annual heat content in joules is for the 0 to ~700 m depth range in ocean waters. The various curves represent estimates by three groups: black line with blue shading for the 90% confidence limits, Levitus *et al.*, 2005; heavy dashed curve, Ishii *et al.*, 2006; and light dashed curve nearer end of record, Willis *et al.*, 2004 (in IPCC, 2007). The time series for sea surface ocean temperatures (two estimates: one in red, one in blue) is generalised and exhibits an average trend of ~ 0.65 °C per century (after Smith *et al.*, 2005).

There are many examples of the changing water chemistry and sediment loads due to human activities of riverine systems that deliver materials to the coastal ocean. One that is especially well documented is shown in Figure 9.3. It can be shown that a correlation exists between the amount of nutrients entering coastal environments and the population of people living in watersheds upstream

of these environments. As the population density of a watershed increases, the nitrate and soluble, biologically reactive phosphorus fluxes of a major river draining that watershed and entering a coastal environment increase. This relationship portends for the future increasing nutrient inputs into coastal environments and their enhanced cultural eutrophication (eutrophication due to human activities) because of increasing population density and the increase in agricultural, transportation, and urban activities associated with that population. The potential for enhanced eutrophication, coupled with increased inputs of pathogenic bacteria, viruses, heavy metals, and synthetic organic compounds, suggests increased degradation of coastal margin ecosystems and loss of habitat and species.

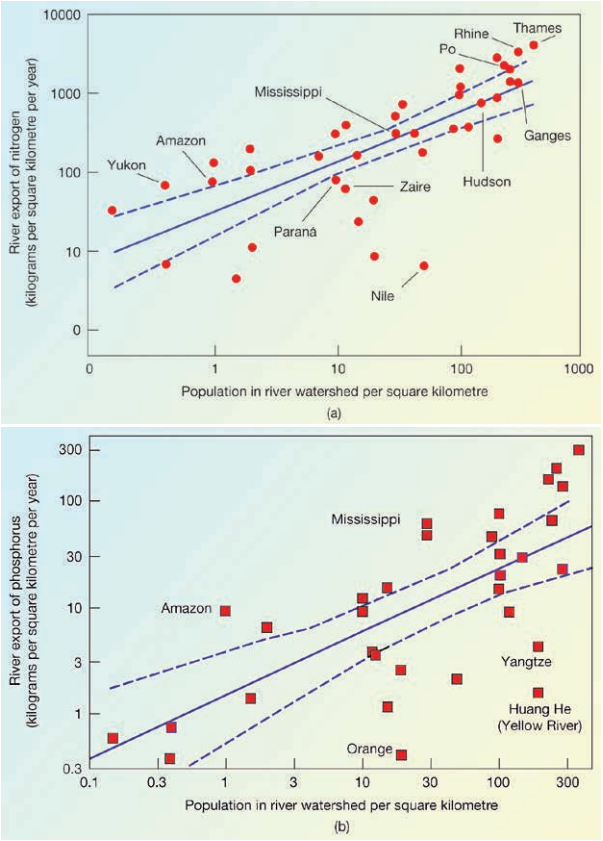

Figure 9.3 Relationship between the population density in a watershed and the export of dissolved NO_3^- **(a)** and phosphorus **(b)** as soluble, biologically available P by a river to the coastal ocean. The dark line represents the linear trend though the data and the dashed lines are measures of the degree of confidence in the relationship [**(a)** after Cole *et al.*, 1993; **(b)** after Caraco, 1995)].

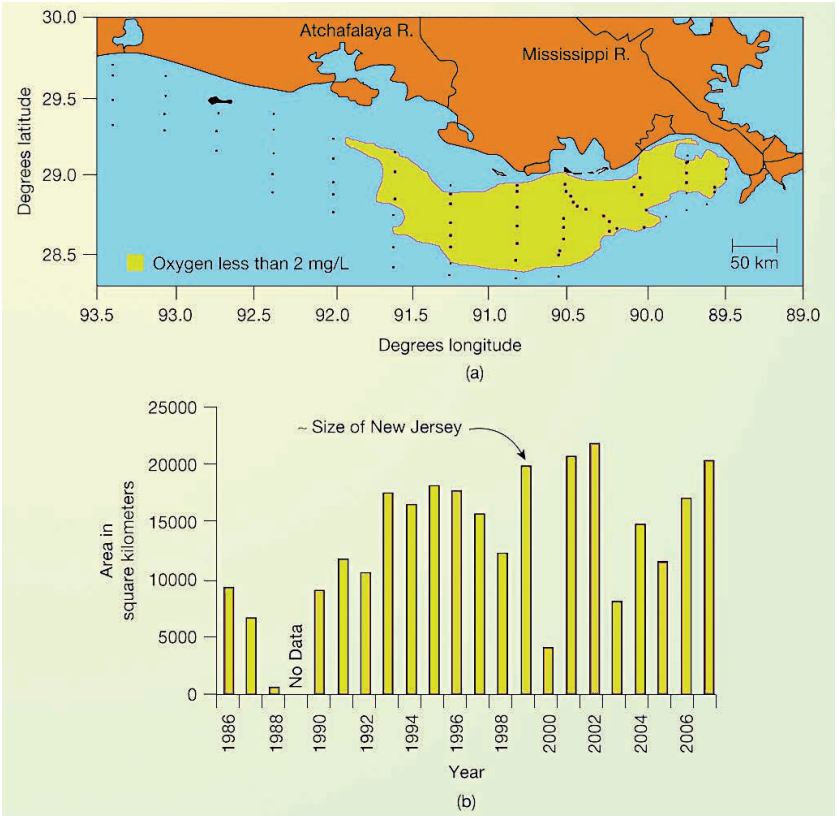

Figure 9.4 The Gulf of Mexico hypoxic zone. The extent of bottom water hypoxia (yellow area, less than 2 mg l^{-1} dissolved O_2) during July 21 to July 25, 1998 **(a)** The area of the hypoxic zone in the northern Gulf of Mexico from 1986 to 2007 in sq km. **(b)** (after Mackenzie, 2011).

An excellent example of what can happen to a coastal environment because of excess nutrient delivery via rivers is that of the development of the Gulf of Mexico hypoxic zone (Fig. 9.4). The Mississippi River and its tributaries in the United States drain two thirds of the conterminous area of the country and deliver nutrients via runoff to the Gulf derived from natural sources and steadily increasing anthropogenic sources of fertiliser and farm wastes, sewage, industrial and urban wastes, and combustion products of nitrogen. The loading of the landscape by nitrogen from nitrogenous fertilisers and by deposition of combustion nitrogen is particularly heavy in the Midwest of the country. The excess nutrients derived from anthropogenic sources reaching the sea enhance algal growth in coastal waters of this region of the Gulf (Fig. 9.4a). The bacterial decomposition

of the dead algae sinking through the water column leads to depletion of oxygen (O_2) dissolved in the water column, and when bottom water levels reach 2 mg l^{-1} O_2 or lower, the water is considered hypoxic. Such low levels lead to the death of most benthic organisms and impact significantly the abundance of fishes and shrimp living in the area. The hypoxic zone is especially well developed in the summer because of the development of a shallow seasonal thermocline. Figure 9.4b shows the comparative size of the Gulf of Mexico hypoxic zone from 1986 to 2007. Owing to the average westward flow of nearshore, shallow-water currents in this coastal region of the Gulf, the pattern of O_2 depletion mimics to some extent the flow pattern of the water.

Hypoxic zones in coastal environments throughout the world are developing more frequently, mainly because of nutrient pollution and subsequent phytoplankton blooms and later decay of organic material. In addition, as average sea surface temperatures increase, the solubility of oxygen in seawater decreases, further complicating the problem. The largest concentrations of these hypoxic and anoxic zones are found in off shore areas of the United States and Europe. These degraded and oxygen-deficient coastal waters can strongly affect the CO_2-carbonic acid system in coastal water bodies and air-sea exchange of CO_2.

9.2 Modelling the Anthropocene Coastal Ocean System

The general problem of the impacts of human activities on the global biogeochemical cycle of carbon, including the links between rising atmospheric CO_2 levels and global climate, gained considerably more attention after WWII. It was reasonably well known by this time that not only was the atmosphere a sink of anthropogenic CO_2 but also the ocean. A consensus that the land phytomass and organic carbon in soils could also be an anthropogenic CO_2 sink did not gain prominence until later in the twentieth century. Thus, both the atmosphere and the ocean as a whole, and later the terrestrial biosphere, became foci of process-based studies, monitoring, and modelling investigations. The degree of interference of human activities in the global carbon balance can be seen in Figure 9.5. Especially noteworthy are (1) the fossil fuel and land use CO_2 emissions, (2) the rate of accumulation of CO_2 in the atmosphere, which is responsible for ~60% of the enhanced greenhouse effect (human-induced global warming), (3) the roughly equal in magnitude land and ocean sinks of anthropogenic CO_2, the latter flux leading to ocean acidification, and (4) the organic carbon load to the ocean, which has increased due to land use activities of humankind.

A number of global carbon cycles for the early twenty-first century are similar to Figure 9.5 with the domain of the coastal ocean either included in the open ocean realm or simply overlooked. Our purpose here is to remedy that oversight using the modelling approaches described in Section 8 coupled with existing observational data from the spatially and temporally highly variable coastal ocean. Emphasis is on the numerical results from the modelling activities.

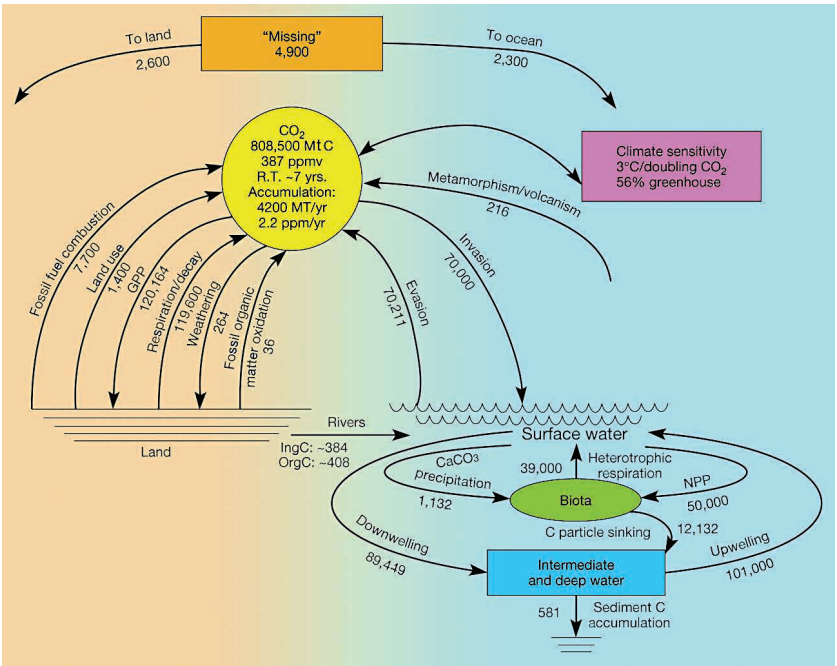

Figure 9.5 Non–steady state global biogeochemical cycle of carbon dioxide as carbon for the early twenty-first century. The processes affecting transfer of carbon as carbon dioxide between the surface of Earth and its atmosphere are shown, as well as the fluxes. Fluxes are in millions of metric tons (Mt) of carbon per year. The reservoir size of carbon dioxide is in millions of tons of carbon. Residence time (R.T.) is calculated with respect to gross primary production on land. The lifetime of CO_2 is on the order of 50 to 100 years but molecules of the gas from anthropogenic activities can remain in the atmosphere from thousands to a hundred thousand of years. The "missing CO_2" is the total of fossil fuel and land-use CO_2 emissions not accumulating in the atmosphere sink and represented primarily by the land uptake and ocean absorption sinks. Fifty-six percent of the enhanced greenhouse effect over the past two centuries is due to carbon dioxide, 16% to methane, 12% to tropospheric ozone, 11% to chlorofluorocarbons (CFCs), and 5% to nitrous oxide. A doubling of the atmospheric concentration of CO_2 could lead to a 3 °C increase in temperature (after Mackenzie, 2011). Fossil fuel and cement emissions, land use emissions, and the strengths of the ocean uptake and land uptake sinks of CO_2, and the atmospheric sink and its concentration in 2011 were ~ 9500, 900, 2500, 4000, 3900 Mt of C yr^{-1} and 390 ppm, respectively (after Mackenzie, 2011; Le Quéré *et al.*, 2012).

For most of the time period since the industrial revolution, our model calculations suggest that the global coastal ocean has served as a net source of CO_2 to the atmosphere owing to net heterotrophy and positive net ecosystem

calcification (Fig. 8.12). Nevertheless, during this time period, both gross primary production and total ecosystem respiration increased owing to increasing inputs of inorganic nutrients and reactive, respirable organic matter from land to the coastal ocean. Although the numerical results indicate that the increase in organic matter primary production (consumption of CO_2) has been roughly balanced by a nearly similar increase in total ecosystem respiration (production of CO_2) up until the present, future projections of the model suggest that nutrient inputs and gross primary production will continue to increase and progressively exceed land organic matter input and total remineralisation in coastal waters, leading to increased net autotrophy. This is mainly due to increased river and groundwater fluxes of N to the coastal zone. Increased autotrophy implies increased storage of organic matter within the global coastal region and/or increased export of organic matter to the open ocean, thereby also enhancing the potential role of the coastal ocean as a sink for atmospheric CO_2.

The residence time of global coastal ocean water is not well known so reasonable upper and lower bounds were adopted of 12 years and 4 years, respectively, in the *(SOCM)*. Numerical results suggest that the global coastal ocean would act as a source of CO_2 of -6 x 10^{12} mol C yr^{-1} (72 Mt C yr^{-1}) in the year 2000 for an average residence time of coastal waters of 12 years and a sink of CO_2 of 30 x 10^{12} mol C yr^{-1} for an average residence time of 4 years (Andersson *et al.*, 2005). The former flux estimate is in agreement with an estimate by Borges (2005) based on the observational CO_2 flux data from different coastal environments extrapolated to the global coastal ocean, including estuaries, whereas the latter estimate agrees with Borges' estimate if estuaries are excluded from this compilation. Thus, the model estimates agree to some extent with observational data. However, it is important to recognise that substantial uncertainty is associated with any generalisation of the global coastal region, which is highly variable and heterogeneous in both time and space. In particular, the model estimates are very sensitive to the average residence time of waters in the global coastal ocean and reflect the potential large influence of upwelling mainly on the distal part of the coastal ocean, *i.e.* the shelf and shelf break. Recent estimates of continental margin and coastal upwelling rates (Chavez and Toggweiler, 1995) indicate that the average residence time of water within the global coastal ocean is approximately two to three years, near the lower bound used in our *SOCM* calculations.

The most recent compilations of the role of the continental shelf in the net air-sea CO_2 exchange flux suggest that this region is on average net autotrophic with a global flux of CO_2 from air to sea ranging from 18.3 x 10^{12} mol C yr^{-1} (n=31; Cai *et al.*, 2006) to 37.5 x 10^{12} mol C yr^{-1} (n=17; Borges *et al.*, 2005). Significant heterogeneity is observed between different coastal regions, and in general, temperate and high latitude waters act as CO_2 sinks (27.5 x 10^{12} mol C yr^{-1} to 40.8 x 10^{12} mol C yr^{-1}), while low latitudes act as CO_2 sources (-2.5 x 10^{12} mol C yr^{-1} to -9.2 x 10^{12} mol C yr^{-1}) to the atmosphere, the latter owing to warm temperature and large inputs of carbon from the terrestrial realm. In contrast to the shelves and the distal region of the coastal ocean, estuaries and the proximal coastal region serve as sources of CO_2 to the atmosphere, which is sustained by

net heterotrophy, and perhaps to a lesser extent, calcification. This conclusion is partly based on the observation that the median of field measurements of air-water CO_2 fluxes in estuaries (-21 mol m^{-2} yr^{-1}, n = 62) is close to the median of field measurements of NEP (-14 mol m^{-2} yr^{-1}, n = 79) (Borges and Abril, 2011), which agrees with estimates of a low contribution (about 10%) of riverine CO_2 inputs to overall estuarine CO_2 emissions (Borges *et al.*, 2006).

As a result of increasing atmospheric CO_2 since late preindustrial time until present, *SOCM* results show that average seawater DIC in the coastal ocean has increased by 4% with associated increases in CO_2 and HCO_3^- by 44% and 8%, respectively, and decreases in pH-total, CO_3^{2-}, and aragonite saturation state by 1.5%, 19%, and 19% respectively (Figs. 8.11 to 8.14). Despite these predicted major changes in seawater carbonic acid system parameters in the coastal ocean, there is no direct observational evidence confirming these changes due to a lack of long-term time series measurements in coastal environments and the large variability in carbon chemistry of their waters in both time and space due to physical and biological processes. An example of this variability in one modern setting is that of the CO_2-carbonic acid system in coastal waters around Oahu, Hawaii, USA, as seen in the pCO_2 record of its surface waters over a period of time of 43 months (Fig. 9.6; see also Fagan and Mackenzie, 2007). Such variability confounds any attempts at modelling of the carbon system of coastal waters globally and even regionally.

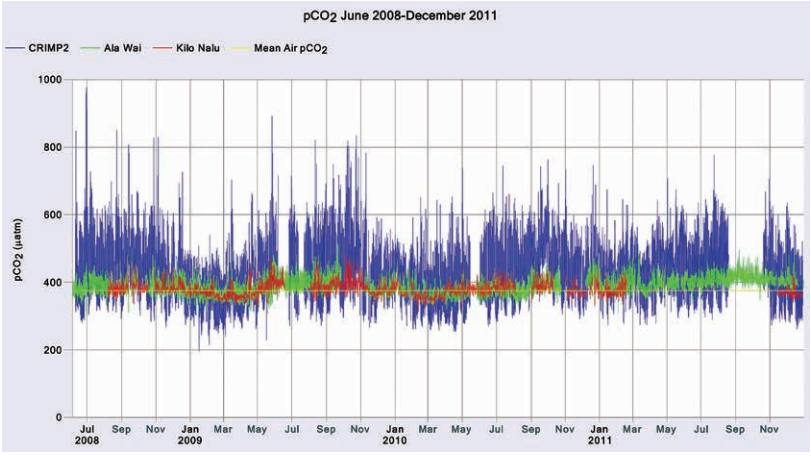

Figure courtesy of Pat Drupp, University of Hawaii.

Figure 9.6 Example of the variability in coastal ocean pCO_2 as observed in coastal surface waters of Oahu, Hawaii, USA. The data were obtained from CO_2 monitoring instrumentation affixed to moored buoys at three sites: CRIMP-2, Ala Wai, and Kilo Nalu and taken every three hours from all three buoys. The records of CO_2 show the long-term seasonal variability, due mainly to temperature changes, as well as the short-term (hourly, weekly) variability, due to both biological and physical forcings. CRIMP-2 (blue) is located in waters bathing the Kaneohe Bay barrier reef on the northeast coast of Oahu and exhibits the

largest variability in pCO_2 due to the high rates of calcification and organic productivity of the reef flat. Ala Wai (green) and Kilo Nalu (red) buoys are located in coastal waters on the south shore of Oahu. Ala Wai pCO_2 is influenced by runoff from the nearby Ala Wai canal and stream. However, Kilo Nalu pCO_2 exhibits little variability and is most representative of the surrounding well mixed waters of the open ocean. The yellow line is the mean air pCO_2 of 377 μatm observed over the study period.

In contrast to the coastal ocean, open-ocean time series stations located in Hawaii (Hawaii Ocean Time-series, HOT), Bermuda (Bermuda Atlantic Time-series Station, BATS), and the Canary Islands (European Station for Time-series Observations in the oCean, ESTOC) have shown a consistent trend in changes of the CO_2-carbonic acid system resulting from increasing atmospheric CO_2 concentrations (Bates, 2007; Bates *et al*., 2012; Dore *et al*., 2008; González-Dávila *et al*., 2010). For example, at BATS surface seawater total dissolved inorganic carbon concentration (DIC) has increased by 1.53±0.12 μmol kg^{-1} yr^{-1} between 1983 and present; pH has decreased at a rate of -0.0016±0.00022 pH units per year, and the saturation state with respect to aragonite has decreased at a rate of -0.01±0.0012 units per year (Bates *et al*., 2012) (Fig. 9.7). These trends although slightly different in pattern and rate of change are also seen at the HOT station and for a shorter period of time at ESTOC (Fig. 9.7). The changes have collectively been referred to as ocean acidification, which mainly refers to the decrease in seawater pH.

Since late preindustrial time, the average surface seawater pH has decreased by 0.1 pH units, which corresponds to a 25% increase in acidity defined as the total hydrogen ion concentration. As a comparison, the average surface seawater pH decreased from approximately 8.35 to 8.18 (Foster, 2008) between the LGM and pre-industrial time, a 60% increase in seawater acidity. The model simulations of *SOCM*, as well as other model predictions, suggest that the pH in both coastal and open ocean waters will decrease by an additional 0.3-0.4 pH units by the year 2100 under a business-as-usual CO_2 emission scenario, which corresponds to an additional increase in acidity of 100% to 150%. These changes in the seawater acid-base balance of the CO_2-carbonic acid system certainly will have a significant impact on marine ecosystems and biogeochemical processes in the global coastal ocean that could significantly influence its role and function as a global ecosystem. We discuss these changes and implications in the next section.

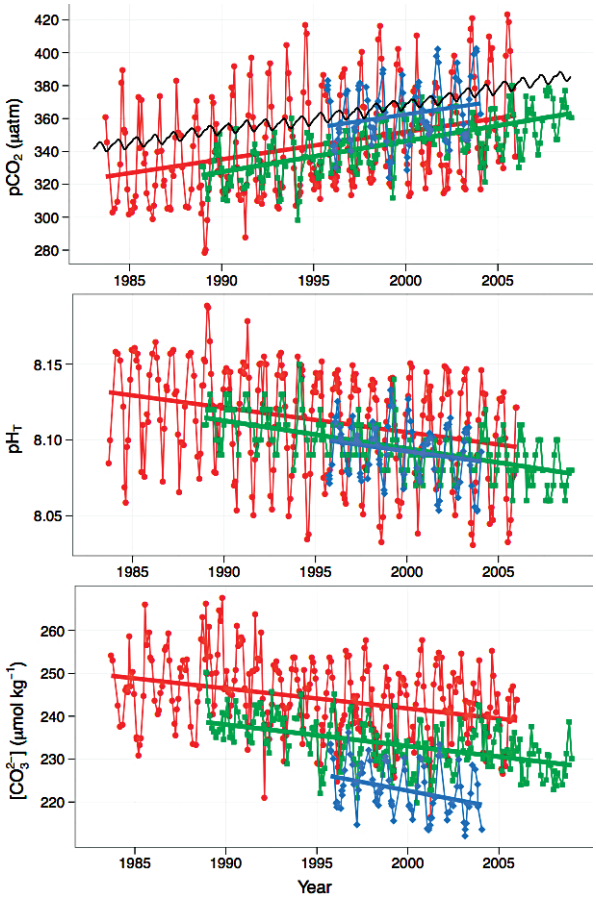

Figure 9.7 Surface seawater pCO_2, pH-total, and $[CO_3^{2-}]$ at Bermuda Atlantic Time-series Station (BATS; red), Hawaii Ocean Time-series (HOT; green), and European Station for Time-series Observations in the ocean (ESTOC; blue) as a function of time. Atmospheric pCO_2 is shown by the black line in the top panel (after Orr, 2011).

10. MODERN ASPECTS OF THE PROBLEM OF OCEAN ACIDIFICATION

In this section we investigate aspects of modern OA concentrating on the biogeochemistry of the problem. Departing somewhat from previous sections of this monograph, we employ a story narrative, mainly reflecting on the work and the questions the two of us, with the help of several colleagues, have pursued beginning in the early 2000s.

10.1 Ocean Acidification (OA) and the Magnesian Salvation Theory

A year or so before we began the initial efforts constructing the *SOCM*, a couple of articles appeared in the literature showing that the calcification rate of corals was strongly dependent on the seawater aragonite saturation state (Ω_a) (Gattuso *et al.*, 1998, 1999). Recognising the implications of this positive correlation, Kleypas *et al.* (1999) modelled changes in surface Ω_a and how $CaCO_3$ production might change in response to rising atmospheric CO_2. This work raised the awareness of the scientific community and the public to the fact that coral reefs might be at risk owing to this anthropogenic biogeochemical perturbation experiment, which we now refer to as ocean acidification. However, it should be pointed out that *Wally Broecker* and *Taro Takahashi* several decades earlier had demonstrated the dependence of rates of $CaCO_3$ precipitation on Ω_a in the Bahamas while studying whitings (milky seawater containing floating patches of $CaCO_3$) (Broecker and Takahashi, 1966). Similarly, a number of pioneers had as early as in the 1920s carried out experiments investigating the effect of seawater pH on various marine organisms (see review in Gattuso and Hansson, 2011) but did not recognise the global problem of ocean acidification. In 1992 Smith and Buddemeier published a paper where the authors made the connection between coral reefs and the threat of OA on their accretion rates. It was also *Bob Buddemeier* who suggested to *Jean-Pierre Gattuso* to investigate how coral calcification was impacted by decreasing seawater aragonite saturation state, but it took *Jean-Pierre* several years before he actually conducted the experiments (J.-P. Gattuso, personal communication). Hence, it was not until the publications of Gattuso *et al.* (1998, 1999) and Kleypas *et al.* (1999), and later a paper by Caldeira and Wickett (2003) that research specifically addressing modern ocean acidification really expanded (Fig. 10.1).

Shortly after the Kleypas *et al.* (1999) article, a couple of abstracts appeared in the International Coral Reef Symposium (held in Bali, Indonesia in the year 2000) abstract volume claiming that marine calcifying organisms would not be negatively affected by OA because dissolution of metastable carbonate minerals, especially the high Mg-calcite skeletal phases (see Supplementary Information SI-1), would occur and buffer seawater pH and Ω_a (Barnes and Cuff, 2000; Halley and Yates, 2000). Publication of this work was followed by a lively discussion online on the coral-list web site (http://coral.aoml.noaa.gov/archive/coral-list-2001.txt)

between several individuals arguing whether or not this process, referred to as the Magnesian Salvation Theory (MST), was important. The idea behind the hypothesis arose from the fact that shallow water carbonate sediments contain a significant proportion of skeletal Mg-calcite minerals (~25%; Land, 1967; Morse and Mackenzie, 1990), and of lesser importance, abiotic Mg-calcite cement. Many compositions of these Mg-calcite phases are more soluble than both aragonite and calcite. If the surficial sediment reservoir (the upper 50 cm or so of modern sediments) containing these minerals dissolved in response to anthropogenic OA, the process would generate alkalinity that consequently could buffer to some extent changes in seawater pH and Ω_a depending on the amount of TA produced by dissolution that accumulated within a system and the increase in TA relative to DIC (Morse *et al.*, 2006; Andersson and Mackenzie, 2012). However, during the ongoing discussion on the online coral-list about the MST, Buddemeier succinctly outlined why dissolution of high Mg-calcite biogenic and abiotic cement phases would not significantly buffer seawater from OA (http://coral.aoml.noaa.gov/archive/coral-list-2001.txt). This fact had also been pointed out previously in a U. S. Department of Energy report edited by Garrels and Mackenzie (1980).

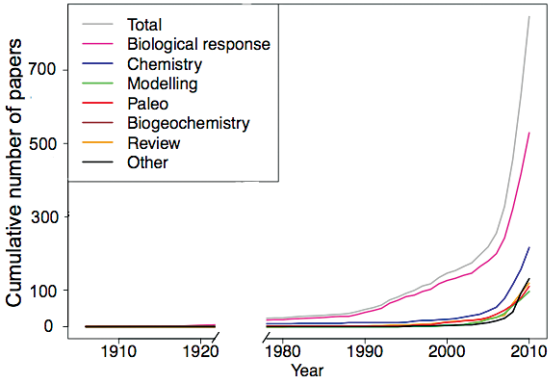

Figure 10.1 Cumulative number of articles published on OA shown as the total number of publications and the number of publications for specific research areas as a function of time (modified from Gattuso and Hansson, 2011).

To further analyse the MST problem, we thought that the *SOCM* described in Chapter 8 of this monograph offered an additional approach to evaluate quantitatively the hypothesis. The resultant modelling results clearly confirmed the conclusion that the CO_2-carbonic acid system of global coastal ocean waters, as well as most shallow water environments in general (including coral reefs), would not be significantly buffered by dissolution of metastable carbonate minerals on time-scales of decades to hundreds of years (Andersson *et al.*, 2003, 2005, 2006; Andersson and Mackenzie, 2012). The major reason for this was that the rates of carbonate mineral dissolution were much too slow and dilution with open ocean

seawater too fast to allow significant amounts of alkalinity to accumulate in shoal-water, marine environments, except perhaps in enclosed marine carbonate sediment regimes with very long water residence times.

The initial publication of the *SOCM* results provides an amusing story of how modern ocean acidification science evolved. As we felt our initial modelling results were quite important, we first submitted the manuscript to Nature, but the manuscript came back almost faster than it was submitted, as the editor did not find this area of research very exciting! Nevertheless, after pointing out the potential implications of OA, the manuscript was sent out for review. However, as one of the reviewers apparently already suspected that dissolution of metastable carbonate minerals would not buffer changes in seawater chemistry arising from increasing atmospheric CO_2, the manuscript was deemed to be not sufficiently novel for publication in the journal Nature. We subsequently submitted it to Geology, where it was published a few months later (Andersson *et al.*, 2003).

Although $CaCO_3$ dissolution will not prevent the negative effects of OA on short timescales, on longer timescales of several thousands of years, dissolution of carbonate sediments in both shallow coastal waters and most importantly at depth in the ocean attendant by the consequent shoaling of the carbonate mineral saturation horizons will act as the ultimate sink of anthropogenic CO_2, the antacid or buffer of the world's oceans (Archer *et al.*, 1998; Broecker, 2003), a process mainly dictated by the overall mixing rate of the ocean, which is on the order of roughly 1,000 years.

Although dissolution of metastable carbonate minerals proved ineffective to buffer OA on short timescales, the *SOCM* model results indicated that carbonate mineral dissolution would significantly increase in the future not only in response to OA, but also owing to the anticipated increasing input, deposition, and remineralisation of organic matter in near-shore environments (Andersson *et al.*, 2003, 2005; Mackenzie *et al.*, 2005). However, the extent of dissolution of metastable Mg-calcite mineral phases depended strongly on which experimental solubility curve was adopted in the modelling calculations (Andersson *et al.*, 2005). As a matter of fact, the solubility and rates of dissolution in seawater solutions of Mg-calcite mineral phases are one of the most controversial and highly debated problems related to this group of mineral phases (*e.g.*, Plummer and Mackenzie, 1974; Thorstenson and Plummer, 1978; Garrels and Wollast, 1978; Mackenzie *et al.*, 1983; Walter and Morse, 1984; Bischoff *et al.*, 1987; see Morse *et al.*, 2006 for a detailed discussion and references therein).

In general, biogenic Mg-calcites with a significant mol% $MgCO_3$ are more soluble than both calcite and aragonite, and the approximate Mg-calcite composition with the same solubility as aragonite ranges from 8 to 12 mol% $MgCO_3$ depending on the experimental solubility curve adopted. There are essentially two different experimental solubility curves expressed as a function of mol% Mg for biogenic Mg-calcite phases that are referred to as the biogenic 'minimally prepared' (Plummer and Mackenzie, 1974) and the biogenic 'cleaned' solubility

curves (*e.g.*, Bischoff *et al.*, 1987) (see Supplementary Information SI-1 and Fig. 10.2). The differences in experimental results are believed to be a result of the methods used in preparation of the experimental materials (Bischoff *et al.*, 1993).

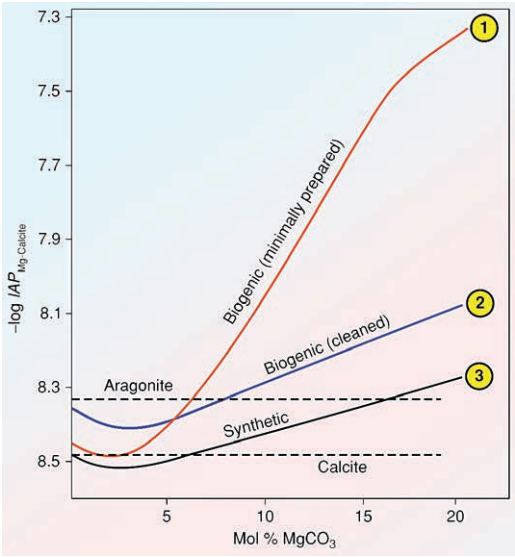

Figure 10.2 Solubility of the magnesian calcites as a function of the $MgCO_3$ in the phase for biogenic phases minimally prepared (1) and well cleaned and annealed (2), and synthetic pure phases prepared at high temperature and pressure in sealed hydrothermal bombs (3) before use in dissolution experiments to obtain the solubility of the Mg-calcites. The smaller the value of the –log IAP, the greater the solubility of the Mg-calcite (see also Supplemental Information SI-1 for details of the various curves, after Bischoff *et al.*, 1993).

At this time, it is not fully understood which solubility curve most accurately reflects the behaviour of the biogenic Mg-calcite minerals in the natural environment (Morse *et al.*, 2006), although suggestions and evidence in favour of the use of the 'minimally prepared' solubility curve are found in the literature (Bischoff *et al.*, 1993: Tribble *et al.*, 1995; Andersson *et al.*, 2007). Problems that compound the determination of the solubility of biogenic calcites arise from their heterogeneous nature, structural disorder, and inclusion of impurities in their structure other than Mg, such as H_2O, OH^-, HCO_3^-, SO_4^{2-}, which commonly are found in biogenic skeletons. The pure synthetic phases used in the solubility dissolution experiments referred to in Figure 10.2 do not have these structural or compositional problems. A further problem, which has been known for some time but largely overlooked, stems from the fact that a true equilibrium cannot be established between a given Mg-calcite composition and a solution (Garrels and Wollast, 1978). In the initial stages of experimental dissolution studies, the

dissolution process occurs congruently (the Mg-calcite phase dissolves producing chemical species in solution with the same ratio as that in the solid), but becomes incongruent (the ratio of dissolved chemical species in solution is different than that of the dissolving solid) as the solution becomes supersaturated with respect to a Mg-calcite phase of lower magnesium content, which then starts to precipitate. To overcome this problem, experimentalists have extrapolated data from the congruent step to infinite time, making the assumption that this stage in reaction progress represents a metastable equilibrium state for the Mg-calcites. This condition is referred to as stoichiometric saturation for the solid solution (see detailed explanation in Plummer and Mackenzie, 1974 and Thorstenson and Plummer, 1978). It should also be mentioned that most studies involving the stability of Mg-calcites at low temperature and pressure have been done in dilute solutions and not in seawater.

Following our initial model simulations concerning whether or not $CaCO_3$ dissolution could buffer the CO_2-carbonic acid system in surface seawater in shallow water environments, we were curious as to what the uncertainty in the solubility of Mg-calcite minerals implied for carbonate sediments and calcifying organisms composed of these mineral phases in the context of ocean acidification. In addition, we wanted to know which solubility curve most accurately represented observations in the natural environment. As a first step, we constructed a very simple dissolution model, essentially mimicking a batch reactor with the properties of the global coastal ocean, which was forced externally by increasing seawater pCO_2 following the timing and projections of the IPCC under the business-as-usual IS92a CO_2 emission scenario and linearly extrapolated to the year 2300 (Andersson *et al*., 2006; Morse *et al*., 2006). As anticipated, the numerical simulations showed radically different results depending on the solubility curve adopted (Fig. 10.3).

In a scenario adopting the biogenic "cleaned" solubility curve, seawater did not become undersaturated with respect to the most soluble Mg-calcite mineral phase, containing 18 mol% $MgCO_3$, until the end of the simulation in the year 2275. Thus, the reactive Mg-calcite mineral reservoir of surficial sediments was little affected by future surface ocean acidification. This model simulation did not take into account modifications of seawater arising from biogeochemical processes in the water column, microenvironments, and sediment pore waters. In contrast, in the scenario adopting the biogenic "minimally" prepared solubility curve, the entire Mg-calcite mineral reservoir of sediments in the range of 11 to 18 mol% dissolved by the year 2175, following a sequential dissolution succession pathway according to mineral stability. As seawater became undersaturated with a particular mineral phase owing to the pCO_2 forcing and consequent ocean acidification, it started to dissolve, reaching a metastable equilibrium with the seawater, which would persist until the mineral phase had completely dissolved and a new metastable equilibrium would be reached with the next most soluble Mg-calcite phase present in the model sediment reservoir. Despite the extensive dissolution observed in this simulation, as well as under a number of sensitivity scenarios

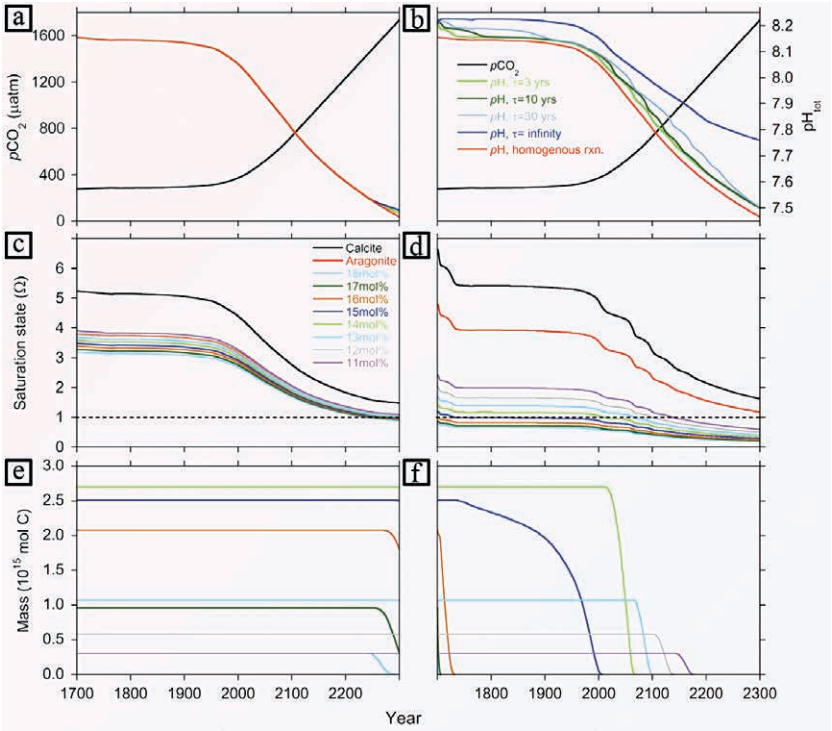

Figure 10.3 Mg-calcite reservoir masses and calculated surface seawater saturation state with respect to calcite, aragonite, and 11 to 18 mol% Mg-calcite based on the biogenic "best fit" solubility data (a, c, e) and the Plummer and Mackenzie (1974) solubility data (b, d, f) as a function of pCO_2 in an open system model scenario, *i.e.* exchange with the open ocean. (a, b) pCO_2 forcing and resulting surface seawater pH in multiple scenarios adopting different shoal-water residence times (τ). The results of panels C-F are based on the scenario of a three year residence time showing (c, d) surface seawater carbonate saturation state (Ω), and (e, f) Mg-calcite reservoir masses (after Morse *et al.*, 2006).

changing the seawater residence time, a significant buffer effect preventing negative effects on calcifying organisms was never observed. This finding confirmed our previous model results with *SOCM*. However, the results showed that the choice of the Mg-calcite solubility curve had important implications for the extent of the predicted effects of OA on Mg-calcite phases found in carbonate sediments in nature. Subsequently, we turned our focus to a natural carbonate environment in Bermuda, referred to as Devil's Hole, which during part of the year experiences elevated CO_2 conditions, to see if we could detect any clues as to the dissolution behaviour of Mg-calcite minerals in nature that would shed some light on our modelling results and perhaps the relevant solubility curve of Mg-calcites.

Devil's Hole is located within Harrington Sound, Bermuda, in the Sargasso Sea region of the North Atlantic Ocean. The Sound is a semi-enclosed body of water that during late spring and early summer develops thermally induced density stratification owing to the exponential decrease in absorption of solar irradiance with depth. Vertical mixing is impeded by this stable stratification, which isolates to some degree the deeper parts of the Sound from the overlying mixed layer (Fig. 10.4).

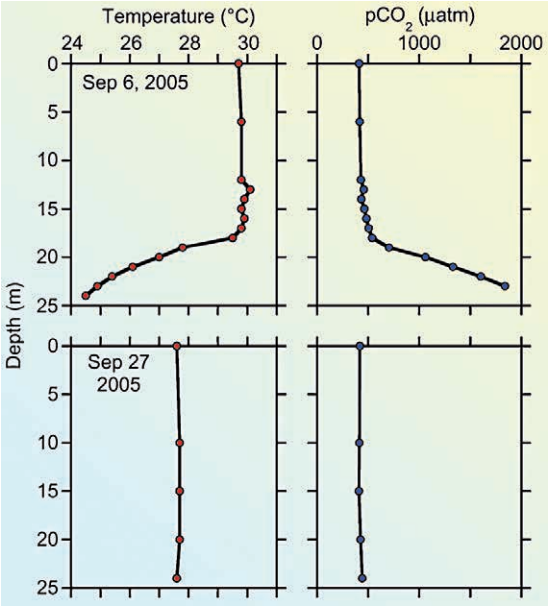

Figure 10.4 Vertical profiles of temperature and pCO_2 in Devil's Hole close to the timing of the maximum stratification of the seasonal thermocline (September 6, 2005), as well as after the overturn of the thermocline (September 27, 2005). The pCO_2 of the subthermocline water is significantly higher than that normally observed in natural shallow surface seawater environments (after Andersson *et al.*, 2007).

As a consequence, organic matter settling through the water column is remineralised below the seasonal thermocline and drives the pCO_2 of the subthermocline region to levels well exceeding CO_2 levels anticipated as a result of OA by the end of the twenty-first century. Since suspended particles and near-surface sediments in Harrington Sound are completely dominated by a metastable assemblage of carbonate minerals of varying composition originating from marine calcifying organisms present within the Sound (*e.g.*, corals, coralline algae, barnacles, holothurians, benthic foraminifera, bryozoans, echinoids, etc.)

or from limestone rocks and eolianites surrounding the Sound, Devil's Hole is an excellent natural laboratory to study the solubility and kinetic behaviour of calcium carbonate minerals under elevated pCO_2 conditions.

Concurrent with high pCO_2 and low seawater saturation state with respect to aragonite in the subthermocline waters of Devil's Hole, strong evidence of $CaCO_3$ dissolution was observed based on the excess total alkalinity and calcium concentrations analytically measured in this layer (Fig. 10.5).

The slope of the best-fit line of the concentration of dissolved calcium [Ca^{2+}] plotted as a function of TA suggested that the average composition of the dissolving $CaCO_3$ phase was roughly equal to a Mg-calcite composition containing 15 mol% $MgCO_3$, but due to large uncertainties in the analytical determination of [Ca^{2+}], no unequivocal conclusion could be made from the data as to the exact composition. However, in a detailed study of the calcifying fauna and sediment properties of Devil's Hole and Harrington Sound conducted in the 1960s, Conrad Neumann observed a distinct trend of decreasing high Mg-calcite content in the silt- to clay-sized sediment classes as a function of depth in Devil's Hole, and thus, increasing pCO_2 and decreasing Ω for part of the year (Neumann, 1965). Our calculations of the seawater saturation state with respect to Mg-calcite mineral phases, based on solubility products determined at stoichiometric saturation, suggested that the bottom waters of Devil's Hole were undersaturated with respect to a ~12 mol% Mg-calcite according to the biogenic 'minimally prepared' solubility curve and a phase with >18 mol% Mg-calcite according to the biogenic 'cleaned' solubility curve. Strictly based on these observations, it appears that the former solubility curve might best represent the solubility behaviour of Mg-calcites in the natural environment.

Until recently, the biogenic 'minimally prepared' solubility curve was only represented by data from one experimental study, that of Plummer and Mackenzie (1974) amended by Thorstenson and Plummer (1978), while the biogenic 'cleaned' solubility curve was represented by data from several experimental investigations using different methodologies (*e.g.*, Chave *et al*., 1962; Land, 1967; Schmalz, 1967; Walter and Morse, 1985; Bischoff *et al*., 1987). However, a recent study by Yamamoto *et al.* (2012) investigating the seawater threshold with respect to aragonite at which a mélange of coral reef carbonate sediments start to dissolve appears to agree with what is predicted by the Plummer and Mackenzie solubility curve. Thus, in conclusion, if the modelling and observational results are correct, we are likely to see a gradual change in the average Mg concentration and average mol% Mg-calcite sediment composition during the next couple of hundred years as a result of ocean acidification, if human activities follow a Business as Usual (IPCC, 2007) or one more onerous scenario in the future (Andersson *et al*., 2005, 2006). In addition, the Magnesian Salvation Theroy will not save the coral reefs of the world.

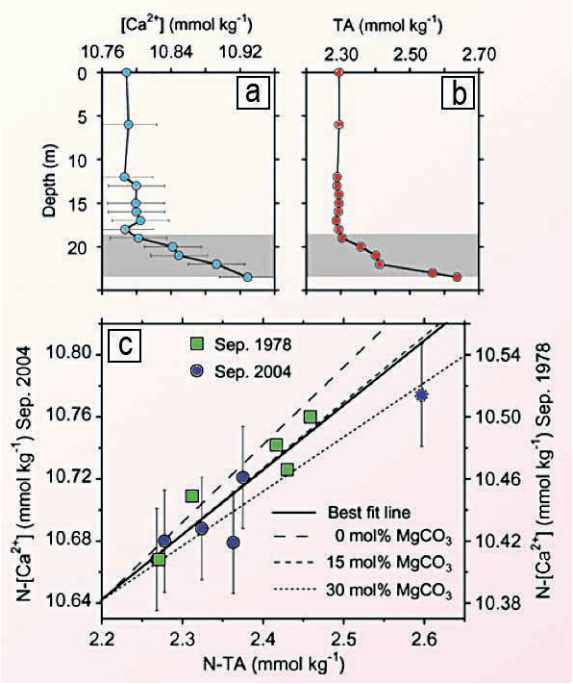

Figure 10.5 **(a)** Calcium concentration and **(b)** total alkalinity as a function of depth in Devil's Hole on September 16, 2004. The subthermocline layer is shown by the shaded area. **(c)** Normalised calcium concentration (N–[Ca^{2+}]; S = 36) as a function of normalised total alkalinity (N-TA) in Devil's Hole in September 1978 and 2004. The dashed lines show the predicted theoretical slopes if the average composition of the dissolving mineral phase was pure calcite or aragonite (0 mol% $MgCO_3$), 15 mol% Mg-calcite, or 30 mol% Mg-calcite. The solid line is the best fit line (slope = 0.42) of the relative changes of the combined data. Error bars indicate the average 1σ precision of triplicate samples (n = 5) (after Andersson *et al.*, 2007).

10.2 "Time Travel" Approach to find Answers about the Effects of Ocean Acidification on Marine Organisms

As significant as the alterations to the average Mg-calcite composition of the surficial reactive carbonate reservoir might be in response to ocean acidification, it is certainly of greater concern as to what the consequences will be for the source of these minerals, *i.e.* marine organisms depositing shells and skeletons made of Mg-calcite. Numerous experiments have shown that the rate of calcification and the ability to build robust calcareous structures made of calcite, aragonite, or Mg-calcite could be negatively affected by decreasing seawater carbonate

saturation state for a range of different marine calcifiers including corals, coralline algae, echinoderms, bivalves, gastropods, bryozoans, foraminifera, pteropods, and coccolithophorids (see reviews in Doney *et al*., 2009; Andersson *et al*., 2011; Riebesell and Tortell, 2011). From a thermodynamic perspective, it becomes increasingly energetically expensive for organisms to calcify at low seawater saturation states with respect to the carbonate phase they deposit, and at undersaturated conditions, this process may become unfeasible as calcareous structures may dissolve faster than organisms are able to build them. It all comes down to energetics, and given sufficient energy resources, organisms may be able to upregulate, that is overcome and counteract the environmental gradients in seawater chemistry. In addition, living organisms may also produce organic coatings that inhibit dissolution (Morse and Mackenzie, 1990).

Although all marine calcifiers will be exposed to lower seawater saturation state with respect to their carbonate mineralogy as a result of ocean acidification, many organisms depositing Mg-calcite mineral phases will be immersed in seawater undersaturated with respect to this group of minerals; the higher the Mg content of the phase, presumably the higher the solubility and vulnerability. Hence, these organisms and mineral phases may act as the first responders to ocean acidification (Morse *et al*., 2006; Andersson *et al*., 2008). However, there is a caveat to this conclusion and this involves the kinetic controls on the dissolution of biogenic carbonate phases in seawater (see Supplementary Information SI-2). The microarchitecture, the size and arrangement of crystals and pores within an organism skeleton, is a property other than solubility that can determine the relative dissolution rates of calcifying organisms. For example, Walter and Morse (Walter, 1985; Walter and Morse, 1985) showed in experimental seawater solutions undersaturated with respect to the aragonitic green algal *Halimeda sp.* and a more soluble Mg-calcite red algal that the *Halimeda* dissolved faster. The Walter and Morse work is the only fundamental and complete laboratory experimental study of the dissolution kinetics of biogenic carbonate phases in seawater solutions. There is an urgent need for more research on the subject as our oceans continue to acidify.

As discussed previously in Section 5, the mechanisms controlling the magnesium content of marine calcifying organisms are not well understood. Marine calcifiers depositing aragonite contain almost none or very little magnesium (<1 mol%) and the same is true for the pelagic calcite producers, which are mostly represented by certain species of coccolithophorids and foraminifera. Among organisms depositing Mg-calcite of various compositions, ranging from a few mol% to as much as 30 mol% $MgCO_3$, there are distinct differences between different species. Clearly, there is a strong taxonomic control on the magnesium content of calcitic skeletons (Chave, 1954). Also, the magnesium content of marine calcifiers depositing Mg-calcite is seen to decrease as a function of increasing latitude (Fig. 10.6). Thus, the Mg content of skeletal hard parts covaries with changes in environmental variables such as temperature, light, and seawater carbonate saturation state, all of which decrease with increasing latitude (Chave, 1954; Mackenzie *et al*., 1983; Andersson *et al*., 2008).

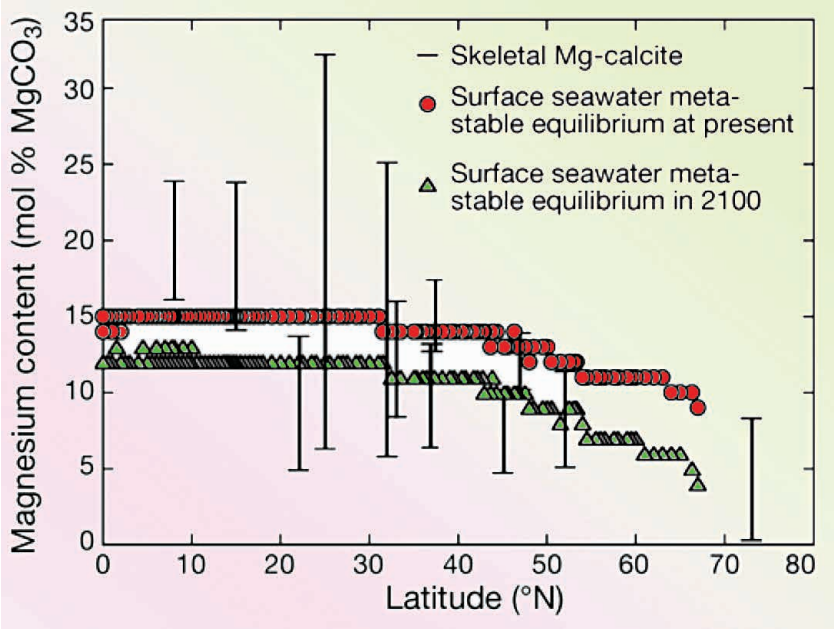

Figure 10.6 Range of magnesium content of calcitic skeletons as a function of latitude (Chave, 1954). The Mg-calcite phase in metastable equilibrium with the surface seawater according to the 'minimally prepared' solubility curve is also shown at present time and in the year 2100 under a Business-as-Usual CO_2 emissions scenario (IS92a) (after Andersson *et al.*, 2008).

The observed variation in the magnesium content of marine calcifying organisms may be attributed to variations in growth rate (Moberly, 1968), which is not only a function of temperature and seawater carbonate saturation state, but also energy availability (*i.e.* food). In addition, in phototrophic organisms (or organisms dependent on phototrophic symbionts), it is also a function of photosynthetic activity and consequently light and nutrient concentrations (see *e.g.*, Mackenzie *et al.*, 1983; Mackenzie and Agegian, 1989; Ries, 2011 for differing opinions on the issue). The "bottom line" is that the ultimate control(s) on the Mg content of marine calcifiers is still incompletely understood and requires additional well-conceived and careful experimental methodologies to resolve the problem. Nevertheless, as the oceans continue to take up anthropogenic CO_2, decreasing seawater pH and saturation state with respect to carbonate minerals, many marine calcifiers will find themselves immersed in seawater undersaturated with respect to the mineral phase they deposit (following the Plummer and Mackenzie, 1974, solubility curve), unless they are able to deposit increasingly less soluble calcareous structures as the seawater chemistry changes. This ability has been observed for some calcifiers. Stolarski *et al.* (2007) discovered that corals

known to deposit aragonite actually secreted calcite during an episode of the Cretaceous Period. Ries *et al.* (2006) observed similar results for corals grown in artificial seawater of variable magnesium to calcium ratio, thus, changing the composition of the mineral phase favoured to precipitate based on thermodynamic and kinetic principles. However, the former conclusion was based on slow changes in seawater carbon chemistry (see Section 4) and the latter on changing the seawater Mg/Ca ratio, which will not occur on the time scale of modern ocean acidification.

Adopting empirical relationships between rates of calcification, $CaCO_3$ dissolution, and the seawater and pore water carbonate saturation states, model simulations of *SOCM* extended to the year 2300 showed that calcification and $CaCO_3$ production in the global coastal ocean would decrease by 42% and 91% by the years 2100 and 2300, respectively, and $CaCO_3$ dissolution increase by 20% and 260% by the years 2100 and 2300, respectively, relative to late preindustrial conditions (Fig. 10.7; Andersson *et al.*, 2005, 2006). Furthermore, the results suggested that sometime during the twenty-second century, $CaCO_3$ dissolution would exceed $CaCO_3$ production and the global coastal ocean would undergo a net loss of $CaCO_3$. The timing of this simulation is highly uncertain, but the trend is robust.

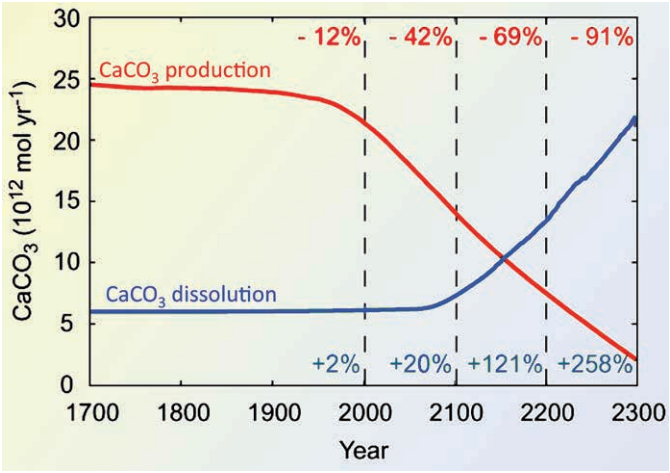

Figure 10.7 Modelled $CaCO_3$ production (red line) and dissolution (blue line) in the global coastal ocean between the years 1700 and 2300 based on the *SOCM* numerical calculations. The percentages in red indicate the years where the original year 1700 $CaCO_3$ production of ~25 x 10^{12} mol C yr^{-1} falls by 12%, 42%, 69%, and 91%. The percentages in blue show the years where the original year 1700 $CaCO_3$ dissolution of ~6 x 10^{12} mol yr^{-1} increases by 2%, 20%, 121%, and 258%.

What are the implications of these projected changes to marine calcifying communities from an ecological perspective? What do slower rates of calcification really mean to calcifying organisms? How are different life stages affected? Are there additional consequences that so far have not been considered? How can we evaluate and address these questions without building a time machine? As we were pondering these questions, *Ilsa Kuffner* and *Paul Jokiel* at the University of Hawaii approached the two of us and wondered if we were interested in starting up a mesocosm experiment to evaluate the effect of future ocean acidification on a subtropical coral reef community. Manipulating seawater CO_2 chemistry in a mesocosm to mimic future conditions was probably the closest we could come to a time machine and we excitingly accepted the invitation (Figs. 10.8 and 10.9).

The experimental approach we devised was intended to maintain the natural properties of the environment to the maximum extent possible, including high flow rates, natural light levels, temperature, and diel cycles while approximately doubling the seawater pCO_2 in the treatment tanks. Because we were pumping about 72,000 litres of seawater through the mesocosms every day at a rate of 48 litres per minute and intended to run the experiment for several months (in the end we ran it for 10 months), we decided it was most feasible to manipulate the seawater CO_2 chemistry by acid addition, a decision we later had to defend every time we presented our results [see Andersson and Mackenzie (2012) for a discussion on acid versus CO_2 gas manipulations]. The benthic community of each mesocosm was initially made up of corals, coralline algae, and the green algal *Halimeda sp.*, but numerous additional organisms would be naturally and inadvertently introduced to the mesocosms via the inflowing seawater throughout the duration of the experiment, including barnacles, crabs, sea hares, vermetids, and several more. On a weekly basis, we monitored the chemistry conditions, prepared new acid, cleaned the inflow and outflow tanks, and on occasion we conducted 24-hour studies to characterise the diel cycle of marine carbon system chemistry and other parameters. As part of the experiment, we also weighed all corals and coralline algae every 2-4 weeks using the buoyant weight technique. With a total of almost 300 individual coral colonies and coralline algae, this was extremely time consuming and looking back we are not exactly sure how we were able to keep up with the experiment. Overall, the experiment was very labour intensive and with both *Andreas* getting close to defending his dissertation in the Department of Oceanography at the University of Hawaii and *Ilsa Kuffner* relocating to Florida, we decided to put an end to the experiment after 10 months duration. Consequently, we pulled the plug in August of 2006, and *Paul Jokiel* and *Ku'ulei Rodgers* began the daunting task of quantifying everything that was in the tanks.

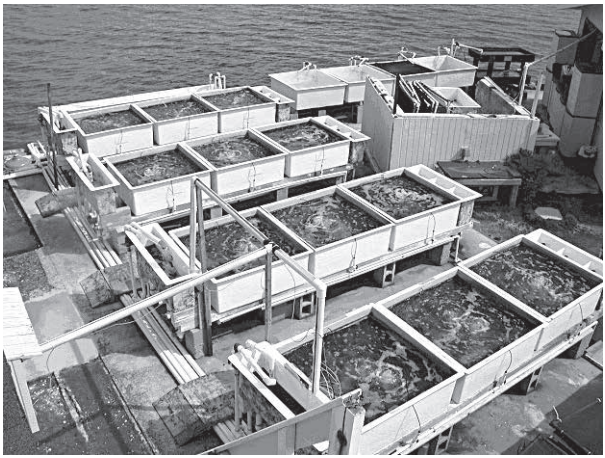

Photo courtesy of Paul Jokiel.

Figure 10.8 Mesocosm facility at the Hawaii Institute of Marine Biology on Coconut Island in Kaneohe Bay used for the experiments described here. Each individual chamber is approximately 1 x 1 x 0.5 m.

Photo courtesy of Andreas Andersson.

Figure 10.9 Andreas, Paul Jokiel, and Ilsa Kuffner discussing the strategy for the mesocosm experiment conducted at Coconut Island, Hawaii.

The results of the mesocosm experiments confirmed previous findings that corals calcified slower under elevated CO_2 conditions (Jokiel *et al.*, 2008). Coral calcification rates were 15% to 20% lower in treatment conditions (average daytime pCO_2 = 669±57 µatm; Ω_a = 1.95±0.13) compared to close to ambient conditions (average daytime pCO_2 = 414±36 µatm; Ω_a = 2.91±0.18). Interestingly, one of the major findings involved a failed experiment! After a few weeks into the experiment, we decided to investigate the effect of elevated CO_2 on some macroalgae, which were initially kept in transparent cylinders enclosed by a fine mesh on both open ends of the cylinders. However, the algae had little interest in staying within these cylinders and grew through the mesh making it impossible to quantify the growth rates. After 50 days we terminated this attempt and when *Ilsa Kuffner* was about to clean the cylinders, she discovered that the cylinders taken from the mesocosms exposed to ambient conditions were completely covered by crustose coralline algae (CCA), while cylinders from treatment conditions had almost none (Fig. 10.10)! We subsequently quantified the difference and published these results (Kuffner *et al.*, 2008).

Image courtesy of Andreas Andersson.

Figure 10.10 Picture showing cylinders incubated in the mesocosms for 50 days. Cylinders from ambient CO_2 conditions were largely covered by crustose coralline algae (CCA), whereas cylinders from acidified seawater treatment conditions were covered by very few CCA.

In the experiments, the recruitment of CCA under treatment conditions was reduced by 85-90% compared to ambient conditions. The experimental results have subsequently been repeated several times in different settings and by manipulating the seawater CO_2-carbonic acid system chemistry by both acid addition and CO_2 gas bubbling and the results have come out the same every

time. Assuming these results are applicable to natural environments under future conditions, they could have serious implications for coral reefs and other shallow water carbonate environments because CCA serve important ecological roles in these environments, and even in some mixed carbonate-terrigenous ecosystems. The CCA act as reef constructing organisms, sometimes even exceeding corals in abundance, cementers and binders, and fill in pores and voids in a reef with their detritus (infilling organisms); thus, they play an important role in the accretion and stabilisation of carbonate reefs. In addition, CCA release chemical cues (chemical messenger compounds) into the water column that coral larvae and abalones are attracted to and use as settlement cues to begin their growth (Morse, 1991; Morse *et al*., 1997). In addition, coral larvae may even settle onto the CCA and use it as a substrate for growth.

Similar to the negative effects on CCA, we observed in the experimental mesocosms that rhodoliths (crustose benthic marine red algae that resemble small coral heads) exposed to elevated CO_2 lost weight at a rate of 0.9 g buoyant weight per year, while those in ambient conditions gained 0.6 g buoyant weight per year. Thus, rhodoliths in future acidified seawater conditions may dissolve faster than they are able to deposit new $CaCO_3$. Both the CCA and rhodoliths deposit Mg-calcite with a significant percentage of Mg in the calcite structure, which in our experimental work had an average composition of 13 to 14 mol% $MgCO_3$.

Other investigators have observed similarly strong negative effects of increased CO_2 concentrations and increased seawater acidity on calcifiers depositing Mg-calcite with a significant Mg content. For example, CCA dominated the epiphythic communities (plants that grow on other plants upon which they depend for mechanical support but not for nutrients) on seagrass blades in average seawater composition of pH equal to 8.0 to 8.2, but were completely absent in seawater of pH less than 7.7 induced by elevated natural subsea volcanic vent CO_2 levels (Martin *et al*., 2008; Hall-Spencer *et al*., 2008). In addition, Anthony *et al*. (2008) observed decreased production rates and high rates of net dissolution for CCA exposed to a seawater pH of 7.6 to 7.7 during an eight-week study. They concluded that *"…sensitive reef-building specie such as CCA may be pushed beyond their thresholds for growth and survival within the next few decades…"* However, contrary to these findings based on a statistical meta-analysis of organism mineralogy, Kroeker *et al*. (2010) concluded that taxa depositing Mg-calcite were more resilient to OA than taxa with tests and skeletons of aragonite or calcite. Later, Andersson and Mackenzie (2011) pointed out that this conclusion may have been based on erroneous assumptions and inadequate recognition and categorisation of carbonate mineral phases according to solubility.

In summary, although organisms respond differently to ocean acidification and some calcifying organisms may be able to deal with lower pH conditions better than others regardless of the mineral composition of their shells, tests, and carapaces, it is important to recognise that the susceptibility of calcifying organisms to dissolution is in general greater for organisms depositing Mg-calcite with

a significant Mg content. Exceptions to this conclusion may arise due to additional impurities incorporated into biogenic mineral structures, organic coatings, and the architectural complexity (microstructure) of the skeleton that can affect the susceptibility of organisms to dissolution (Walter and Morse, 1985; Morse and Mackenzie, 1990) under increasing ocean acidification conditions.

10.3 Will Coral Reefs Disappear as a Result of Ocean Acidification?

As a result of the projected decrease in the rates of calcification of skeletal organisms and increasing rates of $CaCO_3$ dissolution rates as a result of OA, it has been hypothesised that coral reefs at some point in time will transition from a state of net accretion to one of net erosion (Andersson *et al.*, 2005, 2009; Hoegh-Guldberg, 2005; Hoegh-Guldberg *et al.*, 2007; Silverman *et al.*, 2009). However, there still are many questions that remain to be addressed in order to predict the nature and approximate timing of this transition and what it means from an ecological perspective and obviously for the persistence of coral reefs. For example, to make this prediction, we need to know how the seawater carbonate chemistry will change on reefs, which is not as straightforward as it is for the open ocean because reef metabolism significantly modifies the seawater CO_2-carbonic acid system chemistry. At this time, there are actually no non-problematic existing time series observations from coral reef environments that have been maintained long enough to demonstrate the secular trend of OA in this environment. To be able to predict future seawater conditions on coral reefs, we need to understand how open ocean chemistry will change in response to increasing atmospheric CO_2, and also, and importantly, how community structure and biogeochemical processes such as photosynthesis, respiration, calcification, and $CaCO_3$ dissolution will be affected on coral reefs and consequently their influence on the seawater chemistry.

Although substantial efforts have been invested investigating the effect of OA on the ability of corals and other calcifiers to calcify, little attention has been given to the effect of $CaCO_3$ dissolution on NEC (Net Ecosystem Calcification). Because NEC is a function of both calcification and dissolution, it is critical to understand the effect of OA on both of these processes. Furthermore, recent experimental results have suggested that the rate of the dissolution process may be much more affected by OA than the process of calcification (Andersson *et al.*, 2009), which makes it even more imperative to fully understand this process as well as that of bioerosion of carbonate structures in the context of OA. In addition, we need to understand the rates and timescales of breakdown and loss of structural complexity once a reef undergoes net dissolution and what this means to the various inhabitants on the reef. It is obvious that a reef can no longer sustain itself indefinitely if it undergoes net dissolution, but it is necessary to understand the timescale of breakdown in order to evaluate the severity of OA and the potential consequences. If reefs will only lose a marginal mass of $CaCO_3$ and structural

complexity during future decades to centuries, the problem of OA may be minor, but on the other hand, if breakdown is significant over these timescales, OA is obviously a significant problem that threatens the very existence of coral reefs.

10.3.1 Current status of coral reefs

Ocean acidification is only one of many threats to coral reefs and will act synergistically with sea surface warming, overfishing, eutrophication, pollution, sedimentation, increased storm frequency, crown of thorn starfish outbreaks, and disease to undermine the success of this ecosystem. In the most recent evaluation of the status of the world's coral reefs (Wilkinson, 2008), it was concluded that *"… the world has effectively lost 19% of the original area of coral reefs; 15% are seriously threatened with loss within the next 10-20 years; and 20% are under threat of loss in 20-40 years."* It was also concluded that 46% of reefs are relatively healthy and not under immediate threat. However, this evaluation does not take into account the potential threat from climate change and ocean acidification or the potential for effective future management that would address both local and global threats. Gardner *et al.* (2003) reported that coral cover in the Caribbean decreased by 80% from an average of 50% to 10% cover in a period of three decades. The decline was mainly attributed to local processes arising from human activities. In a recent study by De'ath *et al.* (2012), it was concluded that the Great Barrier Reef in Australia has lost half of its coral cover since 1985 owing to storm damage (48%), invasion of crown of thorns starfish (42%), and bleaching (10%). Thus, although it is difficult to determine whether OA has played a direct or indirect role in these observed declines of coral cover, it is obvious that other detrimental forcings are probably more acute on short timescales.

10.3.2 Biogeochemical control of seawater CO_2 chemistry on coral reefs

In recent years, the research community has become increasingly aware of the fact that the dynamics of the seawater CO_2-carbonic acid system and CO_2 air-sea exchange fluxes in near-shore coastal environments, including coral reefs, are much more complex and variable than in the open ocean (Fagan and Mackenzie, 2007; Drupp *et al.*, 2011; Andersson and Mackenzie, 2012; Hofmann *et al.*, 2012). For example, as mentioned previously, dissolved inorganic CO_2 parameters (*e.g.*, pCO_2, pH, Ω) and CO_2 air-sea exchange show large variability on both diel and seasonal timescales, owing to the activity of organisms and the associated biogeochemical processes of photosynthesis, respiration, calcification, and $CaCO_3$ dissolution, as well as changes arising from physical properties such as temperature and mixing. For example, temperature influences the solubility of CO_2 gas in seawater and also the point at which carbonate minerals start to dissolve (*i.e.* Ω). In addition, different benthic habitats and organism groups exert differing influences on the overlying seawater CO_2 chemistry depending on the relative magnitude of the major biogeochemical processes and the resulting effect on the seawater DIC to TA ratio. Under constant temperature, salinity, and pressure, it is

the relative ratio of DIC to TA that controls the speciation of dissolved inorganic carbon in seawater and properties such as pH and Ω (Fig. 10.11). Thus, depending on the relative magnitude of NEP and NEC in a given environment, the relative change in DIC and TA arising from these processes will result in predictable changes in seawater dissolved inorganic carbon speciation, pH, and Ω. For example, under typical DIC and TA conditions observed on present day coral reefs and assuming constant temperature and salinity, if DIC and TA decrease in a ratio of 1.05, there will be no net change in seawater Ω_a. If the relationship is >1.05, Ω_a will increase, and if the relationship is <1.05, Ω_a will decrease (Fig. 10.11). Consequently, if the relative contribution of NEC and NEP and the subsequent changes in DIC and TA were to change owing to future natural or anthropogenic perturbations, the resulting seawater Ω_a will be different from that predicted by oceanic uptake of anthropogenic CO_2 alone (Andersson and Gledhill, 2013).

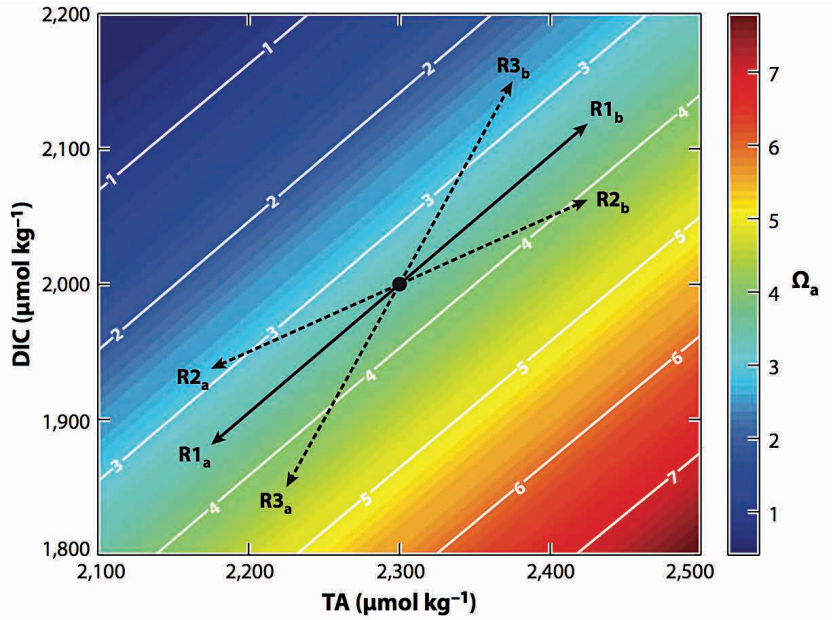

Figure 10.11 Contour plot of seawater aragonite saturation state (Ω) as a function of DIC and TA) at a temperature of 25 °C and a salinity of 35‰. The reaction pathways (R1–R3) show the resulting Ω if net reef metabolism (net ecosystem calcification and net ecosystem production) changes DIC and TA following ΔDIC/ΔTA of 1.05 (R1), 0.5 (R2), and 2 (R3) from a starting condition represented by the solid black circle. The subscript 'a' denotes net reactions consuming DIC and TA; the subscript 'b' denotes net reactions producing DIC and TA (from Andersson and Gledhill, 2013 with permission from Annual Reviews).

This biogeochemical control on seawater CO_2 chemistry in coral reefs and near-shore environments has led researchers to propose that different benthic communities could alleviate or exacerbate future ocean acidification. The coupling and mutual control between biology and chemistry have been observed in several studies on coral reefs. Suzuki *et al.* (1995) proposed a coexisting production enhancement between photosynthesis and calcification at both the colony and the community level in coral reefs; photosynthesis stimulating calcification by raising seawater Ω_a, and calcification regenerating CO_2 that could be used for photosynthesis. Conversely, respiration and decomposition of organic material drive decalcification and $CaCO_3$ dissolution. Bates *et al.* (2010) proposed a coral reef ecosystem feedback hypothesis by which seasonal variations in macroalgae abundance raise seawater Ω and stimulate coral calcification in the spring and later suppress coral calcification when the algae die off and are decomposed in the fall. Semesi *et al.* (2009) showed enhanced calcification in calcareous red algae in the presence of seagrasses, which significantly raised the seawater pH and Ω during daytime. Anthony *et al.* (2011) and Kleypas *et al.* (2011) demonstrated that different community compositions and the proportion of macroalgae and corals influence seawater chemistry differently, and proposed that a change in the community structure in favour of macroalgae could potentially alleviate the effect of OA at the local scale. Whether some benthic communities and biological feedbacks will counteract OA to the extent that they will provide refuge for organisms sensitive to OA remains to be demonstrated, but it is clear that the research community needs to consider these biogeochemical feedbacks in making predictions as to how seawater chemistry in shallow near-shore environments will change in response to OA.

In an effort to more fully understand the temporal variability, air-sea CO_2 gas exchange, and in a search for the secular trend in seawater CO_2 chemistry in coral reef environments, a number of buoy systems capable of continuously measuring pCO_2 in seawater and air have been deployed in numerous coral reef environments around the world including Bermuda, Puerto Rico, Florida, Hawaii, Chuuk, and Australia. This effort is spearheaded by the NOAA Pacific Marine Environmental Laboratory in collaboration with local researchers at these locations. To date, the longest deployment of these buoys in Hawaii is still too short to reveal unambiguously any secular trend arising from increasing atmospheric CO_2. Nevertheless, these data have demonstrated that different coral reef environments are exposed to highly variable and differing seawater CO_2 chemistry (Fig. 10.12). For example, data from Hawaii have shown a reef flat environment exposed to pCO_2 fluctuation ranging from a minimum of 200 μatm during daytime to greater than 1,000 μatm during night time, while a fringing reef in Puerto Rico is exposed to seasonal extreme values in the range of 350 μatm to 550 μatm between winter and summer, respectively. A relatively high latitude reef in Bermuda (32 °N) experiences diel fluctuations of a magnitude sometimes exceeding 100 μatm and 50 μatm at a rim reef and patch reef, respectively, while the seasonal maximum and minimum at these two sites range from 350–600 μatm and 340–500 μatm, respectively.

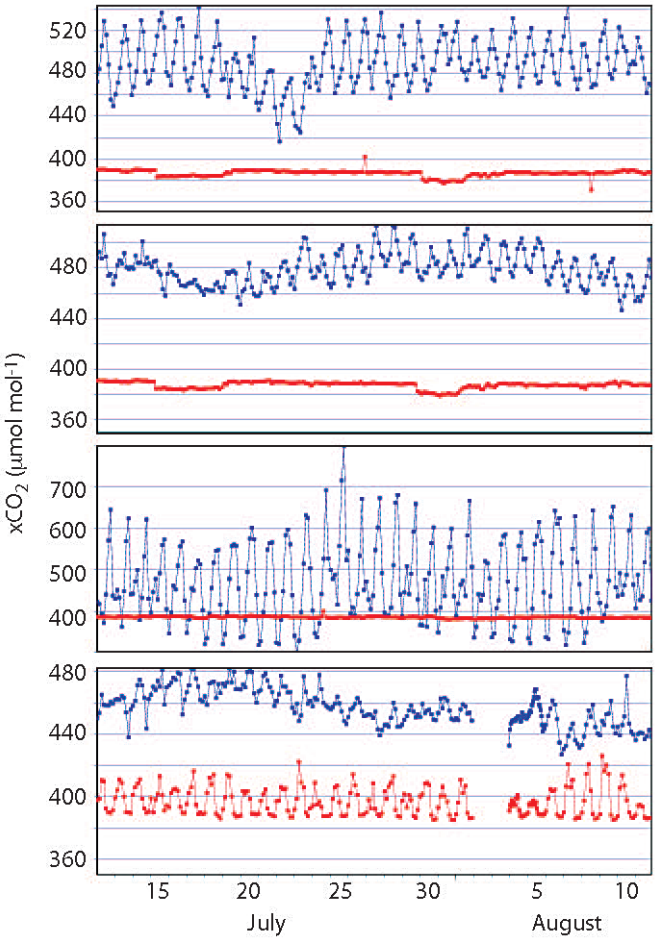

Figure 10.12 Mole fraction CO_2 (xCO_2) in seawater (blue) and air (red) during summertime from different coral reef environments. **From top to bottom**: Bermuda rim reef, Bermuda patch reef, Hawaii reef flat, and Puerto Rico fringing reef. Note that the y-axis scale is different in each panel (based on data from NOAA Pacific Marine Environmental Laboratory Carbon Dioxide Program).

Given that many of these reef environments have several coral species and other organisms in common, we might ask how these organisms are affected by these natural differences in seawater CO_2 chemistry? How will the variability in seawater CO_2 chemistry be affected by OA and how will this affect the living community at these different reefs? Some researchers have proposed

that organisms that are adapted to highly variable seawater CO_2 chemistry may be able to tolerate OA better than those accustomed to more stable conditions. Perhaps this is the case. However, as seawater pH and Ω decrease, the extremes of high variability environments may eventually cross a critical threshold, which could make the existence of certain organisms in these environments improbable. Research and experiments investigating how organisms respond to variability, mean, and/or extreme seawater carbon chemistry conditions are needed to address these fundamental questions.

10.3.3 $CaCO_3$ dissolution and bioerosion on coral reefs

Recent experimental results appear to indicate that some organisms including certain corals are more tolerant to OA than initial results and reports suggested (*e.g.*, Ries *et al*., 2009; McCollaugh *et al*., 2012). In addition, provided sufficient nutrition and energy, many organisms appear to be less negatively affected by OA relative to the effects under conditions of limited energy availability. Nevertheless, on coral reefs and in other environments dependent on the accumulation of $CaCO_3$, including maerl beds and deep-sea coral bioherms, the potential resilience of many organisms to OA may be of little help if the dissolution, bioerosion, and breakdown of these ecosystems increase significantly as a result of OA.

As the seawater saturation state with respect to $CaCO_3$ mineral phases decreases as a result of OA, it is certain that the dissolution and breakdown of these minerals will increase. The increase will occur in both the deep-sea owing to the penetration of anthropogenic CO_2 and the consequent shoaling of the saturation horizons, as well as in shallow seas, owing to the undersaturation of seawater with respect to highly soluble Mg-calcite phases and aragonite in some environments. In addition, the extent of metabolically driven dissolution in sediment porewaters and microenvironments could also increase owing to lower Ω of the overlying and/or surrounding source water. The same may be true for dissolution arising as a result of bioerosion. In support of these predictions, experiments investigating the response of $CaCO_3$ sediments or substrates have shown convincing evidence of dissolution or increasing rates of dissolution as a result of increasing seawater CO_2 and acidity (Keir, 1980; 1983; Walter and Morse, 1985; Tribble and Mackenzie, 1998; Halley and Yates, 2000; Barnes and Cuff, 2000; Morse *et al*., 2006; Andersson *et al*., 2007; Tynan and Opdyke, 2011). Similarly, coral blocks infested with communities of euendolithic and epilithic bioeroding organisms and exposed to seawater pCO_2 levels similar to those anticipated in the atmosphere by the end of the century (750 μatm) dissolved at rates 48% higher than under control conditions (400 μatm; Tribollet *et al*., 2009). In addition, Wisshak *et al*. (2012) demonstrated that dissolution by the sponge *Cliona orientalis*, which specifically targets corals in certain environments, increased significantly as a function of increasing seawater pCO_2 and decreasing pH conditions.

Studies investigating calcifying communities in both experimental settings and in the natural environment have shown consistently lower net calcification and higher net dissolution under conditions of high CO_2 and low pH, many times occurring at night (Leclercq *et al.*, 2000, 2002; Langdon *et al.*, 2003; Yates and Halley, 2006a,b; Andersson *et al.*, 2009; Kline *et al.*, 2012). Andersson *et al.* (2009) attributed a shift from integrated daily net accumulation of $CaCO_3$ under ambient pCO_2 to integrated daily net dissolution under double ambient pCO_2 for subtropical coral reef communities maintained in replicated mesocosms to a decrease in calcification by 24% and an increase in dissolution by 138% (Fig. 10.13).

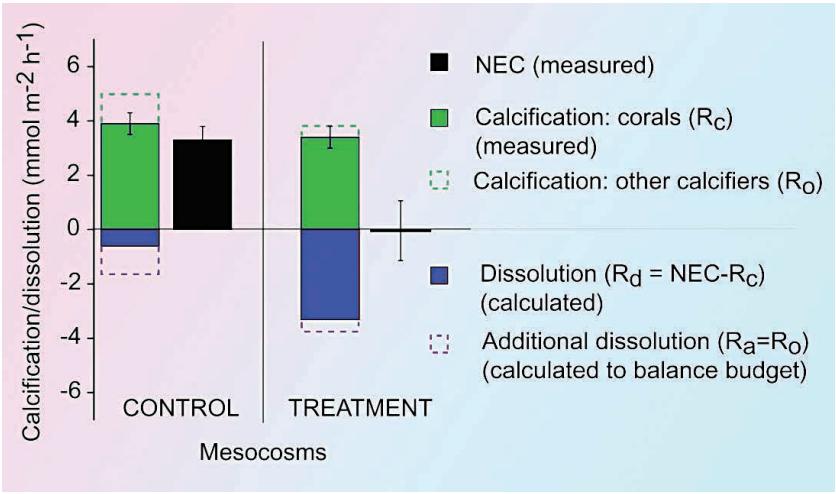

Figure 10.13 Calcification (green bars), $CaCO_3$ dissolution (blue bars), and net ecosystem calcification (NEC; black bars) for subtropical coral reef communities maintained in replicated mesocosms (n=3) under near-ambient (mean pCO_2 = 568 µatm and Ω_a = 2.8) and future (mean pCO_2 = 1147 µatm and Ω_a = 1.4) conditions. The solid green part of calcification bars represents calcification by corals as determined by buoyant weight measurements (Rc), and the dashed green part represents estimated calcification by other calcifiers (*e.g.*, coralline algae, vermetids, barnacles, oysters; R_O). Solid part of blue bars represents dissolution calculated from observed NEC and coral calcification, and the dashed part of blue bars represents additional dissolution required to balance the budget (after Andersson *et al.*, 2009).

Numerical model simulations using empirical relationships between calcification, dissolution, and seawater CO_2 chemistry have also demonstrated increasing dissolution in response to OA (Andersson *et al.*, 2003, 2005, 2006; Silverman *et al.*, 2009). Silverman *et al.* (2009) concluded based on their model simulations that all coral reefs would undergo net dissolution at an atmospheric CO_2 of 560 µatm, whereas Andersson *et al.* (2005, 2009; see Fig. 10.7 for estimate of cross over year) suggested that this transition is more likely to occur at seawater

pCO_2 levels exceeding 1100 µatm based on model simulations and mesocosm experiments. In reality, the timing of this transition is likely to vary from reef to reef and it is anticipated that the transition will occur gradually, *i.e.* net dissolution is first anticipated to occur in wintertime when production and calcification rates are lower compared to summer and then progressively become important for a larger proportion of the year. Such net dissolution during wintertime is already being observed in subtropical coral reef environments of Bermuda and Florida (Bates *et al.*, 2010; Manzello *et al.*, 2012), and probably in many other places, as inferred from total alkalinity offshore to across reef studies during this time of the year. However, at this time we do not know whether and by how much the observed net dissolution in wintertime in Bermuda and Florida has changed since preindustrial conditions, but the future trend is fairly robust given the experimentally derived dependence of calcification and $CaCO_3$ dissolution on seawater CO_2 chemistry and the predicted changes in the latter owing to anthropogenic emissions of CO_2 to the atmosphere.

Although experimental results using aquaria, mesocosms, field enclosures, Free Ocean Carbon Enrichment systems, and models have confirmed that $CaCO_3$ dissolution on coral reefs and in other near-shore environments is likely to increase as a result of ocean acidification, there are many questions remaining to be answered. For example, what is quantitatively more important, metabolic dissolution versus dissolution driven by bioeroders? Will metabolic dissolution in sediments and microenvironments be enhanced by the relatively small changes in surface seawater CO_2 chemistry compared to the large changes in these environments driven by the microbial decomposition of organic material? Our current paradigm suggests that the extent of $CaCO_3$ dissolution in sediments is directly coupled to the extent of remineralisation of organic material (Morse and Mackenzie, 1990). Some research findings suggest that dissolution in sediments will be little affected by the relatively small changes in surface seawater (Leclercq *et al.*, 2002; Andersson *et al.*, 2003), and that the deposition and subsequent microbial decomposition of organic matter is much more important. Thus, what are the major controls of sediment $CaCO_3$ dissolution? How is the extent of dissolution affected by sediment mineralogy, organic matter content and reactivity, bioturbation and bioirrigation, grain size distribution, sediment permeability and porosity, and the rate of flushing of sediment pore waters with overlying surface seawater? Furthermore, as mentioned previously, large uncertainties are associated with the solubility and kinetics of Mg-calcite compositions found in reefs and reef sediments as reef-building, -binding, and -infilling calcareous organisms and abiotic cements. Model predictions of the dissolution of these mineral phases in response to OA based on the different experimentally derived solubility curves as a function of their Mg-content produce widely divergent results (Morse *et al.*, 2006). In terms of the importance and magnitude of bioerosion, it is poorly known to what extent bioeroders cause chemical dissolution versus mechanical breakdown. There is no doubt that the mechanical breakdown into smaller grain sizes with larger surface area to volume ratio is important in facilitating later dissolution of these substrates, but the mechanical

breakdown is distinctly different from the chemical dissolution in terms of its role and importance in the cycling of carbon on coral reefs. As a result of OA, it has also been proposed that marine calcifiers will build weaker calcareous skeletons and structures, a condition similar to osteoporosis in humans, but to date few quantitative data exist confirming that this is the case. Nevertheless, if this prediction is true, the destructive efficiency of bioeroders is likely to increase.

What are the implications for a coral reef that undergoes net dissolution and/or net loss of $CaCO_3$ through the combined effects of chemical dissolution, bioerosion, and export processes? It is important to recognise that net dissolution by itself does not imply the end of all corals and calcifiers because most organisms probably can still build their calcareous carapaces under the chemical conditions existing when this threshold is crossed. The exception might be those organisms depositing highly soluble mineral phases, such as some crustose coralline algae and other coralline algae. As previously discussed, Andersson *et al.* (2009) observed marginal net dissolution in mesocosm experiments with subtropical mixed coral reef communities exposed to an average seawater pCO_2 of 1147 μatm. Nevertheless, individual coral colonies remained healthy and actively calcified at this condition, albeit at slower rates. There are examples of the occurrence of deep-sea corals and other calcifiers living in seawater undersaturated with respect to aragonite, which suggest that some marine calcifiers can deal with conditions of relatively low seawater saturation state with respect to $CaCO_3$. However, and importantly, there is no significant accumulation or development of carbonate structures under these conditions. The complex habitat structures provided by the construction of carbonate reefs and bioherms have been compared to cosmopolitan hubs, which provide a diverse habitat for a myriad of species. Hence, the structural complexity on reefs is considered critical for maintaining the extraordinary biodiversity observed in these ecosystems.

It is estimated that 25% of marine biodiversity is found on tropical coral reefs, but other carbonate structures of maerl beds and deep-sea coral bioherms serve many of the same functions as tropical coral reefs and are critical habitats in the oceanic regions where they are found. Thus, if these carbonate structures were to erode away, they would no longer be able to provide habitat for their current inhabitants. Therefore it is important in the context of OA to understand the potential rates of dissolution and loss of structural complexity. For a healthy reef, these rates may be very low and of little concern even at CO_2 levels anticipated by the end of the century. However, for reefs experiencing disturbances owing to bleaching, overfishing, sedimentation, and/or eutrophication, the combined effect of chemical dissolution and bioerosion may rapidly break down the structural complexity of the reef, and at seawater CO_2 levels higher relative to today, current evidence suggests these processes will become increasingly important. At the present time, evidence from severe bleaching events has shown that reef structures could transition from net deposition to net erosion in a very short time and loose several kilograms of $CaCO_3$ m^{-2} yr^{-1} with profound changes to the reef structure and composition (*e.g.*, Eakin, 1996). With potentially increasing occurrences of mass bleaching events and the possibility of an increase in the intensity

and frequency of hurricanes and cyclones as a result of sea surface warming, it is obvious that increasing rates of dissolution and bioerosion owing to OA will result in a progressively increasing $CaCO_3$ deficit in the $CaCO_3$ budget for many coral reef environments. The major questions that require answers are: will this deficit occur and when and to what extent can the destructive processes exceed the constructive processes? The answers to these questions will take time but OA waits for no one and the world is largely ignorant of this problem and in some cases in political and community circles actually professes disbelief (Fig. 10.14).

Credit: Horsey. Copyright: Los Angeles Times, 2002.

Figure 10.14 A cartoon showing the present status of belief in the problem of ocean acidification in the world's communities.

11. EVER ONWARD: SOME CONCLUDING COMMENTS AND QUESTIONS

Although much has been accomplished regarding our understanding of the behaviour of the Phanerozoic marine CO_2-carbonic acid-carbonate sediment system and ocean acidification, particularly for the modern oceans, the further back in time we go, probably the less we know. This is particularly true for the Palaeozoic Eon (545 Ma to 245 Ma years ago), prior to the rise of the open ocean pelagic foraminfera, coccolithophoridae, and pteropoda, when flooded continents with vast epicontinental shallow seas were common and shoal-water benthic organisms and organo-detrital and abiotic carbonate deposits were the "order of the day". The late Mesozoic seas some 100 Ma years ago were of a similar nature, but at this time pelagic deep-sea biogenic carbonates were ubiquitously present. Even in the modern oceans, there is still some question as to whether the calcium carbonate lysoclines are thermodynamic horizons in which the calcite lysocline and the aragonite lysocline are close to coincident with their respective saturation horizons or whether there is an offset in depths controlled by kinetic factors. There is even dispute as to whether or not sinking $CaCO_3$ shells and tests dissolve above the chemical lysocline, the depth at which there is a rapid increase in the $CaCO_3$ dissolution rate with increasing depth in the water column. This is an important problem in the marine carbon cycle that requires some innovative approaches to resolve. With questions of this nature and many others still outstanding for the modern marine carbon system, attempts to decipher the past are constrained. However, it is likely that continuing environmental concerns and the emergence of the field of Earth system science will be a stimulus to further progress in research involving the marine CO_2-carbonic acid system and sedimentary carbonates—their past, present, and future. In this final section, we list a few future directions and questions for further research in the field.

1. There is a need for more detailed chemical stratigraphic analyses and new types of proxy data to constrain the compositional history of the ocean-atmosphere system, and particularly short-term events, during Phanerozoic time. Despite that in the U.S., this suggestion was put forward in the 1973 book *Orientations in Geochemistry* published by the U. S. National Academy of Sciences, there is much more to be accomplished in this area of research.

2. As a continuation of item 1 above, there is still considerable controversy concerning the mass-age distribution of dolomite and its controls. Dolomite acts as a sink of Mg in the oceans and hence its distribution is critical to modelling the alkaline earth and carbon chemistry of the oceans through geologic time. One major unresolved problem is that a significant mass of extant dolomite found in the sedimentary record might be secondary, that is, formed much later than the carbonate host rock, *e.g.*, by diagenesis in the subsurface. Hence, this secondary dolomite would not be representative of the flux of dolomite at the time

of deposition. A first step in resolution of this dolomite controversy would be a detailed reassessment of the dolomite mass-age distribution perhaps in colloboration with major oil companies that have access to considerable unpublished data. Some attempt should also be made to distinguish "primary" from "secondary" dolomite in the rock record as a function of age using a composite of geologic, geochemical, and isotopic data.

3. Continuing with the theme of item 1, the original carbonate mineralogy of ooids during the Phanerozoic Eon requires reassessment. Changes in the inferred mineralogy of carbonate ooids and cements during Phanerozoic time form the basis of the calcite-dolomite versus aragonite seas hypothesis. There is a need for considerably more data on the inferred mineralogy of ooids covering more time stratigraphic intervals from under-sampled sedimentary basins with wider palaeogeographic coverage. This is particularly necessary in that it is now reasonably well confirmed that the situation is not one of either/or in that ooids of inferred original aragonite mineralogy have been found in carbonate rock units associated with calcite-dolomite seas.
4. The chemistry of fluid inclusions associated with NaCl evaporites, if judiciously interpreted, appears to be a powerful tool for obtaining information concerning palaeo-seawater chemical composition. There is a need for more fluid inclusion data, particularly closely spaced data across stratigraphic intervals of major evolutionary changes in the fossil record.
5. The Phanerozoic long-term sedimentary record of stable isotopes of carbon and sulphur is well constrained but these isotopes are also powerful tools for interpreting shorter-term temporal environmental events in Earth's history. They are being used in this sense today but an expanded database once more across stratigraphic intervals of major evolutionary changes in the fossil record is needed. Furthermore, the use of nitrogen, calcium, and boron isotopes from sedimentary materials is still somewhat in its infancy and requires more attention.
6. Based on an expanded observational database, modelling efforts require parameterisations that reflect quantitatively and robustly the processes that are occurring in nature. It is likely these models will need to be more detailed and involve a network of coupled and interactive processes and in the case of biogeochemical "box" models, a fuller representative array of the major element domains, fluxes, and cycling processes potentially involved in ocean-atmosphere-carbonate sediment evolution and change during the Phanerozoic.
7. Finding the main drivers and the explanatory mechanisms of many of the observed ocean-atmosphere-carbonate sediment-landscape changes in the Pleistocene and Holocene, including the mechanism(s) responsible for the rapid rise in atmospheric CO_2 during the last

deglaciation, should be of high priority. These will provide the necessary framework to quantify the function and feedbacks of the Earth system on timescales of thousands of years.

8. Present-day inorganic and organic carbon fluxes along the landscape-freshwater-estuarine-shelf-open ocean and sediment continuum require further assessment in terms of refining both the late preindustrial and modern-day carbon cycle and the anthropogenic perturbation of the cycle.
9. The global coastal ocean serves a disproportionately important role in the global carbon cycle and for human societies, but it is highly variable and heterogeneous in both time and space. Increased research efforts in both observational oceanography and modelling and synthesis of these approaches are needed to understand quantitatively the carbon cycle biogeochemistry in the coastal ocean. Such an understanding would enable better predictions of the effects of human-induced environmental forcings on this highly dynamical region.
10. Carbonate mineral dissolution and precipitation mechanisms and fluxes in reef sediments necessitate extensive quantitative evaluation particularly as regards to their future response to continuing acidification of our oceans and their role in what may be a progressively increasing $CaCO_3$ deficit in the $CaCO_3$ budget for many coral reef ecosystems. Their redefinition will lead to a better prediction of the future response of coral reefs to ocean acidification.
11. The previous statement is especially true for the metastable biogenic Mg-calcite mineral phases of varying Mg content, and especially, in terms of their solubility and dissolution kinetics in natural environments. In fact, the solubility and rates of dissolution in seawater solutions of Mg-calcite mineral phases are still one of the most controversial and highly debated problems related to this group of mineral phases. In addition, the work of Walter and Morse (1985) is the only fundamental laboratory experimental study of the dissolution kinetics of biogenic carbonate phases in seawater solutions. Thus, there is an urgent need for more research on the subject as our oceans continue to acidify.
12. Despite extensive work going back to *Keith Chave* in 1954, the mechanistic controls on the Mg content of Mg-calcite shells and skeletons are not fully understood and a careful set of well-devised experiments is required to address this problem.
13. Whether some benthic communities and biological feedbacks will counteract ocean acidification and provide a refuge for organisms sensitive to OA remains to be demonstrated. It is clear, however, that the research community needs to consider these biogeochemical feedbacks in making predictions as to how seawater chemistry in shallow nearshore environments will change in response to ocean acidification.

Research and experiments investigating how organisms respond to variability, mean, and/or extreme seawater carbon chemistry conditions are needed to address the fundamental questions.

14. Based on our research efforts and analysis of the ocean CO_2-carbonic acid-carbonate system during Phanerozoic time, it is evident that the rate of the present human-induced ocean acidification event is most likely unprecedented in the geologic record for the past 800,000 years, the time of record of atmospheric CO_2 and temperature as obtained from the ice cores. Given the recorded changes in abiotic and biotic carbonate mineralogy, organism assemblages, and ecosystem functions in response to changes in seawater carbonate chemistry, temperature, and/or oxygen concentration during the Phanerozoic, it is evident that the current ocean acidification event will significantly influence marine ecosystems. In our opinion, it would be wise to address aggressively the world's current dependence on 85% of our commercial energy requirements coming from the fossil fuels of coal, oil, and gas in order to slow down the rates of CO_2 emissions and consequent ocean acidification (Fig. 11.1).

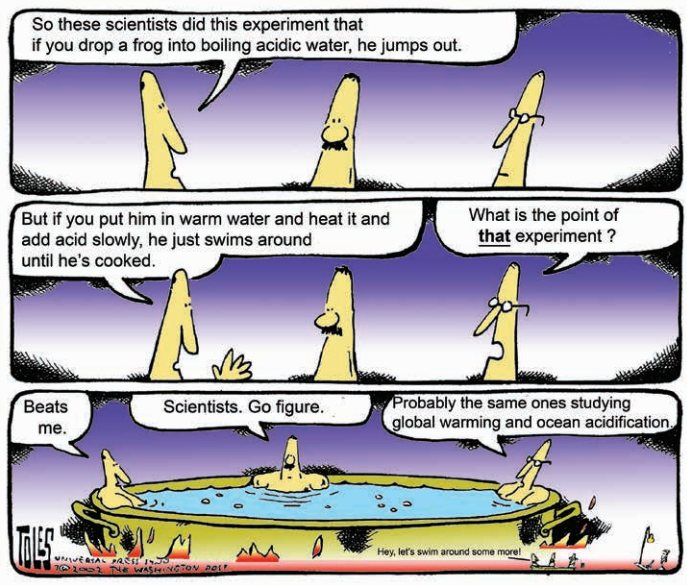

Credit: Toles. Copyright: Los Angeles Times, 2002 (modified).

Figure 11.1 Cartoon illustrating the hesitancy of the global community to deal with the first (global climate change) and second (ocean acidification) problems of anthropogenic CO_2 emissions to the atmosphere because of the burning of the fossil fuels of coal, oil, and gas.

REFERENCES

AGEGIAN, C.R. (1985) The biogeochemical ecology of *Porolithon gardineri* (Foslie). Ph. D. Dissertation. University of Hawaii, Honolulu.

ALGEO, T.J., INGALL, E. (2007) Sedimentary C_{org}: P ratios, paleocean ventilation, and Phanerozoic atmospheric pO_2. *Palaeogeography Palaeoclimatology Palaeoecology* 256, 130-155.

ALT, J.C., TEAGLE, D.A.H. (1999) The uptake of carbon during alteration of ocean crust. *Geochimica et Cosmochimica Acta* 63, 1527-1535.

ANDERSSON, A.J. (2013) The oceanic $CaCO_3$ cycle. In: Mottl, M. (Ed.) Treatise on Geochemistry: The Oceans and Marine Geochemistry. Elsevier, Oxford, in press.

ANDERSSON, A.J., MACKENZIE, F.T. (2004) Shallow-water oceans: a source or sink of atmospheric CO_2? *Frontiers in Ecology and the Environment* 2, 348-353.

ANDERSSON, A.J., MACKENZIE, F.T. (2011) Technical comment on Kroeker et al. 2010. Meta-analysis reveals variable responses of ocean acidification on marine organisms. *Ecology Letters* 14, E1-E2, doi: 10.1111/j.1461-0248.2011.01646.x.

ANDERSSON, A.J., MACKENZIE, F.T. (2012) Revisiting four scientific debates in ocean acidification research. *Biogeosciences* 9, 893-905.

ANDERSSON, A. J., GLEDHILL, D. (2013) Ocean acidification and coral reefs: Effects on breakdown, dissolution and net ecosystem calcification. *Annual Reviews* 5, doi:10.1146/annurev-marine-121211-172241.

ANDERSSON, A.J., MACKENZIE, F.T., VER, L.M. (2003) Solution of shallow-water carbonates: an insignificant buffer against rising atmospheric CO_2. *Geology* 31, 513-516.

ANDERSSON, A.J., MACKENZIE, F.T., LERMAN, A. (2005) Coastal ocean and carbonate systems in the high CO_2 world of the Anthropocene. *American Journal of Science* 305, 875-918.

ANDERSSON, A.J., MACKENZIE, F.T., LERMAN, A. (2006) Coastal ocean CO_2-carbonic acid-carbonate sediment system of the Anthropocene. *Global Biogeochemical Cycles* 20, GB4S09.

ANDERSSON, A.J., BATES, N., MACKENZIE, F.T. (2007) Dissolution of carbonate sediments under rising pCO_2 and ocean acidification: observations from Devil's Hole, Bermuda. *Aquatic Geochemistry* 13, 237-264.

ANDERSSON, A.J., MACKENZIE, F.T., BATES, N.R. (2008) Life on the margin: implications of ocean acidification on Mg-calcite, high latitude and cold-water calcifiers. *Marine Ecology Progress Series* 373, 265-273.

ANDERSSON, A.J., KUFFNER, I.B., MACKENZIE, F.T., JOKIEL, P.L., RODGERS, K.S., TAN, A. (2009) Net loss of $CaCO_3$ from a subtropical calcifying community due to seawater acidification: mesocosm-scale experimental evidence. *Biogeosciences* 6, 1811-1823.

ANDERSSON, A.J., MACKENZIE, F.T., GATTUSO, J.-P. (2011) Effects of ocean acidification on benthic processes, organisms, and ecosystems. In: Gattuso, J.-P., Hansson, L. (Eds.) Ocean acidification. Oxford University Press, New York. 122-153.

ANTHONY, K.R.N., KLINE, D.I., DIAZ-PULIDO, G., DOVE, S., HOEGH-GULDBERG, O. (2008) Ocean acidification causes bleaching and productivity loss in coral reef builders. *Proceedings of the National Academy of Sciences* 105, 17442-17446.

ANTHONY, K.R.N., KLEYPAS, J.A., GATTUSO, J.-P. (2011) Coral reefs modify their seawater carbon chemistry: implications for impacts of ocean acidification. *Global Change Biology* 17, 3655-3666.

ARCHER, D., MAIER-REIMER, E. (1994) Effect of deep-sea sedimentary calcite preservation on atmospheric CO_2 concentration. *Nature* 367, 260-263.

ARCHER, D., KHESHGI, H., MAIER-REIMER, E. (1998) Dynamics of fossil fuel CO_2 neutralization by marine $CaCO_3$. *Global Biogeochemical Cycles* 12, 259-276.

ARNDT, S., REGNIER, P., GODDÉRIS, Y., DONNADIEU, Y. (2011) GEOCLIM reloaded (v 1.0): a new coupled earth system model for past climate change. *Geoscientific Model Development Discussions* 3, 2109-2187.

ARVIDSON, R.S., MACKENZIE, F.T. (1997) Tentative kinetic model for dolomite precipitation rate and its application to dolomite distribution. *Aquatic Geochemistry* 2, 273-298.

ARVIDSON, R.S., MACKENZIE, F.T. (1999) The dolomite problem: control of precipitation kinetics by temperature and saturation state. *American Journal of Science* 299, 257-288.

ARVIDSON, R.S., MACKENZIE, F.T. (2000) Temperature dependence of mineral precipitation rates along the $CaCO_3$-$MgCO_3$ join. *Aquatic Geochemistry* 6, 249-256.

ARVIDSON, R.S., MORSE, J.W. (2013) Formation and diagenesis of carbonates. In: Mackenzie, F.T. (Ed.) Treatise on Geochemistry: Sediments, Diagenesis and Sedimentary Rocks, Vol. 9. Second edition, Elsevier-Pergamon, Oxford.

ARVIDSON, R.S., MACKENZIE, F.T., GUIDRY, M. (2000) Ocean/atmosphere history and carbonate precipitation rates: a solution to the dolmite problem. In: Glenn, C.R., Prevot-Lucas, L., Lucas, J. (Eds.) Society of Economic Paleontologists and Mineralogists Special Publication No. 65, Tulsa, OK, pp. 1-5.

ARVIDSON, R.S., ERTAN, I.E., AMONETTE, J.E., LUTTGE, A. (2003) Variation in calcite dissolution rates: a fundamental problem? *Geochimica et Cosmochimica Acta* 67, 1623-1634.

ARVIDSON, R.S., GUIDRY, M., MACKENZIE, F.T. (2006) MAGic: a Phanerozoic model for the geochemical cycling of major rock-forming components. *American Journal of Science* 306, 135-190.

ARVIDSON, R.S., GUIDRY, M.W., MACKENZIE, F.T. (2011) Dolomite controls on Phanerozoic seawater chemistry. *Aquatic Geochemistry* 17, 735-747.

BABEL, M., SCHREIBER, B.C. (2013) Geochemistry of evaporites and evolution of seawater. In: Mackenzie, F.T. (Ed.) Treatise on Geochemistry: Sediments, Diagenesis and Sedimentary Rocks, Vol. 9. Second edition, Elsevier, Oxford.

BACASTOW, R., KEELING, C.K. (1973) Atmospheric carbon dioxide and radiocarbon in the natural carbon cycle: II. changes from A. D. 1700 to 2070 as deduced from a geochemical model. *Brookhaven Symposia in Biology* 30, 86-135.

BAKER, P.A., KASTNER, M. (1981) Constraints on the formation of sedimentary dolomite. *Science* 213, 214-216.

Balthasar, U., Cusack, M., Faryma, L., Chung, P., Holmer, L.E., Jin, J., Percival, I., Popov, L. (2011) Relic aragonite from Ordovician-Silurian brachiopods: implications for the evolution of calcification. *Geology* 39, 967-970.

Bard, E., Hamelin, B., Fairbanks, R.G. (1990a) U-Th ages obtained by mass-spectrometry in corals from Barbados: sea-level during the past 130,000 years. *Nature* 346, 456-458.

Bard, E., Hamelin, B., Fairbanks, R.G., Zindler, A. (1990b) Calibration of the C-14 timescale over the past 30,000 years using mass-spectrometric U-Th ages from Barbados corals. *Nature* 345, 405-410.

Barnes, D.J., Cuff, C. (2000) Solution of reef rock buffers seawater against rising atmospheric CO_2. In: Hopley, D., Hopley, M., Tamelander, J., Done, T. (Eds.) Proceedings of the 9th International Coral Reef Symposium, Abstracts. State Ministry for the Environment, Indonesia.

Bates, N.R. (2007) Interannual variability of the oceanic CO_2 sink in the subtropical gyre of the North Atlantic Ocean over the last 2 decades. *Journal of Geophyical Research* 112, C09013.

Bates, N.R., Brand, U. (1990) Secular variation of calcium carbonate mineralogy: an evaluation of ooid and micrite chemistries. *Geologische Rundschau* 79, 27-46.

Bates, N.R., Amat, A., Andersson, A.J. (2010) Feedbacks and responses of coral calcification on the Bermuda reef system to seasonal changed in biological processes and ocean acidification. *Biogeosciences* 7, 2509-2530.

Bates, N.R., Best, M.H.P., Neely, K., Garley, R., Dickson, A.G., Johnson, R.J. (2012) Detecting anthropogenic carbon dioxide uptake and ocean acidification in the North Atlantic Ocean. *Biogeosciences* 9, 2509-2522.

Bathurst, R.G.C. (1974) Marine diagenesis of shallow water calcium carbonate sediments. *Annual Review of Earth and Planetary Sciences* 2, 257-274.

Bathurst, R.G.C. (1975) Carbonate sediments and their diagenesis. Elsevier Publishing Co., Amsterdam.

Beerling, D., Berner, R.A., Mackenzie, F.T., Harfoot, M.B., Pyle, J.A. (2009) Methane and the CH_4 related greenhouse effect over the past 400 million years. *American Journal of Science* 309, 97-113.

Berger, W.H. (1982) Increase of carbon-dioxide in the atmosphere during deglaciation: the coral reef hypothesis. *Naturwissenschaften* 69, 87-88.

Bergman, N.M., Lenton, T.M., Watson, A.J. (2004) COPSE: a new model of biogeochemical cycling over Phanerozoic time. *American Journal of Science* 304, 397-437.

Berner, R.A. (1971) Principles of Chemical Sedimentology. McGraw-Hill, New York.

Berner, R. (1975) The role of magnesium in the crystal growth of calcite and aragonite from sea water. *Geochimica et Cosmochimica Acta* 39, 489-504.

Berner, R.A. (2001) Modeling atmospheric O_2 over Phanerozoic time. *Geochimica et Cosmochimica Acta* 65, 685-694.

Berner, R.A. (2004) The Phanerozoic Carbon Cycle: CO_2 and O_2. Oxford University Press, Oxford.

Berner, R.A. (2006) GEOCARBSULF: a combined model for Phanerozoic atmospheric O_2 and CO_2. *Geochimica et Cosmochimica Acta* 70, 5653-5664.

Berner, R.A., Morse, J.W. (1974) Dissolution kinetics of calcium carbonate in sea water: IV. Theory of calcite dissolution. *American Journal of Science* 274, 108-134.

Berner, R.A., Canfield, D.E. (1989) A new model for atmospheric oxygen over Phanerozoic time. *American Journal of Science* 289, 333-361.

Berner, R.A., Kothavala, Z. (2001) Geocarb III: A revised model of atmospheric CO_2 over Phanerozoic time. *American Journal of Science* 301, 182-204.

Berner, R.A., Mackenzie, F.T. (2011) Burial and preservation of carbonate rocks over Phanerozoic time. *Aqueous Geochemistry* 17, 727-733.

Berner, R.A., Westrich, J.T., Graber, R., Smith, J., Martens, C.S. (1978) Inhibition of aragonite precipitation from supersaturated seawater: a laboratory and field study. *American Journal of Science* 278, 816-837.

Berner, R.A., Lasaga, A.C., Garrels, R.M. (1983) The carbonate-silicate geochemical cycle and its effect on atmospheric carbon dioxide over the past 100 million years. *American Journal of Science* 283, 641-683.

Bertram, M.A., Mackenzie, F.T., Bishop, F.C., Bischoff, W.D. (1991) Influence of temperature on the stability of magnesian calcite. *American Mineralogist* 76, 1889-1896.

Bischoff, J.L. (1968) Kinetics of calcite nucleation: magnesium ion inhibition and ionic strength catalysis. *Journal of Geophysical Research* 73, 3315-3322.

Bischoff, J.L., Fyfe, W.S. (1968) Catalysis, inhibition, and the calcite-aragonite problem: 1. The aragonite-calcite transformation. *American Journal of Science* 266, 65-79.

Bischoff, W.D., Mackenzie, F.T., Bishop, F.C. (1987) Stabilities of synthetic magnesian calcites in aqueous solution: Comparison with biogenic materials. *Geochimica et Cosmochimica Acta* 51, 1413-1423.

Bischoff, W.D., Bertram, M.A., Mackenzie, F.T., Bishop, F.C. (1993) Diagenetic stabilization pathways of magnesian calcites. *Carbonates and Evaporites* 8, 82-89.

Borges, A. (2005) Do we have enough pieces of the jigsaw to integrate CO_2 fluxes in the coastal ocean? *Estuaries and Coasts* 28, 3-27.

Borges, A., Abril, G. (2011) Carbon dioxide and methane dynamics in estuaries. In: Wolanski, E., McLusky, D.S. (Eds.) Treatise on Estuarine and Coastal Science, Vol. 5.Academic Press, Waltham, pp. 119-161.

Borges, A.V., Delille, B., Frankignoulle, M. (2005) Budgeting sinks and sources of CO_2 in the coastal ocean: diversity of ecosystems counts. *Geophysical Research Letters* 32, L14601.

Borges, A.V., Schiettecatte, L.S., Abril, G., Delille, B., Gazeau, F. (2006) Carbon dioxide in European coastal waters. *Estuarine, Coastal and Shelf Science* 70, 375-387.

Boss, S.K., Wilkinson, B.H. (1991) Planktogenic eustatic control on cratonic-oceanic carbonate accumulation. *Journal of Geology* 99, 497-513.

Bots, P., Benning, L.G., Rickaby, R.E.M., Shaw, S. (2011) The role of SO_4 in the switch from calcite to aragonite seas. *Geology* 39, 331-334.

Brady, P.V., Krumhansl, J.L., Papenguth, H.W. (1996) Surface complexation clues to dolomite growth. *Geochimica et Cosmochimica Acta* 60, 727-731.

Brennan, S.T., Lowenstein, T.K. (2002) The major-ion composition of Silurian seawater. *Geochimica et Cosmochimica Acta* 66, 2683-2700.

Brennan, S.T., Lowenstein, T.K., Horita, J. (2004) Seawater chemistry and the advent of biocalcification. *Geology* 32, 473-476.

Broecker, W.S. (1971) Calcite accumulation rates and glacial to interglacial changes in ocean mixing. In: Turekian, K.K. (Ed.) The Late Cenozoic Glacial Ages. Yale University Press, New Haven, CT, pp. 239- 265.

Broecker, W.S. (1995) The glacial world according to Wally. Lamont-Doherty Geological Observatory, Columbia University, Palisades, NY.

Broecker, W.S. (2002) Constraints on the glacial operation of the Atlantic Ocean's conveyor circulation. *Israel Journal of Chemistry* 42, 1-14.

Broecker, W.S. (2003) The oceanic $CaCO_3$ cycle. In: Turekian, K.K., Holland, H.D. (Eds.) Treatise on Geochemistry. Elsevier, Palisades, NY, pp. 529-549.

Broecker, W.S. (2012) The Carbon Cycle and Climate Change: Memoirs of my 60 Years in Science. *Geochemical Perspectives* 1, 221-340.

Broecker, W.S., Takahashi, T. (1966) Calcium carbonate precipitation on the Bahama Banks. *Journal of Geophysical Research* 71, 1575-1602.

Broecker, W.S., Peng, T.H. (1982) Tracers in the Sea. Eldigio Press, Palisades, NY.

Broecker, W.S., Stocker, T.F. (2006) The Holocene CO_2 rise, anthropogenic or natural? *Eos* 87, 27.

Broecker, W.S., Li, Y.H., Peng, T.H. (1971) Carbon dioxide: man's unseen artifact. In: Hood, D.H. (Ed.) Impingement of Man on the Oceans. John Wiley and Sons, Inc., New York, pp. 287-324.

Budd, A. (2000) Diversity and extinction in the Cenozoic history of Caribbean reefs. *Coral Reefs* 19, 25-35.

Buddemeier, R.W., Hopley, D. (1988) Turn-ons and turn-offs: causes and mechanisms of the initiation and termination of coral reef growth. In: Proceedings of the Sixth International Coral Reef Symposium. Townsville, Australia. 8th-12th August 1988. pp. 253-261.

Buggisch, W., Joachimski, M.M., Lehnert, O., Bergstrom, S.T., Repetski, J.E. (2010) Did intense volcanism trigger the fisrt Late Ordovician icehouse? *Geology* 38, 327-330.

Burton, E.A., Walter, L.M. (1987) Relative precipitation rates of aragonite and Mg calcite from seawater: temperature or carbonate ion control? *Geology* 15, 111-114.

Burton, E.A., Walter, L.M. (1990) The role of pH in phosphate inhibition of calcite and aragonite precipitation rates in seawater. *Geochimica et Cosmochimica Acta* 54, 797-808.

Busenberg, E., Plummer, L.N. (1982) The kinetics of dissolution of dolomite in CO_2-H_2O systems at 1.5°C to 65°C and 0 atm to 1 atm pCO_2. *American Journal of Science* 282, 45-78.

Busenberg, E., Plummer, L.N. (1986) A comparative study of the dissolution and crystal growth kinetics of calcite and aragonite. In: Mumpton, F.A. (Ed.) Studies in Diagenesis: U.S. Geological Survey Bulletin 1578, United States Government Printing Office, pp. 139-168.

Busenberg, E., Niel Plummer, L. (1989) Thermodynamics of magnesian calcite solid-solutions at 25°C and 1 atm total pressure. *Geochimica et Cosmochimica Acta* 53, 1189-1208.

Cai, W.-J., Dai, M., Wang, Y. (2006) Air-sea exchange of carbon dioxide in ocean margins: a province-based synthesis. *Geophysical Research Letters* 33, L12603.

Caldeira, K., Wickett, M.E. (2003) Oceanography: Anthropogenic carbon and ocean pH. *Nature* 425, 365-365.

Caraco, N.F. (1995) Influence of human populations on P transfers to aquatic aquatic systems: a regional scale study using large rivers. In: Tiessen, H. (Ed.) Phosphorus in the Global Environment: Transfers, Cycles, and Management. John Wiley, New York.

Carlson, W.D. (1980) The calcite-aragonite equilibrium; effects of Sr substitution and anion orientational disorder. *American Mineralogist* 65, 1252-1262.

Catling, D.C., Claire, M.W. (2005) How Earth's atmosphere evolved to an oxic state: a status report. *Earth and Planetary Science Letters* 237, 1-20.

Chave, K.E. (1954) Aspects of the biogeochemistry of magnesium: 2. Calcareous sediments and rocks. *The Journal of Geology* 62, 587-599.

Chave, K.E., Suess, E. (1967) Suspended minerals in seawater. *Transactions of the New York Academy of Sciences* 29, 991-1000.

Chavez, F.P., Toggweiler, J.R. (1995) Physical estimates of global new production: the upwelling contribution. In: Summerhayes, C.P., Emeis, C.-L., Angel, M.V., Smith, R.L., Zeitzschel, B. (Eds.) Upwelling in the Ocean: Modern Processes and Ancient Records. Wiley, New York, pp. 313-320.

Chave, F.T., Mackenzie, F.T. (1961) A statistical technique applied to the geochemistry of pelagic muds. *Journal of Geology* 69, 572-582.

Chave, K.E., Garrels, R.M., Thompson, M.E., Deffeyes, K.S., Weyl, P.K. (1962) Observations on solubility of skeletal carbonates in aqueous solutions. *Science* 137, 33-34.

Chen, C.-T.A., Liu, K.-K., Macdonald, R. (2003) Continental margin exchanges. In: Fasham, M.J.R. (Ed.) Ocean Biogeochemistry: The Role of the Ocean Carbon Cycle in Global Change. Springer-Verlag, Berlin, pp. 53-97.

Chen, C.-T.A., Wang, S.L., Lu, X.X., Zhang, S.R., Lui, H.K., Tseng, H.C., Wang, B.J., Huang, H.I. (2008) Hydrogeochemistry and greenhouse gases of the Pearl River, its estuary and beyond. *Quaternary International* 186, 79-90.

Chou, L., Garrels, R.M., Wollast, R. (1989) Comparative study of the kinetics and mechanisms of dissolution of carbonate minerals. *Chemical Geology* 78, 269-282.

Cicero, A.D., Lohmann, K.C. (2001) Sr/Mg variation during rock-water interaction: implications for secular changes in the elemental chemistry of ancient seawater. *Geochimica et Cosmochimica Acta* 65, 741-761.

Cloud, P.E.J. (1962) Environment of calcium carbonate deposition west of Andros Island, Bahamas *U.S. Geology Survey Professional Papers* 350, 1-138.

Cohen, J.E., Small, C., Mellinger, A., Gallup, J., Sachs, J. (1997) Estimates of coastal populations. *Science* 278, 1209-1213.

Cole, J.J., Pace, M.L., Caraco, N.F., Steinhart, G.S. (1993) Bacterial biomass and cell-size distributions in lakes: more and larger cells in anoxic waters. *Limnology and Oceanography* 38, 1627-1632.

Crowley, T.J., Berner, R.A. (2001) CO_2 and climate change. *Science* 292, 870-872.

Curl, R.L. (1962) The aragonite-calcite problem. Bulletin of the National Speleological Society 24, 57-73.

Davis, K.J., Dove, P.M., De Yoreo, J.J. (2000) The role of Mg2+ as an impurity in calcite growth. *Science* 290, 1134-1137.

De Villiers, S., Nelson, B.K. (1999) Detection of low-temperature hydrothermal fluxes by seawater Mg and Ca anomalies. *Science* 285, 721-723.

De'ath, G., Fabricius, K.E., Sweatman, H., Puotinen, M. (2012) The 27-year decline of coral cover on the Great Barrier Reef and its causes. *Proceedings of the National Academy of Sciences of the United States of America* 109, 17995-17999.

Demicco, R.V. (2004) Modeling seafloor-spreading rates through time. *Geology* 32, 485-488.

Demicco, R.V., Lowenstein, T.K., Hardie, L.A. (2003) Atmospheric pCO_2 since 60 Ma from records of seawater pH, calcium, and primary carbonate mineralogy. *Geology* 31, 793-796.

Demicco, R.V., Lowenstein, T.K., Hardie, L.A., Spencer, R.J. (2005) Model of seawater composition for the Phanerozoic. *Geology* 33, 877-880.

Dickson, J.A.D. (1995) Palaeozoic Mg calcite preserved: implications for the Carboniferous ocean. *Geology* 23, 535-538.

Dickson, J.A.D. (2002) Fossil echinoderms as monitor of the Mg/Ca ratio of Phanerozoic oceans. *Science* 298, 1222-1224.

Dickson, J.A.D. (2004) Echinoderm skeletal preservation: calcite-aragonite seas and the Mg/Ca ratio of Phanerozoic oceans. *Journal of Sedimentary Research* 74, 355-365.

Doney, S.C., Fabry, V.J., Feely, R.A., Kleypas, J.A. (2009) Ocean Acidification: The Other CO2 Problem. *Annual Review of Marine Science* 1, 169-192.

Dore, J.E., Letelier, R.M., Church, M.J., Lukas, R., Karl, D.M. (2008) Summer phytoplankton blooms in the oligotrophic North Pacific Subtropical Gyre: historical perspective and recent observations. *Progress In Oceanography* 76, 2-38.

Drupp, P., De Carlo, E.H., Mackenzie, F.T., Bienfang, P., Sabine, C.L. (2011) Nutrient inputs, phytoplankton response, and CO_2 variations in a semi-enclosed subtropical embayment, Kaneohe Bay, Hawaii. *Aquatic Geochemistry* 17, 473-498.

Durack, P.J., Wijffels, S.E. (2010) Fifty-year trends in global ocean salinities and their relationship to broad-scale warming. *Journal of Climate* 23, 4342-4362.

Eakin, C.M. (1996) Where have all the carbonates gone? A model comparison of calcium carbonate budgets before and after the 1982-1983 El Nino at Uva Island in the eastern Pacific. *Coral Reefs* 15, 109-119.

Ebelmen, J.J. (1845) Sur les produits de la décomposition des espèces minérales de la famille des silicates. *Annales des Mines* 7, 3-66.

Edmond, J.M., Huh, Y. (2003) Non-steady state carbonate recycling and implications for the evolution of atmospheric pCO_2. *Earth and Planetary Science Letters* 216, 125-139.

Egli-Stoffyn, P., Mackenzie, F.T. (1984) Mass balance of dissolved lithium in the ocean. *Geochimica et Cosmochimica Acta* 48, 859-872.

Elsig, J., Schmitt, J., Leuenberger, D., Schneider, R., Eyer, M., Leuenberger, M., Joos, F., Fischer, H., Stocker, T.F. (2009) Stable isotope constraints on Holocene carbon cycle changes from an Antarctic ice core. *Nature* 461, 507-510.

Fagan, K.E., Mackenzie, F.T. (2007) Air-sea CO_2 exchange in a subtropical estuarine-coral reef system, Kaneohe Bay, Oahu, Hawaii. *Marine Chemistry* 106, 174-191.

Fairbanks, R.G. (1989) A 17,000-year glacio-eustatic sea-level record: influence of glacial melting rates on the younger dryas event and deep-ocean circulation. *Nature* 342, 637-642.

Folk, R.L., Land, L.S. (1975) Mg/Ca ratio and salinity: two controls over crystallization of dolomite. *AAPG Bulletin* 59, 60-68.

Foster, G.L. (2008) Seawater pH, pCO_2 and $[CO^{2-}_3]$ variations in the Caribbean Sea over the last 130 kyr: a boron isotope and B/Ca study of planktic foraminifera. *Earth and Planetary Science Letters* 271, 254-266.

Frakes, L.A., Francis, J.E., Syktus, J.I. (1992) Climate Modes of the Phanerozoic. Cambridge University Press, Cambridge.

Fyfe, W.S., Bischoff, J.L. (1965) The calcite-aragonite problem. In: Dolomitization and Limestone Diagenesis, Vol. 13. Society for Economic Paleontologists and Mineralogists Special Publication, pp. 3-13.

Gardner, T.A., Côté, I.M., Gill, J.A., Grant, A., Watkinson, A.R. (2003) Long-term region-wide declines in Caribbean corals. *Science* 301, 958-960.

Garrels, R.M., Mackenzie, F.T. (1967) Origin of the chemical compositions of some springs and lakes. In: Stumm, W. (Ed.), Equilibrium Concepts in Natural Water Systems, Advances in Chemistry Series 67, pp. 222-242.

Garrels, R.M., Mackenzie, F.T. (1971) Evolution of Sedimentary Rocks. W.W. Norton and Company, New York.

Garrels, R.M., Mackenzie, F.T. (1972) A quantitative model for the sedimentary rock cycle. *Marine Chemistry* 1, 27-41.

Garrels, R., Wollast, R. (1978) Equilibrium criteria for two-component solids reacting with fixed composition in an aqueous phase: example- the magnesian calcites; discussion. *American Journal of Science* 278, 1469-1474.

Garrels, R.M., Mackenzie, F.T. (1980) Some aspects of the role of the shallow ocean in global carbon dioxide uptake. Workshop Report, United States Department of Energy, Carbon Dioxide Effects Research and Assessment Program.

Garrels, R.M., Thompson, M.E., Siever, R. (1960) Stability of some carbonates at 25°C and one atmosphere total pressure. *American Journal of Science* 258, 402-418.

Garrels, R.M., Perry, E.A., Mackenzie, F.T. (1973) Genesis of Precambrian iron-formations and the development of atmospheric oxygen. *Economic Geology* 68, 1173-1179.

Garrels, R.M., Mackenzie, F.T., Hunt, C. (1975) Chemical Cycles and the Global Environment-Assessing Human Influences. W. Kaufman, Inc., Los Altos, CA.

Garrels, R.M., Lerman, A., Mackenzie, F.T. (1976) Controls of atmospheric O_2 and CO_2: past, present, and future. *American Scientist* 64, 306-315.

Gattuso, J.-P., Hansson, L. (2011) Ocean Acidification. Oxford University Press, New York.

Gattuso, J.P., Frankignoulle, M., Bourge, I., Romaine, S., Buddemeier, R.W. (1998) Effect of calcium carbonate saturation of seawater on coral calcification. *Global and Planetary Change* 18, 37-46.

Gattuso, J.-P., Allemand, D., Frankignoulle, M. (1999) Photosynthesis and calcification at cellular, organismal and community levels in coral reefs: a review on interactions and control by carbonate chemistry. *American Zoologist* 39, 160-183.

Goldsmith, J.R. (1953) A "simplexity principle" and its relation to "ease" of crystallization. *Journal of Geology* 61, 439-451.

Goldsmith, J.R., Heard, H.C. (1961) Subsolidus phase relations in the system $CaCO_3$-$MgCO_3$. *Journal of Geology* 69, 45-74.

González-Dávila, M., Santana-Casiano, J.M., Rueda, M.J., Llinás, O. (2010) The water column distribution of carbonate system variables at the ESTOC site from 1995 to 2004. *Biogeosciences* 7, 3067-3081.

Gradstein, F.M., Ogg, J.C., Smith, A.G. (2004) A Geologic Time Scale 2004. Cambridge University Press, New York.

GRAF, D.L., GOLDSMITH, J.R. (1955) Dolomite-magnesian calcite relations at elevated temperatures and CO_2 pressures. *Geochimica et Cosmochimica Acta* 7, 109-126.

GRAF, D.L., GOLDSMITH, J.R. (1958) The solid solubility of $MgCO_3$ in $CaCO_3$ - a revision. *Geochimica et Cosmochimica Acta* 13, 218-219.

GREGOR, C.B., GARRELS, R.M., MACKENZIE, F.T., MAYNARD, J.B. (1988) Chemical Cycles in the Evolution of the Earth. John Wiley & Sons, New York.

GRIGG, R.W. (1982) Coral reef development at high latitudes in Hawaii. *Manila* 1, 687-693.

GRIGG, R.W. (1997) Paleoceanography of coral reefs in the Hawaiian-Emperor Chain - revisited. *Coral Reefs* 16, S33-S38.

GUIDRY, M.W., MACKENZIE, F.T. (2003) Experimental study of igneous and sedimentary apatite dissolution: control of pH, distance from equilibrium, and temperature on dissolution rates. *Geochimica et Cosmochimica Acta* 67, 2949-2963.

GUIDRY, M.W., ARVIDSON, R.S., MACKENZIE, F.T. (2007) Biological and geochemical forcings to Phanerozoic change in seawater, atmosphere, and carbonate precipitate composition. In: Falkowski, P.G., Knoll, A.H. (Eds.) Evolution of Primary Producers in the Sea. Elsevier, Amsterdam, pp. 377-403.

HALL-SPENCER, J.M., RODOLFO-METALPA, R., MARTIN, S., RANSOME, E., FINE, M., TURNER, S.M., ROWLEY, S.J., TEDESCO, D., BUIA, M.-C. (2008) Volcanic carbon dioxide vents show ecosystem effects of ocean acidification. *Nature* 454, 96-99.

HALLAM, A. (1984) Pre-Quaternary sea-level changes. *Annual Review of Earth and Planetary Sciences* 12, 205-243.

HALLEY, E. (1715) A short account of the cause of the saltness of the ocean, and of the several lakes that emit no rivers; with a proposal, by help thereof, to discover the age of the world. *Philosophical Transactions of the Royal London Society* 29, 296-300.

HALLEY, R.B., YATES, K.K. (2000) Will reef sediments buffer corals from increased global CO_2? In: Hopley, D., Hopley, M., Tamelander, J., Done, T. (Eds.) Proceedings of the 9th International Coral Reef Symposium, 248. State Ministry for the Environment, Bali, Indonesia.

HANSEN, K.W., WALLMANN, K. (2003) Cretaceous and Cenozoic evolution of seawater composition, atmospheric O_2 and CO_2: a model perspective. *American Journal of Science* 303, 94-148.

HARDIE, L.A. (1987) Dolomitization; a critical view of some current views. *Journal of Sedimentary Research* 57, 166-183.

HARDIE, L.A. (1991) On the significance of evaporites. *Annual Review of Earth and Planetary Sciences* 19, 131-168.

HARDIE, L.A. (1996) Secular variation in seawater chemistry: an explanation for the coupled secular variation in the mineralogies of marine limestones and potash evaporites over the past 600 m.y. *Geology* 24, 279-283.

HARKER, R.I., TUTTLE, O.F. (1955a) Studies in the system CaO-MgO-CO_2. 1. The thermal dissociation of calcite, dolomite and magnesite. *American Journal of Science* 253, 209-224.

HARKER, R.I., TUTTLE, O.F. (1955b) Studies in the system CaO-MgO-CO_2. 2. Limits of solid solution along the binary join $CaCO_3$-$MgCO_3$. *American Journal of Science* 253, 274-282.

HARVIE, C.E., WEARE, J.H. (1980) The prediction of mineral solubilities in natural waters: the Na-K-Mg-Ca-Cl-SO_4-H_2O system from zero to high concentration at 25 °C. *Geochimica et Cosmochimica Acta* 44, 981-997.

HARVIE, C.E., EUGSTER, H.P., WEARE, J.H. (1982) Mineral equilibria in the six-component seawater system, Na-K-Mg-Ca-SO_4-Cl-H_2O at 25 °C. 2. Compositions of the saturated solutions. *Geochimica et Cosmochimica Acta* 46, 1603-1618.

HAWORTH, M., HESSELBO, S.P., MCELWAIN, J.C., ROBINSON, S.A., BRUNT, J.W. (2005) Mid-Cretaceous pCO_2 based on stomata of the extinct conifer *Pseudofrenelopsis* (Cheirolepidiaceae). *Geology* 33, 749-752.

HAY, W.W. (1985) Potential errors in estimates of carbonate rock accumulating through geologic time. In: Sundquist, E. T., Broecker, W.S. (Eds.) The Carbon Cycle and Atmospheric CO_2: Natural Variations Archean to Present. AGU, Washington, DC, pp. 573-583.

Helgeson, H.C. (1968) Evaluation of irreversible reactions in geochemical processes involving minerals and aqueous solutions, I. Thermodynamic relations. *Geochemica et Cosmochimica Acta* 32, 853-877.

Helgeson, H.C., Mackenzie, F.T. (1970) Silicate-sea water equilibria in the ocean system. *Deep Sea Research and Oceanographic Abstracts* 17, 877-892.

Helgeson, H.C., Garrels, R.M., Mackenzie, F.T. (1969) Evaluation of irreversible reactions in geochemical processes involving minerals and aqueous solutions. II. Applications. *Geochimica et Cosmochimica Acta* 33, 455-481.

Herrmann, A.D., MacLeod, K.G., Leslie, S.A. (2010) Did a volcanic mega-eruption cause global cooling during the Late Ordovician? *Palaios* 25, 831–836.

Hoegh-Guldberg, O. (2005) Low coral cover in a high-CO_2 world. *Journal of Geophysical Research* 110, C09S06.

Hoegh-Guldberg, O., Mumby, P.J., Hooten, A.J., Steneck, R.S., Greenfield, P., Gomez, E., Harvell, C.D., Sale, P.F., Edwards, A.J., Caldeira, K., Knowlton, N., Eakin, C.M., Iglesias-Prieto, R., Muthiga, N., Bradbury, R.H., Dubi, A., Hatziolos, M.E. (2007) Coral reefs under rapid climate change and ocean acidification. *Science* 318, 1737-1742.

Hoffman, J.S., Carlson, A.E., Winsor, K., Klinkhammer, G.P., LeGrande, A.N., Andrews, J.T., Strasser, J.C. (2012) Linking the 8.2 ka event and its freshwater forcing in the Labrador Sea. *Geophysical Research Letters* 39, L18703.

Holland, H.D. (1972) Geologic history of sea-water- attempt to solve problem. *Geochimica et Cosmochimica Acta* 36, 637-651.

Holland, H.D. (1978) The Chemical Evolution of the Atmosphere and Oceans. Princeton University Press, Princeton, New Jersey.

Holland, H.D. (1984) The Chemical Evolution of the Atmosphere and Oceans. Princeton University Press, Princeton.

Holland, H.D. (2004) The geologic history of seawater. In: Elderfield, H. (Ed.) The Oceans and Marine Chemistry. Elsevier, Amsterdam, pp. 583-625.

Holland, H.D. (2005) Sea level, sediments and the composition of seawater. *American Journal of Science* 305, 220-239.

Holland, H.D., Zimmerman, H. (2000) The dolomite problem revisited. *International Geology Review* 42, 481-490.

Holland, H.D., Horita, J., Seyfried, W.E. (1996) On the secular variations in the composition of Phanerozoic marine potash evaporites. *Geology* 24, 993-996.

Holser, W.T. (1963) Chemistry of brine inclusions in Permian salt from Hutchinson, Kansas. *Symposium on Salt 1*, Northern Ohio Geological Society, 86-95.

Holser, W.T. (1984) Gradual and abrupt shifts in ocean chemistry during Phanerozoic time. In: Holland, H.D., Trendall, A.F. (Eds.) Patterns of Change in Earth Evolution. Springer-Verlag, Berlin, pp. 123-144.

Holser, W., Schidlowski, M., Mackenzie, F., Maynard, J. (1988) Geochemical cycles of carbon and sulfur. *Chemical Cycles in the Evolution of the Earth*, 105-173.

Hönisch, B., Hemming, N.G. (2005) Surface ocean pH response to variations in pCO_2 through two full glacial cycles. *Earth and Planetary Science Letters* 236, 305-314.

Hönisch, B., Ridgwell, A., Schmidt, D.N., Thomas, E., Gibbs, S.J., Sluijs, A., Zeebe, R., Kump, L., Martindale, R.C., Greene, S.E., Kiessling, W., Ries, J., Zachos, J.C., Royer, D.L., Barker, S., Marchitto, T.M., Moyer, R., Pelejero, C., Ziveri, P., Foster, G.L., Williams, B. (2012) The geological record of ocean acidification. *Science* 335, 1058-1063.

Horita, J., Friedman, T.J., Lazar, B., Holland, H.D. (1991) The composition of Permian seawater. *Geochimica et Cosmochimica Acta* 55, 417-432.

Horita, J., Zimmermann, H., Holland, H.D. (2002) Chemical evolution of seawater during the Phanerozoic: implications from the record of marine evaporites. *Geochimica et Cosmochimica Acta* 66, 3733-3756.

HOUGHTON, R.A. (1995) Land-use change and the carbon-cycle. *Global Change Biology* 1, 275-287.

HUTCHEON, I., OLDERSHAW, A., GHENT, E.D. (1980) Diagenesis of Cretaceous sandstones of the Kootenay Formation at Elk Valley (southeastern British Columbia) and Mt Allan (southwestern Alberta). *Geochimica et Cosmochimica Acta* 44, 1425-1435.

IMBRIE, J., HAYS, J., MARTINSON, D., MCINTYRE, A., MIX, A., MORLEY, J., PISIAS, N., PRELL, W., SHACKLETON, N. (1984) The orbital theory of Pleistocene climate: support from a revised chronology of the marine $\delta^{18}O$ record. In: Berger, A., Schneider, S., Duplessy, J.C. (Eds.) Climate and Geosciences. Kluwer Academic Publishers, Dordrecht, Holland, pp. 121-164.

INDERMÜHLE, A., STOCKER, T.F., JOOS, F., FISCHER, H., SMITH, H.J., WAHLEN, M., DECK, B., MASTROIANNI, D., TSCHUMI, J., BLUNIER, T., MEYER, R., STAUFFER, B. (1999) Holocene carbon-cycle dynamics based on CO_2 trapped in ice at Taylor Dome, Antarctica. *Nature* 398, 121-126.

IPCC (2001) Climate change 2001: the scientific basis, Contribution of Working Group I to the Third Assessment Report of the Inter-governmental Panel on Climate Change. Cambridge University Press, New York.

IPCC (2007) Climate change 2007: the scientific basis. Contribution of Working Group I to the Fourth Assessment Report of the Intergovernmental Panel on Climate Change. Cambridge University Press, New York.

ISHII, M., KIMOTO, M., SAKAMOTO, K., IWASAKI, S.I. (2006) Steric sea level changes estimated from historical ocean subsurface temperature and salinity analyses. *Journal of Oceanography* 62, 155-170.

JAHNKE, R.A. (2010) Global synthesis. In: Liu, K.-K., Atkinson, L., Quiñones, R., Talaue-McManus, L. (Eds.) Carbon and Nutrient Fluxes in Continental Margins. Springer, Berlin, pp. 597-615.

JOKIEL, P., RODGERS, K., KUFFNER, I., ANDERSSON, A., COX, E., MACKENZIE, F. (2008) Ocean acidification and calcifying reef organisms: a mesocosm investigation. *Coral Reefs* 27, 473-483.

JOLY, J. (1899) An estimate of the geological age of the Earth. *The Scientific Transactions of the Royal Dublin Society* 7, 23-66.

KAMPSCHULTE, A. (2001) Schwefelisotopenuntersuchungen an strukturell substituierten Sulfaten in marinen Karbonaten des Phanerozoikums: Implikationen für die geochemische Evolution des Meerwassers und die Korrelation verschiedener Stoffkreisläufe. Fakultät für Geowissenschaften, Ruhr-Universität Bochum.

KAMPSCHULTE, A., STRAUSS, H. (1998) The isotopic composition of trace sulphates in Palaeozoic biogenic carbonates: implications for coeval seawater and geochemical cycles. *Mineralogy Magazine* 62, 744-745.

KASTING, J.F., TOON, O.B., POLLACK, J.B. (1988) How climate evolved on the terrestrial planets. *Scientific American* 258, 90-97.

KATZ, M.E., WRIGHT, J.D., MILLER, K.G., CRAMER, B.S., FENNEL, K., FALKOWSKI, P.G. (2005) Biological overprint of the geological carbon cycle. *Marine Geology* 217, 323-338.

KATZ, M.E., FENNEL, K., FALKOWSKI, P.G. (2007) Geochemical and biological consequences of phytoplankton evolution. *Evolution of Primary Producers in the Sea*, 405-430.

KEIR, R.S. (1980) The dissolution kinetics of biogenic calcium carbonates in seawater. *Geochimica et Cosmochimica Acta* 44, 241-252.

KEIR, R.S. (1983) Variation in the carbonate reactivity of deep-sea sediments: determination from flux experiments. *Deep-Sea Research Part A: Oceanographic Research Papers* 30, 279-296.

KERR, R.A. (2002) Deep life in the slow, slow lane. *Science* 296, 1056-1058.

KIESSLING, W. (2002) Secular variations in Phanerozoic reef ecosystem. In: Kiessling, W., Flügel, E., Golonka, J.A.N. (Eds.) Phanerozoic Reef Patterns. Society of Economic Paleontologists and Mineralogists Special Publication, Tulsa, OK. pp. 625-690.

KIESSLING, W. (2009) Geologic and biologic controls on the evolution of reefs. *Annual Review of Ecology, Evolution, and Systematics* 40, 173-192.

KIESSLING, W., FLÜGEL, E., GOLONKA, J. (2003) Patterns of Phanerozoic carbonate platform sedimentation. *Lethaia* 36, 195-225.

Kleypas, J.A. (1997) Modeled estimates of global reef habitat and carbonate production since the last glacial maximum. *Paleoceanography* 12, 533-545.

Kleypas, J.A., Buddemeier, R.W., Archer, D., Gattuso, J.-P., Langdon, C., Opdyke, B.N. (1999) Geochemical consequences of increased atmospheric carbon dioxide on coral reefs. *Science* 284, 118-120.

Kleypas, J.A., Anthony, K.R.N., Gattuso, J.-P. (2011) Coral reefs modify their seawater carbon chemistry – case study from a barrier reef (Moorea, French Polynesia). *Global Change Biology* 17, 3667-3678.

Kline, D.I., Teneva, L., Schneider, K., Miard, T., Chai, A., Marker, M., Headley, K., Opdyke, B., Nash, M., Valetich, M., Caves, J.K., Russell, B.D., Connell, S.D., Kirkwood, B.J., Brewer, P., Peltzer, E., Silverman, J., Caldeira, K., Dunbar, R.B., Koseff, J.R., Monismith, S.G., Mitchell, B.G., Dove, S., Hoegh-Guldberg, O. (2012) A short-term in situ CO_2 enrichment experiment on Heron Island (GBR). *Scientific Reports* 2, 1-9.

Köhler, P., Fischer, H., Munhoven, G., Zeebe, R.E. (2005) Quantitative interpretation of atmospheric carbon records over the last glacial termination. *Global Biogeochemical Cycles* 19, GB4020.

Kroeker, K.J., Kordas, R.L., Crim, R.N., Singh, G.G. (2010) Meta-analysis reveals negative yet variable effects of ocean acidification on marine organisms. *Ecology Letters* 13, 1419-1434.

Kroopnick, P.M. (1980) The distribution of ^{13}C in the Atlantic-Ocean. *Earth and Planetary Science Letters* 49, 469-484.

Ku, T.C.W., Walter, L.M., Coleman, M.L., Blake, R.E., Martini, A.M. (1999) Coupling between sulfur recycling and syndepositional carbonate dissolution: evidence from oxygen and sulphur isotope composition of pore water sulfate, South Florida Platform, U.S.A. *Geochimica et Cosmochimica Acta* 63, 2529-2546.

Kuffner, I.B., Andersson, A.J., Jokiel, P.L., Rodgers, K.u.S., Mackenzie, F.T. (2008) Decreased abundance of crustose coralline algae due to ocean acidification. *Nature Geoscience* 1, 114-117.

Kump, L.R. (1989) Alternative modeling approaches to the geochemical cycles of carbon, sulfur, and strontium isotopes. *American Journal of Science* 289, 390-410.

Kump, L.R. (2004) The geochemistry of mass extinction. In: Mackenzie, F.T. (Ed.) Treatise on Geochemistry, Volume 7. Elsevier, New York, pp. 351-367.

Kump, L.R., Bralower, T.J., Ridgwell, A. (2009) Ocean acidification in deep time. *Oceanography* 22, 94-107.

Land, L.S. (1967) Diagenesis of skeletal carbonates. *Journal of Sedimentary Research* 37, 914-930.

Land, L.S. (1985) The origin of massive dolomite. *Journal of Geological Education* 33, 112-125.

Land, L.S. (1989) The carbon and oxygen isotopic chemistry of surficial Holocene shallow marine carbonate sediment and Quaternary limestone and dolomite. In: Fritz, P., Fontes, J.C. (Eds.) The Marine Environment. Elsevier, Amsterdam, pp. 191-218.

Land, L.S. (1995) Comment on "Oxygen and carbon isotopic composition of Ordovician brachiopods: Implications for coeval seawater" by H. Qing and J. Veizer. *Geochimica et Cosmochimica Acta* 59, 2843-2844.

Land, L.S., Mackenzie, F.T., Gould, S.J. (1967) Pleistocene history of Bermuda. *Geological Society of America Bulletin* 78, 993-1006.

Langdon, C., Broecker, W.S., Hammond, D.E., Glenn, E., Fitzsimmons, K., Nelson, S.G., Peng, T.-H., Hajdas, I., Bonani, G. (2003) Effect of elevated CO_2 on the community metabolism of an experimental coral reef. *Global Biogeochemical Cycles* 17, 1011.

Lantzy, R., Mackenzie, F.T. (1979) Atmospheric trace metals: Global cycles and assessment of man's impact. *Geochimica et Cosmochimica Acta* 43, 511-525.

Lasaga, A.C., Berner, R.A., Garrels, R.M. (1985) An improved geochemical model of atmospheric CO2 fluctuations over the past 100 million years. *Geophysical Monograph Series* 32, 397-411.

Lazar, B., Holland, H.D. (1988) The analysis of fluid inclusions in halite. *Geochimica et Cosmochimica Acta* 52, 485-490.

Le Quéré, C., Andres, R.J., Boden, T., Conway, T., Houghton, R.A., House, J.I., Marland, G., Peters, G.P., van der Werf, G., Ahlström, A., Andrew, R.M., Bopp, L., Canadell, J.G., Ciais, P., Doney, S.C., Enright, C., Friedlingstein, P., Huntingford, C., Jain, A.K., Jourdain, C., Kato, E., Keeling, R.F., Klein Goldewijk, K., Levis, S., Levy, P., Lomas, M., Poulter, B., Raupach, M.R., Schwinger, J., Sitch, S., Stocker, B.D., Viovy, N., Zaehle, S., Zeng, N. (2012) The global carbon budget 1959-2011. *Earth System Science Data Discussion* 5, 1107-1157.

Leclercq, N., Gattuso, J.-P., Jaubert, J. (2000) CO_2 partial pressure controls the calcification rate of a coral community. *Global Change Biology* 6, 329-334.

Leclercq, N., Gattuso, J.-P., Jaubert, J. (2002) Primary production, respiration, and calcification of a coral reef mesocosm under increased CO_2 partial pressure. *Limnology and Oceanography* 47, 558-564.

Lee, J., Morse, J.W. (2010) Influences of alkalinity and pCO_2 on $CaCO_3$ nucleation from estimated Cretaceous composition seawater representative of "calcite seas". *Geology* 38, 115-118.

Lees, A., Buller, A.T. (1972) Modern temperate-water and warm-water shelf carbonate sediments contrasted. *Marine Geology* 13, M67-M73.

Leitmeier, H. (1909) Die Absätze des Mineralwassers von Rohitsch-Sauerbrunn in Steiermark. *Zeitschrift Krystallographie Mineralogie* 47, 104-123.

Lerman, A., Clauer, N. (2004) Stable isotopes in the sedimentary record. In: Mackenzie, F.T. (Ed.) Treatise on Geochemistry: Sediments, Diagenesis, and Sedimentary Rocks, Vol. 7. Elsevier, pp. 1-55.

Lerman, A., Mackenzie, F. (2005) CO_2 air–sea exchange due to calcium carbonate and organic matter storage, and its implications for the global carbon cycle. *Aquatic Geochemistry* 12, 389-390.

Lerman, A., Clauer, N. (2013) Stable isotopes in the sedimentary record. In: Mackenzie, F.T. (Ed.) Treatise on Geochemistry: Sediments, Diagenesis and Sedimentary Rocks, Vol. 9. Second edition, Elsevier, Oxford.

Lerman, A., Mackenzie, F., Garrels, R. (1975) Modeling of geochemical cycles: Phosphorus as an example. In: Whitten, E. H. T. (Ed.) Quantitative Studies in the Geological Sciences, Geological Society of America Memoir 142, pp. 205-218.

Lerman, A., Guidry, M., Andersson, A., Mackenzie, F. (2011) Coastal ocean last glacial maximum to 2100 CO_2-carbonic acid-carbonate system: a modeling approach. *Aquatic Geochemistry* 17, 749-773.

Levitus, S., Antonov, J., Boyer, T. (2005) Warming of the world ocean, 1955-2003. *Geophysical Research Letters* 32, L02604.

Li, G., Elderfield, H. (2013) Evolution of carbon cycle over the past 100 million years. *Geochimica et Cosmochimica Acta* 103, 11-25.

Lippmann, F. (1960) Versuche zur Aufklarung der Bildungsbedingungen von Calcit und Aragonit. *Fortschritte der Mineralogie* 38, 156-161.

Lippmann, F. (1973) Sedimentary Carbonate Minerals. Springer-Verlag, New York.

Locklair, R.E., Lerman, A. (2005) A model of Phanerozoic cycles of carbon and calcium in the global ocean: evaluation and constraints on ocean chemistry and input fluxes. *Chemical Geology* 217, 113-126.

Lough, J.M., Barnes, D.J. (2000) Environmental controls on growth of the massive coral *Porites*. *Journal of Experimental Marine Biology and Ecology* 245, 225-243.

Lowenstam, H.A. (1986) Mineralization processes in monerans and protoctists. *Systematics Association Special Volume Series*, 1-17.

Lowenstam, H.A., Weiner, S. (1989) On biomineralization. Oxford University Press, Oxford.

Lowenstein, T.K., Hardie, L.A., Timofeeff, M.N., Demicco, R.V. (2003) Secular variation in seawater chemistry and the origin of calcium chloride basinal brines. *Geology* 31, 857-860.

Lowenstein, T.K., Timofeeff, M.N., Kovalevych, V.M., Horita, J. (2005) The major-ion composition of Permian seawater. *Geochimica et Cosmochimica Acta* 69, 1701-1719.

Lüthi, D., Le Floch, M., Bereiter, B., Blunier, T., Barnola, J.M., Siegenthaler, U., Raynaud, D., Jouzel, J., Fischer, H., Kawamura, K. (2008) High-resolution carbon dioxide concentration record 650,000-800,000 years before present. *Nature* 453, 379-382.

Machel, H.-G., Mountjoy, E.W. (1986) Chemistry and environments of dolomitization- a reappraisal. *Earth-Science Reviews* 23, 175-222.

Mackenzie, F.T. (1975) Sedimentary cycling and the evolution of seawater. In: Riley, J.P., Skirrow, G. (Eds.) Chemical Oceanography, Vol. 1. Second edition, Academic Press, London, pp. 309-364.

Mackenzie, F.T. (2011) Our Changing Planet: An Introduction to Earth System Science and Global Environmental Change. Fourth edition, Prentice Hall, Upper Saddle River, NJ.

Mackenzie, F.T., Garrels, R.M. (1966a) Chemical mass balance between rivers and oceans. *American Journal of Science* 264, 507-525.

Mackenzie, F.T., Garrels, R.M. (1966b) Silica-bicarbonate balance in the ocean and early diagenesis. *Journal of Sedimentary Research* 36, 1075-1084.

Mackenzie, F.T., Pigott, J.D. (1981) Tectonic controls of Phanerozoic sedimentary rock cycling. *Journal of the Geological Society* 138, 183-196.

Mackenzie, F.T., Agegian, C.R. (1989) Biomineralization and tentative links to plate tectonics. In: Crick, R.E. (Ed.) Origin, Evolution, and Modern Aspects of Biomineralization in Plants and Animals. Plenum Press, New York, pp. 11-28.

Mackenzie, F.T., Morse, J.W. (1992) Sedimentary carbonates through Phanerozoic time. *Geochimica et Cosmochimica Acta* 56, 3281-3295.

Mackenzie, F.T., Lerman, A. (2006) Carbon in the Geobiosphere: Earth's Outer Shell. Springer, Dordreeht, Netherlands.

Mackenzie, F.T., Lantzy, R., Paterson, V. (1979) Global trace metal cycles and predictions. *Journal of the International Association of Mathematical Geologists,* 11, 99-142.

Mackenzie, F.T., Ristvet, B., Thorstenson, D., Lerman, A., Leeper, R. (1981) Reverse weathering and chemical mass balance in a coastal environment. In: Marten, J.M., Burton, J.D., Eisma, D. (Eds.) River Inputs to Ocean Systems. UNEP and UNESCO, Switzerland, pp. 152-187.

Mackenzie, F.T., Bischoff, W.D., Bishop, F.C., Loijens, M., Schoonmaker, J., Wollast, R. (1983) Magnesian calcites: low-temperature occurrence, solubility and solid-solution behavior. *Reviews in Mineralogy and Geochemistry* 11, 97-144.

Mackenzie, F.T., Ver, L.M., Lerman, A. (2002) Century-scale nitrogen and phosphorus controls of the carbon cycle. *Chemical Geology* 190, 13-32.

Mackenzie, F.T., Andersson, A.J., Lerman, A., Ver, L.M. (2005) Boundary exchanges in the global coastal margin: implications for the organic and inorganic carbon cycles. In: Robinson, A.R., Brink, K.H. (Eds.) The Sea: Ideas and Observations on Progress in the Study of the Seas. Harvard University Press, Cambridge, MA, pp. 193-225.

Mackenzie, F.T., Arvidson, R.S., Guidry, M. (2008) Chemostatic modes of the ocean-atmosphere-sediment system through Phanerozoic time. *Mineralogical Magazine* 72, 329-332.

Mackenzie, F.T., Andersson, A.J., Arvidson, R.S., Guidry, M.W., Lerman, A. (2011) Land-sea carbon and nutrient fluxes and coastal ocean CO_2 exchange and acidification: past, present, and future. *Applied Geochemistry* 26, S298-S302.

Macqueen, R.W., Ghent, E.D. (1970) Electron microprobe study of magnesium distribution in some mississippian echinoderm limestones from western Canada, *Canadian Journal of Earth Sciences* 7, 1308-1316.

Macqueen, R.W., Ghent, E.D., Davies, G.R. (1974) Magnesium distribution in living and fossil specimens of the echinoid Peronella lesueuri Agassiz, Shark Bay, Western Australia. *Journal of Sedimentary Research* 44, 60-69.

Manzello, D.P., Enochs, I.C., Melo, N., Gledhill, D.K., Johns, E.M. (2012) Ocean acidification refugia of the Florida reef tract. *PLoS ONE* 7, e41715.

Margulis, L., Schwartz, K.V. (1998) Five kingdoms: an illustrated guide to the phyla of life on Earth. Third edition, Freeman, New York.

Martin, S., Rodolfo-Metalpa, R., Ransome, E., Rowley, S., Buia, M.-C., Gattuso, J.-P., Hall-Spencer, J. (2008) Effects of naturally acidified seawater on seagrass calcareous epibionts. *Biology Letters* 4, 689-692.

McCulloch, M., Falter, J., Trotter, J., Montagna, P. (2012) Coral resilience to ocean acidification and global warming through pH up-regulation. *Nature Climate Change* 2, 623-633.

McKenzie, J.A. (1991) The dolomite problem: an outstanding controversy. In: Müller, D.W., McKenzie, J.A., Weissert, H. (Eds.) Controversies in Modern Geology: Evolution of Geological Theories in Sedimentology. Academic Press, London, pp. 37-54.

McKenzie, J.A., Vasconcelos, C. (2009) Dolomite Mountains and the origin of the dolomite rock of which they mainly consist: historical developments and new perspectives. *Sedimentology* 56, 205-219.

Meybeck, M. (1979) Concentrations des eaux fluviales en éléments majeurs et apports en solution aux océans. *Revue de Géologie Dynamique et de Géographie Physique* 21, 215-246.

Meybeck, M. (1982) Carbon, nitrogen, and phosphorus transport by world rivers. *American Journal of Science* 282, 401-450.

Meybeck, M., Ragu, A. (1995) River Discharges to Oceans: An Assessment of Suspended Solids, Major Ions and Nutrients. United Nations Environment Programme, Nairobi.

Michalopoulos, P., Aller, R.C. (1995) Rapid clay mineral formation in Amazon delta sediments: reverse weathering and oceanic elemental cycles. *Science* 270, 614-614.

Milankovitch, M. (1941) Kanon der Erdbestrahlung und seine Anwendung auf das Eiszeitenproblem (Canon of Insolation and the Ice Age Problem). *Royal Serbian Sciences, Special Publications 132* Section of Mathematical and Natural Sciences 33, Belgrade. Translated by Israel Program for Scientific Translations, Jerusalem, available from U. S. Department of Commerce, Clearinghouse for Scientific and Technical Information, Springfield, Va.

Millero, F.J. (1996) Modeling the effect of ionic interactions on radionuclides in natural waters. *Abstracts of Papers of the American Chemical Society* 212, 85-NUCL.

Millero, F.J. (2006) Chemical Oceanography. CRC Press.

Milliken, K.L. (2004) Elemental transfer in sandstone-shale sequences: Chapter 5. In: Mackenzie, F.T. (Ed.) Treatise on Geochemistry: Sediments, Diagenesis, and Sedimentary Rocks, Vol. 7. Elsevier, pp. 159-190.

Milliman, J.D. (1993) Production and accumulation of calcium carbonate in the ocean: budget of a nonsteady state. *Global Biogeochemical Cycles* 7, 927-957.

Milliman, J.D. (1997) Blessed dams or damned dams? *Nature* 386, 325-327.

Milliman, J.D. (2001) Delivery and fate of fluvial water and sediment to the sea: a marine geologist's view of European rivers. *Scientia Marina* 65, 121-131.

Milliman, J., Droxler, A. (1996) Neritic and pelagic carbonate sedimentation in the marine environment: ignorance is not bliss. *Geologische Rundschau* 85, 496-504.

Moberly, R. (1968) Composition of magnesian calcites of algae and pelecypods by electron microprobe analysis. *Sedimentology* 11, 61-82.

Monaghan, P.H., Lytle, M.L. (1956) The origin of calcareous ooliths. *Journal of Sedimentary Research* 26, 111-118.

Montaggioni, L. (2000) Postglacial reef growth. *Comptes Rendus de l'Académie des Sciences-Series IIA-Earth and Planetary Science* 331, 319-330.

Montañez, I.P. (2002) Biological skeletal carbonate records changes in major-ion chemistry of paleooceans. *Proceedings of the National Academy of Sciences* 99, 15852-15854.

Mora, C.I., Driese, S.G., Colarusso, L.A. (1996) Middle to Late Palaeozoic atmospheric CO_2 levels from soil carbonate and organic-matter. *Science* 271, 1105-1107.

Morrow, D.W. (1982) Diagenesis 1. Dolomite- Part 1. The chemistry of dolomitization and dolomite precipitation. *Geoscience Canada* 9, 5-13.

Morse, A.N.C., Iwao, K., Baba, M., Shimoike, K., Hayashibara, T., Omori, M. (1996) An ancient chemosensory mechanism brings new life to coral reefs. *The Biological Bulletin* 191, 149-154.

Morse, D.E., Morse, A.N.C. (1991) Enzymatic characterization of the morphogen recognized by *Agaricia humilis* (scleractinian coral) larvae. *The Biological Bulletin* 181, 104-122.

Morse, J.W. (1983) The kinetics of calcium carbonate dissolution and precipitation. *Reviews in Mineralogy and Geochemistry* 11, 227-264.

Morse, J.W., Berner, R.A. (1972) Dissolution Kinetics of Calcium-Carbonate in Sea-Water .2. Kinetic Origin for Lysocline. *American Journal of Science* 272, 840-851.

Morse, J.W., Mackenzie, F.T. (1990) Geochemistry of Sedimentary Carbonates. Elsevier, New York.

Morse, J.W., Mucci, A., Walter, L.M., Kaminsky, M.S. (1979) Magnesium interaction with the surface of calcite in seawater. *Science* 205, 904-905.

Morse, J.W., Zullig, J.J., Bernstein, L.D., Millero, F.J., Milne, P.J., Mucci, A., Choppin, G.R. (1985) Chemistry of calcium carbonate-rich shallow water sediments in the Bahamas. *American Journal of Science* 285, 147-185.

Morse, J.W., Wang, Q., Tsio, M.Y. (1997) Influences of temperature and Mg:Ca ratio on $CaCO_3$ precipitates from seawater. *Geology* 25, 85-87.

Morse, J.W., Andersson, A.J., Mackenzie, F.T. (2006) Initial responses of carbonate-rich shelf sediments to rising atmospheric pCO_2 and "ocean acidification": role of high Mg-calcites. *Geochimica et Cosmochimica Acta* 70, 5814-5830.

Morse, J.W., Arvidson, R.S., Lüttge, A. (2007) Calcium carbonate formation and dissolution. *Chemical Reviews* 107, 342-381.

Moser, H., Stichler, W. (1980) Environmental isotopes in ice and snow. In: Fritz, P., Fontes, J.C. (Eds.) The Terrestrial Environment, A. Elsevier, Amsterdam, pp. 141-178.

Mottl, M.J., Wheat, C.G. (1994) Hydrothermal circulation through mid-ocean ridge flanks: fluxes of heat and magnesium. *Geochimica et Cosmochimica Acta* 58, 2225-2237.

Mucci, A. (1986) Growth kinetics and composition of magnesian calcite overgrowths precipitated from seawater: quantitative influence of orthophosphate ions. *Geochimica et Cosmochimica Acta* 50, 2255-2265.

Mucci, A., Morse, J.W. (1983) The incorporation of Mg^{2+} and Sr^{2+} into calcite overgrowths: influences of growth rate and solution composition. *Geochimica et Cosmochimica Acta* 47, 217-233.

Mucci, A., Morse, J.W. (1984) The solubility of calcite in seawater solutions of various magnesium concentration, It=0.697 M at 25°C and one atmosphere total pressure. *Geochimica et Cosmochimica Acta* 48, 815-822.

Mucci, A., Canuel, R., Zhong, S. (1989) The solubility of calcite and aragonite in sulfate-free seawater and the seeded growth kinetics and composition of the precipitates at 25°C. *Chemical Geology* 74, 309-320.

Munhoven, G. (2007) Glacial-interglacial rain ratio changes: implications for atmospheric CO_2 and ocean-sediment interaction. *Deep-Sea Research Part II-Topical Studies in Oceanography* 54, 722-746.

Nelson, C.S. (1988) An introductory perspective on non-tropical shelf carbonates. *Sedimentary Geology* 60, 3-12.

Neumann, A.C. (1965) Processes of recent carbonate sedimentation in Harrington Sound, Bermuda. *Bulletin of Marine Science* 15, 987-1035.

Nordt, L., Atchley, S., Dworkin, S. (2002) Palaeosol barometer indicates extreme fluctuations in atmospheric CO_2 across the Cretaceous-Tertiary boundary. *Geology* 30, 703-706.

Opdyke, B.N., Wilkinson, B.H. (1990) Paleolatitude distribution of Phanerozoic marine ooids and cements. *Palaeogeography, Palaeoclimatology, Palaeoecology* 78, 135-148.

Opdyke, B.N., Walker, J.C.G. (1992) Return of the coral reef hypothesis: basin to shelf partitioning of $CaCO_3$ and its effect on atmospheric CO_2. *Geology* 20, 733-736.

Orr, J. (2011) Recent and future changes in ocean carbonate chemistry. In: Gattuso, J.-P., Hansson, L. (Eds.) Ocean Acidification. Oxford University Press, New York, pp. 41-66.

Paytan, A., Kastner, M., Campbell, D., Thiemens, M.H. (1998) Sulfur isotopic composition of Cenozoic seawater sulfate. *Science* 282, 1459-1462.

PAYTAN, A., KASTNER, M., CAMPBELL, D., THIEMENS, M.H. (2004) Seawater sulphur isotope fluctuations in the cretaceous. *Science* 304, 1663-1665.

PEARSON, P.N., PALMER, M.R. (2000) Atmospheric carbon dioxide concentrations over the past 60 million years. *Nature* 406, 695-699.

PERRIN, C. (2002) Tertiary: the emergence of modern reef ecosystems. In: Kiessling, W., Flügel, Golonka, J. (Eds.) Phanerozoic Reef Patterns. SEPM Special Publication 72, pp. 587-624.

PETIT, J.R., JOUZEL, J., RAYNAUD, D., BARKOV, N.I., BARNOLA, J.M., BASILE, I., BENDER, M., CHAPPELLAZ, J., DAVIS, M., DELAYGUE, G., DELMOTTE, M., KOTLYAKOV, V.M., LEGRAND, M., LIPENKOV, V.Y., LORIUS, C., PEPIN, L., RITZ, C., SALTZMAN, E., STIEVENARD, M. (1999) Climate and atmospheric history of the past 420,000 years from the Vostok ice core, Antarctica. *Nature* 399, 429-436.

PITZER, K.S. (1973) Thermodynamics of electrolytes. I. Theoretical basis and general equations. *The Journal of Physical Chemistry* 77, 268-277.

PITZER, K.S. (1975) Thermodynamics of electrolytes. V. Effects of higher-order electrostatic terms. *Journal of Solution Chemistry* 4, 249-265.

PITZER, K.S. (1979) Relativistic effects on chemical properties. *Accounts of Chemical Research* 12, 272-276.

PLUMMER, L.N., MACKENZIE, F.T. (1974) Predicting mineral solubility from rate data; application to the dissolution of magnesian calcites. *American Journal of Science* 274, 61-83.

PLUMMER, L.N., WIGLEY, T.M.L., PARKHURST, D.L. (1978) The kinetics of calcite dissolution in CO_2 -water systems at 5° to 60°C and 0.0 to 1.0 atm CO_2. *American Journal of Science* 278, 179-216.

PYTKOWICZ, R.M. (1965) Rates of inorganic calcium carbonate nucleation. *The Journal of Geology*, 196-199.

PYTKOWICZ, R. (1973) Calcium carbonate retention in supersaturated seawater. *American Journal of Science* 273, 515-522.

RAILSBACK, L.B. (1993) Stability of carbonate minerals: a thermodynamic perspective and its implications for carbonate petrology. *Journal of Geological Education* 41, 12-14.

RAILSBACK, L.B., ANDERSON, T.F. (1987) Control of Triassic seawater chemistry and temperature on the evolution of post-Palaeozoic aragonite-secreting faunas. *Geology* 15, 1002-1005.

RAISWELL, R., CANFIELD, D.E. (2012) The iron biogeochemical cycle past and present. *Geochemical Perspectives* 1, 1-220.

RAO, C.P., JAYAWARDANE, M.P.J. (1994) Major minerals, elemental and isotopic composition in modern temperate shelf carbonates, eastern Tasmania, Australia - implications for the occurrence of extensive ancient nontropical carbonates. *Palaeogeography Palaeoclimatology Palaeoecology* 107, 49-63.

RAYMO, M., RUDDIMAN, W.F. (1992) Tectonic forcing of late Cenozoic climate. *Nature* 359, 117-122.

RAYMO, M.E., RUDDIMAN, W.F., FROELICH, P.N. (1988) Influence of late Cenozoic mountain building on ocean geochemical cycles. *Geology* 16, 649-653.

REDDY, M.M., PLUMMER, L.N., BUSENBERG, E. (1981) Crystal growth of calcite from calcium bicarbonate solutions at constant pCO_2 and 25 °C: a test of a calcite dissolution model. *Geochimica et Cosmochimica Acta* 45, 1281-1289.

RETALLACK, G.J. (2001) A 300-million-year record of atmospheric carbon dioxide from fossil plant cuticles. *Nature* 411, 287-290.

RIDGWELL, A.J. (2003) Implications of the glacial CO_2 "iron hypothesis" for Quaternary climate change. *Geochemistry Geophysics Geosystems* 4, 1076.

RIDGWELL, A.J. (2005) Changes in the mode of carbonate deposition: implications for Phanerozoic ocean chemistry. *Marine Geology* 217, 339-357.

RIDGWELL, A.J., ZEEBE, R.E. (2005) The role of the global carbonate cycle in the regulation and evolution of the Earth system. *Earth and Planetary Science Letters* 234, 299-315.

RIDGWELL, A.J., WATSON, A.J., MASLIN, M.A., KAPLAN, J.O. (2003) Implications of coral reef buildup for the controls on atmospheric CO_2 since the Last Glacial Maximum. *Paleoceanography* 18, 1083.

RIDING, R., LIANG, L. (2005a) Geobiology of microbial carbonates: metazoan and seawater saturation state influences on secular trends during the Phanerozoic. *Palaeogeography, Palaeoclimatology, Palaeoecology* 219, 101-115.

RIDING, R., LIANG, L. (2005b) Seawater chemistry control of marine limestone accumulation over the past 550 million years. *Revista Española de Micropaleontología* 37, 1-11.

RIEBESELL, U., TORTELL, P.D. (2011) Effects of ocean acidification on pelagic organisms and ecosystems. In: Gattuso, J.-P., Hansson, L. (Eds.) Ocean acidification. Oxford University Press, New York, pp. 99-121.

RIES, J.B. (2004) Effect of ambient Mg/Ca ratio on Mg fractionation in calcareous marine invertebrates: A record of the oceanic Mg/Ca ratio over the Phanerozoic. *Geology* 32, 981-984.

RIES, J.B. (2009) Review: the effects of secular variation in seawater Mg/Ca on marine biocalcification. *Biogeosciences Discussion* 6, 7325-7452.

RIES, J.B. (2011) Skeletal mineralogy in a high-CO_2 world. *Journal of Experimental Marine Biology and Ecology* 403, 54-64.

RIES, J.B., STANLEY, S.M., HARDIE, L.A. (2006) Scleractinian corals produce calcite, and grow more slowly, in artificial Cretaceous seawater. *Geology* 34, 525-528.

RIES, J.B., COHEN, A.L., MCCORKLE, D.C. (2009) Marine calcifiers exhibit mixed responses to CO_2-induced ocean acidification. *Geology* 37, 1131-1134.

RISTVET, B.L. (1971) Reverse weathering reactions within recent nearshore marine sediments, Kaneohe Bay, Hawaii. Test Directorate Field Command, Kirtland Air Force Base, New Mexico, 314 pp.

ROBERTS, J.A., BENNETT, P.C., GONZALEZ, L.A., MACPHERSON, G.L., MILLIKEN, K.L. (2004) Microbial precipitation of dolomite in methanogenic groundwater. *Geology* 32, 277-280.

ROBIE, R.A., HEMINGWAY, B.S., FISHER, J.R. (1979) Thermodynamic properties of minerals and related substances at 298.15 K and 1 bar (10^5 Pascals) pressure and at higher temperatures. *U.S. Geological Survey Bulletin* 1452, pp. 456.

RONOV, A.B. (1980) Sedimentary Cover of the Earth. Nauka, Moscow.

ROYER, D.L. (2006) CO_2-forced climate thresholds during the Phanerozoic. *Geochimica et Cosmochimica Acta* 70, 5665-5675.

ROYER, D.L., BERNER, R.A., BEERLING, D.J. (2001) Phanerozoic atmospheric CO_2 change: evaluating geochemical and paleobiological approaches. *Earth Science Reviews* 54, 349-392.

ROYER, D.L., BERNER, R.A., MONTANEZ, I.P., TABOR, N.J., BEERLING, D.J. (2004) CO_2 as a primary driver of Phanerozoic climate. *GSA Today* 14, 4-10.

RUBEY, W.W. (1951) Geologic history of sea water: an attempt to state the problem. *Geological Society of America Bulletin* 62, 1111-1148.

RUDDIMAN, W.F. (2003) The anthropogenic greenhouse era began thousands of years ago. *Climatic Change* 61, 261-293.

RUNNEGAR, B., BENGTSON, S. (1990) Origin of hard parts-early skeletal fossils. In: Briggs, D.E.G., Crowther, P.R. (Eds.) Palaeobiology: A Synthesis. Blackwell Scientific Publications, pp. 24-29.

SABINE, C.L., MACKENZIE, F.T. (1995) Bank-derived carbonate sediment transport and dissolution in the Hawaiian Archipelago. *Aquatic Geochemistry* 1, 189-230.

SANDBERG, P.A. (1975) New interpretation of Great Salt Lake ooids and of ancient non-skeletal carbonate moneralogy. *Sedimentology* 22, 497-538.

SANDBERG, P.A. (1983) An oscillating trend in Phanerozoic non-skeletal carbonate mineralogy. *Nature* 305, 19-22.

SANDBERG, P.A. (1985a) Aragonite cements and their occurrence in ancient limestones. In: Schneidermann, N., Harris, P.M. (Eds.) Society of Economic Paleontologists and Mineralogists Special Publication 36, pp. 33-57.

SANDBERG, P.A. (1985b) Nonskeletal aragonite and pCO_2 in the Phanerozoic and Proterozoic. In: Sunquist, E.T., Broecker, W.S. (Eds.) The Carbon Cycle and Atmospheric CO_2: Natural Variations Archean to Present. AGU Monograph 32, Washington, DC., pp. 585-594.

SCHLAGER, W., JAMES, N. (1978) Low-magnesian calcite limestones forming at the deep-sea floor, Tongue of the Ocean, Bahamas. *Sedimentology* 25, 675-702.

SCHMALZ, R.F. (1967) Kinetics and diagenesis of carbonate sediments. *Journal of Sedimentary Petrology* 37, 60-67.

Scoffin, T.P., Tudhope, A.W., Brown, B.E., Chansang, H., Cheeney, R.F. (1992) Patterns and possible environmental controls of skeletogenesis of *Porites lutea*, South Thailand. *Coral Reefs* 11, 1-11.

Semesi, I.S., Beer, S., Björk, M. (2009) Seagrass photosynthesis controls rates of calcification and photosynthesis of calcareous macroalgae in a tropical seagrass meadow. *Marine Ecology Progress Series* 382, 41-47.

Shields, G., Veizer, J. (2002) Precambrian marine carbonate isotope database: Version 1.1. *Geochemistry, Geophysics, Geosystems* 3, 1-12.

Siegenthaler, U., Stocker, T.F., Monnin, E., Lüthi, D., Schwander, J., Stauffer, B., Raynaud, D., Barnola, J.-M., Fischer, H., Masson-Delmotte, V., Jouzel, J. (2005) Stable carbon cycle-climate relationship during the Late Pleistocene. *Science* 310, 1313-1317.

Sigman, D.M., Boyle, E.A. (2000) Glacial/interglacial variations in atmospheric carbon dioxide. *Nature* 407, 859-869.

Sillén, L.G. (1967) Gibbs phase rule and marine sediments. In: Gould, R.F. (Ed.) Equilibrium Concepts in Natural Water Systems. American Chemical Society, Washington, D.C., pp. 57-69.

Silverman, J., Lazar, B., Cao, L., Caldeira, K., Erez, J. (2009) Coral reefs may start dissolving when atmospheric CO_2 doubles. *Geophysical Research Letters* 36, L05606.

Simkiss, K. (1964) Variation in the crystallization form of calcium carbonate from artificial sea water. *Nature* 201, 492-493.

Sjöberg, E.L., Rickard, D.T. (1984) Temperature dependence of calcite dissolution kinetics between 1 and 62°C at pH 2.7 to 8.4 in aqueous solutions. *Geochimica et Cosmochimica Acta* 48, 485-493.

Smith, S.V. (2013) Parsing the Oceanic Calcium Carbonate Cycle: A Net Atmospheric Carbon Dioxide Source, or a Sink., L&O e-Books, *Association for the Sciences of Limnology and Oceanography (ASLO)*, Waco,TX, 10.4319/svsmith.2013.978-0-9845591-2-1.

Smith, S.V., Kinsey, D.W. (1976) Calcium-carbonate production, coral-reef growth, and sea-level change. *Science* 194, 937-939.

Smith, S.V., Buddemeier, R.W. (1992) Global change and coral reef ecosystems. *Annual Review of Ecology and Systematics* 23, 89-118.

Smith, S.V., Veeh, H.H. (1989) Mass balance of biogeochemically active materials (C,N,P) in a hypersaline gulf. *Estuarine Coastal and Shelf Science* 29, 195-215.

Smith, T.M., Peterson, T.C., Lawrimore, J.H., Reynolds, R.W. (2005) New surface temperature analyses for climate monitoring. *Geophysical Research Letters* 32.

Sorby, H.C. (1879) The structure and origin of limestone. *Proceedings of the Geological Society of London* 35, 56-59.

Speer, J.A. (1983). Crystal chemistry and phase relations of orthrombic carbonates. In: Reeder, R.J. (Ed.) Carbonates: Mineralogy and Chemistry. Mineralogical Society of America. pp. 249-540.

Spencer, R., Hardie, L. (1990) Control of seawater composition by mixing of river waters and mid-ocean ridge hydrothermal brines. *Fluid-mineral interactions: A tribute to HP Eugster: Geochemical Society Special Publication* 19, 409-419.

Stanley, S.M. (2006) Influence of seawater chemistry on biomineralization throughout Phanerozoic time: paleontological and experimental evidence. *Palaeogeography, Palaeoclimatology, Palaeoecology* 232, 214-236.

Stanley, S.M., Hardie, L.A. (1998) Secular oscillations in the carbonate mineralogy of reef-building and sediment-producing organisms driven by tectonically forced shifts in seawater chemistry. *Palaeogeography, Palaeoclimatology, Palaeoecology* 144, 3-19.

Stanley, S.M., Hardie, L.A. (1999) Hypercalcification: paleontology links plate tectonics and geochemistry to sedimentology. *GSA Today* 9, 1-7.

Stanley, S.M., Ries, J.B., Hardie, L.A. (2002) Low-magnesium calcite produced by coralline algae in seawater of Late Cretaceous composition. *Proceedings of the National Academy of Sciences* 99, 15323-15326.

Stanley, S.M., Ries, J.B., Hardie, L.A. (2005) Seawater chemistry, coccolithophore population growth, and the origin of Cretaceous chalk. *Geology* 33, 593-596.

Stein, C.L., Krumhansl, J.L. (1988) A model for the evolution of brines in salt from the lower Salado Formation, southeastern New Mexico. *Geochimica et Cosmochimica Acta* 52, 1037-1046.

Steuber, T., Veizer, J. (2002) Phanerozoic record of plate tectonic control of seawater chemistry and carbonate sedimentation. *Geology* 30, 1123-1126.

Stoffyn, M., Mackenzie, F.T. (1982) Fate of dissolved aluminum in the ocean. *Marine Chemistry* 11, 105-127.

Stolarski, J., Meibom, A., Przeniosło, R., Mazur, M. (2007) A Cretaceous Scleractinian coral with a calcitic skeleton. *Science* 318, 92-94.

Suzuki, A., Nakamori, T., Kayanne, H. (1995) The mechanism of production enhancement in coral-reef carbonate systems: model and empirical results. *Sedimentary Geology* 99, 259-280.

Taft, W.H., Harbaugh, J.W. (1964) Modern Carbonate Sediments of Southern Florida, Bahamas, and Espíritu Santo Island, Baja California: A Comparison of Their Mineralogy and Chemistry, Volume 8. Stanford University Press, Palo Alto, CA.

Takahashi, T., Sutherland, S.C., Sweeney, C., Poisson, A., Metzl, N., Tilbrook, B., Bates, N., Wanninkhof, R., Feely, R.A., Sabine, C., Olafsson, J., Nojiri, Y. (2002) Global sea-air CO_2 flux based on climatological surface ocean pCO_2, and seasonal biological and temperature effects. *Deep Sea Research Part II: Topical Studies in Oceanography* 49, 1601-1622.

Tan, F.C. (1988) Stable carbon isotopes in dissolved inorganic carbon in marine and estuarine environments. In: Fritz, P., Fontes, J. C. (Eds.) Handbook of Environmental Isotope Geochemistry, volume 3, The Marine Environment. Elsevier, Amsterdam, pp. 171-190.

Thompson, G. (1983) Basalt-seawater interaction. In: Rona, P.A., Bostrom, K., Laubjer, L., Smith, K.L. (Eds.) Hydrothermal Processes at Seafloor Spreading Centers. Plenum Press, New York, pp. 225-278.

Thorstenson, D.C., Plummer, L.N. (1977) Equilibrium criteria for two-component solids reacting with fixed composition in an aqueous phase- Example: the magnesian calcites. *American Journal of Science* 277, 1203-1223.

Thorstenson, D.C., Plummer, L.N. (1978) Equilibrium criteria for two-component solids reacting with fixed composition in an aqueous phase- Example: the magnesian calcites; reply. *American Journal of Science* 278, 1478-1488.

Timofeeff, M.N., Lowenstein, T.K., Da Silva, M.A.M., Harris, N.B. (2006) Secular variation in the major-ion chemistry of seawater: evidence from fluid inclusions in Cretaceous halites. *Geochimica et Cosmochimica Acta* 70, 1977-1994.

Tribble, J.S., Mackenzie, F.T. (1998) Recrystallization of magnesian calcite overgrowths on calcite seeds suspended in seawater. *Aquatic Geochemistry* 4, 337-360.

Tribble, J.S., Arvidson, R.S., Lane III, M., Mackenzie, F.T. (1995) Crystal chemistry, and thermodynamic and kinetic properties of calcite, dolomite, apatite, and biogenic silica: applications to petrologic problems. *Sedimentary Geology* 95, 11-37.

Tribollet, A., Godinot, C., Atkinson, M., Langdon, C. (2009) Effects of elevated pCO_2 on dissolution of coral carbonates by microbial euendoliths. *Global Biogeochemical Cycles* 23, GB3008.

Tynan, S., Opdyke, B.N. (2011) Effects of lower surface ocean pH upon the stability of shallow water carbonate sediments. *Science of The Total Environment* 409, 1082-1086.

Tyrrell, T., Zeebe, R.E. (2004) History of carbonate ion concentration over the last 100 million years. *Geochimica et Cosmochimica Acta* 68, 3521-3530.

Vail, P.R., Mitchum, R.W., Thompson, S. (1977) Seismic stratigraphy and global changes of sea level, part 3: relative changes of sea level from coastal onlap. In: Payton, C. E. (Ed.) Seismic Stratigraphy Applications to Hydrocarbon Exploration. AAPG Memoir 26, pp. 63-82.

Vasconcelos, C., McKenzie, J.A. (1997) Microbial mediation of modern dolomite precipitation and diagenesis under anoxic conditions (Lagoa Vermelha, Rio de Janeiro, Brazil). *Journal of Sedimentary Research* 67, 378-390.

Vecsei, A., Berger, W.H. (2004) Increase of atmospheric CO_2 during deglaciation: constraints on the coral reef hypothesis from patterns of deposition. *Global Biogeochemical Cycles* 18, GB1035.

VEIZER, J. (1995) Reply to the Comment by L. S. Land on "Oxygen and carbon isotopic composition of Ordovician brachiopods: implications for coeval seawater". *Geochimica et Cosmochimica Acta* 59, 2845-2846.

VEIZER, J., MACKENZIE, F.T. (2004) Evolution of sedimentary rocks. In: Mackenzie, F.T. (Ed.) Sediments, Diagenesis and Sedimentary Rocks. Elsevier-Pergamon, Oxford, pp. 369-407 (also 2013 edition of the Treatise on Geochemistry).

VEIZER, J., MACKENZIE, F.T. (2013) Evolution of sedimentary rocks. In: Mackenzie, F.T. (Ed.) Treatise in Geochemistry, Volume 9. Elsevier, New York.

VEIZER, J., ALA, D., AZMY, K., BRUCKSCHEN, P., BUHL, D., BRUHN, F., CARDEN, G.A.F., DIENER, A., EBNETH, S., GODDERIS, Y., JASPER, T., KORTE, C., PAWELLEK, F., PODLAHA, O.G., STRAUSS, H. (1999) $^{87}Sr/^{86}Sr$, $\delta^{13}C$ and $\delta^{18}O$ evolution of Phanerozoic seawater. *Chemical Geology* 161, 59-88.

VER, L.M.B., MACKENZIE, F.T., LERMAN, A. (1999) Biogeochemical responses of the carbon cycle to natural and human perturbations: past, present, and future. *American Journal of Science* 299, 762-801.

VIDETICH, P.E. (1985) Electron microprobe study of Mg distribution in recent Mg calcites and recrystallized equivalents from the Pleistocene and Tertiary. *Journal of Sedimentary Research* 55, 421-429.

VÖRÖSMARTY, C., LETTENMAIER, D., LEVEQUE, C., MEYBECK, M., PAHL-WOSTL, C., ALCAMO, J., COSGROVE, W., GRASSL, H., HOFF, H., KABAT, P., LANSIGAN, F., LAWFORD, R., NAIMAN, R. (2004) Humans transforming the global water system. *Eos Transactions AGU* 85, 509-514.

WALLMANN, K. (2001) The geological water cycle and the evolution of marine $\delta^{18}O$ values. *Geochimica et Cosmochimica Acta* 65, 2469-2485.

WALSH, J.J. (1991) Importance of continental margins in the marine biogeochemical cycling of carbon and nitrogen. *Nature* 350, 53-55.

WALTER, L.M. (1985) Relative reactivity of skeletal carbonates during dissolution: implications for diagenesis. In: Schneidermann, N., Harris, P.M. (Eds.) Carbonate Sediments. Society of Economic Paleontologists and Mineralogists, Tulsa, OK, pp. 3-16.

WALTER, L.M. (1986) Relative efficiency of carbonate dissolution and precipitation during diagenesis: a progress report on the role of solution chemistry. In: Gautier, D.L. (Ed) Roles of Organic Matter in Mineral Diagenesis. SEPM Special Publication 38, pp. 1-12.

WALTER, L.M., MORSE, J.W. (1984) Reactive surface area of skeletal carbonates during dissolution: effect of grain size. *Journal of Sedimentary Research* 54, 1081-1090.

WALTER, L.M., MORSE, J.W. (1985) The dissolution kinetics of shallow marine carbonates in seawater: a laboratory study. *Geochimica et Cosmochimica Acta* 49, 1503-1513.

WALTER, L.M., BURTON, E.A. (1986) The effect of ortho-phosphate on carbonate mineral dissolution rates in seawater. *Chemical Geology* 56, 313-323.

WALTER, L.M., BURTON, E.A. (1990) Dissolution of recent platform carbonate sediments in marine pore fluids. *American Journal of Science* 290, 601-643.

WALTER, L.M., BISCHOF, S.A., PATTERSON, W.P., LYONS, T.W., O'NIONS, R.K., GRUSZCZYNSKI, M., SELLWOOD, B.W., COLEMAN, M.L. (1993) Dissolution and recrystallization in modern shelf carbonates: evidence from pore water and solid phase chemistry [and discussion]. *Philosophical Transactions of the Royal Society of London. Series A: Physical and Engineering Sciences* 344, 27-36.

WALTER, L.M., KU, T.C.W., MUEHLENBACHS, K., PATTERSON, W.P., BONNELL, L. (2007) Controls on the $\delta^{13}C$ of dissolved inorganic carbon in marine pore waters: an integrated case study of isotope exchange during syndepositional recrystallization of biogenic carbonate sediments (South Florida Platform, USA). *Deep Sea Research Part II: Topical Studies in Oceanography* 54, 1163-1200.

WARTHMANN, R., VAN LITH, Y., VASCONCELOS, C., MCKENZIE, J.A., KARPOFF, A.M. (2000) Bacterially induced dolomite precipitation in anoxic culture experiments. *Geology* 28, 1091-1094.

WEYL, P.K. (1965) The solution behavior of carbonate minerals in sea water. *EPR Publication* 428, 1-59.

WHITE, A.F. (1977) Sodium and potassium coprecipitation in aragonite. *Geochimica et Cosmochimica Acta* 541, 613-625.

WHITE, A.F. (1978) Sodium coprecipitation in calcite and olomite. *Chemical Geology* 23, 65-72.

WILKINSON, B.H. (1979) Biomineralization, paleoceanography, and the evolution of calcareous marine organisms. *Geology* 7, 524-527.

WILKINSON, B.H., GIVEN, R.K. (1986) Secular variation in abiotic marine carbonates: constraints on Phanerozoic atmospheric carbon dioxide contents and oceanic Mg/Ca ratios. *The Journal of Geology* 94, 321-333.

WILKINSON, B.H., ALGEO, T.J. (1989) Sedimentary carbonate record of calcium-magnesium cycling. *American Journal of Science* 289, 1158-1194.

WILKINSON, B.H., WALKER, J.C.G. (1989) Phanerozoic cycling of sedimentary carbonate. *American Journal of Science* 289, 525-548.

WILKINSON, B.H., BUCZYNSKI, C., OWEN, R.M. (1984) Chemical control of carbonate phases: implications from Upper Pennsylvanian calcite-aragonite ooids of southeastern Kansas. *Journal of Sedimentary Research* 54, 932-947.

WILKINSON, B.H., OWEN, R.M., CARROLL, A.R. (1985) Submarine hydrothermal weathering, global eustasy, and carbonate polymorphism in Phanerozoic marine oolites. *Journal of Sedimentary Research* 55, 171-183.

WILKINSON, C. (2008) Status of Coral Reefs of the World: 2008. Global Coral Reef Monitoring Network & Reef and Rainforest Research Centre, Townsville.

WILLIS, J.K., ROEMMICH, D., CORNUELLE, B. (2004) Interannual variability in upper ocean heat content, temperature, and thermosteric expansion on global scales. *Journal of Geophysical Research-Oceans* 109, C12036.

WILSON, P.A., DICKSON, J.A.D. (1996) Radiaxial calcite: alteration product of and petrographic proxy for magnesian calcite marine cement. *Geology* 24, 945-948.

WISSHAK, M., SCHOENBERG, C.H.L., FORM, A., FREIWALD, A. (2012) Ocean acidification accelerates reef bioerosion. *PLoS ONE* 7, E45124.

WOLLAST, R. (1971) Kinetic aspects of the nucleation and growth of calcite from aqueous solutions. In: Bricker, O.P. (Ed.) Carbonate Cements. John Hopkins University Press, Baltimore, MD, pp. 264-273.

WOLLAST, R. (1998) Evaluation and comparison of the global carbon cycle in the coastal zone and in the open ocean. In: Brink, K., Robinson, A.R. (Eds.) The Sea: Ideas and Observations on Progress in the Study of the Seas. Wiley & Sons, New York, pp. 213-252.

WOLLAST, R., MACKENZIE, F.T. (1983) Global cycle of silica. In: Aston, S.R. (Ed.) Silicon Geochemistry and Biogeochemistry. Academic Press, pp. 39-76.

YAMAMOTO, S., KAYANNE, H., TERAI, M., WATANABE, A., KATO, K., NEGISHI, A., NOZAKI, K. (2012) Threshold of carbonate saturation state determined by CO_2 control experiment. *Biogeosciences* 9, 1441-1450.

YAPP, C.J., POTHS, H. (1992) Ancient atmospheric CO_2 pressures inferred from natural goethites. *Nature* 355, 342-344.

YATES, K.K., HALLEY, R.B. (2006a) CO_2^{-3} concentration and pCO_2 thresholds for calcification and dissolution on the Molokai reef flat, Hawaii. *Biogeosciences Discussions* 3, 123-154.

YATES, K.K., HALLEY, R.B. (2006b) Diurnal variation in rates of calcification and carbonate sediment dissolution in Florida Bay. *Estuaries and Coasts* 29, 24-39.

ZEEBE, R.E. (1999) An explanation of the effect of seawater carbonate concentration on foraminiferal oxygen isotopes. *Geochimica et Cosmochimica Acta* 63, 2001-2007.

ZEEBE, R.E. (2001) Seawater pH and isotopic paleotemperatures of Cretaceous oceans. *Palaeogeography, Palaeoclimatology, Palaeoecology* 170, 49-57.

ZEEBE, R. (2012a) LOSCAR: Long-term ocean-atmosphere-sediment carbon cycle reservoir model v2. 0.4. *Geoscientific Model Development* 5, 149-166.

ZEEBE, R. (2012b) History of seawater carbonate chemistry: Atmospheric CO_2, and ocean acidification. *Annual Review of Earth and Planetary Sciences* 40, 141-165.

ZEEBE, R.E., WOLF-GLADROW, D. (2001) CO_2 in Seawater - Equilibrium, Kinetics, Isotopes. Elsevier, Amsterdam.

ZEEBE, R.E., RIDGWELL, A. (2011) Past changes of ocean carbonate chemistry. In: Gattuso, J.-P., Hansson, L. (Eds.) Ocean Acidification. Oxford University Press, New York, pp. 21-40.

ZHONG, S., MUCCI, A. (1989) Calcite and aragonite precipitation from seawater solutions of various salinities: precipitation rates and overgrowth compositions. *Chemical Geology* 78, 283-299.

SUPPLEMENTARY INFORMATION

SI-1

Sedimentary Carbonate Minerals and Stability

Exploration of the evolution of atmospheric CO_2 and the seawater CO_2-carbonic acid-carbonate system during the Phanerozoic Eon requires some information on the fundamental properties of the carbonate minerals. In this section we consider the mineralogy and chemistry of the solid carbonate phases and their stability relationships. Much of this section and others in the Supplementary Information sections of this monograph is derived from the books *Geochemistry of Sedimentary Carbonates* by Morse and Mackenzie (1990) and *Carbon in the Geobiosphere—Earth's Outer Shell* by Mackenzie and Lerman (2006) and based extensively on papers by Mackenzie and colleagues.

Sediments and sedimentary rocks contain a variety of carbonate minerals. Table SI-1.1 lists the various carbonate minerals found in nature and some of their properties. Despite the variety of carbonate mineral species, calcite (trigonal crystal system) and dolomite, (trigonal crystal system) are by far the most abundant carbonate minerals in ancient sedimentary rocks (Fig. SI-1.1). Preserved aragonite ($CaCO_3$, orthorhombic

crystal system) is rare in rocks older than Cenozoic and other carbonate minerals are largely confined to special deposits, such as evaporite sediments, iron formation deposits, or are present as minor minerals, such as ankerite [$CaFe(CO_3)_2$], in other sedimentary deposits. Calcitic and dolomitic sedimentary rocks constitute 10% to 15% of the mass of sedimentary rocks and approximately 30% of the sedimentary rock mass younger than 545 Ma (the Phanerozoic Eon). Carbonate rocks are important reservoirs of oil and gas and contain commercial ore bodies, and of importance to this article, contain valuable information, in the form of biological, chemical, mineralogical, and isotopic signatures, concerning the evolution of the Earth's exogenic system and ecosphere.

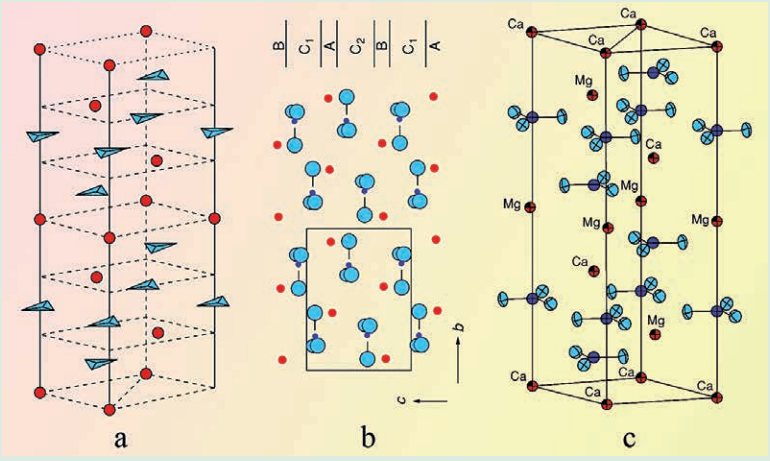

Figure SI-1.1 Structure of **(a)** calcite, trigonal $CaCO_3$; **(b)** aragonite, orthorhombic $CaCO_3$; and **(c)** dolomite, trigonal $(CaMg(CO_3)_2$. The arrangement of carbonate anion groups (triangular shapes) and the atoms of Ca and Mg (small open or filled circles) are shown within the mineral structures. In **(a)** and **(c)**, the c-axis of the minerals is perpendicular to the planes of the carbonate anion groups and Ca and Mg cations (after Mackenzie and Lerman, 2006).

There are three major polymorphs (minerals of the same chemical composition but different crystal structure) of $CaCO_3$ that occur in sediments and in the structures of organisms. The rhombohedral mineral calcite is the most abundant and is thermodynamically stable near the Earth's surface. Aragonite, the orthorhombic form, is also abundant but found primarily in younger sediments of Cenozoic age and the skeletal structures of marine organisms. Aragonite has a density greater than that of calcite

Table SI-1.1 Various carbonate minerals found in nature and their properties including the formula weight, density, crystallographic system, the Gibbs free energy of formation in joules per mol, and various estimates of the solubility (Ksp) of the phase as pKsp = -log Ksp (table modified from Morse and Mackenzie, 1990).

Mineral	Formula	Formula wt ($g\ mol^{-1}$)	Density ($g\ cm^{-3}$)	Crystal System	Gf,298 ($J\ mol^{-1}$)	Various estimates of $-\log K_{sp}$
Calcite	$CaCO_3$	100.09	2.71	Trig.	–1128842	8.30, 8.35, 8.48, 8.46
Aragonite	$CaCO_3$	100.09	2.93	Ortho.	–1127793	8.12, 8.22, 8.34, 8.30
Vaterite	$CaCO_3$	100.09	2.54	Hex.	–1125540	7.73, 7.91
Monohydrocalcite	$CaCO_3 \cdot H_2O$	118.10	2.43	Hex.	–1361600	7.54, 7.60
Ikaite	$CaCO_3 \cdot 6H_2O$	208.18	1.77	Mono.	—	7.12
Magnesite	$MgCO_3$	84.32	2.96	Trig.	–1723746	8.20, 7.46, 5.10, 8.10
Nesquehonite	$MgCO_3 \cdot 3H_2O$	138.36	1.83	Trig.	–1723746	5.19, 4.67
Artinite	$Mg2CO_3(OH)_2 \cdot 3H_2O$	196.68	2.04	Mono.	–2568346	18.36
Hydromagnesite	$Mg4(CO_3)_3(OH)_2 \cdot 3H_2O$	359.27	—	Mono.	–4637127	36.47, 30.6
Dolomite	$CaMg(CO_3)_2$	184.40	2.87	Trig.	–2161672	17.09
Huntite	$CaMg3(CO_3)_4$	353.03	2.88	Trig.	–4203425	30.46
Strontianite	$SrCO_3$	147.63	3.70	Ortho.	–1137645	8.81, 9.03, 9.13, 9.27
Witherite	$BaCO_3$	197.35	4.43	Ortho.	–1132210	7.63, 8.30, 8.56
Barytocalcite	$CaBa(CO_3)_2$	297.44	—	Trig.	–2271494	17.68
Rhodochrosite	$MnCO_3$	114.95	3.13	Trig.	–816047	10.54, 9.30, 10.59
Kutnohorite	$CaMn(CO_3)_3$	215.04	—	Trig.	–195058	55.79
Siderite	$FeCO_2$	115.85	3.80	Trig.	–666698	10.50, 10.68, 10.91
Cobaltocalcite	$CoCO_3$	118.94	4.13	Trig.	–650026	11.87, 9.68
—	$CuCO_3$	123.56	—	Trig.	—	9.63, 11.51

Mineral	Formula	Formula wt ($g\ mol^{-1}$)	Density ($g\ cm^{-3}$)	Crystal System	Gf,298 ($J\ mol^{-1}$)	Various estimates of $-\log K_{sp}$
Gaspeite	$NiCO_3$	118.72	—	Trig.	–613793	7.06, 6.87
Smithsonite	$ZnCO_3$	125.39	4.40	Trig.	–731480	9.87, 10.00
Otavite	$CdCO_3$	172.41	4.26	Trig.	–669440	11.21, 13.74
Cerussite	$PbCO_3$	267.20	6.60	Ortho.	–625337	12.80, 13.13, 12.15
Malachite	$Cu2CO_3(OH)_2$	221.11	4.00	Mono.	—	33.78, 33.46
Azurite	$Cu3(CO_3)2(OH)_2$	344.65	3.88	Mono.	—	45.96
Ankerite	$CaFe(CO_3)_2$	215.95	—	Trig.	–1815200	19.92
Natronite	$Na2CO_3 \cdot 1OH_2O$	285.99	—	Ortho.	–3428997	1.03
Thermonatrite	$Na2CO_3 \cdot H_2O$	124.00	—	Ortho.	–1286538	0.403, 0.54
Trona	$NaHCO_3 \cdot Na_2CO_3 \cdot 2H_2O$	229.00	2.25	Mono.	–2386554	2.07, 1.00
Nahcolite	$NaHCO_3$	84.01	2.16	Mono.	–851862	0.545, 0.39
Natron	$NaHCO_3 \cdot H_2O$	102.03	—	—	—	0.80

and hence is the $CaCO_3$ phase stable at higher pressure and temperature but unstable relative to calcite at low pressure and temperature. It is about 1.5 times more soluble than calcite at 25 °C and 1 atmosphere. Vaterite is the third anhydrous $CaCO_3$ phase, has a hexagonal structure, and is metastable relative to aragonite and calcite under the environmental conditions that characterise sediments and sedimentary rocks. It is approximately 3.7 times more soluble than calcite and 2.5 times more soluble than aragonite. It rarely is observed in natural systems but can be produced in the laboratory under experimental conditions that are designed to produce high precipitation rates of carbonate phases but converts relatively rapidly to calcite (Fig. SI-1.2). In addition to the anhydrous $CaCO_3$ minerals found in sediments, there are scarce occurrences of hydrated $CaCO_3$ minerals; an example is ikaite ($CaCO_3 \cdot 6H_2O$), which has been observed, *e.g.*, in Antarctic shelf sediments.

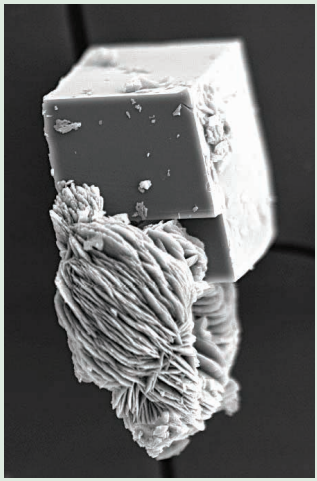

Image courtesy of John Morse.

Figure SI-1.2 Vaterite rose converting to a calcite rhomb in an experimental aqueous solution.

Dolomite, a 50:50 mol% mixture of $CaCO_3$ and $MgCO_3$, and calcite are the main carbonate phases that make up carbonate rocks. However, dolomite does not occur as a skeletal structural component of organisms as do calcite and aragonite. Even after years of study, the mode of formation of dolomite remains controversial. Its properties under the environmental conditions at and near the surface of the Earth are less well known than those of calcite and aragonite. This is partly a reflection of the fact that the synthesis of dolomite in low temperature laboratory experiments has proven to be difficult.

In contrast to much of the *preserved* rock record of carbonate sediments, which is dominated by calcite and dolomite, the carbonate mineral composition of modern skeletons and tests of organisms is quite variable (Table SI-1.2). The variability of biogenic carbonate minerals in composition and the microstructure of the carbonate edifice of the organism control both the stability of a $CaCO_3$ inorganic skeleton and its reactivity in natural aqueous solutions. Because of the predominant abundance of calcite and dolomite, and the lesser but important abundance of aragonite in the sedimentary rock record, in the next sections, we consider the stability of inorganic and skeletal $CaCO_3$ compositions. Their reactivity in aqueous solutions is discussed in Supplemental Information Section SI-2.

Table SI-1.2 Mineral composition of various groups of calcifying organisms, their trophic state, common name, and ecological habitat (after Mackenzie and Lerman, 2006).

Mineral[1]	Kingdom and Phylum[1],[2]	Trophic state or production mode[2]	Common name, ecological habitat[2], comments
	Bacteria (Monera)		
Calcite	Cyanobacteria	Photoautotrophs	Blue-green algae or bacteria
Aragonite	Cyanobacteria	Photoautotrophs	Blue-green algae or bacteria
	Pseudomands	Heterotrophs	Also classified as Protobacteria or purple bacteria
	Protoctista		
Calcite	Haptophyta	Photoautotrophs	Coccoliths, predominantly marine plankton
	Chlorophyta	Photoautotrophs	Green algae, marine and freshwater
	Rhodophyta	Photoautotrophs	Red or coralline algae, vast majority marine
	Rhizopoda	Heterotrophs	Amoebas, ocean and fresh water, soils
	Dinoflagellata	Some photoautotrophs, some heterotrophs	Mostly marine plankton
	Zoomastigina	Heterotrophs	Zooflagellates, largely fresh water
	Foraminifera	Heterotrophs	Marine plankton and benthos
	Ciliophora	Heterotrophs	Ciliates, marine and freshwater
	Myxomycota	Heterotrophs	Plasmodial slime molds
Aragonite	Haptophyta	Photoautotrophs	Coccoliths
	Chlorophyta	Photoautotrophs	Green algae, marine and freshwater
	Rhodophyta	Photoautotrophs	Red or coralline algae, vast majority marine
	Phaeophyta	Photoautotrophs	Brown algae, littoral and pelagic
	Foraminifera	Heterotrophs	Superfamily *Robertinacea*, benthonic
Vaterite	Rhodophyta	Photoautotrophs	In genus *Galaxaura*
	Fungi		
Calcite	Ascomycota	Heterotrophs	Lichens, formerly Mycophycophyta

Mineral[1]	Kingdom and Phylum[1],[2]	Trophic state or production mode[2]	Common name, ecological habitat[2], comments
	Plantae		
Calcite		Photoautotrophs	Mosses
			Ferns
	Angiospermophyta		Flowering plants, also classified as Anthophyta
Aragonite	Angiospermophyta		same
Vaterite	Angiospermophyta		same
	Animalia		
Calcite	Cnidaria	Heterotrophs	Tabulate and rugose corals (extinct); Octocorallia (except Helioporida)
	Porifera		Sponges, Calcarea (calcareous sponges)
	Platyhelminthes		Flat worms, freshwater, marine, soils
	Sipuncula		Peanut worms, mostly benthonic
	Annelida		Marine worms, Polychaeta, serpulid worms
	Ectoprocta		Bryozoans, mostly marine
	Arthropoda		Carapace and cuticle: Trilobitomorpha (trilobites, extinct), ostracods, barnacles (Cirripedia), Malacostraca
	Mollusca		Shells only: Bivalvia and Gastropoda (snails)
	Brachiopoda		Fossil and extant lamp shells
	Echinodermata		Plates, spicules, spines of Mg-calcite in all groups: sea urchins, sea stars, brittle starts (ophiuroids), sea lilies (crinoids), sea cucumbers (holothurians).
Aragonite	Cnidaria		Madreporian corals and groups Milliporina, Helioporida, Scleractinia
	Porifera		Sponges, Calcarea (calcareous sponges)
	Platyhelminthes		Flat worms, freshwater, marine, soils

Mineral[1]	Kingdom and Phylum[1],[2]	Trophic state or production mode[2]	Common name, ecological habitat[2], comments
	Annelida		Marine worms, Polychaeta, serpulid worms
	Ectoprocta		Bryozoans, mostly marine
	Mollusca		Shells only: Aplacophora, Monoplacophora, Polyplacophora, Bivalvia, Gastropoda (including planktonic Pteropoda), Cephalopoda
	Arthropoda		Cuticle in some Malacostraca, base plate in some barnacles
Vaterite	Platyhelminthes		Flat worms, freshwater, marine, soils

(1) Lowenstam (1986), Lowenstam and Weiner (1989), Mackenzie *et al.* (1983), Runnegar and Bengtson (1990).
(2) Margulis and Schwartz (1998).

Stability of the Calcites. Calcites constitute major and very important biogenic and inorganic constituents of modern marine sediments, Pleistocene, and older rocks as skeletal clasts and cements. They can contain up to 30 mol% $MgCO_3$, and higher Mg content phases have been produced in the laboratory and observed sparingly in nature. Calcites with more than a few percent $MgCO_3$ are usually referred to as magnesian calcites or magnesium calcites (Mg calcites). Generally, for the same $MgCO_3$ content, the biogenic calcites have greater concentrations of sodium, sulphate, water, hydroxide, and bicarbonate and tend to have larger cell volumes and greater carbonate anion and cation positional disorder in their structure than natural or synthetic inorganic phases. Chemical and microstructural heterogeneities especially characterise biogenic magnesian calcites, and dislocations and plane defects are common in their crystals. All of these characteristics may affect the thermodynamic and kinetic properties and reactivity of these phases in aqueous solution.

The solubilities of calcites depend on their $MgCO_3$ content, in addition to other chemical constituents and environmental parameters. The solubilities of calcites can be expressed as a function of their $MgCO_3$ content and the ion activity product (IAP) of a solution in equilibrium with the solid (Plummer and Mackenzie, 1974; Thorstenson and Plummer, 1977):

$$Ca_{1-x}Mg_xCO_3 = (1-x)Ca^{2+} + xMg^{2+} + CO_3^{2-} \qquad \text{(SI-1.1)}$$

$$IAP_{calcite} = K_{sp} = \{(Ca^{2+})^{1-x}(Mg^{2+})^{x}(CO_3^{2-})\}, \qquad \text{(SI-1.2)}$$

where curly brackets in the latter expression denote the *activities* of the ions in aqueous solution, x is the mole fraction of $MgCO_3$ in the solid, and K_{sp} is the solubility product. For pure calcite, the mole fraction of $MgCO_3$ is zero. The generalised trend in solubility with $MgCO_3$ content of these phases at 25 °C and 1 atmosphere total pressure appears reasonably well defined (Fig. SI-1.3) owing to the work of Plummer and Mackenzie (1974), Thorstenson and Plummer (1977), Walter and Morse (1984), Bischoff *et al.* (1987, 1993), and Busenberg and Plummer (1989). Bertram *et al.* (1991) have made preliminary estimates of the change in solubility with temperature demonstrating that as with pure calcite, the magnesian calcites have retrograde solubility (solubility decreases with increasing temperature).

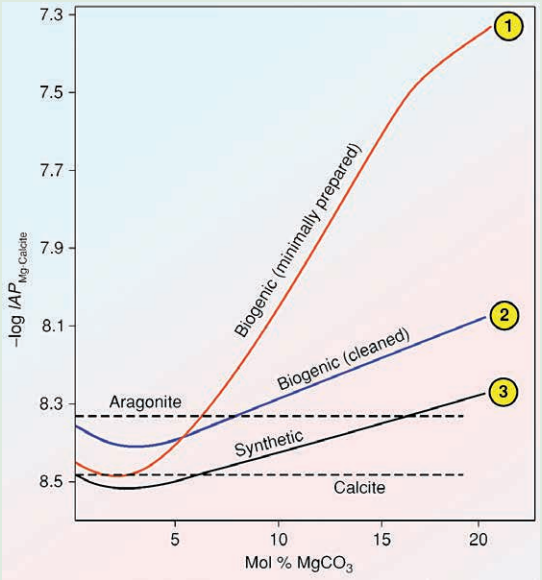

Figure SI-1.3 Solubility of the magnesian calcites as a function of the $MgCO_3$ in the phase. See text for further explanation (after Bischoff *et al.*, 1993).

The solubilities of the calcites expressed in terms of IAP exhibit a minimum around two mole percent $MgCO_3$, beyond which their solubility increases nearly linearly with increasing $MgCO_3$ content. The *thermodynamic solubility product*, which is only a function of pressure and temperature, of pure calcite at 25 °C and 1 atmosphere is about $10^{-8.46}$. There appear to be three recognisable trends in the solubility-composition data: one for inorganic solids that are well crystallised, compositionally homogeneous,

and chemically pure (Fig. SI-1.3, curve 3), and the other for biogenic phases and inorganic solids that exhibit substantial lattice defects, carbonate positional disorder, and substitution of such foreign ions as sulphate and sodium (Fig. SI-1.3, curve 2). The third solubility-composition curve is that of Plummer and Mackenzie (1974) for biogenic materials subjected to minimal cleaning procedures in the laboratory before use in dissolution experiments designed to determine the solubilities of these phases (Fig. SI-1.3, curve 1). This curve probably reflects primarily kinetic rather than thermodynamic factors, but it may be the curve that best reflects the effective solubility of the biogenic magnesian calcites in nature as a function of $MgCO_3$ content. Biogenic and some inorganic calcites are unstable in aqueous solutions relative to synthetic phases of similar $MgCO_3$ content. Their solubilities differ by roughly 0.15 pIAP units (pIAP = -log IAP), or about 4.6 kJ mol^{-1} (1.1 kcal mol^{-1}). This difference arises because of physical and chemical differences between the two types of solids. The complex microarchitecture, greater positional disorder of the CO_3^{2-} anion group, and chemical impurity of the biogenic phases and some inorganic calcites result in higher solubilities of these solids. It is likely that the solubility-composition curve 3 for pure, compositionally homogeneous, and structurally well-ordered calcite phases represents the true metastable equilibrium solubility of calcites in aqueous solution at 25 °C and 1 atmosphere.

Stability of Aragonite. The most abundant orthorhombic carbonate considered in this monograph is aragonite, the dimorph of calcite. At near Earth surface pressure and temperature, aragonite is found as the inorganic component of many common invertebrate skeletons (Table SI-1.2), as sediments derived from the physical and biological disintegration and erosion of these skeletons, as cements in modern marine sediments and Neogene limestones, in some carbonate cave deposits and travertine precipitated by hot springs, and often as a replacement mineral in igneous and metamorphic rocks and ore deposits (Speer, 1983). Although aragonite has larger cation sites, the phase is denser than calcite and hence is stable relative to calcite at elevated pressure and temperature (Fig. SI-1.4). The solubility product of aragonite at 25 °C and 1 atmosphere is about $10^{-8.30}$. Aragonites exhibit only limited solid solution, primarily with Pb and Sr. Plumbian aragonites with up to 2.5 mol% are common, and strontian aragonites occurring in hot springs may contain up to 14 mol% $SrCO_3$ (Speer, 1983). The limited solid solution of Sr is of importance because of the fact that the degree of solid solution varies among different groups of organisms having aragonitic shells, and the Sr content of some skeletal species has been used to obtain the Sr/Ca ratio or the temperature of the water from which the organism precipitated its skeleton. However, the Sr content is a function of the mechanism by which the organism precipitates its skeleton

and it varies from organism to organism producing a "species or vital effect", complicating the use of the Sr/Ca ratio as a means of predicting environmental conditions.

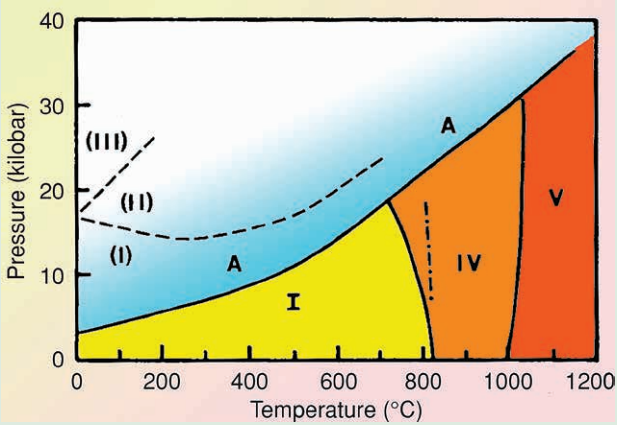

Figure SI-1.4 Stability fields of aragonite and different polymorphs of calcite as a function of temperature and pressure. A: aragonite; I through IV: calcite polymorphs with metastable fields shown by parentheses; dash-dot line at 800°C represents aragonite-calcite transition encountered on experimental cooling runs; solid line at lower temperature represents transition encountered on experimental heating runs (after Carlson, 1980).

Because aragonite is unstable relative to calcite at near Earth surface pressures and temperatures, with time and changes in environmental conditions, such as exposure to meteoric waters or burial in the subsurface, inorganic and biogenic aragonite can be converted to calcite or dolomite. Thus the original texture of the aragonite can be altered and the chemical and isotopic information contained in the phase lost. Rocks older than Neogene contain very little aragonite because of diagenetic reactions that lead to leaching of the components of the phase from the rock or its recrystallisation to another mineral. Scant aragonite has been found in rocks as old as Pennsylvanian in age. The recrystallisation process can lead to a loss of information concerning the environment of formation of a biogenic or inorganic aragonitic precipitate.

Stability of Dolomite. The mineral dolomite is a major constituent of especially ancient carbonate rocks. Dolomite is distinguished from calcite and the other rhombohedral carbonates by its stoichiometry. Ideal dolomite has equal numbers of Ca and Mg atoms, and the Ca and Mg are segregated in distinct lattice planes (Fig. SI-1.1). These planes are oriented

normal to the *c*-axis, each alternating with *c*-normal trigonal CO_3 groups that are also in essentially planar orientation. Dolomite was named in honour of Dieudonné Dolomieu (also known as Déodat Dolomieu), a geologist who worked in the Pyrenees and Alps in the eighteenth century and first described the mineral's characteristics and occurrence. For geologists dolomite has been the centre of an enduring debate regarding its mode of formation in surface environments, its past abundance relative to other sedimentary carbonates, and its overall significance in the geologic record (*e.g.*, Land, 1985; Machel and Mountjoy, 1986; Hardie, 1987; McKenzie, 1991; Mackenzie and Morse, 1992; McKenzie and Vasconcelos, 2009).

In terms of dolomite stability relationships, determination of the univariant temperature-CO_2 curve for the calcite-dolomite-magnesite system was made by Harker and Tuttle (1955a) at high to moderate temperatures and pressures. The order of decomposition with increasing temperature was shown to be magnesite, dolomite, and calcite. The location of the calcite-dolomite and dolomite-magnesite solvi along the $CaCO_3$-$MgCO_3$ binary join (Fig. SI-1.5) was established through the collective work of Harker and Tuttle (1955b), Graf and Goldsmith (1955), Graf and Goldsmith (1958), and Goldsmith and Heard (1961). The top of the calcite-dolomite solvus was located by Goldsmith and Heard (1961) at 1075 °C, giving a composition of $Ca_{0.57.5}Mg_{0.42.5}CO_3$, a slightly calcium-rich phase. Note in Figure SI-1.4 that the composition of calcite in terms of its Mg content at Earth's surface temperature and pressure in equilibrium with dolomite contains only a couple of mol% Mg in solid solution. All calcites containing more Mg than this are unstable relative to nearly pure calcite $CaCO_3$. Calcium-rich, somewhat disordered dolomite, protodolomite, is commonly found in younger sediments and with aging of the rock, progressively converts to a stochiometric dolomite with distinct ordering (Land, 1985).

Stability of Carbonate Minerals in Seawater. Since much of this monograph deals with ocean water, it is worth exploring the stabilities of the major carbonate minerals in a solution of seawater composition. Figure SI-1.6 shows equilibrium relationships at 25 °C and 1 atmosphere between stable (Fig. SI-1.6a) and metastable (Fig. SI-1.6b) important carbonate phases found in modern marine sediments and in sedimentary rocks. It is the case that in equatorial surface seawater of average composition, the ion activity products of the minerals calcite, aragonite, and an average magnesian calcite composition of 15 mol% $MgCO_3$ are all greater than their stoichiometric saturation constants (K_{sp}) and therefore theoretically could precipitate from surface seawater. As one moves poleward and surface seawater temperatures fall and the CO_2-carbonic acid system chemistry of surface seawater changes with increases in dissolved inorganic carbon (DIC), the saturation state (Ω) of the seawater with respect to all these minerals decreases, and the seawater may even become

undersaturated at high latitude with respect to the 15 mol% magnesian calcite phase (based on the Plummer and Mackenzie (1974) solubility curve, a 15 mol% Mg-calcite is in metastable equilibrium with tropical surface seawater; see Fig. 10.6). This assertion will depend on the choice of the stoichiometric saturation constant used in the saturation state calculation. With depth in the present-day oceans, seawater saturation with respect to aragonite, calcite, and dolomite, becomes progressively lower in that order, because of decreasing temperature and increasing pressure and CO_2 content with depth. Aragonite and calcite produced mainly biologically in surface seawater dissolve as the minerals transit the water column and in deep ocean basins below their respective carbonate compensation depths (CCD, the depth where dissolution rate equals sedimentation rate), they are no longer generally found in modern marine sediments. The aragonite compensation depth (ACD) is shallower than that of calcite (CCD) because of the former mineral's greater solubility.

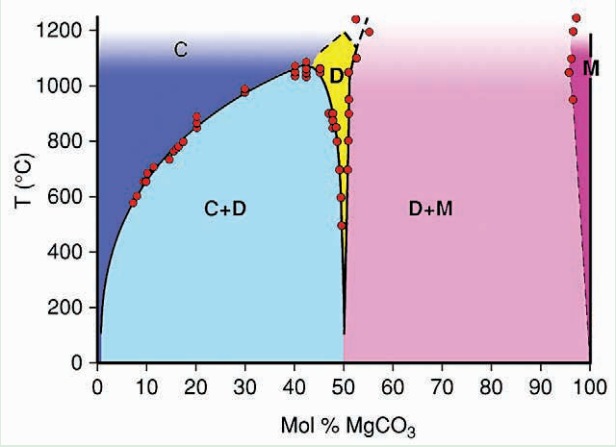

Figure SI-1.5 Subsolvus relationships for the $CaCO_3$-$MgCO_3$ join. The top of the calcite-dolomite immisibility gap occurs at 1075°C. At this temperature, the phase composition is $Ca_{57.5}Mg_{42.5}(CO_3)_2$. Dotted line represents limit of detectable ordering in the dolomite structure. C = calcite; M = magnesite; and D = dolomite [after Tribble *et al.*, 1995; data from Goldsmith and Graf (1958) and Goldsmith and Heard (1961)].

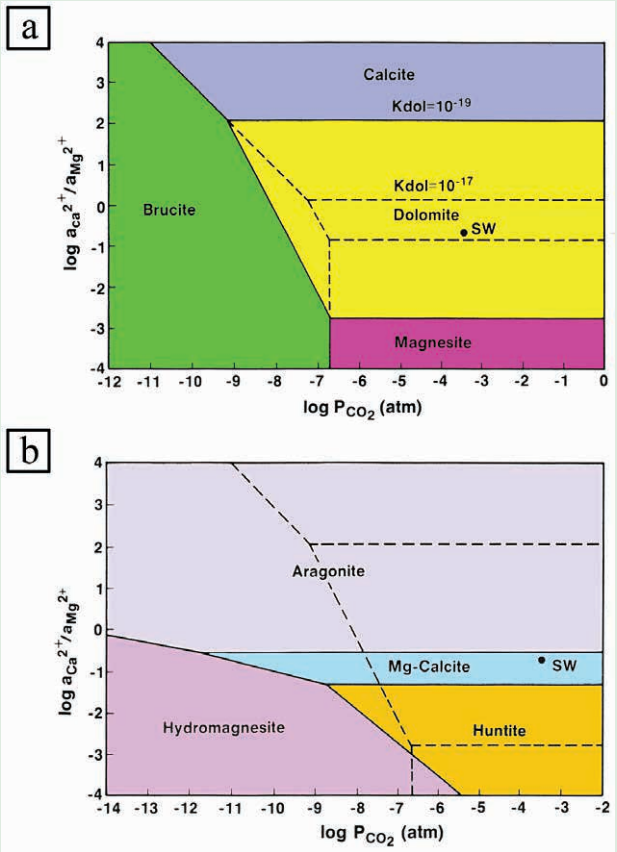

Figure SI-1.6 An equilibrium activity diagram illustrating phase relationships among calcium and magnesium carbonate minerals at 25 °C and 1 atmosphere total pressure as a function of the logarithm of the activity ratio of Ca^{2+}/Mg^{2+} ($a_{Ca}2+/a_{Mg}2+$) and logarithm of the partial pressure of CO_2 (P_{CO2}). **(a)** Equilibrium relationships among stable carbonate mineral phases showing two configurations: an expanded dolomite stability field consistent with an equilibrium constant for dolomite dissolution of 10^{-19} and a contracted field consistent with a constant equal to 10^{-17}. **(b)** Equilibrium relationships among metastable carbonate mineral phases; the magnesian calcite composition portrayed contains 15 mol% $MgCO_3$; dashed lines show calcite ($CaCO_3$), dolomite [$CaMg(CO_3)_2$], magnesite ($MgCO_3$), and brucite ($Mg(OH)_2$) phase relations as in **(a)**. The dark round circle represents the composition of average surface seawater (after Morse and Mackenzie, 1990).

Figure SI-1.6 also demonstrates that in solution of average seawater composition at 25 °C and 1 atmosphere, calcite, aragonite, and a 15 mol% magnesian calcite are all metastable with respect to dolomite and should convert spontaneously to this phase. The energy associated with this metastability depends, in part, on the choice of the free energy of formation value chosen for dolomite, whether one selects a value consistent with an equilibrium constant of dolomite dissolution of 10^{-17} (Robie *et al.*, 1979) or 10^{-19} (Garrels *et al.*, 1960). The phase boundaries shown in Figure SI-1.6 are calculated using both values. Whatever the case, it is likely that the lack of conversion of carbonate phases to dolomite, or the latter's precipitation, in the modern marine environment is due to kinetic factors, which still remain problematic and have been a major factor hindering the resolution of the long-standing controversy involving the "dolomite problem"—why the lack of dolomite in the modern marine sediment record but its abundance in ancient carbonate deposits?

SI-2

Carbonate Dissolution and Precipitation Kinetics

Carbonate minerals are chemically moderately reactive minerals under Earth surface conditions. They are not as "easy" to dissolve or precipitate as the simple salts of NaCl (halite) or $CaSO_4{\cdot}2H_2O$ (gypsum) or as "difficult" to dissolve or precipitate as the aluminosilicate minerals. An understanding of their reactivity (dissolution and precipitation) is important in consideration of a range of topics in geochemistry, including those addressed in this monograph. The vast majority of kinetic studies have focused on calcite and aragonite with less attention being given to the third most important carbonate mineral, dolomite, mainly because of its slow reactivity under low temperature and pressure conditions. In addition, most of the dissolution research has involved carbonate mineral reactions in dilute aqueous solutions. Furthermore, there are few kinetic studies of the calcites containing 4 or more mol% $MgCO_3$, the magnesian calcites, in any composition aqueous solution. The reader is referred to the recent paper of Arvidson and Morse (2013) for some new insights and promising new directions in research on carbonate mineral reactivity.

Dissolution of Carbonate Minerals. The most commonly used equation to describe the rate of carbonate mineral dissolution at constant pH is (e. g., Morse and Berner, 1972):

$$R = -dm_{(carbonate)}/dt = (kA/V)\ (1 - \Omega)^n \qquad \text{(SI-2.1)}$$

where R is the rate, m is number of moles of carbonate mineral, and t is time. A is the total surface area of the solid, V is the volume of solution, k is the rate constant, Ω is the ratio of the ion activity product (IAP) of the carbonate mineral to its solubility product (K_{sp}), and n is a positive constant known as the order of reaction. A, V, and k are often combined into a single constant $k^* = kA/V$. The ratio of $IAP/K_{sp} = \Omega$ is a measure of disequilibrium between the carbonate solid and solution; that is, a measure of the Gibbs free energy drive for dissolution (or precipitation). For undersaturation it must range from 0 to 1 and for supersaturation from 1 to higher values. It follows from equation (SI-2.1) that by taking the logarithm of both sides of the equation we have

$$\log R = n \log(1 - \Omega) + \log k^* \qquad \text{(SI-2.2)}$$

Thus a plot of log R vs. log (1-Ω) yields a straight line with the intercept log k* and the slope n. This equation and variations of it have been used to obtain n for calcite, aragonite, and dolomite.

Figure SI-2.1 is one example of experimental rate data for dissolution of the inorganic carbonate minerals aragonite, calcite, dolomite, magnesite, and witherite ($BaCO_3$) in which the rates have been determined over a range of pH in simple aqueous solutions. The experimental data were fit by equations of the *nature* of that for calcite:

$$R = k_1 a_{H+} + k_3 - k_6 m_{Ca}^{2+} m_{CO3}^{2-} \qquad \text{(SI-2.3)}$$

where k_1, k_3, and k_6 are rate constants that are temperature dependent. Aragonite and calcite have about the same rate of dissolution, whereas not surprisingly, dolomite and magnesite ($MgCO_3$) dissolve at rates one to three orders of magnitude slower. These results confirm the geological observations that dolomite is considerably less reactive than calcite or aragonite in nature. Notice that the rates decrease by two to three orders of magnitude from low pH values to high. Preliminary experiments on magnesian calcites show that the overall dissolution rate of calcites containing Mg is higher than that of pure calcite but bear similarities to calcite dissolution results (Bertram *et al.*, 1991).

One major conclusion that has been drawn from experiments of this nature is that an increase in the acidity (pH decrease) or an increase in the partial pressure of CO_2 or temperature of the environment will increase the rate of dissolution of carbonate minerals. Another conclusion mentioned above is that dolomite at Earth surface temperatures and pressures is difficult to dissolve, or for that matter, precipitate. In extremely dilute solutions,

the rate of dissolution of dolomite is 100 times slower that of calcite and aragonite. In addition, relatively low concentrations of HCO_3^- can almost completely inhibit dolomite dissolution far from equilibrium. This difficulty in dissolving dolomite in experimental aqueous solutions to determine its solubility is part of the reason for the range in the estimates of the solubility product for dolomite of 10^{-17} to 10^{-19}.

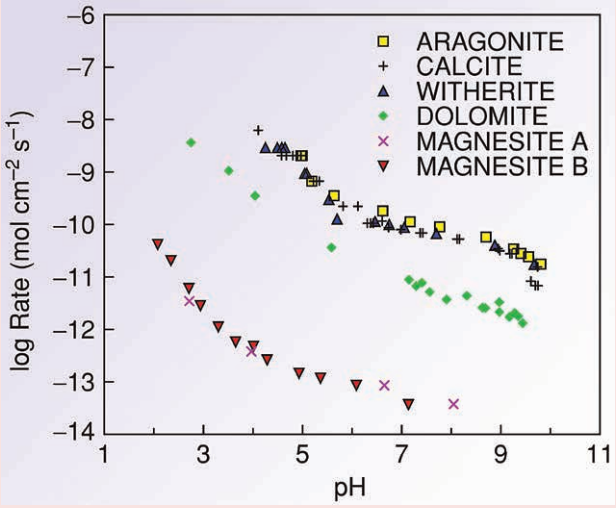

Figure SI-2.1 Comparison of the logarithm of the rates of dissolution of several carbonate minerals in mol cm^{-2} s^{-1} in dilute solutions (after Chou *et al.*, 1989; see also Plummer *et al.*, 1978).

Precipitation of Carbonate Minerals. The kinetics of carbonate mineral precipitation in chemically simple solutions has received considerably less attention than that of dissolution reactions. The work of Busenberg and Plummer (1982, 1986) dealing with a comparative study of the crystal growth kinetics and dissolution of calcite and aragonite, and dissolution of dolomite is an exception and is of particular interest. The authors investigated the crystal growth kinetics and dissolution of calcite and aragonite in pure water, and in the presence of HCl, $CaCl_2$, $KHCO_3$, and KOH at various CO_2 partial pressures at 25 °C. The rate of crystal growth of calcite and aragonite was investigated in $Ca(HCO_3)_2$ solutions at CO_2 partial pressures of $10^{-3.5}$ (atmospheric) to 1 atmosphere and the rate can be described by the following rate equation:

$$R_{(precipitation)} = k_4\,(c\,[(Ca^{2+}{}_{eq})\,(HCO_3^-{}_{eq})] - [(Ca^{2+}{}_s)\,(HCO_3^-{}_s)] \qquad \text{(SI-2.4)}$$

where the parentheses represent the activities of the ions, k_4 and c are constants, and the ion activity products are for Ca^{2+} and HCO_3^- at equilibrium with the specific $CaCO_3$ dimorph and in the aqueous solution (s) at the CO_2 partial pressure of the experiment. Figure SI-2.2 is a summary of some of the results. It can be seen from the figure that for supersaturated $Ca(HCO_3)$ solutions, the rates of precipitation of calcite are significantly faster than those of aragonite whereas the rates of dissolution of aragonite are slightly greater than those for calcite in solutions of similar composition. For reasonable dilute, mainly Ca-HCO_3^- natural solutions, like soil and ground waters, these results to some extent explain why aragonite when exposed to natural freshwater meteoric solutions is dissolved and its chemical components leached from the environment or reprecipitated as calcite.

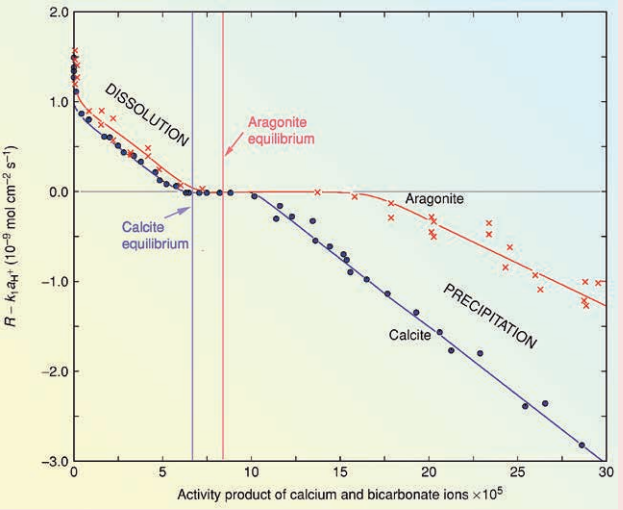

Figure SI-2.2 Comparison of dissolution and precipitation rates of calcite and aragonite single crystals as a function of the activity product of Ca^{2+} and HCO_3^- at 0.96 P_{CO2}. Note that the rates of precipitation of calcite are significantly faster than those for aragonite; however, aragonite dissolves at a rate only slightly faster than calcite, as also seen in Figure SI-2.1 (after Busenberg and Plummer, 1986).

With respect to dolomite, little has been done experimentally at near Earth-surface environmental conditions in terms of precipitation of the phase because of its recalcitrance to precipitate from compositionally simple or complex solutions except at significantly higher temperatures. This is probably due in part to the fact that the dolomite structure is highly

ordered, exerting a limit on the rate at which dolomite can precipitate. It is also plausible that the slow dehydration kinetics of the Mg^{2+} ion and its subsequent incorporation into the dolomite structure play a role in the rate of precipitation (Lippmann, 1973). Nevertheless, as with all inorganic carbonate precipitates, the overall precipitation rate of dolomite is probably a function of the saturation state and temperature (Morse and Mackenzie, 1990; Arvidson and Mackenzie, 1999) and follows the parabolic rate law

$$R_D = k\ (\Omega - 1)^n \qquad \text{(SI-2.5)}$$

where R_D is precipitation rate, Ω is the dolomite saturation index, n is the order of the reaction, and k is the rate constant.

Indeed, Arvidson and Mackenzie (1997, 1999, 2000) were able to demonstrate from theoretical considerations and continuous flow, dolomite-seeded, reactor experiments in reasonably dilute solutions that the dolomite precipitation reaction rate is strongly dependent on temperature and moderately dependent on the saturation state of the solution from which the dolomite is forming. The authors were able to precipitate dolomite at temperatures as low as 60 °C. The dolomite produced in their experiments was variable in composition but typically was a calcium-rich phase termed protodolomite that formed epitaxial overgrowths on the seed material (see Fig. 2.5 in text). The activation energy for this protodolomite precipitation reaction was found to be 31.9 kcal mol^{-1}, lower than that for reactions involving ordered dolomite. The energy required to convert a calcium-rich protodolomite to an ordered dolomite was found to about 5.5 kcal mol^{-1}, and the solubility product for ordered dolomite at 25 °C and 1 atmosphere was reported as about 10^{-17}. The above experimental work led the authors to conclude that both protodolomite and dolomite growth can occur at low to moderate temperatures on relatively short time scales, given an appropriate solution chemistry and temperature.

Carbonate Dissolution and Precipitation in Marine Waters. The reaction kinetics of carbonate minerals in complex solutions such as seawater is more difficult to investigate than that in simple solutions. However for the "constant ionic solution" of seawater, there is quite a bit of information, briefly summarised here. From the dissolution side of the coin, it has been known for some time that Mg^{2+} inhibits the dissolution rate of both calcite and aragonite (Sjöberg, 1978; Morse *et al*., 1979). The only other *major* seawater component that has been identified as a dissolution inhibitor is SO_4^{2-} (Sjöberg, 1978; Mucci *et al*., 1989). Of the minor components in seawater, phosphate ion, which is highly variable in concentration in the ocean, is the most notorious in inhibiting the dissolution rate of both calcite and aragonite (Berner and Morse, 1974; Walter and Burton, 1986). It appears to do so for these carbonate minerals by changing the critical degree of undersaturation necessary for the onset of rapid dissolution of the phases (Berner and Morse, 1974; Walter and Burton, 1986). Organic compounds in

seawater do not seem to exert a strong influence on carbonate dissolution rates but do inhibit precipitation rates (*e.g.*, Berner *et al.*, 1978).

In terms of the precipitation of calcite and aragonite from seawater, the effect of Mg^{2+} ion on rate has been studied in most detail (*e.g.*, Weyl, 1965; Pytkowicz, 1965; Berner, 1975; Mucci and Morse, 1984). Berner (1975) using calcite and aragonite seeds in seawater solutions of different concentrations of Mg^{2+} demonstrated that Mg^{2+} had no influence on aragonite precipitation kinetics but the amount of Mg^{2+} in solution significantly affected the rate of precipitation of calcite. A major retardation of the rate was found in solutions containing Mg^{2+} but at low concentrations of Mg^{2+}, there was no retardation of the growth rate of calcite. The experimental work on Mg^{2+} led to a major hypothesis concerning the retention of the high supersaturation state of seawater with respect to calcite. The central idea is that when calcite nuclei attempt to form in seawater, magnesium absorbs on the surface of the growing nuclei preventing the growth of the nuclei beyond a critical size. This raises the surface free energy of the growing nuclei and likely causes a magnesian calcite to form of significantly higher solubility. The latter mechanism was in part confirmed by the work of Tribble and Mackenzie (1998).

The minor seawater constituent, phosphate, has been found to inhibit the precipitation rates of calcite (Burton and Walter, 1990), magnesian calcite (Mucci, 1986), and aragonite (Berner *et al.*, 1978) from seawater. This inhibition may be most strong in the pore waters of sediments where dissolved phosphate concentrations are relatively high and variable. For calcite versus aragonite precipitation rates, pH fluctuations in phosphate-enriched pore waters leading to varying PO_4^{3-} to HPO_4^{2-} ratios may be responsible for controlling small scale variations in the mineralogy of the carbonate precipitate. Organic compounds also seem to influence carbonate mineral precipitation rates. The influence seems to be directly proportional to the strength of the organic complex with Ca^{2+}. Strong organic inhibitors, like citrate and malate because of Ca^{2+} complexation, slow carbonate precipitation rates and actually can lead to calcite precipitation rather than aragonite.

Biogenic Carbonate Dissolution Kinetics. Most carbonate minerals forming in the modern oceans are a result of biological processes. The mechanisms of biomineralisation take place within the internal fluids of the organism, which can be quite different in composition from the external ambient seawater. This can result in the formation of biogenic carbonate phases very different than those that would be produced by direct precipitation from seawater. The metastability and microstructure of the biogenic phases result in unique behaviour in solution. On the contrary, ooids and marine cements, although their composition may be influenced to some degree by biological processes, are mainly the result of the inorganic precipitation of $CaCO_3$ from seawater or modified seawater.

When seawater is undersaturated with respect to calcite, it has been shown that solubility may not simply control dissolution rate even for grains of the same size, and that the internal arrangement of the carbonate crystals and their voids within the shell or test, or the microarchitecture (microstructure) of the biogenic phase, plays a strong role in the rate of dissolution of biogenic phases. In one of the only complete experimental studies of the dissolution rates of biogenic phases in seawater, using the pH-stat method at S = 35‰, 25 °C, and a P_{CO2} of $10^{-2.5}$ atmosphere, Walter and Morse (Walter, 1985; Walter and Morse, 1985) showed that the relative dissolution rates of various biogenic carbonates as a function of seawater $CaCO_3$ ion activity product were related to both mineral stability and grain microstructure. For example, in seawater undersaturated with respect to aragonite, finely crystalline aragonites dissolved more rapidly than thermodynamically less stable high Mg-calcites (15–18 mol% $MgCO_3$) with lower reactive surface areas. Therefore, under certain conditions, differences in grain microstructural complexity can override thermodynamic constraints and lead to selective dissolution of a thermodynamically more stable mineral phase (Fig. SI-2.3). This finding is especially important to the problem of modern day acidification of our oceans where the lowering of the pH of surface ocean waters not only affects biogenic mineral formation rates but also after death the dissolution rates of their skeletal parts.

Carbonate Mineral Kinetic Equations in Modelling. In this section we discuss briefly some kinetic equations that are used for the precipitation and dissolution of carbonate minerals that are primarily relevant to the monograph sections dealing with the modelling of ocean acidification during the recovery from the Last Glacial Maximum and on into the future of the Anthropocene.

The biogenic calcification rate R, as with inorganic $CaCO_3$ precipitation, certainly depends on carbonate saturation state and temperature. Its dependence on carbonate saturation state for some organisms can be expressed by a linear relationship derived from multiple experiments on corals (aragonite) and coralline algae (magnesian calcite), at least up to moderate degrees of oversaturation (Gattuso *et al.*, 1999):

$$R_\Omega = 21.3\Omega + 12 \qquad \text{(SI-2.6)}$$

where R_Ω is the relative rate of calcification expressed as a percentage of the rate at preindustrial conditions (approximately equal to 100%) and Ω is the carbonate saturation state of the ambient seawater with respect to the carbonate phase of interest. However in the case of saturation state experiments utilising the aragonitic coral *Stylophora pistillata* (Gattuso *et al.*, 1998; Leclerq *et al.*, 2002), the calcification rate was best fit by a curvilinear relationship of the form:

$$R_\Omega = 228(1-e^{-\Omega/0.69}) - 128 \qquad \text{(SI-2.7)}$$

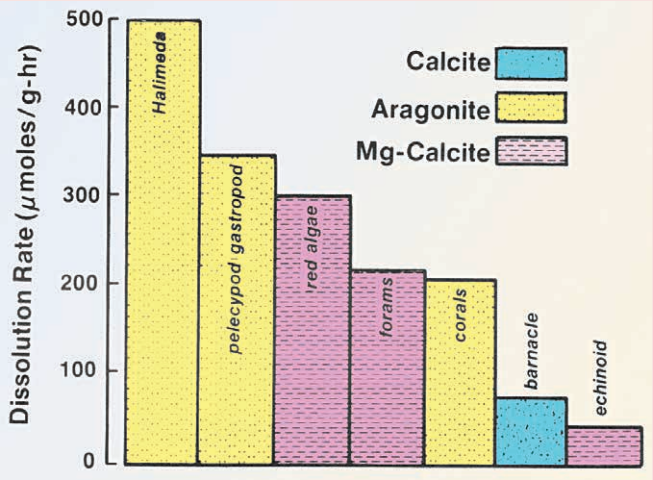

Figure SI-2.3 Relative dissolution rates of biogenic carbonate minerals in seawater undersaturated with respect to calcite (after Walter, 1985).

where R_Ω is the relative rate of calcification expressed as above and Ω is the surface water aragonite saturation state. Thus sensitivity analysis can be run using these two equation (SI-2.6) and (SI-2.7) in modelling the effect of carbonate saturation state on calcification rate.

The dependence of biogenic calcification on temperature can also be expressed by two different relationships and thus once more as with saturation state, both equations can be used in a model sensitivity analysis to gain some idea of the effect of each relationship on model output. In one case, the negative parabolic relationship obtained from experimental results for a red coralline alga, *Porolithon gardineri* (Agegian, 1985; Mackenzie and Agegian, 1989) can be used and normalised to the maximum rate of calcification:

$$R_T = 100 - 1.32\Delta T^2, \qquad \text{(SI-2.8)}$$

where R_T is the relative rate of calcification expressed as a percentage of the rate at the initial temperature and ΔT is the temperature change in degrees Celsius. In the second case, a positive linear relationship can be utilised as obtained from the observed rates of calcification of multiple coral colonies from the Great Barrier Reef, Hawaii, and Thailand (Grigg, 1982, 1997; Scoffin *et al.*, 1992; Lough and Barnes, 2000):

$$R_T = 100 + 28\Delta T \qquad \text{(SI-2.9)}$$

In addition, inorganic dissolution (R_d) and precipitation (R_p) of carbonate minerals within the pore water–sediment model system can be described in models by kinetic rate equations of the general form:

$$R_d = k_d(1 - \Omega)^{n_d} \quad \text{(SI-2.10)}$$

and,

$$R_p = k_p(\Omega - 1)^{n_p} \quad \text{(SI-2.11)}$$

where k_d is the rate constant for dissolution and k_p is the rate constant for precipitation, Ω is the pore water carbonate saturation state, and n_d and n_p are reaction orders for dissolution and precipitation, respectively (Table SI-2.1). The constant parameters can be obtained from the experimental results of Zhong and Mucci (1989) for precipitation and Walter and Morse (1985) for dissolution. Reaction rates can be calculated based on the total mass of calcium carbonate in the sediments by converting the calculated rates per unit area to mass per unit time using average specific surface areas of the minerals (0.1–0.5 $m^2\ g^{-1}$) and the ratio between reactive surface area and total area (0.003-0.66) for typical shallow–water biogenic sediment components (Walter and Morse, 1985). Inhibition by dissolved phosphate (10 µmol l^{-1}) and dissolved organic matter (10 mg kg^{-1}) (Morse *et al.*, 1985) can also be taken into consideration by modifying the uninhibited rates by factors derived from the relationship between the concentrations of these constituents and the rates (Morse *et al.*, 1985). The application of the above relationships can be found in this monograph in the sections that discuss the effects of changing carbonate saturation state and temperature on future biogenic calcification and carbonate dissolution rates in the coastal ocean.

Table SI-2.1 **Constants adopted in modelling work in this monograph for inorganic carbonate mineral precipitation and dissolution rates (R) (after Andersson *et al.*, 2005).**

Precipitation $R_p = k_p(\Omega - 1)^{n_p}$ (Zhong and Mucci, 1989)	Rate constant (k) (µmol $m^{-2}\ h^{-1}$)	Reaction order (n)
Calcite	$10^{-0.20}$	2.80
15 mol % Mg-calcite*	$10^{-0.20}$	2.80
Aragonite	$10^{1.00}$	2.36
Dissolution $R_d = k_d(1 - \Omega)^{n_d}$ (Walter and Morse, 1985)	(µmol $g^{-1}\ h^{-1}$)	
Calcite	$10^{2.82}$	2.86
15 mol % Mg-calcite	$10^{2.62}$	3.34
Aragonite	$10^{2.89}$	2.48

* Assuming same rate as calcite

SI-3

CO_2-Carbonic Acid-Carbonate System and Seawater

This section presents some of the basic physicochemical relationships relevant to understanding the behaviour of CO_2 in aqueous solution in Earth's surface environments. Readers are referred to the books, for example, by Broecker and Peng (1982), Morse and Mackenzie (1990), Mackenzie and Lerman (2006), Zeebe and Wolf-Gladrow (2001), and Millero (2006) for a detailed development of the subject material.

The carbonate ion (CO_3^{2-}) is part of a complex chemical system in natural waters. This is the carbonic acid system that also includes the bicarbonate ion (HCO_3^-), undissociated carbonic acid ($H_2CO_{3(aq)}$), dissolved carbon dioxide (CO_{2aq}), and often exchanges with gaseous carbon dioxide (CO_{2gas}). Changes in the energy content of a system are most easily compared if everyone agrees on a set of reference conditions. In chemistry the standard state of a material (pure substance, mixture, or solution) is a reference point used to calculate its properties under different conditions. In principle, the choice of standard state is arbitrary. In classical thermodynamics, one often chooses a standard state for a substance in solution (solute) where it exhibits infinite-dilution behaviour . The reason for this unusual definition is that the behaviour of a solute at the limit of infinite dilution is described by equations that are very similar to the equations for ideal gases. A very common standard state in geochemistry is chosen as a temperature and pressure (NTP) of 25 °C and 1 atmosphere pressure, and solutes have an activity of 1 in a 1 M (molal), such that at infinite dilution the activity coefficient of the solute is equal to one. Thus, mass action equations written in terms of equilibrium constants are expressed as activities of the chemical species of interest and are a function of only pressure and temperature.

Because of the difficulties in determining the values of activity coefficients in seawater, another standard state has been developed, that of the composition of seawater at S = 35‰, 25 °C and 1 atmosphere total pressure. Thus for calculations of seawater CO_2-carbonic acid system chemistry, "apparent" or stoichiometric constants have been adopted and these vary with pressure, temperature, *and* salinity. In this monograph because of the large changes in seawater chemistry throughout the Phaerozoic Eon, a classical thermodynamic approach was employed to calculate the distribution of chemical species in seawater over deep time based on Pitzer type equations (Pitzer, 1979; Harvie and Weare, 1980; see Morse and Mackenzie, 1990 for review of the subject). In contrast, for glacial/interglacial time and

for the Anthropocene into the future, stoiochiometric constants were used to calculate seawater chemistry. With this in mind, let us look briefly at the dissolution and dissociation of CO_2 in water.

Dissolution and Dissociation of CO_2 in Water. Dissolution of carbon dioxide in water is the first step that enables photosynthetic production of organic matter in aqueous environments, precipitation of carbonate minerals from aqueous solutions, and chemical weathering of the Earth's crust and sediments. Carbon dioxide dissolves in water and reacts with it producing negatively charged bicarbonate and carbonate ions. In pure water the electrical charges are balanced by the hydrogen ion or in natural or experimental more complex aqueous solutions by other metal cations and the hydrogen ion. Dissolution and dissociation of the gaseous species $CO_2(g)$ in water are represented by the following reactions:

$$CO_{2(g)} = CO_{2(aq)} \quad \text{(SI-3.1)}$$

$$CO_{2(aq)} + H_2O_{(l)} = H_2CO_{3(aq)} \quad \text{(SI-3.2)}$$

$$H_2CO_{3(aq)} = H^+_{(aq)} + HCO_3^-{}_{(aq)} \quad \text{(SI-3.3)}$$

$$HCO_3^-{}_{(aq)} = H^+_{(aq)} + CO_3^{2-}{}_{(aq)} \quad \text{(SI-3.4)}$$

Although aqueous uncharged CO_2 can include the species $H_2CO_{3(aq)}$, this species constitutes only a small fraction, about 1/400, of CO_2 in solution. As such the use of either $CO_{2(aq)}$ or $H_2CO_{3(aq)}$ for all of the aqueous species CO_2 is acceptable without a loss of meaning or accuracy (Millero, 1996).

For each of the mass action equations (SI-3.1) to (SI-3.4), one can write a thermodynamic equilibrium constant (using H_2CO_3* to represent both undissociated inorganic carbon species of $H_2CO_{3(aq)}$ and $CO_{2(aq)}$), which have values at 25 °C and 1 atmosphere total pressure as follows:

$$K_o = \{H_2CO_3^*\}/P_{CO2} = 10^{-1.47} \quad \text{(SI-3.5)}$$

$$K_1 = \{H^+\}\ \{HCO_3^-\}/\{H_2CO_3^*\} = 10^{-6.34} \quad \text{(SI-3.6)}$$

$$K_2 = \{H^+\}\ \{CO_3^{2-}\}/\{HCO_3^-\} = 10^{-10.33} \quad \text{(SI-3.7)}$$

where curly brackets designate activities of the chemical species and P_{CO2} is the partial pressure of CO_2. In seawater the mass action equations and the CO_2-carbonic acid system stoichiometric equilibrium constants (K primes) have a similar formulation as the thermodynamic constants but the expressions are written in terms of the concentrations of the dissolved inorganic carbon chemical species, have different values, and are a function of salinity as well as temperature and pressure. As an example, for an average seawater salinity of 35‰ and at a temperature of 25 °C and a total pressure of 1 bar (= ~1 atmosphere), the stoichiometric constants and their values corresponding to equations (SI-3.5) to (SI-3.7) are

$$K'_0 = [H_2CO_3^*]/P_{CO2} = 2.84 \times 10^{-2} \quad \text{(SI-3.8)}$$

$$K'_1 = [H^+]\,[HCO_3^-]/[H_2CO_3^*] = 1.39 \times 10^{-6} \quad \text{(SI-3.9)}$$

$$K'_2 = [H^+]\,[CO_3^{2-}]\,/[HCO_3^-] = 1.19 \times 10^{-9} \quad \text{(SI-3.10)}$$

where brackets denote concentrations of the chemical species.

Because of the formation of the aqueous ions HCO_3^- and CO_3^{2-} from CO_2 in solution, the total concentration of dissolved inorganic carbon is the sum of all the inorganic carbon species, $CO_{2(aq)}$, HCO_3^-, and CO_3^{2-}. This parameter is termed dissolved inorganic carbon, to distinguish it from dissolved organic compounds, and it is usually denoted as ΣCO_2 or DIC:

$$DIC = CO_{2(aq)} + HCO_3^- + CO_3^{2-} \quad \text{(SI-3.11)}$$

With the above equations and discussion in mind, we can now consider a pictorial representation of the distribution of dissolved inorganic carbon chemical species in the CO_2-carbonic acid system. The relative distribution of chemical species is commonly shown as a function of pH relative to DIC in a plot known as a Bjerrum diagram (Fig. SI-3.1). The individual values of the three fractions of DIC (CO_2 plus H_2CO_3 as CO_2), (HCO_3^- and CO_3^{2-}) are shown in the figure for different sets of conditions, as a function of the solution pH, between pH = 2 and 12, at two temperatures of 5 and 25 °C, and 1 bar total pressure and for seawater S = 35‰ and 1 and 300 bar total pressure. In a solution of zero ionic strength (Fig. SI-3.1a), that is a very dilute solution, HCO_3^- is the dominant DIC species over the pH range from roughly 6.5 to slightly more than 10. This is the range in pH of most dilute natural waters, such as soil and many ground waters. In addition, in dilute waters, lower temperature favours relatively higher concentrations of undissociated CO_2 and lower concentrations of the carbonate anion, CO_3^{2-}; that is, the equal concentration points of 50% shift to the left, towards lower pH values.

The effects of salt concentration and pressure on the distribution of the dissolved carbon species are shown in Figure SI-3.1b. Notice first that HCO_3^- is by far the dominant species in seawater. In addition, at 5 and 25 °C, the effect of a mean seawater salinity of 35‰ on the abundance of the various DIC species is pronounced: from a dilute solution of salinity 0 to 35‰, the abundance of the bicarbonate ion, HCO_3^-, decreases at the expense of the other two species of $CO_{2(aq)}$ and CO_3^{2-}. However, the effect of pressure is small at a mean ocean water salinity of 35‰: a total pressure increase from atmospheric to 300 bars of pressure has only a small effect on the shift in the relative abundance of the DIC chemical species.

One other variable of the CO_2-carbonic acid system that is important in our discussion of the evolution of seawater in this monograph is that of total alkalinity. For seawater the difference between the charges of the

conservative cations and anions is equal to the algebraic sum of the charges of the H^+-dependent ions, and this difference is called the total alkalinity of the solution, denoted [TA]:

$$2[Ca^{2+}] + 2[Mg^{2+}] + [Na^+] + [K^+] - [Cl^-] - 2[SO_4^{2-}] = [HCO_3^-] + 2[CO_3^{2-}] + [B(OH)_4^-] + [OH^-] - [H^+] \quad \text{(SI-3.12)}$$

and for the major species in seawater that contribute to the total alkalinity:

$$[TA] = [HCO_3^-] + 2[CO_3^{2-}] + [B(OH)_4^-] + [OH^-] - [H^+]. \quad \text{(SI-3.13)}$$

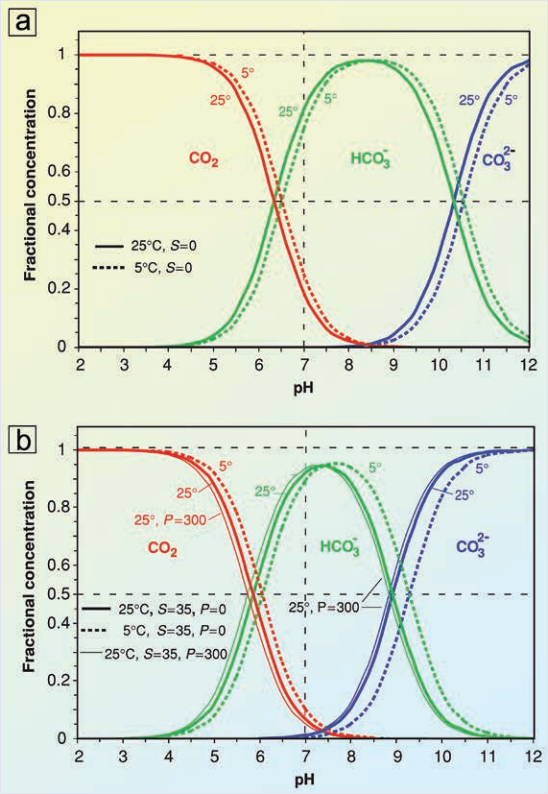

Figure SI-3.1 Bjerrum diagram showing **(a)** Fractional concentrations of dissolved inorganic carbon species in pure water (salinity S = 0‰) as a function of pH at 5 ° and 25 °C. **(b)** Fractional concentrations of dissolved inorganic carbon species in seawater (S = 35‰) at 5 ° and 25 °C at atmospheric pressure, and at a pressure of 300 bar (after Mackenzie and Lerman, 2006).

The determination of TA and DIC in ocean waters is a powerful tool to use to trace water masses in the ocean and to obtain estimates of primary productivity and the dissolution and precipitation of carbonate minerals. Also if you know the values of these two variables, you can calculate the complete carbonic acid system including pH and pCO_2 of seawater.

Saturation State. It is also possible to write reactions and equilibrium constants for the solution (dissolution) and precipitation of minerals in aqueous solutions. The carbonate minerals are especially important minerals found in the ocean as the skeletons and tests of marine organisms and as cements in marine sediments (see SI-1). Calcite (hexagonal $CaCO_3$), aragonite (orthorhombic $CaCO_3$), and dolomite [hexagonal $CaMg(CO_3)_2$] are important marine minerals. As previously discussed, the latter mineral is not found in great abundance in the modern oceans, but it is an important carbonate mineral found in ancient rocks deposited in the marine environment. The mass action equation for both calcite and aragonite is written

$$CaCO_3 = Ca^{2+} + CO_3^{2-}, \quad \text{(SI-3.14)}$$

and at 25 °C and 1 atmosphere total pressure, the thermodynamic equilibrium constants are

$$K_{cal} = \{Ca^{2+}\}\{CO_3^{2-}\} = 10^{-8.46}, \quad \text{(SI-3.15)}$$

and

$$K_{arag} = \{Ca^{2+}\}\{CO_3^{2-}\} = 10^{-8.3} \quad \text{SI-3.16)}$$

and in seawater of S = 35‰ under the same P and T conditions:

$$K'_{cal} = [Ca^{2+}][CO_3^{2-}] = 10^{-6.37}, \quad \text{(SI-3.17)}$$

and

$$K'_{arag} = [Ca^{2+}][CO_3^{2-}] = 10^{-6.19}. \quad \text{(SI-3.18)}$$

Despite the two minerals having the same composition, they differ in their atomic structure, and thus the K values for the two minerals differ. These K values basically represent the solubilities of the two minerals. The larger K value for aragonite than for calcite implies that aragonite is a more soluble mineral than calcite and is unstable relative to calcite under the environmental conditions specified above. However for these minerals to dissolve, the aqueous solution in which the minerals are bathed must be undersaturated with respect to the two minerals. This implies that the product of the activities or concentrations of Ca^{2+} and CO_3^{2-}, termed the ion activity product (IAP) or ion concentration product (ICP), respectively, in the solution must be smaller than the K values for the minerals; that is the ratio of IAP/K or ICP/K′ = **Ω**, the carbonate saturation state, must be < 1. The converse is true for the minerals to precipitate, where $Ca^{2+} + CO_3^{2-} =$

$CaCO_3$ and $\Omega > 1$. Both calcite and aragonite contain other elements in minor or trace amounts and this affects their solubilities. Strontium (Sr) is especially important in aragonite and magnesium (Mg) in calcite. Indeed Mg can be so plentiful in biologically and inorganically produced calcite that a special term has been applied to the calcites containing more than about 4 wt% Mg, the magnesian calcites, which generally have greater solubilities than pure calcite, and for some magnesian calcite compositions, even aragonite. The general mass action equation and thermodynamic equilibrium constant for calcites with Mg in them is written as

$$Ca_{(1-x)}Mg_x(CO_3) = (1-x)Ca^{2+} + xMg^{2+} + CO_3^{2-} \qquad \text{(SI-3.19)}$$

and

$$K_{MgCalcite} = \{Ca^{2+}\}^{(1-x)} \{Mg^{2+}\}^{(x)} \{CO_3^{2-}\} \qquad \text{(SI-3.20)}$$

where x is the mole fraction of $MgCO_3$. The solubility of magnesian calcites is discussed in SI-1.

For dolomite the mass action equation is

$$CaMg(CO_3)_2 = Ca^{2+} + Mg^{2+} + 2CO_3^{2-} \qquad \text{(SI-3.21)}$$

and

$$K_{dol} = \{Ca^{2+}\} \{Mg^{2+}\} \{CO_3^{2-}\}^2 = \sim 10^{-17}. \qquad \text{(SI-3.22)}$$

To our knowledge the K´ for dolomite has never been determined experimentally in seawater because of the difficulty in doing experiments involving this phase at low temperatures due to its slow reactivity in aqueous solution (see SI-2).

The general relationships discussed above for the CO_2-carbonic acid-carbonate mineral system are true for all natural waters. It is worthwhile in terms of the emphasis on ocean waters in this monograph to discuss some of the trends in carbon system variables in the modern ocean. Although biological productivity and mixing can complicate the picture, as one moves poleward from the tropical regions, the surface seawaters of the various major ocean basins generally increase in DIC and decrease in P_{CO2} (Fig. SI-3.2 and SI-3.3) due to decreasing temperature and its effect on the solubility of CO_2 in seawater. Exceptions to this trend can be found in upwelling regions in the equatorial region and in eastern boundary regions where deep-water enriched in DIC and with high P_{CO2} is brought to the surface.

Total alkalinity mainly depends on salinity and mixing and closely follows the salinity distribution of the ocean. For example, total alkalinity is significantly higher in the Atlantic Ocean than in the Pacific Ocean owing to the higher salinity of the former. The saturation state of surface waters with respect to all major marine carbonate minerals generally decreases

with increasing latitude, although virtually all surface seawaters remain oversaturated with respect to calcite, aragonite, and dolomite. With depth in all ocean basins DIC and TA increase while carbonate saturation state and pH decline (Fig. SI-3.3), mainly due to the microbial respiration of sinking organic matter producing CO_2 and lowering pH. Increasing pressures and decreasing temperatures with oceanic depth also lead to an increase in the solubility of the major carbonate minerals with increasing depth.

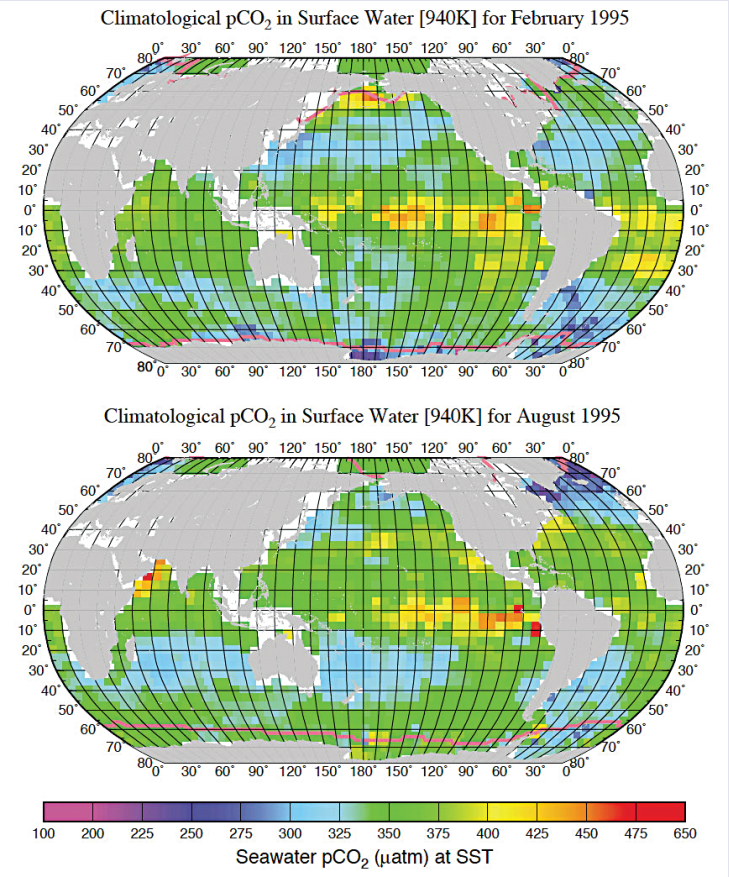

Figure SI-3.2 Climatological mean distribution of surface seawater P_{CO2} in February **(top)** and August **(bottom)** in 1995 at *in situ* temperature (after Takahashi *et al.*, 2002).

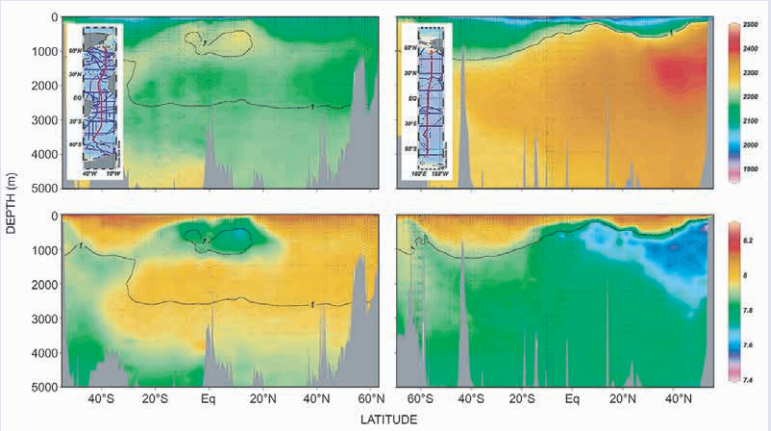

Figure SI-3.3 Meridional sections across the Atlantic (left) and Pacific (right) oceans showing DIC and pH-total in seawater. The depth of the saturation horizon with respect to aragonite (Ω-aragonite) is shown by the black lines (after Andersson, 2013).

Thus at varying depth horizons in the ocean depending on the carbonate mineral phase in question, the carbonate saturation state (**Ω**) of ocean water with respect to a particular carbonate mineral phase becomes less than 1 and the waters become undersaturated with respect to that phase. This depth horizon is shallowest for aragonite and deeper for calcite. The saturation horizons for the carbonate minerals are deepest in the Atlantic Ocean and shallowest in the Pacific Ocean, reflecting the movement of deep waters from the Atlantic Ocean through the Indian Ocean to the Pacific Ocean and the accumulation on route of CO_2 in these waters from microbial respiration of sinking organic detritus. Furthermore, there is a depth horizon in the ocean, termed the carbonate compensation depth (CCD), at which depth the rate of deposition of $CaCO_3$ is equal to its dissolution rate, and below which $CaCO_3$ is generally no longer present in deep-sea marine sediments. This horizon again is shallower for aragonite than for calcite. Dolomite is not produced biologically in the shallow waters of the ocean nor is it produced at depth, except as a diagenetic phase in shelf/slope sediments (so-called organogenic dolomites), so the concept of a saturation horizon for this mineral is not applicable *sensu stricto* in the modern ocean setting.

SI-4

Modelling Global Biogeochemical Cycles

Because much of this monograph is based on the modelling of the biogeochemical cycles of carbon and associated elements, some important factors involved in the construction of biogeochemical cycling models are considered in this informational section. These factors include:

1. Definition of the boundaries of a global natural system and subsystems (reservoirs or boxes),
2. Prediction and evaluation of transport paths,
3. Problems of evaluating fluxes, and
4. Mathematics of modelling of global systems.

Reservoirs. In developing a biogeochemical-cycling model, it is necessary to separate the system of interest from its natural surroundings. In general, the boundaries of a natural system are defined by the scale of the phenomena of interest and by previous knowledge of possible interactions between the system and its surroundings. Global biogeochemical cycling models consider phenomena on a worldwide scale. In such models, the Earth is divided into a number of physically well-defined spheres referred to as "boxes" or "reservoirs." The term box model is commonly applied to models of this type. The number of reservoirs considered in modelling the global movement of a substance depends on previous knowledge of the manner in which the substance is distributed about the Earth's surface in its oceans, atmosphere, biota, sediments, etc. If it can be demonstrated that a substance is transported from one Earth sphere to another, then the spheres are considered boxes or reservoirs within a global model. If there are several sources within a reservoir for transport of materials from that reservoir to another but there are no known transport paths for these sources, then the individual sources within a reservoir are considered as compartments in a global model.

Transport Paths and Fluxes. Transport paths are directional properties of a system. They represent the major agents or processes responsible for movement of materials about Earth's surface and their nature may have various origins. They may be physical, chemical, or biological. Associated with a transport path is a flux and it is a quantitative measure of the mass of the substance transferred along a transport path between reservoirs. Flux is usually defined in terms of mass per unit time (*e.g.*, grams or moles of a substance per year).

Fundamentally, the way a substance, be it an element or compound, is transferred from one box to another depends on its physical and chemical properties and processes controlling the distribution of that substance in the natural environment. For example, a substance with a high solubility in water, such as sodium chloride (NaCl), would be expected to move about the Earth's surface via agents involving water movement, such as rivers. However, a substance with a high solubility in fatty tissue, for instance, DDT (dichlorodiphenyl-trichloromethane), might be expected to be involved in biological processes. For example, DDT accumulates in the fatty tissue of some fish and can be transported by fish from place to place. Carbon as a gas in the atmosphere is directly available for terrestrial plant photosynthesis and because of the gas's moderate solubility in aqueous solutions, it is available in aquatic systems for photosynthesis.

The quantitative evaluation of transport paths and their relative contributions are probably the most critical point of model building. It necessitates both a good knowledge of all the interactions possible between the reservoirs and the dynamics of the physical, chemical, and biological processes involved. The complexity of the task increases rapidly if subsystems are considered. In this case, it is necessary to understand the physical processes of movement (mixing by advection and diffusion), as well as biological processes, within the reservoirs. Although it might be easy to estimate the transport of a dissolved substance from the land to the oceans via rivers, it is more difficult to estimate the substance's movement within the ocean by advective and diffusive flows interacting with the biological processes of organic production and decomposition. Once transport paths are defined in a model, they must be quantified. This step involves estimates of rates of transfer (fluxes) involved with the transport paths. Herein lies a major problem. In many cases basic data and an understanding of the processes operating in the system of interest are lacking. Many material cycles have innumerable processes and fluxes. Some are better known than others, and some are quantitatively unknown. Our knowledge of many biogeochemical cycles, particularly their dynamics and potential for feedback (see below) during perturbations, for example, natural or human-induced climatic change, is progressing rapidly but is still incomplete.

Modelling. Figure SI-4.1 illustrates a simple global biogeochemical box model of a hypothetical substance A, consisting of three reservoirs with transport paths between reservoirs. Each reservoir receives fluxes from the other two and delivers fluxes to them. The chemical or biological form of the element may differ from reservoir to reservoir. Any transformations or chemical reactions, such as oxidation or reduction and solution or precipitation, are not represented in the diagram of the cycle. The ocean reservoir is subdivided into the compartments of water, biota, and sediment. The land reservoir includes the compartments of plants, animals, and soil.

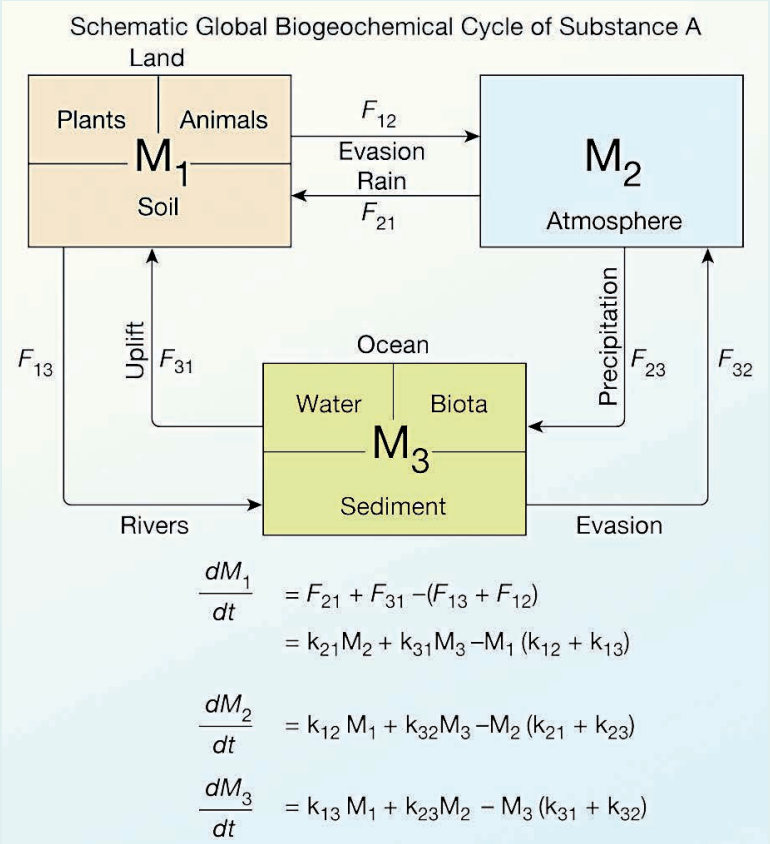

Figure SI-4.1 Schematic diagram of the global biogeochemical cycle of a hypothetical substance A. The differential equations for the rate of change of the mass of substance A in each reservoir are also shown (after Mackenzie, 2011).

The atmosphere is represented as a single reservoir. The masses of substance A in the compartments are known. However, although transport paths among the compartments are suspected, no values for the fluxes are known for these paths. The flows between the reservoirs involve the masses of A transported. The rates of transport (fluxes) are measured in units of mass per unit of time. The nature of the biogeochemical processes that

are responsible for the transformation of the components from one form to another, and the physical and biological processes that are responsible for the flows determine in detail the rates of transport.

The transport of substance A involves (1) gaseous transport from the land and sea surface to the atmosphere (evasion, F_{12} and F_{32}) and return in rainfall (F_{21}) and precipitation (F_{23}), (2) river transport of dissolved and solid materials (F_{13}), and (3) return of the substance to the land via uplift of sedimentary rocks (F_{31}). Fluxes of substance A are known for these transport paths. dM_i/dt is the change in mass of a reservoir per unit of time and in a steady state system by definition is equal to zero. In a non–steady or transient state system, it differs from zero. Knowledge of the fundamental processes and of the driving forces behind the flows may not be sufficient to enable development of a quantitative relationship between them and the material fluxes. Thus, the fluxes of materials (denoted in the figure for the flux from box i to box j) are commonly measured and related to the conditions in the system according to some chosen model. The two simplest flux models are of zeroth- and first-order fluxes. The zeroth-order flux is a constant:

$$F_{ij} = \text{constant.} \qquad \text{(SI-4.1)}$$

and a first-order flux is one that is proportional to the reservoir mass:

$$F_{ij} = k_{ij}\, M_i. \qquad \text{(SI-4.2)}$$

M_i is the mass of a substance in a reservoir i, and k_{ij} is a rate parameter for the flux going from reservoir i to j. In general, k_{ij} may vary with reservoir size and time and may be a function of environmental conditions within a system. However, in the preceding equation (SI-4.2), it is treated as a constant. In a steady-state (unchanging) system, reservoir concentrations or masses of a substance do not change with time. This requires that the input and output fluxes for every reservoir are equal. If one of the fluxes changes, the steady state of the system becomes perturbed. The system is no longer at steady state, and the system is described as transient or non–steady state system. Such a condition can result in changes in all the reservoir masses.

In some models the representation of fluxes and their variation with time are more complicated than indicated above. For example, the flux of carbon related to calcification may be parameterised in an equation that has temperature and carbonate saturation state, and perhaps other variables, as parameters that affect the calcification rate. In addition, the accumulation of dolomite might be parameterised by not only the saturation state of seawater with respect to dolomite and temperature but also because dolomite does not accumulate in the deep sea, shelf area might also be considered as a variable governing dolomite accumulation rate.

Residence Time and Feedback. The residence time of a substance in a reservoir M_i is an important concept. It provides some clue as to the reactivity of a substance within a reservoir. It is defined as the ratio of the mass of the reservoir to the sum of either input or output fluxes of the substance at steady state. The residence time (λ) is equal to 1 divided by the rate constant:

$$\lambda = M_i/F_{ji(in)} = 1/k_{ji}. \quad \text{(SI-4.3)}$$

In this case, the subscript (in) refers to the flux into the reservor of interest.

A perturbation of a biogeochemical cycle caused by a change in an input flux will result in a change in reservoir mass. For a fixed change in input, up or down, the reservoir mass will come to within 5% of a new steady-state value after three residence times have elapsed. Thus, most of the change (95%) caused by a perturbation in input would be completed in a time period equal to three times the residence time. This time is known as the renewal or recovery time. Consequently, reservoirs of short residence times respond rapidly to external perturbations. In reservoirs of long residence time, perturbations require more time to work their way through.

Feedback is an important concept in our studies of biogeochemical cycles and environmental change. Feedback is a self-perpetuating mechanism or process of change and response to that change. Natural systems react to perturbations in a positive or negative fashion. In a positive feedback loop, the effects of a perturbation are amplified; in a negative feedback loop, the effects of the disturbance are diminished.

To provide a further idea of the construction of biogeochemical cycles and their complexity, Figure SI-4.2 shows the global biogeochemical cycles of organic and inorganic carbon in the global coastal ocean as coupled to the continental slope and open ocean. The fluxes are in units of 10^{12} mol C yr^{-1}. In this representation, both fluxes between reservoirs and within reservoirs are shown: P and R represent organic productivity and respiration fluxes, respectively, in the organic C cycle, and production and dissolution of $CaCO_3$ are shown for the inorganic C cycle. Notice in particular the small flux due to open ocean organic productivity that is eventually buried in the sediments (0.01%) as opposed to shelf productivity (3.8%) and that $CaCO_3$ accumulation in shelf sediments represents 45% of total $CaCO_3$ accumulated on the sea floor, despite the fact that coral reefs, banks, and continental shelves constitute only 7% to 8% of total ocean area.

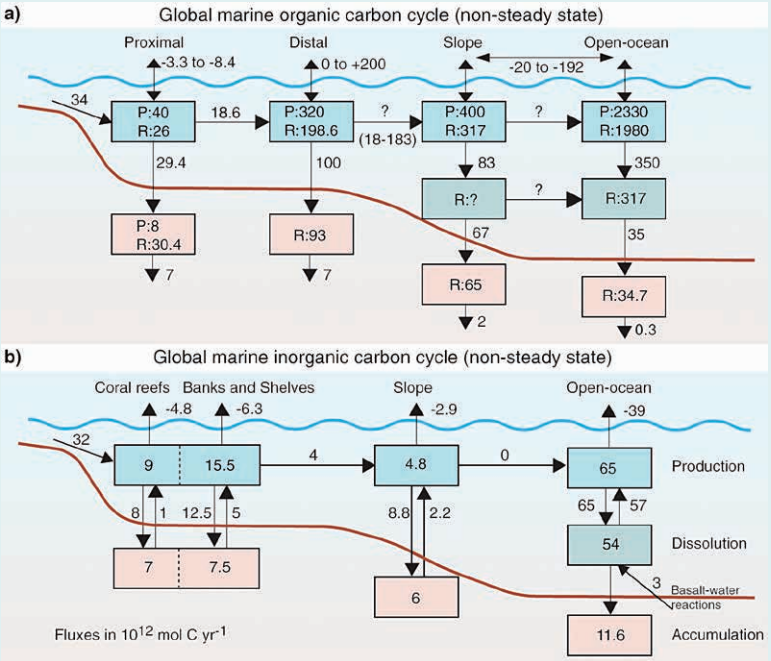

Figure SI-4.2 Late preindustrial, non-steady state global marine organic **(a)** and inorganic **(b)** carbon cycles. Fluxes are in units of 10^{12} mol yr^{-1} of C (1 gigaton of C is 1 x 10^{15} g C and approximately 83 x 10^{12} mol of C). Less well-known fluxes are denoted by a question mark and/or by a range of values. Negative values indicate a net flux of CO_2 from the surface ocean to the atmosphere. Positive values the opposite direction of the air-sea flux. Air–sea CO_2 exchange fluxes resulting from the imbalance between gross primary production and total respiration of organic matter and precipitation and dissolution of $CaCO_3$ in the sub-reservoirs (domains) of the ocean are also shown. The precipitation of $CaCO_3$ always results in a flux of CO_2 out of the ocean (negative value). The air–sea CO_2 flux related to organic metabolism in the ocean or its sub-reservoirs (domains) may be negative or positive, depending on whether the region is a net source (autotrophic) or a net sink (heterotrophic) of atmospheric CO_2, respectively. During late pre-industrial time, it is likely that the shallow-water coastal ocean environment served as a net source of ~18 x 10^{12} mol C yr^{-1} to the atmosphere (after Andersson and Mackenzie, 2004).

GLOSSARY

Acid Rain: rainfall with a pH of generally less than 5 on an annual basis because of the presence of acidic compounds of nitrogen and sulphur dissolved in the rainwater.

Aerobic: with oxygen; requiring the presence of free oxygen for life, or an environment that contains oxygen.

Total Alkalinity (TA): a measure of the ability of a solution to neutralise acids and is equivalent to the stoichiometric sum of the bases in solution. Practically its measurement involves titration of the solution usually with hydrochloric acid to the equivalence point of carbonate ion or bicarbonate ion; that is, the point at which these ions are completely converted to dissolved carbon dioxide. Common natural chemical species that contribute to the total alkalinity of a solution are carbonate, bicarbonate, borate, hydroxide, phosphate, silicate, dissolved ammonia, sulphide, and some organic acids. A special case of alkalinity is that of carbonate alkalinity involving only bicarbonate, carbonate, hydrogen, and hydroxyl ions.

Anaerobic: without oxygen; an organism that does not require oxygen to carry on its metabolism, or an environment without oxygen.

Angiosperm: a flowering plant that produces seeds encased in a fruit or seed case, like oak, maple, and eucalyptus trees.

Anoxic: without oxygen.

Anthropogenic: of, relating to, or influenced by the impact of humans on nature.

Anthropogenic CO_2 increase: steadily increasing concentrations of CO_2 in the atmosphere over the past century mostly due to human activities.

Aquatic: of or pertaining to water; growing or living in or frequenting water.

Autotroph: an organism that requires carbon dioxide as a source of carbon and a simple inorganic nitrogen compound for synthesis of organic matter.

Autotrophic system: an environment in which the difference between gross photosynthesis and gross respiration is positive. In such a terrestrial or aquatic environment, the net transfer of carbon dioxide is into the system.

Autotrophy: the biochemical pathway by which an organism utilises carbon dioxide as a source of carbon and simple nutrient compounds for synthesis of organic matter.

Basalt rock: a dark, dense basic igneous rock of a lava flow or intrusion into Earth's crust composed principally of the minerals labradorite (a plagioclase) and pyroxene.

Benthic: of, relating to, or occurring at the bottom of a body of water.

Benthic organisms: organisms that inhabit the surface of, or live within, the sediments at the bottom of a body of water.

Biogeochemical cycle: representation of biological, geological, and chemical processes that involve the movement of an element or compound about Earth's surface.

Biological production: the rate of production of organic matter by producer organisms.

Biological productivity: rate of production per unit area of organic matter by producer organisms. There are several types of productivity. **Gross primary productivity** (GPP) refers to the total amount of plant material produced by photosynthesis in a defined area in an interval of time. **Net primary productivity** (NPP) is the net amount of plant material produced per unit area per unit of time and is the difference between GPP and cell respiration. **Net ecosystem productivity** (NEP) is the difference between GPP and cell respiration plus heterotrophic processes of decay.

Biomass: the amount of living matter in a unit area or volume of habitat.

Biosphere: the living and dead organic components of the planet.

Blue-green algae: a widely distributed group of predominately photosynthetic prokaryotic organisms of the kingdom Monera that occur singularly or in colonies; also called cyanobacteria.

Box model: a representation of a system that includes reservoirs (boxes), processes, and fluxes of materials.

C-3 pathway: a photosynthetic metabolic pathway involving the initial synthesis of a three-ring organic acid by which most trees and shrubs (95% of all land vegetation) remove CO_2 from the air.

C-4 pathway: a photosynthetic metabolic pathway involving the initial synthesis of a four-ring organic acid by which about 5% of all land plants extract CO_2 from the air.

Carbon isotopes: isotopes of carbon with different atomic masses; ^{13}C and ^{12}C can be used to distinguish the sources of different kinds of carbon, and ^{14}C and ^{12}C can be used to determine the elapsed time since formation of a carbon-containing compound.

Chemical weathering: the dissolving or other alteration of minerals and rocks in the presence of water and acids like carbonic acid to yield dissolved constituents and solid reaction products.

Chlorofluorocarbons (CFCs): synthetic organic compounds composed of methyl (CH_3) groups, chlorine, and fluorine.

Climate: the characteristic long-term environmental conditions of temperature, precipitation, winds, etc., in a region or for the globe presently and in the past (palaeoclimate).

Climate forcing: the ability of a variable, like the concentration of a greenhouse gas in the atmosphere, to induce a change in climate.

Coccolithophoridae: a family of planktonic algae that build a skeleton of micrometre-size disc-shaped plates of calcite ($CaCO_3$).

Continental ice sheet: mass of ice on the order of several kilometres in thickness covering the continent or a portion thereof and moving independently of the underlying topography.

Continental shelf: the shallow, submarine plain of varying width that forms the border of a continent and terminates seaward at the continental slope.

Coupling: a feature or characteristic of a system implying that information from one part of the system is provided to, and influences the behaviour of, other parts. The biogeochemical cycles of the elements necessary for life are coupled through processes that are essential for life—e.g., photosynthesis and respiration.

Crust: Earth's outer layer, enriched in silicon, sodium, and potassium and having a thickness of 35 km beneath the continents and 10 km beneath the oceans.

Cultural eutrophication: the various processes leading to overnourishment of an aquatic system in nutrients, rapid plant growth and death, and oxygen deficiency brought about by human-derived nutrient and carbon inputs to the aquatic system.

Cyanobacteria: the blue-green algae, a widely distributed group of predominantly photosynthetic prokaryotic organisms of the kingdom Monera that occur singularly or in colonies.

Decay: the oxidative process of conversion of organic tissue to simpler organic and inorganic compounds. The oxidising agent may be diatomic oxygen, nitrate, sulphate or other chemical compounds.

Diagenesis: the collection of physical, chemical, and biological processes that operate on a sediment after deposition.

Diatom: planktonic and benthic freshwater and marine algae that commonly use silicon to build a skeleton of opal.

Dissolution: the solution of solid substances, such as the minerals in rock or salt, in water that leads to the production of ions dissolved in an aqueous solution.

Dolomite: a sedimentary rock consisting predominantly of the carbonate $CaMg(CO_3)_2$.

Dissolved inorganic carbon (DIC): the summation of the concentrations of carbonate ion (CO_3^{2-}), bicarbonate ion (HCO_3^-), and aqueous CO_2 in an aqueous solution.

Earth system science: that branch of knowledge or study dealing with Earth as a whole; study of the sum of processes operating in the atmosphere, hydrosphere, biosphere, cryosphere, and lithosphere and the interactions among these components.

Ecosphere: the system that includes the biosphere and its interactions with the physical systems of planet Earth.

Enhanced greenhouse: the additional greenhouse effect produced by the accumulation of greenhouse gases in the atmosphere derived from human activities.

Equilibrium: a stable balanced system in which all influences are countered by others.

Erosion: the processes by which the surface of Earth is worn away by the action of water, wind, glacial ice, etc.

Estuary: an arm of the ocean where freshwater from the land mixes with seawater.

Eutrophication: the various processes leading to over-nourishment of an aquatic system in nutrients, rapid plant growth and death, and oxygen consumption and deficiency in the system. These processes occur naturally in some aquatic systems but may be speeded up by additions of nutrients from human activities (e.g., fertiliser application) to the systems. Human-induced eutrophication is often called **cultural eutrophication**.

Exogenic system: Earth's outer sphere, which includes the atmosphere, hydrosphere, biosphere, cryosphere, and shallow lithosphere.

Feedback: a process or mechanism that generates a feedback loop in which some fraction of the output is returned or "fed back" to the input. Feedback loops may act in such a way as to stabilise (negative feedback) or destabilise (positive feedback) a system undergoing a perturbation. These feedback loops exist in both the biogeochemical cycles and the climate system.

Flux: the rate of transfer of a material; a parameter used, for example, in box models.

Foraminifer: any chiefly marine protozoan of the sarcodinian order Foraminifera. Also called foram. These microscopic creatures typically have a linear, spiral, or concentric shell perforated by small holes or pores through which pseudopodia extend. Their shells are commonly calcium carbonate in composition.

Forcing function or driver: a parameter that controls the behaviour of a system. Such a function often makes the behaviour of the system regular and predictable.

Glacial stage: a relatively cold period of time recognised during the Pleistocene Epoch during which much of the Northern Hemisphere was covered by great ice sheets.

Greenhouse effect: the phenomenon of the warming of Earth's atmosphere and surface by the atmospheric greenhouse gases. These gases absorb and reradiate long-wave Earth radiation, making the global temperature of the planet reasonable. Without the natural greenhouse effect, the planet would be about 33 °C cooler than its global mean annual temperature of 15 °C that is, -18 °C. Because of inputs to the atmosphere of greenhouse gases from human activities, these gases are increasing in concentration in the atmosphere. This may lead to an **enhanced greenhouse effect** and warming of the planet.

Greenhouse gas: an atmospheric gas that absorbs and radiates energy in the infrared part of the electromagnetic spectrum. Such gases include water vapour, carbon dioxide, methane, nitrous oxide, tropospheric ozone, and the synthetic chlorofluorocarbon gases. These gases warm the atmosphere and Earth's surface below. This phenomenon is frequently referred to as the **greenhouse effect** or warming.

Gymnosperm: plants with seeds that are not enclosed in a fruit or seed case, including pine, fir, spruce, and other cone-bearing trees and shrubs.

Heterotroph: an organism requiring complex organic compounds of carbon for metabolic synthesis.

Heterotrophic system: an environment in which the difference between gross photosynthesis and gross respiration is negative. In such a terrestrial or aquatic environment, the net transfer of carbon dioxide is out of the system.

Heterotrophy: biochemical pathway in which organic substrates are used by organisms to make organic matter.

Hothouse: an extended period of geologic time during which Earth was warm.

Hydrothermal reaction: a chemical reaction involving hot water and minerals in a rock.

Hydrothermal vent: a hot water spring on the seafloor or the land through which water and chemical substances from depth exit.

Ice age: a glacial epoch, especially the last, or Pleistocene Epoch, beginning about 1.8 million years ago.

Icehouse: an extended period of geologic time during which Earth was cool.

Ice sheet: a thick and extensive blanket of ice found on land and often covering a large portion of the continent.

Interglacial stage: a relatively warm period of time recognised during the Pleistocene Epoch during which great ice sheets retreated from the continents of the Northern Hemisphere.

Intergovernmental Panel on Climate Change (IPCC): a large group of scientists from the international community that develops consensus statements and documents on the present scientific investigations regarding the impact of greenhouse gases and aerosols on climate.

Isotope: any of two or more forms of a chemical element having the same atomic number—that is, the same number of protons in the nucleus—but having different numbers of neutrons in the nucleus, therefore having different atomic weights. There are 275 isotopes of the stable elements and over 800 radioactive isotopes.

Lifetime: a measure of the reactivity of an atmospheric chemical compound. The more reactive the compound, the shorter its atmospheric lifetime; analogous to the term residence time.

Limestone: a sedimentary rock consisting predominately of calcium carbonate minerals.

Limiting nutrient: the chemical compound, generally inorganic, that limits productivity in a terrestrial or aquatic environment. Examples are nitrate, phosphate, and iron.

Lithosphere: the dynamic subdivision of Earth on the order of 100 km in thickness forming the outer rigid part of the planet. Also, the solid portion of Earth comprised of minerals, rocks, and soil; a reservoir in Earth's surface system.

Mantle: the portion of Earth between the crust and the core that is enriched in magnesium and iron and has a thickness of about 2,900 km.

Mass balance equation: an equation describing the balance of materials in a system on a mass basis. For example, the total mass of dissolved inorganic carbon in the ocean is equal to the sum of the masses of bicarbonate (HCO_3^-) carbonate (CO_3^{2-}) and dissolved CO_2.

Metamorphic rock: a rock formed from a preexisting rock by an increase in temperature and pressure.

Metamorphism: the set of processes that lead to a change in the structure or constitution of a rock due to pressure and temperature.

Milankovitch hypothesis (theory): the hypothesis that orbitally controlled fluctuations in high-latitude solar radiation (insolation) during the summer control the size of ice sheets and the periodicity of glacial-interglacial stages.

Model: a simplified representative of a system or phenomenon whose description is often mathematical and portrayed pictorially.

Mole or mol: one gram atomic weight of an element or one gram molecular weight of a compound. One gram atomic weight of an element is its atomic weight expressed in grams. One gram molecular weight of a compound is its molecular weight expressed in grams.

Negative feedback: a process or mechanism that relieves or subtracts from an initial perturbation to a system.

Net primary production (NPP): the net amount of plant material produced per unit area per unit time; photosynthesis minus respiration equals net primary production.

Non–steady state: the state of a system in which a variable(s) is (are) changing with time. For example, the atmospheric concentrations of carbon dioxide and other greenhouse gases are changing with time. Thus, the atmosphere is a non-steady-state system with respect to composition.

Ocean acidification (OA): the increase in the acidity of the ocean due to emissions of CO_2 to the atmosphere from human activities and the absorption of part of this CO_2 in surface ocean water leading to a decrease in the pH of the water. This phenomenon has been called "the other CO_2 problem". Acidification will have important consequences for marine organisms from bacteria on up the trophic chain. Coral reefs are particularly at risk of degradation due to acidification of the waters bathing them.

Oxidation: the process by which electrons are removed from an atom or molecule. In such a process a substance like iron may combine with oxygen and be converted into an oxide like iron oxide (rust).

Ozone: a form of oxygen, O_3, having a peculiar odour of weak chlorine. It can be produced by an electric spark or ultraviolet light passing through air or oxygen. It is found in both the troposphere and stratosphere as a trace gas. In the stratosphere it absorbs UV radiation, preventing much of that energy from reaching Earth's surface.

Pelagic: of, relating to, or occurring in lake water or the open ocean.

pH: the negative logarithm of the effective hydrogen ion concentration or hydrogen ion activity used in expressing both acidity and alkalinity on a scale whose values range from 0 to 14, with 7 representing neutrality; numbers less than 7 denote increasing acidity, and numbers greater than 7, increasing alkaline conditions.

Photosynthesis: the process of synthesis of complex organic materials; e.g., carbohydrates, from carbon dioxide, water and nutrients, using sunlight as a source of energy and with the aid of chlorophyll and associated pigments.

Plankton: minute plant and animal life of the ocean ranging in size from 5 micrometres to 3 centimetres. The plant plankton are the **phytoplankton**; the animal plankton are the **zooplankton**.

Plate tectonics: the theory of global tectonics in which the lithosphere is divided into a number of crustal plates that move on the underlying plastic **asthenosphere**. These plates may collide with, slide under, or move past adjacent plates in a nearly horizontal direction. The sources of the plates are the great **midocean ridges** of the world's oceans, where hot molten material upwells from within Earth. The plates are destroyed at **subduction zones**, such as the western margin of the Pacific Ocean, where the plates sink down into the underlying asthenosphere.

Polymorph: a mineral with a specific composition that can crystallise in at least two different structural forms. A dimorph is a mineral that crystallises in two distinct structural forms.

Positive feedback: a process or mechanism that reinforces or adds to an initial perturbation to a system.

Protozoan: an eukaryotic organism of the kingdom Protoctista, phylum Protozoa, with a membrane-bound nucleus and organelles within a mass of protoplasm. Planktonic foraminifera and radiolarians, which secrete shells of calcium carbonate and opal, respectively, are members of this group.

Proxy: a quantifiable indicator of climatic or other environmental changes that is found in an historical record and precede direct instrument measurements of change.

Radiolarian: a planktonic protozoan that constructs an intricate skeleton of spicules made up of opal.

Redfield ratio: the relatively constant ratio of 106:16:1 of the bioessential elements carbon, nitrogen, and phosphorus in marine plankton.

Reduction: the process by which electrons are added to an atom or molecule.

Reservoir or stock: that part of a system that can store or accumulate and be a source of a quantity of one of the system's variables or substances.

Residence time: the total mass of a substance in a reservoir divided by its inflow or outflow. The residence time is a measure of the reactivity of the substance in the reservoir.

Respiration: the physical and chemical processes by which an organism supplies its cells and tissues with the oxygen needed for metabolism and releases carbon dioxide formed in the energy-producing reactions.

Salinity: a measure of the salt content of water; for example, the salinity of seawater is 35 (often shown as 35%) and that of average river water is 0.12.

Saturation: the degree to which a solution or a gas is at equilibrium with one of its components. It is measured in several different ways. For example, saturation of seawater with respect to the mineral calcite ($CaCO_3$) of 50% would mean that the seawater was 50% undersaturated with respect to calcite.

Saturation state of an aqueous solution (W**):** the measure of the degree of saturation of a solution with respect to a phase like a mineral. It is equal to the ion activity product or the ion concentration product of the components in the solution divided by the thermodynamic equilibrium product or the stoichiometric solubility product, respectively. If W is greater than 1, the solution is oversaturated with respect to the phase under consideration, If less than 1, undersaturated, and if equal to 1, at equilibrium.

Seafloor accretion: the creation and migration of new seafloor by the separation of lithospheric plates generally at midocean ridges and the filling of the gap with lava and igneous intrusive rocks.

Sedimentary rock: a rock formed from the erosion of preexisting rocks and the deposition of the eroded materials as sediment. Sedimentary rocks are also formed by inorganic or biological precipitation of minerals from natural waters.

Space scale: a particular three-dimensional realm or expanse in which material objects are located and events occur.

Steady state: the property of a system that implies no change in space and time.

Stoichiometry: the quantitative relationship between reactants and products in a chemical reaction.

Subduction zone: the juncture of two lithospheric plates where collision of the plates results in one plate being drawn down or overridden by another plate. This region is the sink of the crustal plates of Earth.

System: a selected set of interactive components. A biogeochemical system consists of reservoirs, processes and mechanisms, and associated fluxes involving material transport. The global climate system is very complex and involves all the physical, chemical, and biological interactions that control the long-term environmental conditions of the world.

Time scale: a particular period of time encompassing the duration of an event.

Transport path: the process or mechanism that moves materials in and out of a reservoir. A transport path is associated with a flux for a substance.

Upwelling: the upward movement of water from depths of typically 50 to 150 metres at speeds of approximately 1 to 3 metres per day. The upwelling of water generally results from the lateral movement of surface water. Upwelling zones in the ocean are found along the western margins of the continents, in equatorial regions, and at high latitudes of the Southern Hemisphere.

Vascular plant: a gymnosperm or angiosperm plant.

Weathering: the chemical, physical, and biological processes that lead to the disintegration of minerals, kerogen, and rocks.

LIST OF ACRONYMS

ALOHA	A Long-term Oligotrophic Habitat Assessment
BATS	Bermuda Atlantic Time-series Station
CCA	Crustose Coralline Algae
DIC	Dissolved Inorganic Carbon
ESM	Earth System Model
ESTOC	European Station for Time-series Observations in the Ocean
HOT	Hawaii Ocean Time-series
LGM	Last Glacial Maximum
MAGic	Mackenzie, Arvidson, Guidry interactive cycles
MST	Magnesian Salvation Theory
NEC	Net Ecosystem Calcification
NEM	Net Ecosystem Metabolism
NEP	Net Ecosystem Productivity
NOAA	National Oceanic and Atmospheric Administration
SOCM	Shallow-water Ocean Carbonate Model
SOCM-GLACIAL	Shallow-water Ocean Carbonate Model-Glacial
TA	Total Alkalinity
TOTEM	Terrestrial Ocean aTmosphere Ecosystem Model

INDEX

C

D

E

F

SUBSCRIBE TO

Geochemical Perspectives

Geochemical Perspectives is provided to all members of the European Association of Geochemistry.

To join the European Association of Geochemistry visit:

www.eag.eu.com/membership

Volume 1, Number 1

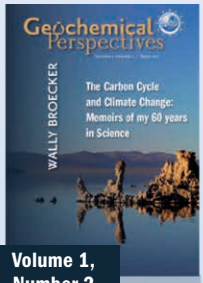

Volume 1, Number 2

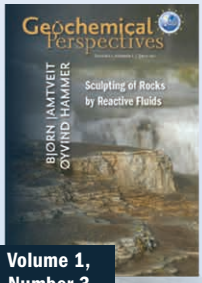

Volume 1, Number 3

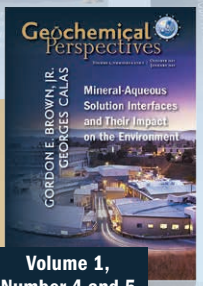

Volume 1, Number 4 and 5

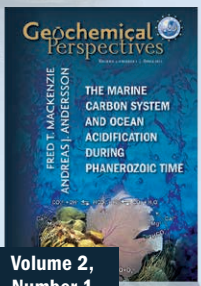

Volume 2, Number 1

Future issues will be written by:
Manuel Moreira & Mark Kurz, Charlie Langmuir, Bruce Yardley, Henry Dick and others.

For information, contact us at:
office@geochemicalperspectives.org

www.geochemicalperspectives.org

Geochemical Perspectives is an official journal of the European Association of Geochemistry

The European Association of Geochemistry, EAG, was established in 1985 to promote geochemistry, and in particular, to provide a platform within Europe for the presentation of geochemistry, exchange of ideas, publications and recognition of scientific excellence.

Officers of the EAG Council

President	Chris Ballentine, University of Manchester, UK
Vice-President	Liane G. Benning, University of Leeds, UK
Past-President	Bernard Bourdon, ENS Lyon, France
Treasurer	Christa Göpel, IPG Paris, France
Goldschmidt Officer	Bernard Marty, CNRS Nancy, France
Goldschmidt Officer	Bernie Wood, University of Oxford, UK

www.eag.eu.com

FRED MACKENZIE is Emeritus Professor of Oceanography and Geology & Geophysics in the School of Ocean and Earth Science and Technology, University of Hawaii. Fred's research includes modelling of the Earth surface system through geologic time; biogeochemical cycling of carbon, nutrients and CO_2 exchange in coastal oceans; effects of ocean acidification on carbonate ecosystems; kinetics and thermodynamics of mineral-solution reactions; and implications of global change for sustainability in Pacific island nations and Hawaii. Aside from academic pursuits, Fred is an ardent athlete, lifetime traveller, and mountaineer, climbing peaks in the Colorado and Canadian Rockies, the Cascades, the European Alps, Scotland, Corsica, Ecuador, Peru, Bolivia, and Chile. His last expedition was to the 6,348 m Volcan Parinacota on the Bolivia/Chile border. Fred is a Fellow of six professional societies, including The Explorer's Club. Some awards are: Université Libre de Bruxelles Francqui International Medal of Science, Society for Sedimentary Geology Pettijohn Medal, Geochemical Society Patterson Medal, International Association of Geochemistry Vernadsky Medal, and American Chemical Society Geochemistry Medal.

ANDREAS ANDERSSON is Assistant Professor of Oceanography at Scripps Institution of Oceanography, University of California San Diego. Andreas' research interest deals with global environmental change owing to both natural and anthropogenic processes, and the subsequent effects on the function, role, and cycling of carbon in marine environments. His current research is mainly concerned with ocean acidification in coral reefs and in near-shore coastal environments. Andreas was born and raised in Sweden but relocated to Hawaii to attend college and later graduate school. After completion of his PhD under the supervision of Fred Mackenzie, his academic career has taken him to the Bermuda Institute of Ocean Sciences, and most recently to San Diego, California. Andreas has a strong emotional affection for the ocean and while not working in or near the ocean, he enjoys spending his spare time surfing, kite surfing or diving.